Molecular Mechanisms of Peripheral T cell Tolerance: Identification of Dickkopf 3 as a Novel Immune Modulator

INAUGURAL-DISSERTATION

Maria Papatriantafyllou

Heidelberg, October 2008

INAUGURAL-DISSERTATION

Submitted to the
Fakultät für Biowissenschaften of
Ruprecht Karl Universität
Heidelberg

Presented by
Maria Papatriantafyllou
Born in Athens, Greece
Oral-examination: 31st of October 2008

Molecular mechanisms of peripheral T cell tolerance: Identification of Dickkopf 3 as a novel immune modulator

Supervisor:

Prof. Dr. Bernd Arnold

1st Referee: Prof. Dr. Günter J. Hämmerling

2nd Referee: Prof. Dr. Lutz Gissmann

TABLE OF CONTENTS

FIGURE AND TABLE INDEX

ACKNOWLEDGEMENTS

This PhD thesis was accomplished in the period of September 2005 to September 2008 in the Department of Molecular Immunology of the German Cancer Research Centre with the priceless contribution of many people.

First and foremost I would like to express my deepest gratitude to my supervisor, Prof Dr Bernd Arnold. Not only did he provide me with the opportunity to work on a highly interesting project, but he also supported me with his valuable ideas and his vast knowledge throughout the three years of my PhD study. Moreover, his critical reading and sharp comments have made this dissertation more rigorous. Last but not least, I am grateful to him because his guidance strengthened my fascination about science.

In addition, I am thankful to the head of the Department of Molecular Immunology and my first referee, Prof Dr Günter Hämmerling, for supporting the present work with his invaluable scientific ideas and his insightful critical comments.

I would like to give the warmest thanks to Dr Thilo Oelert. I appreciate his continuous contribution to this project with stimulating discussions, interesting ideas as well as with the critical reading of this thesis.

I am very grateful to Dr Gerd Moldenhauer who laboriously worked on the production of the anti-Dickkopf 3 monoclonal antibody. Moreover, I would like to acknowledge Prof Dr Hermann-Josef Gröne who contributed all the histological analyses of this project and Prof Dr Christof Niehrs who provided the Dickkopf 3 deficient mice. I also kindly thank Prof Dr Kari Hemminki, Rajiv Kumar and Dagmar Beige for providing the Affymetrix microarray equipment and technical assistance for the microarray chip hybridization respectively. Furthermore, I am indebted to Gorana Hollmann, Alexandra Klevenz, Günter Küblbeck, Georg Pougialis and Sandra Prokosch for their expert technical assistance.

My special thanks goes to Dr Kristin Hochweller who supported me, at both a scientific and a personal level. I would also like to thank her, together with Dr Petra Lindemann and Dr Konstantina Bourkoula for critically reading this thesis. Additionally, I would like to express my gratitude to previous and present colleagues from my lab for the friendly and stimulating working environment.

Many friends helped me and I greatly value their encouragement and support. Without their friendship my time in Heidelberg would have not been so nice.

Finally, I would like to deeply thank my parents, my sister and Lefteris for their genuine love and understanding. Despite being far away, they were the strongest supporters of my efforts throughout the three years of my PhD.

ABBREVIATIONS

Ab	Antibody
ACAID	Anterior chamber associated immune deviation
AICD	Activation-induced cell death
AIRE	Autoimmune regulator
AML1/RUNX1	Acute myeloid leukemia 1/ Runt-related transcription factor 1
AP-1	Activator protein 1
APCs	Antigen presenting cells
APS	Ammonium persulfate
aRNA	amplified RNA
BMDC	Bone marrow dendritic cells
BRAID	Brain-associated immune deviation
BSA	Bovine serum albumin
cAMP	cyclic adenosine monophosphate
CBL-B	Cas-Br-M (murine) ecotropic retroviral transforming sequence b
CCL3	Chemokine (C-C motif) ligand 3
CCL4	Chemokine (C-C motif) ligand 4
CCR7	C-C motif chemokine receptor 7
CFA	Complete Freud's adjuvant
CFSE	5(6)-Carboxyfluorescein diacetate *N*-succinimidyl ester
CNS	Central nervous system
CRP	C-reactive protein
CTL	cytotoxic T cell
CTLA-4	Cytotoxic T-Lymphocyte Antigen 4
DAG	Diacylglycerol
DCs	Dendritic cells
Des-TCR	Desire T cell receptor
DGKα	Diacylglycerol kinase α
DISC	Death-inducing signaling complex
DKK	Dickkopf
DMSO	Dimethyl sulfoxide
DNA	Deoxyribonucleic acid
dNTPs	deoxynucleosides
DP T cells	Double positive T cells
dPBS	Dubelcco's Phosphate buffered saline
EAE	Experimental autoimmune encephalitis
EBI-3	Eipstein Barr virus induced gene 3
EDTA	Ethylenediaminetetraacetic
EGR	Early growth response factor

ELISA	Enzyme-Linked ImmunoSorbent Assay
ERK	Extracellular regulated kinase
FasL	Fas ligand
FCS	Fetal calf serum
FoxP3	Forkhead box protein P3
GFAP	Glial fibrillary acidic protein
GFP	Green fluorescent protein
GM-CSF	granulocyte monocyte colony stimulating factor
GRAIL	Gene related to anergy in lymphocytes
GTP	Guanosine triphosphate
GTPase	Guanosine triphosphatase
HBSS	Hank's balanced salt solution
HEK	Human embryonic kidney cells
HLA	Human leukocyte antigen
ICAM-I	Intercellular adhesion molecule-I
IDO	Indolamine 2,3 dioxygenase
IFA	Incomplete Freud's adjuvant
IFN-γ	Interferon-γ
IPEX	Immune dysregulation, polyendocrinopathy, enteropathy, X-linked syndrome
JNK	Jun N-terminal kinase
LPS	Lipopolysaccharide
LRP5/6	Lipoprotein-receptor-related proteins 5/6
LSEC	liver sinusoidal endothelial cells
MAPK	Mitogen activated protein kinase
MBP	Myelin basic protein
MHC I	Major histocompatibility complex class I
MHC II	Major histocompatibility complex class II
MMP2	Metalloproteinase 2
MOG	Myelin oligodendrocyte protein
mRNA	messenger RNA
mTECs	medullary thymic epithelial cells
NFAT	Nuclear factor of activated T cells
NK	Natural killer cell
Nrp-1	Neuripilin 1
OD	Optical density
PBS	Phosphate buffered saline
PCP	Planar cell polarity
PCR	Polymerase chan reaction
PKCθ	Protein kinase Cθ
PLC-γ	Phospholipase C-γ
PLP	Proteolipid protein

PMA	Phorbol 12- myristate 13- acetate
RAG1/2	Recombination activating genes 1 and 2
RANK	Receptor activator of NF-B ligand
RASGRP1	Ras guanyl-releasing protein 1
RNA	Ribonucleic acid
RT	Room temperature
RT-PCR	Reverse transcription PCR
SAPE	Streptavidin-phycoerythrin
SDS	sodium dodecyl sulfate
Sgy	Soggy
TCR	T cell receptor
TEMED	N,N,N',N'-Tetramethylethylenediamine
TGF-β	Tumor growth factor-β
Th1	T helper cells 1
Th17	T helper cells 17
Th2	T helper cells 2
TLR	Toll-like receptors
TNF	Tumor necrosis factor
TNFR	Tumor necrosis factor receptor
TRAIL	Tumor necrosis factor-related apoptosis-inducing ligand
TRAs	Tissue restricted antigens
Treg	Regulatory T cell
UTP	uracil triphosphate
VCAM-I	Vascular cell adhesion molecule I
VEGF	Vascular endothelial growth factor
VIP	Vasoactive intestinal peptide
α-MSH	α-melanocyte-stimulating hormone

1 SUMMARY

Protection of tissues from the devastating effects of immune responses is essential for the integrity of the organism. Tolerance mechanisms, such as T cell depletion or anergy induction by natural and adaptive regulatory T cells, tolerogenic dendritic cells and parenchymal cells control potentially auto-reactive lymphocytes. In addition, organs that are particularly sensitive to damage by inflammation, so called immune privileged sites, are protected by tissue barriers and contain an immunosuppressive microenvironment.

There is increasing evidence that processes establishing immune privilege overlap with those associated with tolerance induction. However, there is much yet to learn about the molecules with a role in immune regulation. This knowledge could help in the understanding of systemic diseases, such as autoimmunity and cancer, and introduce novel principles concerning transplantation tolerance.

Aim of this study was the identification of novel molecules that are potential mediators of peripheral tolerance. Starting from a transgenic mouse model for peripheral CD8 T cell tolerance, identification of such candidate genes was attempted by wide range gene expression analysis. Dickkopf 3 (Dkk3) was 10-fold upregulated in regulatory CD8 T cells. Interestingly, Dkk3 mRNA was previously shown to be present in peripheral tissues, such as the brain, the eye, the spinal cord, the ovary and the uterus, pointing to a possible role in immune priviledge. Moreover, Dkk3 was reported to inhibit the ERK MAPK pathway in tumor cells, which is also crucial for T cell receptor signal transduction. Taking all the above into consideration, it was hypothesized that Dkk3 might be involved in immune regulation.

Here, Dkk3 was identified as a novel modulator of immune responses. Dkk3 protein was shown to be expressed by the transgenic regulatory CD8 T cells and was indispensable for the suppression of naïve T cells. In detail, Dkk3 deficient transgenic mice displayed no CD8 T cell tolerance and regulatory CD8 T cells could not exert their suppressive function in the presence of anti-Dkk3 blocking antibody.

The immune regulatory function of Dkk3 was not limited to the transgenic mouse model of CD8 T cell tolerance. Polyclonal T cells from Dkk3 deficient mice showed hyperproliferation and increased IL-2 production. This effect could be explained by the fact that the ERK MAPK is overactivated in the absence of Dkk3.

Among the tissues that express Dkk3 in high amounts are the immune privileged organs (central nervous system (CNS), ovaries, placenta), the liver, which is a crucial site for the establishment of T cell tolerance to oral antigens, the heart and the lung. On the other hand, Dkk3 expression could not be detected in the lymphoid organs and the serum. Given the

observed suppressive activity of Dkk3. it might control potentially harmful T cell responses in the above mentioned immune privileged organs.

Indeed, the immune regulatory role of Dkk3 in the CNS could be demonstrated in the context of experimental autoimmune encephalitis (EAE). Absence of neuron-derived Dkk3 led to severe and persistent EAE, due to lack of suppression of activated CD8 T cells. In addition, blocking of the secreted Dkk3 with the respective anti-Dkk3 antibody resulted in increased disease chronicity.

In conclusion, Dkk3 is a universal immune regulator, employed by transgenic tolerant CD8 T cells and immune privileged organs in order to control excessive T cell responses.

2 ZUSAMENFASSUNG

Der Schutz von Organstrukturen vor zerstörerischen Effekten durch Immunreaktionen ist essentiell für die Integrität des Organismus. Toleranzmechanismen wie T-Zelldepletion, Anergieinduktion oder Kontrolle durch regulatorische T-Zellen, tolerogene Dendritische Zellen und parenchymale Zellen kontrollieren autoreaktive Lymphozyten. Des Weiteren sind besonders empfindliche Organe, mit sehr begrenzter Möglichkeit der Regeneration, so genannte immunprivilegierte Organe, durch anatomische Barrieren und ein immun suppressives Mikromilieu geschützt.

Es gibt verstärkte Hinweise, dass die Mechanismen, welche lokale Immunsuppression innerhalb von Organen etablieren, mit denen überlappen, die systemische T-Zelltoleranz erzeugen. Jedoch herrscht weiterhin Unklarheit über die wesentlichen Moleküle, die für die Immunregulation die zentrale Rolle spielen. Dieses Wissen könnte für Therapieoptionen von Autoimmun- oder Krebserkrankungen sowie für die Induktion von Transplantationstoleranz hilfreich sein.

Ziel dieser Arbeit war die Identifikation neuer Moleküle, welche für die periphere Toleranz von Bedeutung sind. Das im Labor etablierte transgene Mausmodel der peripheren CD8 T-Zelltoleranz wurde für die Beschreibung solcher Kandidatengene mittels Genexpressionsanalysen genutzt. Dickkopf 3 (Dkk3) wurde als 10-fach hoch-reguliert in toleranten CD8 T-Zellen identifiziert. Dkk3 mRNA war bis dahin in peripheren Geweben inklusive dem Gehirn, dem Auge, den Eierstöcken und der Gebärmutter gefunden worden. Zusätzlich war beschrieben worden, dass Dkk3 überexpremiert in Tumorzelllinien, den ERK MAPK Signalweg inhibiert, welcher auch in die T-Zellsignalübertragung involviert ist. Daher wurde die Hypothese aufgestellt, dass Dkk3 eine Funktion in der Immunregulation haben könnte.

In dieser Arbeit wird Dkk3 als neuer Modulator von Immunantworten identifiziert. Die Induktion von Dkk3 Protein wurde in transgenen regulatorischen CD8 T-Zellen gefunden und war notwendig für deren regulatorische Funktion. So waren die Dkk3-defizientnen transgenen Mäuse nicht tolerant gegenüber dem Modellantigen und die regulatorische Funktion der CD8 T-Zellen war aufgehoben in Anwesenheit von Dkk3-blockierendem Antikörpern.

Die immunregulatorische Funktion von Dkk3 war nicht auf das transgene Mausmodel begrenzt. Polyklonale T-Zellen von Dkk3-defizienten Mäusen waren hyper-proliferativ und produzierten verstärkt IL-2. Diese Beobachtung konnte durch eine verstärkte Aktivierung der ERK MAP-Kinase erkärt werden.

Zu den Organen mit hoher Expression von Dkk3 gehören immunpriviligierte Organe (ZNS, Plazenta), die Leber, welche eine zentrale Bedeutung für die orale Toleranz inne hat, das Herz und die Lunge. Dkk3 konnte hingegen nicht in den lymphoiden Organen und dem Serum nachgewiesen werden. Insofern wurde vermutet, dass Dkk3 an der Etablierung eines lokalen immunsuppressiven Mikromillieus beteiligt sein könnte.

In der Tat konnte die immunregulatorische Funktion von Dkk3 im Model der Experimentellen Autoimmunen Enzephalitis (EAE) demonstriert werden. Ohne die Produktion von Dkk3 durch Neuronen in den Dkk3 defizienten Tieren war der Verlauf von EAE durch die fehlende Kontrolle aktivierter CD8 T-Zellen stärker und länger anhaltend. So führte auch die Applikation des Dkk3-spezifischen Antikörpers eine Woche nach der peripheren Aktivierung der T-Zellen zu verstärkter Chronizität von EAE.

Somit wird hier Dkk3 als universeller Immunregulator identifiziert, welcher von der regulatorischen transgenen CD8 T-Zellpopulation und von Zellen immunpriviligierter Organe genutzt wird.

3 INTRODUCTION

3.1 Introduction to the immune system

The immune system employs diverse elaborate mechanisms to protect the organism against pathogens. The immunological responses are classified in two main branches, the innate and adaptive immunity. The innate immune system responds to a microbial infection in a generic, non specific way. On the other hand, the adaptive immune system can successfully discriminate between self and foreign antigens and involves antigen-specific responses to viruses, bacteria and extracellular parasites. The main effector cells of the adaptive immunity are the lymphocytes. The lymphocytes are cells of hematopoietic origin that carry antigen-specific receptors of great diversity. The B cells are the mediators of humoral adaptive responses. Their main role is the antigen recognition and antigen-specific antibody secretion, which in turns leads e.g. to the complement-mediated killing of microbes or to the neutralization of microbial products that are toxic for the host.

Apart from the humoral responses, adaptive immunity is achieved by T cell responses. T cells originate from the bone marrow and further develop in the thymus (Moore et al. 1965; Micklem et al. 1966; Moore et al. 1967). The thymus-derived mature CD4 and CD8 T cells display a T cell receptor (TCR) repertoire of at least $2.5x10^7$ diverse specificities. Therefore they can recognize a broad spectrum of antigenic peptides, presented on MHC class I molecules by the host cells and MHC class II molecules by professional antigen presenting cells (APCs). Antigen recognition by the TCR in combination with costimulatory signals, delivered by the APCs, lead to T cell activation and proliferation (June et al. 1994).

CD4 T cells are otherwise called helper T cells and upon activation they proliferate and produce proinflammatory cytokines. Thereby they promote the activation and proliferation of CD8 T cells and the function of phagocytes and macrophages in response to intracellular bacterial infections. Moreover, CD4 helper cells play a central part in the destruction of extracellular pathogens by activating B cells. There are three classes of CD4 T cell responses, depending on the nature of the antigen and the cytokine-milieu at the site of inflammation. Th1 CD4 T cells develop in the presence of IL-12, secrete mainly IFN-γ and respond to intracellular microbes (Schmitt et al. 1994). Th2 responses are characterized by IL-4 secretion upon encounter of extracellular pathogens in the presence of IL-4 (Street et al. 1991; Cardell et al. 1992). The IL-17-producing Th17 CD4 T cells have been recently identified (Harrington et al. 2006). They have been reported to differentiate in the presence of TGF-β and IL-6 (Stockinger et al. 2007) and to respond to extracellular bacteria by inducing strong

inflammation (Korn et al. 2007; Ouyang et al. 2008). Independently of what their target pathogen is, all CD4 T cells are activated upon antigen presentation on MHC class II complexes by professional APCs, most usually dendritic cells (DCs).

CD8 T cells mediate cytotoxic T cell responses. They recognize antigenic peptides presented on MHC class I complexes by host cells or cross-presented by DCs (Zinkernagel et al. 1979; Azuma et al. 1992; Albert et al. 1998). Upon activation CD8 T cells kill the infected cells or the tumor cells by release of perforin and granzymes. Perforin forms pores to the target's cell membrane through which granzymes can enter the cell and induce apoptosis (Griffiths 1995).

The potency of the mammalian adaptive immune system lies on the mentioned highly sophisticated effector responses but also the long-lasting immunologic memory. Memory CD4 and CD8 T cells are developed during the anti-microbial responses, survive for long time and effectively prevent disease upon a second encounter with the same pathogen (Zinkernagel et al. 1996).

3.2 Immunological Tolerance

3.2.1 The role of immunological tolerance

The mammalian immune system protects the host from a broad spectrum of pathogenic microorganisms while avoiding misguided or excessive immune reactions that would be deleterious to the individual. Adaptive immune responses are characterized by enormous diversity in antigen recognition, high antigen specificity, potent effector activity and long-lasting immunologic memory. Because of this potency, serious damage to the host may ensue if aberrant immune responses are triggered against self, such as in case of autoimmunity or allergy. Immunological tolerance assures the unresponsiveness of the adaptive immune system to self antigens and the control of the quality and magnitude of the adaptive immune responses, so that host is protected and immune homeostasis is preserved.

The diverse mechanisms by which T cell tolerance is established will be explicitly discussed below. First the basic principles of central tolerance will be described. Next, all strategies reported to suppress self reactive T cells and T cell hypereactivity in peripheral tissues will be addressed. Furthermore, the mechanisms of local protection against the devastating results of T cell responses, which are vital for the immune privileged organs, will be reviewed. Since in this thesis the role of Dickkopf 3 as a mediator of peripheral T cell tolerance and immune privilege will be explored, the last paragraphs of this chapter will focus on the current knowledge about the expression, structure and function of this protein.

3.2.2 Central T cell Tolerance

The term central tolerance is used to describe the mechanisms taking place in the thymus during T cell development, which result in the elimination and control of auto-reactive T cells. The two major branches of central tolerance are the clonal deletion of self-specific T cells and the intrathymic induction of natural $CD4^+CD25^+Foxp3^+$ regulatory T cells (nTregs).

3.2.2.1 Clonal Deletion

The proper function of the adaptive immune system is firmly dependent on the diversity of the TCR repertoire. The development of a T cell population that carries a wide spectrum of antigen specificities and is able to recognize MHC-bound antigenic peptides takes place in the thymus. Progenitor T cells described as double negative, i.e. lacking expression of CD4 and CD8, the molecules that will ultimately define the functional status of T cells, are generated in the bone marrow and migrate to the thymus. There, initially the TCRβ and, after entering the double positive ($CD4^+CD8^+$, DP) stage, the TCRα genes undergo random recombination by the RAG1/RAG2 enzymatic complex (Figure 1).

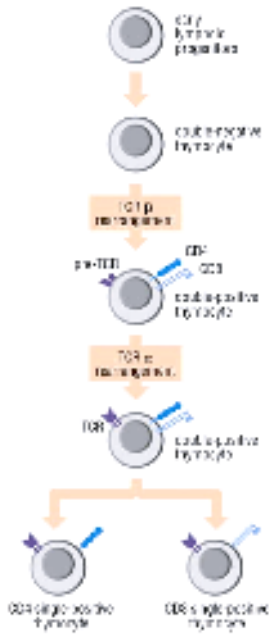

Figure 3-1. Schematic representation of T cell development in the thymus. T cell progenitors, described as double negative thymocytes undergo random recombination of the TCRβ genes and become double positive thymocytes. Followingly the TCRα genes are rearranged and the TCR-positive thymocytes differentiate to CD4 and CD8 single positive T cells. Adapted from Immunity:The immune response in infectious and inflammatory disease (DeFranco, Locksley and Robertson)

The randomly generated TCRs are next tested for their ability to recognize the host's MHC molecules, in a process called positive selection. Positive selection is conducted in the thymic cortex (Anderson et al. 1994). Only the T cells with a TCR able to recognize self-MHC molecules get a survival signal and are positively selected (Zinkernagel et al. 1974; Kisielow 1988; Wagner 2007). An estimated 90-95% of DP T cells that are not able to bind to the available MHC complexes undergo death by neglect (Huesmann et al. 1991).

The risk of randomly developing a T cell population with an extremely high TCR diversity would be high, if a checkpoint for the elimination of auto-reactive specificities was not present. The possibility of autoimmunity is minimized by deleting the auto-reactive T cells before they escape the thymus. This process is described as negative selection or clonal deletion and takes place in the thymic medulla. Clonal deletion occurs upon self antigen presentation by the medullary thymic epithelial cells (mTECs) (Burkly et al. 1993; Volkmann et al. 1997) and the thymic dendritic cells (Brocker et al. 1997). mTECs promiscuously express a variety of tissue restricted antigens (TRAs), under the transcriptional regulation of Autoimmune Regulator (AIRE). Self-antigens expressed by mTECs represent virtually all the parenchymal organs, thereby mirroring the peripheral self (Derbinski et al. 2001). TRAs have been shown to be either presented by mTECs themselves or transferred to and cross-presented by thymic dendritic cells (Gallegos et al. 2004). The MHC-self antigen recognition by a TCR usually leads to the deletion of the respective T cell.

Even though this process is highly efficient, since approximately 50-70% of the positively selected T cells are thought to be subject to negative selection (van Meerwijk et al. 1997), not all auto-reactive T cells are eliminated by clonal deletion. An additional mechanism of central tolerance is the thymic development of regulatory T cells (Kappler et al. 1987; Modigliani et al. 1996; Itoh et al. 1999).

3.2.2.2 Naturally arising $CD4^+CD25^+FoxP3^+$ regulatory T cells (nTregs)

Naturally arising $CD4^+CD25^+FoxP3^+$ regulatory T cells are a specialized subset of T cells with suppressive and regulatory properties. They have been shown to suppress proliferation of naïve T cells, their differentiation into effector T cells and the effector functions of activated CD4 and CD8 T cells. Moreover, they have been reported to regulate the function of natural killer cells, natural killer T cells, B cells, macrophages and dendritic cells (Sakaguchi et al. 2008). The suppressive activity of nTreg cells requires their prior activation through their T cell receptor. Once activated, nTreg cells can also suppress other T cells in an antigen-nonspecific way. Their importance in immune regulation is demonstrated by the development of autoimmune diseases following their ablation (Shevach et al. 2001; Kim et al. 2007). The transcription factor forkhead box protein P3 (Foxp3) is expressed specifically in the natural Treg cell lineage and is a master regulator of Treg cell development (Fontenot et al. 2003; Hori et al. 2003).

Like conventional T cells, nTreg cells develop in the thymus, through positive selection (Itoh et al. 1999). Data from a variety of systems indicate that the development of functional

peripheral Treg from their intrathymic precursors also involves an extrathymic phase, dependent on the presence, in the periphery, of the relevant self-antigen (Seddon et al. 2000). Until recently it was believed that they express a TCR repertoire enriched in self specificities, distinct from that of conventional T cells (Hsieh et al. 2006). The development of Treg cells was thought to be driven by high-affinity interactions between TCRs on developing thymocytes and self peptide–MHC complexes on thymic epithelial cells (Jordan et al. 2001; Kawahata et al. 2002). The affinities of such interactions were proposed to be somewhere between the affinities of interactions triggering positive and negative selection of thymocytes (Figure 2) (Apostolou et al. 2002; Kawahata et al. 2002). However, this view was challenged by a recent study indicating that TCR repertoire of Treg cells was as diverse as in conventional T cells and self TCR specificities in the Treg population were rare (Pacholczyk et al. 2007). Thus it is possible that one result of commitment to the Treg cell lineage is an increased resistance to negative selection in the thymus resulting in a population of Treg cells with a TCR repertoire similar to conventional T cells but likely with slightly higher affinity to self (Stephens et al. 2007).

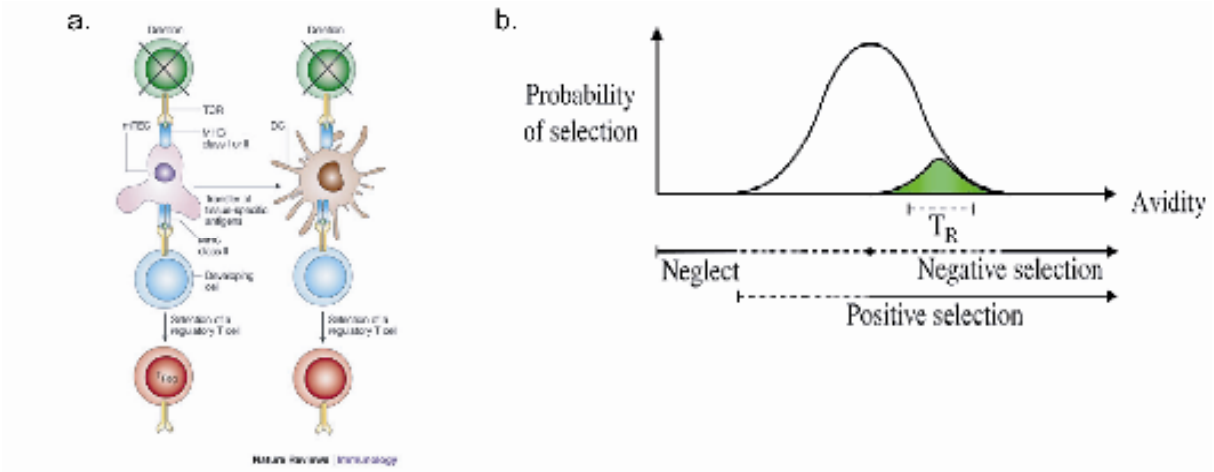

Figure 3-2. Development of naturally arising regulatory T cells in the thymus. (**a**) The promiscuously expressed TRAs are presented and cross-presented by mTECs respectively. This leads to the deletion of auto-reactive T cells but also to the development of CD4CD25Foxp3 regulatory T cells that are self antigen-specific. Adapted from: Self representation in the thymus: an extended view. Bruno Kyewski & Jens Derbinski, Nat Rev Immunol, 2004. (**b**) Developing T cells with affinity for self peptide-MHC complexes that is higher than in conventional T cells and lower than in negatively selected thymocytes are positively selected to become nTreg cells. Adapted from: Regulatory T cells in the control of immune pathology, Kevin J. Maloy & Fiona Powrie, Nat Immunol, 2001.

3.2.3 Peripheral T cell Tolerance

Central tolerance is very efficient, but it is still incomplete. Self-reactive T cells, especially those with a lower affinity for self-antigens, can escape negative selection (Bouneaud et al.

2000). Also, certain antigens, for which tolerance is required, may not be expressed in the thymus. This is the case for most harmless environmental proteins, to which chronic immune reactivity must not develop.

Furthermore, T cell responses mounted against pathogens need to be controlled in order to avoid extended tissue damage. Apart from the naturally occurring regulatory T cells that develop in the thymus and regulate the immune responses in the periphery there are additional mechanisms for controlling autoreactive T cells in the tissues. Cell intrinsic processes, which control excessive T cell activation, include the deletion of or anergy induction in self-specific T cells. On the other hand, systemic regulation of cell populations is based on self-antigen presentation by immature dendritic cells and parenchymal cells, as well as regulatory T cell induction in the tissues.

3.2.3.1 Deletion by activation induced cell death

Activation induced cell death (AICD) restrains the for the host tissues devastating consequences of T cell hyperactivation. Additionally, the molecular mechanisms of AICD are employed by immune regulators (i.e. tolerogenic dendritic cells and Tregs) to extinguish self-reactive T cells, as it will be later on discussed.

Following repeated T cell activation by their specific antigen, T cells undergo apoptosis by AICD. AICD is brought about by the crosslinking of death receptors on T cells. Death receptors are a subclass of the tumor necrosis factor receptor (TNFR) family, which trigger apoptosis. The best studied mechanism of AICD is Fas-mediated T cell death (Alderson et al. 1995; Mogil et al. 1995). Resting naïve T cells carry the Fas molecule (CD95) on their surface. TCR stimulation in the presence of IL-2 results in Fas upregulation (Refaeli et al. 1998) and upon repeated antigen stimulation, the Fas ligand (FasL) is also expressed on activated T cells (Lenardo et al. 1999). Additionally, FasL is expressed by immune privileged organs. Ligation of Fas to the FasL leads to the formation of the death-inducing signaling complex (DISC) with subsequent activation of caspases, resulting in caspase-mediated apoptosis (Nagata 1997). Other death ligands and receptors, such as the TRAIL molecule and its receptor have also been implied to contribute to AICD. (Jeremias et al. 1998; Mariani et al. 1998).

3.2.3.2 T cell anergy

Anergy has been described as a long lasting cell intrinsic state of T cell unresponsiveness (Jenkins et al. 1987; Fathman et al. 2007). It is associated with a nearly complete block of T cell proliferation and IL-2 production (Quill et al. 1987). Secretion of other cytokines, such as

IFNγ, is reduced during anergy but this can be reversed with strong stimuli (i.e. the presence of IL-2 and IL-15). T cell anergy is suggested to be a result of suboptimal TCR activation, due to the lack of costimulatory molecules on the antigen presenting cells (Quill et al. 1987; Schwartz 2003) or due to T cell stimulation by peptide-MHC complexes with low TCR avidity (Sloan-Lancaster et al. 1993). *In vivo* T cell anergy has been observed after systemic delivery of superantigens (Kawabe et al. 1990), adoptive transfer of TCR transgenic T cells into hosts that express the cognate antigen as a self antigen (Kearney et al. 1994) and the administration of soluble peptide antigen into TCR transgenic mice (Kearney et al. 1994; Dubois et al. 1998).

At the molecular level, T cell anergy is the result of the overactivation of the nuclear factor of activated T cells (NFAT), which then becomes disproportionate to the activator protein 1 (AP-1) levels (Kang et al. 1992; Lyakh et al. 1997; Macian et al. 2002). Defective extracellular regulated kinase (ERK) and Jun N-terminal kinase (JNK) MAPK signaling is the cause of reduced AP-1 DNA binding and subsequent IL-2 transcription (Li et al. 1996). The small GTPase Ras which is upstream of the MAPK pathways is fully activated after coactivation with CD28. However, in anergic T cells, Ras GTP-loading is defective (Fields et al. 1996). In detail, diacylglycerol kinase α (DGKα) upregulation in anergic T cells prevents diacylglycerol analog (DAG) signalling from inducing to the GTP loading of the Ras molecules by Ras guanyl-releasing protein 1 (RASGRP1) (Figure 4) (Fathman et al. 2007).

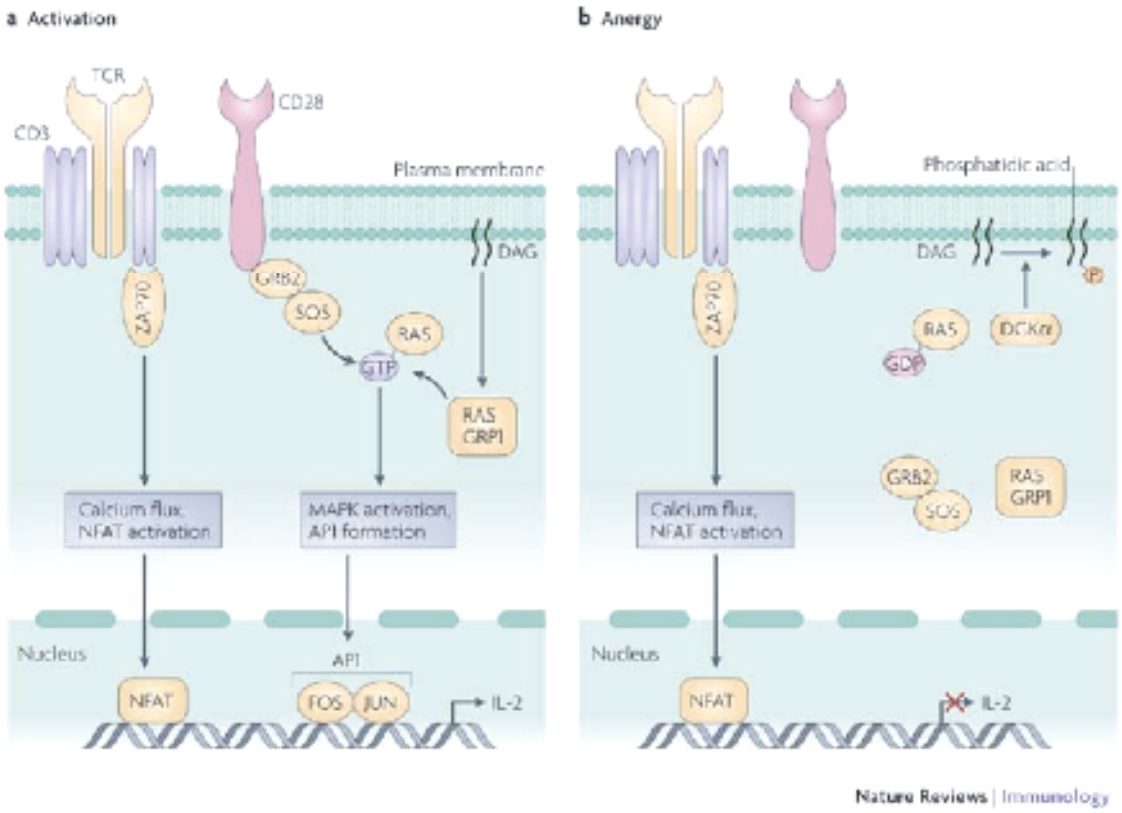

Figure 3-3. Schematic representation of the signalling pathways in T cell activation and T cell anergy induction. (a) T cell activation involves both TCR and CD28 stimulation, which finally lead to NFAT activation and AP1 formation, leading to IL-2 transcription. (b) Absence of T cell costimulation leads to anergy induction. This involves NFAT activation as well as defective Ras activation due to the inhibition of DAG signaling by DGKα. Adapted from: Molecular mechanisms of CD4+ T-cell anergy, C. Garrison Fathman and Neil B. Lineberry, Nat Rev Immunol, 2007.

Moreover, the induction of the EGR transcription factor by the upregulated NFAT has also been shown to contribute to the anergic state (Harris et al. 2004; Safford et al. 2005). Additionally, many reports have implicated an important role for E3 ubiquitin ligases in anergy. Protein poly-ubiquitination is a post-translational mechanism of governing cellular events by leading to proteasomal protein degradation (Pickart et al. 2004). The E3 ubiquitin ligases CBL-B, GRAIL and ITCH have been demonstrated to be crucial for the establishment of T cell anergy *in vitro* and *in vivo* (Heissmeyer et al. 2004; Loeser et al. 2007; Schartner et al. 2007) .

3.2.3.3 Natural regulatory T cells

Naturally arising FoxP3$^+$ regulatory T cells, which are developed in the thymus as described above, greatly contribute to the maintenance of systemic tolerance. FoxP3 loss-of-function mutations result in the lethal X-linked lymphoproliferative disorder of the naturally arising scurfy mouse strain, and the homologous human disorder IPEX syndrome (‘immune

dysregulation, polyendocrinopathy, enteropathy, X-linked' syndrome), which are attributed to impaired Treg development (Chatila et al. 2000; Bennett et al. 2001). FoxP3 has been shown to interact with the transcription factors NFAT (Wu et al. 2006) and AML1/Runx1 (Ono et al. 2007), that otherwise induce gene-expression related to the differentiation and proliferation of effector T cells. Thereby it represses the transcription of proinflammatory cytokines and induces immune-suppressive molecules.

A range of molecular mechanisms for Treg mediated immune regulation have been identified by *in vitro* and *in vivo* studies of their function. Since natural Tregs constitutively express CD25, which is the high-affinity receptor for IL-2, they have been reported to suppress effector T cells *in vitro* and *in vivo* by IL-2 deprivation-mediated apoptosis (Pandiyan et al. 2007). Additionally, Tregs have been shown to act by immunosuppressive cytokine secretion, cell-contact suppression and functional modification or killing of APCs. Treg-secreted cytokines such as IL-10 (Belkaid et al. 2002), TGF-β (Maloy et al. 2003; Li et al. 2007) and the newlly identified IL-35 (Collison et al. 2007) have been demonstrated to be mediators of suppression either *in vivo* or *in vitro*. Moreover, during inflammation Treg cells are able to kill the activated T cells or APCs through cell-contact by a granzyme B- (Gondek et al. 2005) and perforin- (Grossman et al. 2004) dependent mechanism (Cao et al. 2007). Furthermore they have been indicated to inhibit T cell proliferation *in vitro* by delivering cAMP through gap junctions (Bopp et al. 2007), or to suppress activated T cells *in vitro* and *in vivo* by generating pericellular adenosine with CD39 and CD73 enzymatic activity (Deaglio et al. 2007). Finally, activated Tregs downmodulate CD80/86 expression on APCs and stimulate dendritic cells, in a CTLA-4 dependent manner, to form the enzyme indolamine 2, 3 dioxygenase (IDO). IDO is a potent immunosuppressive enzyme, which catalyzes the catabolism of tryptophan, an aminoacid that is essential for T cell proliferation (Puccetti et al. 2007).

All the mechanisms mentioned above, contribute to the regulatory role of nTreg cells during the steady state (immune homeostasis) or during an active immune response. These mechanisms can act independently of each other or in combination, depending on the local microenvironment as well as on the strength and duration of the antigenic stimulus (Figure 3) (Tang et al. 2008).

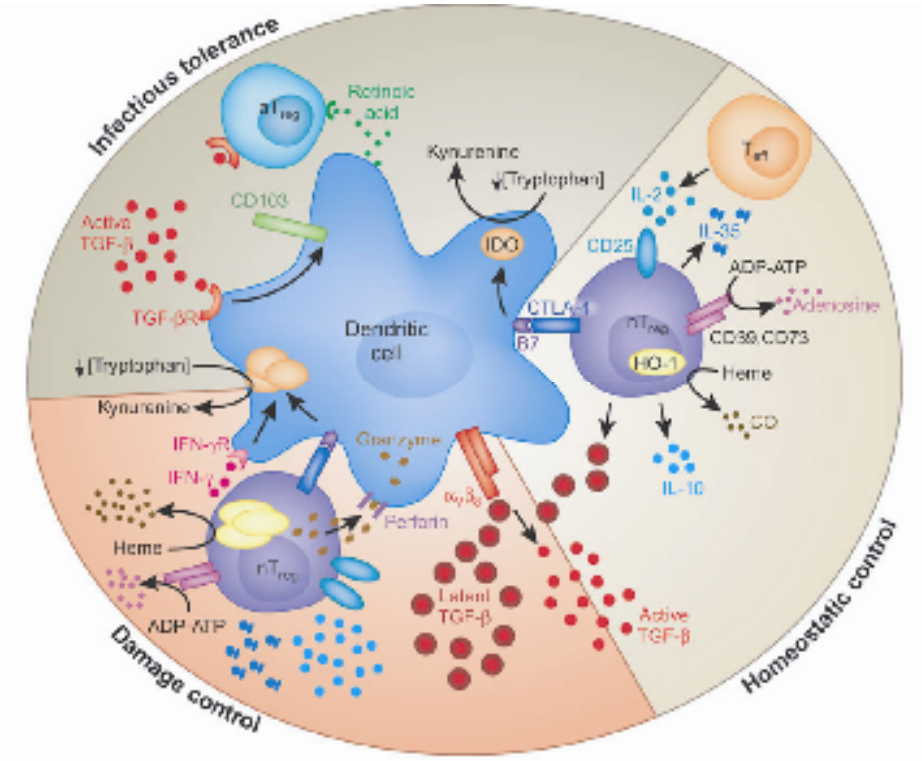

Figure 3-4. Schematic representation of the molecular mechanisms reported to contribute to the regulatory role of nTregs. The potential contribution of the above mentioned mechanisms in homeostatic control (steady state), damage control (inflammation) and infectious tolerance are depicted. Adapted from: The FoxP3+ regulatory T cell: a jack of all trades, master of regulation, Qizhi Tang & Jeffrey A Bluestone, Nat Immunol, 2008.

3.2.3.4 Adaptive regulatory T cells

Apart from the nTreg cells many regulatory T cell populations have been described to develop in the periphery. The $CD4^+CD25^+$ regulatory T cells that differentiate from naïve T cells in the periphery are called adaptive or induced regulatory T cells. They are suggested to be triggered by low-affinity antigen or altered TCR signal transduction and, unlike the natural Tregs, do not necessarily display biased anti-self TCR repertoire (Bluestone et al. 2003). This implicates their regulatory function in the context of anti-pathogen immune response suppression and oral- or probiotic-antigen tolerance (Groux 2001). Adaptive regulatory T cells mainly suppress immune responses in a cytokine dependent manner (Maloy et al. 2001). Naïve T cells have been shown to acquire FoxP3 expression and consequently Treg function in the periphery in several experimental models. It has been observed *in vitro* that antigenic stimulation in the presence of TGF-β triggers naïve T cell differentiation to FoxP3+ T cells (Chen et al. 2003; Apostolou et al. 2004; Kretschmer et al. 2005). FoxP3 induction by TGF-β is due to demathylation of CpG motifs within the foxp3 locus. Strikingly this chromatin modification is incomplete, when compared to the methylation state in the foxp3 locus of

nTreg cells. Therefore, induced FoxP3+ regulatory T cells can loose FoxP3 expression and suppressive function when deprived of TGF-β (Floess et al. 2007).

Interestingly, the presence of TGF-β, IL-2 and retinoic acid (which is secreted by a particular subset of dendritic cells in the gut-associated lymphoid tissue) facilitate the generation of FoxP3+ T cells *in vitro*. Hence FoxP3 Treg induction upon oral antigen-presentation by retinoic acid-producing dendritic cells could be a plausible mechanism of oral tolerance. Yet, what remains to be determined is the stability of the peripherally induced FoxP3 Tregs *in vivo* and their contribution to the peripheral pool of the regulatory T cells (Sakaguchi et al. 2008).

Besides FoxP3+ Tregs, several other types of inducible regulatory T cells have been described. For example, repeated antigen stimulation of CD4 T cells in the presence of IL-10 *in vitro* leads to the development of so called Tr1 cells (Chen et al. 1994; Groux et al. 1997). Tr1 cells secrete IL-10 and TGF-β. They have been shown to control the activation of naïve and memory T cells *in vivo* and *in vitro* and to suppress Th1 and Th2 responses to pathogens, tumors and alloantigens, antibody production by B cells and the APC stimulatory capacity. The presence of Tr1 cells in the small intestine has been associated with the protection against colitis.

It is noteworthy to mention that a variety of other T cell subpopulations, including $CD8^+CD122^+$ (Endharti et al. 2005), $CD8^+CD28^-$ T cells (Filaci et al. 2004), $CD4^-CD8^-$ (Chen et al. 2004) and γδ T cells (Hayday et al. 2003) have also been reported to exert an immunosuppressive activity.

3.2.3.5 Tolerance induction by dendritic cells

Dendritic cells are highly specialized antigen presenting cells (APCs), that process and present antigenic peptides to T cells (Steinman et al. 1978; Banchereau et al. 1998). During inflammation DCs process both microbial and self proteins (e.g. derived from dead cells). However, they induce a specific immune response against pathogens but not against self antigens. Thus, they contribute to peripheral autoreactive T cell tolerance (Steinman et al. 2003). The exact mechanism of tolerance induction by dendritic cells is still unclear, so only an overview of the most accepted notions will be given below.

Initially, it has been proposed that in the steady state immature DCs in peripheral tissues take up soluble proteins or apoptotic bodies arising from cell turnover. Upon migration to the secondary lymphoid organs, they present or cross-present (Heath et al. 1998; Kurts et al. 1998) these self antigens, inducing either deletion or anergy of the autoreactive CD4 and CD8 T cells respectively (Steinman et al. 2002; Morelli et al. 2003). Alternatively, short-lived

migratory DCs may function as antigen-transporting cells that transfer self antigens to longer-lived spleen- and lymphnode-resident DCs with inherent tolerogenic function.
Later it has been shown that DC migration, as well as self antigen processing and presentation for tolerance induction, require partial DC maturation (Lutz et al. 2002). Semi-mature DCs, or otherwise named quiescent mature DCs, exhibit upregulated levels of surface MHC and T cell-costimulatory molecules and produce low amounts of IL-10 and no IL-12. The tolerogenic quiescent mature DCs have been demonstrated to promote FoxP3+ Treg and Tr1 differentiation and expansion and release the suppressive mediators IL-10 and IDO (Morelli et al. 2003).
The tolerogenic features of DCs are lost after full maturation, which occurs in the presence of TLR-ligands (e.g. dsRNA, LPS, CpG oligunucleotides), proinflammatory cytokines (i.e.GM-CSF, IL-1β, TNF-α, IFN-α, prostaglandin E2) and interaction of the TNFR family molecules on the DC surface (i.e. CD40, TNFR, RANK) with their ligands. Activated DCs upregulate MHC class II, costimulatory molecules (such as CD80 (B7.1), CD86 (B7.2), CD40) and CCR7 on their surface and secrete proinflammatory cytokines like IL-1α, IL-1β, IL-6, IL-12 and IFNα. This in turn allows the initiation of an effective immune response in the draining lymphnodes. Although activated DCs still present self antigens, the prior establishment of self tolerance prevents detrimental autoimmune responses.

3.2.3.6 Tolerance induction by parenchymal cells

3.2.3.6.1 Tolerance induction in the liver

The liver is continuously exposed to both potential pathogens and commensal bacterial- or food-derived antigens through the portal vein. Tolerance to oral antigens is assured not only by the generation of adaptive CD4 regulatory T cells in the gut associated lymphoid tissue (GALT) (Sun et al. 2007), but importantly by the induction of suppressive T cells in the liver. Intraportal antigen application results in systemic antigen-specific tolerance, suggesting that the liver is particularly capable of actively inducing peripheral tolerance. In addition, it has been shown that concomitant liver transplantation from the same donor prolongs allograft survival (Calne et al. 1969; Praseedom et al. 2001). Many mechanisms are proposed to underlie tolerance induction in the liver. For instance, liver dendritic cells have been demonstrated to produce high amounts of suppressive IL-10. Importantly, liver parenchymal cells are also crucial for the establishment of CD8 T cell peripheral tolerance in the liver (Crispe et al. 2006).

When leukocytes pass with the blood flow through the liver sinusoids, they come in contact with the liver sinusoidal endothelial cells (LSEC) that line the sinusoids. Since LSEC constitutively express various surface molecules associated with professional APCs, such as MHC class I and II, CD54 (ICAM-I), CD106 (VCAM-I), the costimulatory molecules CD80, CD86 (Lohse et al. 1996) and CD40 (Leifeld et al. 1999), they are able to present soluble antigen to CD4 T cells and cross-present antigen to CD8 T cells. Following priming by LSEC *in vitro*, CD4 T cells do not differentiate into Th1 cells (Knolle et al. 1999). *In vivo*, intravenously applicated ovalbumin is cross-presented by LSEC to CD8 T cells, which then become non-cytotoxic (Limmer et al. 2000).

LSEC do not constitute the only liver cell type capable of inducing T cell tolerance. Hepatocytes are also thought to be involved in T cell peripheral tolerance induction. This was shown in transgenic mice, expressing the MHC class I K^b molecule only on hepatocytes, under the control of the C-reactive protein (CRP) promoter, and carrying K^b specific Des-TCR CD8 T cells (Des-TCRxCRP-K^b mice). The Des-TCR CD8 T cells recognize only an intact K^b antigen presented by the hepatocytes and are thus rendered tolerant. As a result K^b positive skin grafts are accepted by the DesTCRxCRP-K^b mice (Ferber et al. 1994).

3.2.3.6.2 Tolerance induction in the skin

During adult life naïve T cells do not access peripheral tissues, such as the skin and the lung, but traffic only in the secondary lymphoid organs (Kimpton et al. 1995; Alferink et al. 1998). However, it has been shown that CD8 T cells are tolerized against antigens expressed by skin parenchymal cells. More specifically, transgenic mice expressing the K^b antigen under the KeratinIV promoter on hair follicle keratinocytes and carrying the K^b-specific Des-TCR T cells are tolerant to K^b. Notably, they have been demonstrated to accept K^b positive skin and tumor grafts (Alferink et al. 1995). The observed tolerance cannot be assigned to K^b cross-presentation by DCs, since the Des-TCR can recognize only an intact K^b molecule and does not react with the peptides of a degraded K^b molecule presented by another MHC class I molecules. Interestingly, it has been demonstrated that CD8 T cells can pass through the endothelium during the neonatal phase and recognize self-antigens on the keratinocytes. Contact with parenchymal cells renders these CD8 T cells tolerant (Alferink et al. 1998). Tolerant CD8 T cells persist during adulthood and are capable of regulating the reactivity of naïve Des-TCR CD8 T cells against K^b positive tumor and skin grafts (Figure 5). The molecular mechanism underlying this CD8 T cell tolerance remains to be elucidated and this is subject of this study. So far it has been demonstrated that regulatory Des-TCR CD8 T cells

upregulate mRNA of molecules, such as TGF-β, that have already been described to play a role in the natural Treg mediated suppression (Reibke et al. 2006).

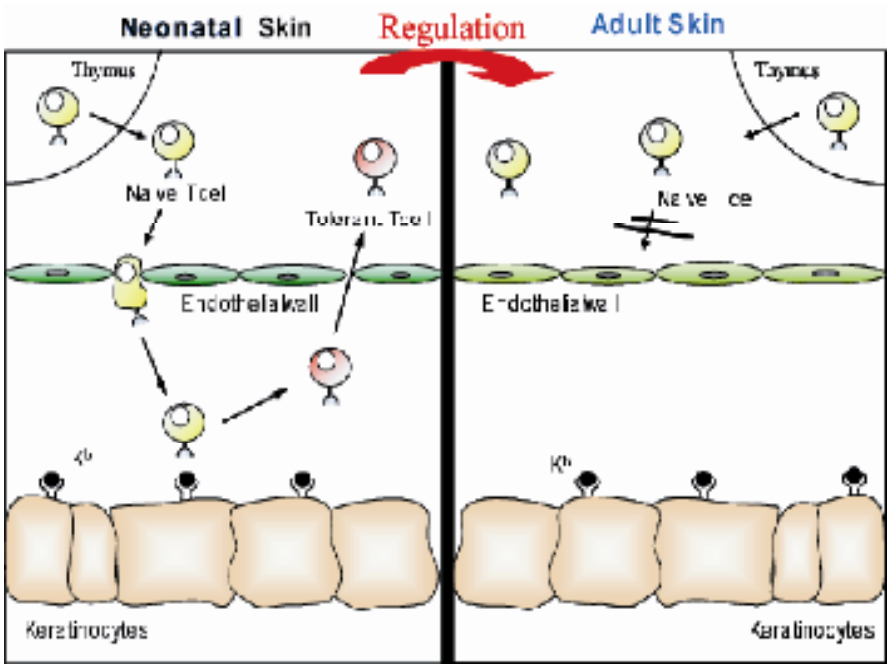

Figure 3-5. CD8 T cell tolerance induction by keratinocytes during the neonatal phase. In neonates naïve T cells pass through the endothelium and are rendered tolerant to self-antigens that are presented by parenchymal cells. Tolerant CD8 T cells survive until adulthood and can regulate naïve CD8 T cells with the same TCR specificity.

3.2.4 Immunological privilege

Described above are the mechanisms that are important for the establishment of a systemic immunological tolerance. In addition, certain organs are predisposed to establish an immune-privileged microenvironment in order to assure local protection. The term immunological privilege was first assigned to organs, where prolonged allogeneic graft survival was observed (Medawar 1948). In detail, the anterior chamber of the eye, the brain, the hamster cheek pouch, the testes and the ovary were all shown to accept allogeneic grafts. Pregnancy is another example of immunological privilege, since the fetus, which also carries foreign antigens of paternal origin, is not recognized as an allograft and rejected.

Initially it was proposed that immune privilege is the consequence of the absence of lymphatic drainage in the eyes, brain and endometrium, which would lead to ignorance of antigens (Medawar 1948). However, peripheral blood contains antibodies against antigen injected in the brain (Harling-Berg et al. 1989; Harling-Berg et al. 1991; Gordon et al. 1992), allogenic cells transplanted in the eye (Kaplan et al. 1977) or fetal HLAs of paternal origin (McLean et al. 1970). Yet, immune privilege is the result of active regulation, namely local suppression or deviation of potentially harmful T cell responses (Niederkorn 2006).

Numerous mechanisms of local immune suppression have been described. Interestingly, MHC I molecules are absent from the neurons (brain) (Lampson et al. 1984), the corneal

endothelium and the retina (eye) (Abi-Hanna et al. 1988) as well as from the trophoblast. This prevents the CTL responses in the particular tissues. Furthermore, the expression of non-classical MHC Ib molecules (HLA-G, HLA-E in human and Qa2 in mice) results in the inhibition of NK cells and the cell death of activated CD8 T cells (Streilein 2003; Niederkorn 2006).

Apart from the non-classical MHC Ib molecules, some more cell surface proteins have been indicated to contribute to the immunological privilege of the eye, the brain and the fetus. For example, the FasL is expressed on ocular cells, cytotrophoblasts and the placenta and is upregulated on microglia, astrocytes, oligodendrocytes and neurons upon inflammation (Askenasy et al. 2005). As already mentioned FasL binds to the Fas receptor on activated T cells, thus inducing AICD. Proapoptotic TNF-realted apoptosis inducing ligand (TRAIL) has also been found in ocular (Wang et al. 2003) and fetal tissues (Phillips et al. 1999) but not in the CNS (Dorr et al. 2002). Yet its function in maintaining immunological privilege is still to be established. Finally, some secretory molecules with T cell suppressive role, such as TGF-β, soluble FasL and IDO are traced in the anterior chamber of the eye and the placenta (Askenasy et al. 2005; Niederkorn 2006). The functional relevance of anti-inflammatory molecules in the brain is poorly understood. It has been suggested that the neuropeptides VIP, α-MSH and somatostatin are regulating T cell immune responses in the CNS (Reinke et al. 2006).

The phenomenon of immune deviation has mainly been described in the anterior chamber of the eye and is known as ACAID (anterior chamber associated immune deviation). Upon antigen deposition in the anterior chamber unique, tolerogenic $F4/80^+$ APCs in the iris-ciliary body are believed to capture it and enter the thymus via blood circulation. There, they induce $CD4^-CD8^-NK1.1^+$ thymocytes, which in turn enter the circulation as recent thymic emigrants and home to the spleen, contributing to the generation of splenic suppressor cells. $F4/80^+$ APCs are also claimed to migrate directly from the eye to the spleen, where they contribute to the development of CD8 regulatory T cells. CD4 regulatory T cells and γδ T cells are also involved in ACAID. Soluble antigen introduced to the brain induces an immune deviation that bears notable resemblance to ACAID and is therefore called brain-associated immune deviation (BRAID). It seems that BRAID does not follow the same splenic pathway as described for ACAID, since it could not be induced in splenectomized mice, but it could be adoptively transferred by cells isolated from the cervical lymph nodes (Wenkel et al. 2000).

3.2.5 Failure of peripheral T cell tolerance: the example of experimental autoimmune encephalitis

Experimental autoimmune encephalitis (EAE) is a model for multiple sclerosis and an example of T cell-mediated autoimmunity. It is an autoimmune disease that is driven mainly by CD4 and also by CD8 T cells specific for myelin sheath, a component of the CNS. EAE can be induced in mice by active immunization with CNS-self antigens mixed with complete Freund's adjuvant (CFA) and administration of pertussis toxin, which breaks the blood brain barrier and provides to the activated autoreactive T cells access to the CNS. The most commonly used CNS-derived antigens are the myelin basic protein (MBP), the myelin oligodendrocyte glycoprotein (MOG) and the proteolipid protein (PLP). Alternatively EAE can be also induced by the adoptive transfer of MBP- or MOG-reactive T cells with subsequent pertussis toxin administration.

In EAE, autoreactive CD4 and CD8 T cells traffic to the CNS parenchyma, resulting in focal areas of inflammation and demyelination throughout the CNS. Until recently, research done in the EAE model was focused on Th1 CD4 T cells and their resulting cytokines and chemokines, which were thought to be involved in the pathogenesis of the disease. The cytokine IL-12 was considered to be essential for the development of Th1 mediated autoimmunity. However, during the last few years this view has been challenged. It has been shown that the cytokine IL-23, which promotes the survival and expansion of Th17 cells, plays a major role in the establishment of EAE (Thakker et al. 2007) and that Th17 cells are the major disease mediators (Aranami et al. 2008). Moreover, the role of IFN-gamma producing CD8 T cells in EAE pathogenesis is not to be overseen, since two independent EAE models involve MBP or MOG specific CD8 T cells (Steinman 2001; Ji et al. 2007).

3.3 Dickkopf 3

3.3.1 The Dickkopf family of proteins and Dickkopf3

Dickkopf3 (Dkk3) is a member of the Dickkopf family of five secreted proteins, DKK1-4 and Soggy, which share 37-50% sequence identity (Krupnik et al. 1999; Barrantes Idel et al. 2006). Dkk proteins contain a signal sequence and share two conserved cystein-rich domains, separated by a linker domain (Figure 6). Each of the cystein-domains contains ten conserved cystein residues (Glinka et al. 1998; Krupnik et al. 1999). The N-terminal cysteine-rich domain, Dkk_N (formerly called Cys1) is unique to the Dkk protein family while the C-terminal cysteine-rich domain (formerly called Cys2) has a pattern of ten cysteines related to that of the colipase fold (Niehrs 2006). According to structure-function analysis of vertebrate Dkk1,2 and 4, the colipase fold domain alone is sufficient for their biological activity, which

is the Wnt pathway modulation. Colipases facilitate the interaction of pancreatic lipases with lipid micelles, therefore, it has been suggested that the Cys2 domain may enable Dkk proteins to interact with lipids in order to regulate Wnt signaling (Krupnik et al. 1999).

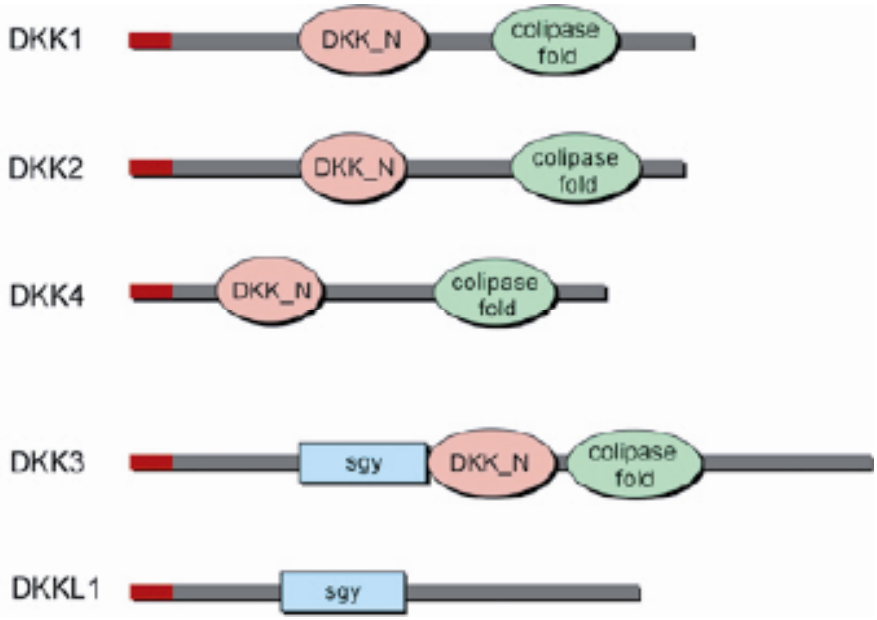

Figure 3-6. Domain structure of the Dkk family. Dkk1–4, as well as DkkL1 (sgy) are shown with their domains corresponding to DKK_N and colipase fold. The sgy-domain is only found in DKK3 and DKKL1 (sgy). Adapted from: Function and biological roles of the Dickkopf family of Wnt modulators, C Niehrs, Oncogene, 2006.

Contrary to the conserved cysteine-rich domains, the linker region is highly variable between Dkk proteins and it is notably larger in Dkk1, 2 and 4 (50-55 amino acids), when compared to Dkk3 (12 amino acids). The mammalian Dkk1 possesses one potential N-glycosylation site located close to the C-terminus of the protein. Chicken and mammalian Dkk3 displays four potential N-glycosylation sites (Krupnik et al. 1999). Additionally, Dkk proteins carry several potential proteolytic cleavage sites for furin-type proteases (Nakayuma, 1997), suggesting that the proteins may be subject to post-translational proteolytic processing.

Dkk3 and Soggy (Sgy), which display high sequence similarity, share an N-terminal signal peptide, due to which it is predicted that they can be secreted. Sequence homology between these two proteins is most pronounced within the N-terminal domain of Dkk3, although significant amino-acid identities are seen beyond this domain that extend into the cysteine-rich domains of Dkk3. The residues shared by Sgy and Dkk3 are poorly conserved in other Dkks, implicating that the two proteins are uniquely related (Krupnik et al. 1999).

3.3.2 Function of the Dkk proteins

As mentioned above the Dkk family members were characterized as regulators of the Wnt signaling pathway. The Wnt pathway has been shown to play an essential role during embryonic development (Micsenyi et al. 2004; Nelson et al. 2004). Moreover, during

adulthood this pathway has been reported to regulate cell proliferation, motility, cell polarity and cell fate (Etheridge et al. 2004). Wnt proteins are secreted molecules that trigger at least two (possibly three) pathways that employ Wnt receptors of the frizzled seven transmembrane class. These are the canonical or Wnt/b-catenin pathway (Cadigan et al. 2006), the planar cell polarity pathway (PCP), which does not involve β-catenin but recruits small GTPases of the rho/ cdc42 family to activate JNK and the Wnt/Ca^{2+} cascade that is still controversial and may be partly overlapping with the PCP pathway (Kohn et al. 2005). Of the various pathways employed by Wnt proteins, Dkk proteins specifically affect the canonical or Wnt/β-catenin cascade. In the canonical Wnt pathway, ligation of the Frizzled and lipoprotein-receptor-related (LRP5/6) proteins lead to the activation of the cytoplasmic protein Dishevelled, which in turn destabilizes the complex formed by APC, Axin and glycogen synthetase kinase 3 (GSK3). Since APC/Axin/GSK3 complex promotes phosphorylation and degradation of β-catenin, the Wnt signaling leads to the stabilization and nuclear translocation of β-catenin, which in turn forms a complex with TCF transcription factors (Figure 7) (Cadigan et al. 2006). Dkk1, 4 and occasionaly Dkk2 have been shown to inhibit Wnt signaling by binding on LRP5/6 and Kremen coreceptors. This leads to the formation of a ternary complex, which is internalized by endocytosis. As a result the Wnt receptors are eliminated from the plasma membrane, thus preventing Wnt-LRP5/6 complex formation (Mao et al. 2002).

All Dkk proteins show distinct and elevated expression patterns in tissues that mediate mesechyme-epithelial transitions, indicating that they may participate in the development of the heart, tooth, hair follicles, limb and bone (Monaghan et al. 1999). In Xenopus embryos Dkk1 is expressed in the Spemann organizer region and is essential for head development (Glinka et al. 1998). In the mouse Dkk1 is essential for head development and is involved in distal limb patterning (Mukhopadhyay et al. 2001), osteoblast and cardiac myocyte proliferation (Kawano et al. 2003).

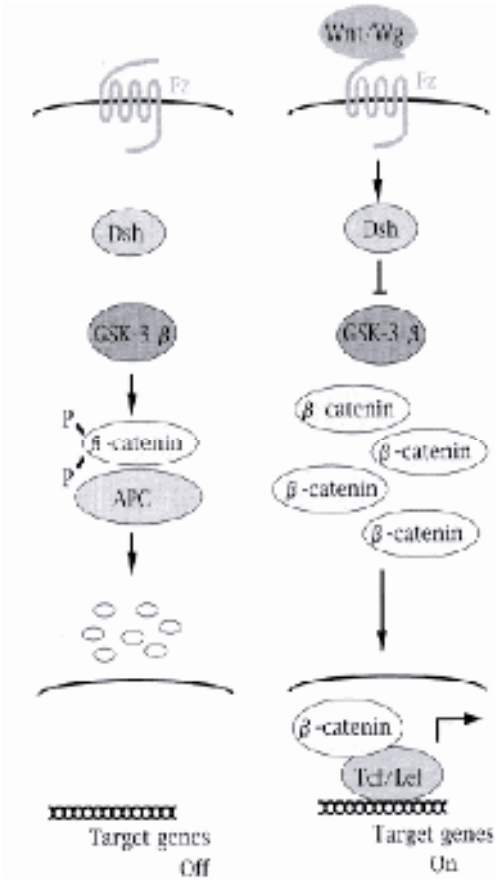

Figure 3-7. The Wnt signalling pathway. Upon activation by the Wnt signal, Dsh inhibits the activity of GSK-3β. In the absence of the Wnt signal, GSK-3β is thought to phosphorylate and consequently induce the degradation of β-catenin. Therefore, the Wnt signal stabilizes and causes the accumulation of β-catenin, which in turn associates with TCF/LEF family transcription factors. Adapted from: Regulation of hematopoiesis and hematopoietic stem cell niche by Wnt signaling pathways, Michael J Nemeth & David M Bodine, Cell Res, 2007.

3.3.3 Dkk3 is a divergent member of the Dickkopf family

By a number of criteria Dkk3 appears to be a divergent member of the Dkk family. First, by DNA sequence similarity, vertebrate Dkk1, 2 and 4 are more related to each other than they are to Dkk3 (Glinka et al. 1998). Additionally, Sgy, the distant member of the Dkk family, shares sequence similarity with Dkk3 but not with other Dkk family members (Krupnik et al. 1999). Two Cnidaria, Hydra and Nematostella, have two Dkk genes only, one related to vertebrate Dkk1, 2 and 4 (Guder et al. 2006) and one related to vertebrate Dkk3 (Fedders et al. 2004). Human Dkk1, 2 and 4 are located within the well-characterized chromosome 4/5/8/10 paralogy group (Dkk1 maps to 10q11, Dkk2 to 4q25 and Dkk4 to 8p11). Genes within this paralogy region were duplicated early in vertebrate evolution (Pollard et al. 2000). In contrast, human Dkk3 maps to 11p15.3, which is not part of the same paralogous chromosome group. Taken together, these observations suggest a deep split into Dkk3 and

Dkk1/2/4 gene families during early metazoan evolution, and more recent gene duplications accompanied by functional divergence of the two Dkk subfamilies (Guder et al. 2006). Strikingly, Dkk3 and sgy do not seem to function in Wnt signaling (Glinka et al. 1998; Krupnik et al. 1999; Mao et al. 2001).

3.3.4 The functions of Dkk3

Like other Dkk members, Dkk3 is expressed during vertebrate development in suggestive patterns in many organs. In adult rodents, a prominent expression of Dkk3 is observed in the brain and in fibroblasts. Dkk3 protein was also found in the the zona glomerulosa of the human adrenal cortex, where it inhibits steroidogenesis (Suwa et al. 2003). Additionally, significant Dkk3 expression at the RNA level has been reported for the spinal cord, eye, lung, heart, colon, ovary, uterus and hair follicle (Niehrs 2006). Moreover a study using human pancreatic tissue revealed Dkk3 mRNA and protein expression in a subpopulation of the human pancreatic beta cells (Hermann et al. 2007).

Dkk3 knockout mice ($Dkk3^{-/-}$) are, however, viable and fertile, possibly due to complementation of the Dkk3 function by the highly homologous Sgy. $Dkk3^{-/-}$ only display increased lung ventilation and hyperactivity. It is worth pointing out that minor changes in the frequency of NK cells, immunoglobulin M, hemoglobin and hematocrite levels have also been reported (Barrantes Idel et al. 2006).

Dkk3 is also known as 'REIC' (Reduced Expression in Immortalized Cells) (Tsuji et al., 2000), since it has been proposed to act as tumor suppressor. Dkk3 has been claimed to be downregulated in a number of tumors, including hepatocellular carcinoma, lymphoblastic leukemia, prostate cancer, renal cell carcinoma, lung carcinoma, melanoma, ovarian cancer and neuroblastoma (Koppen, 2008). Lack of Dkk3 expression in tumor cells has been attributed to hypermethylation of the Dkk3 promoter. For example, the second of the two CpG islands in the promoter region is up to 90% methylated in lung carcinoma (Yue et al. 2008).

Dkk3 overexpression suppresses tumor cell proliferation (Abarzua et al. 2005; Lodygin et al. 2005; Kawano et al. 2006) and induces an apoptotic phenotype (cytoplasm shrinking, membrane blebbing and nucleus condensation). In Dkk3-transduced lung carcinoma cells proliferation is inhibited by activation of caspase-3. NIH3T3 cells infected with adenovirus expressing Dkk3 undergo apoptosis via JNK activation and subsequent mitochondrial translocation of the proapoptotic Bax protein (Abarzua et al. 2007)

Interesingly, Dkk3-transfected RM9 cells exhibit decreased motility due to Dkk3-mediated downregulation of metalloproteinase 2 (MMP2), which degrades type IV collagen (Edamura

et al. 2007). Kuphal *et al.* have also indicated that Dkk3 transfected cells upregulate E-cadherin, which restrains their migratory capacity (Kuphal et al. 2006).

Although hypermethylation of Dkk3 correlates with certain cancers (Kobayashi et al. 2002; Roman-Gomez et al. 2004; Lodygin et al. 2005), the physiological relevance of altered Dkk3 expression in tumors and its potential growth inhibitory effect are unknown. Notably, Dkk3 deficient mice show no enhanced tumorigenesis (Barrantes Idel et al. 2006) and the role of Dkk3 in the regulation of cell proliferation and migration remains to be studied.

3.4 Aim of the study

Protection of tissues from the devastating effects of immune responses is essential for the integrity of the organism. Tolerance mechanisms that are summarized above are controlling potentially auto-reactive lymphocytes. In addition, organs that are particularly sensitive to damage by inflammation, so called immune privileged sites, are protected by tissue barriers and contain an immunosuppressive microenvironment.

There is increasing evidence that processes establishing immune privilege overlap with those associated with tolerance induction. For example, the proapoptotic molecule FasL (Nagata 1997; Lenardo et al. 1999; Askenasy et al. 2005) and the immunosuppressive enzyme IDO (Morelli et al. 2003; Niederkorn 2006; Puccetti et al. 2007) are involved in both the peripheral immune regulation by T cells or dendritic cells and in the maintenance of the immune privileged status of some tissues. However, there is much yet to learn about the molecules with a potential universal role in immune regulation. This knowledge could help in the understanding of systemic diseases, such as autoimmunity and cancer, and introduce novel principles concerning transplantation tolerance.

Aim of this study was the identification of novel molecules that are potential mediators of both peripheral tolerance and immune privilege. Starting from a transgenic mouse model for peripheral CD8 T cell tolerance, identification of such candidate genes was attempted by wide range gene expression analysis. Consequently, Dkk3 was chosen for further characterization. On the one hand, Dkk3 was found to be upregulated in the tolerant CD8 T cells. On the other hand, Dkk3 mRNA was previously shown to be present in peripheral tissues, such as the brain, the eye, the spinal cord, the ovary and the uterus (Niehrs 2006).

The subsequent objective of the study was the functional characterization of Dkk3 in the context of immune regulation. First, the role of Dkk3 in the establishment and maintenance of peripheral CD8 T cell tolerance was investigated. Moreover the potential of Dkk3 to regulate polyclonal T cell responses was examined and its regulatory properties at the cellular and molecular level were defined. The study was completed by the determination of the importance of Dkk3 in the establishment of immune privilege and in the protection from autoimmunity of vital organs, such as the brain.

4 MATERIALS AND METHODS

4.1 Materials

4.1.1 Chemicals

- Acrylamide and TEMED were purchased from ROTH.
- PMA, Ionomycin, Bovine Serum Albumin (BSA) and CFSE were from Sigma.
- Pertussis Toxin was from Calbiochem.
- Incomplete Freud's adjuvant (IFA) and M. Tuberculosis (attenuated) were obtained from Dufco.
- RPMI, Glutamine, Penicillin and Streptavidinwere purchased from Gibco.
- Fetal calf serum (FCS) was from Biochrom AG.
- Propidium Iodide was from BD.
- Protease Inhibitor Cocktail was purchased from Roche.
- Phosphatase inhibitor cocktail was from Calbiochem.
- SuperSignal West Dura Extended Duratio Substrate was purchased from PIERCE.
- Fixation and Permeabilization kit was obtained from BD Biosciences.

FoxP3 staining kit was from eBioscience.

4.1.2 Antibodies

The monoclonal antibodies for FACS are listed on the following table.

Antigen	Conjugate	Company
Annexin V	FITC	BD
CD3e	PE/Cy7	Natutec
CD3e	FITC	BD
CD3e	Biotin	BD
CD3e	PE	BD
CD3e	purif.	Natutec
CD3e	APC	BD
CD3e	PerCP/Cy5.5	BD
CD3e	APC-Cy7	BD
CD4	FITC	BD
CD4	FITC	BD
CD4	PE	BD
CD4	APC	BD
CD4	APC-Cy7	BD
CD4	PerCP-Cy5.5	BD
CD8a	APC	BD
CD8a	FITC	BD

CD8a	PE	BD
CD8a	APC	BD
CD8a	PE-Cy7	BD
CD8a	PerCP-Cy5.5	BD
CD11b	APC	BD
CD11c	PE-Cy7	BD
CD19	PE	BD
CD19	PerCP/Cy5.5	BD
CD19	Biotin	BD
CD19	APC	BD
CD25 (IL2Ra)	PE	BD
CD45 R (B220)	PerCP/Cy5.5	BD
CD45 R (B220)	FITC	BD
CD45 R (B220)	PE	Natutec
CD45.1	FITC	BD
CD45.1	Biotin	BD
CD45.1	PE-Cy7	natutec
CD45.1	PE	BD
CD45.2	FITC	BD
CD45.2	Alexa750-APC	natutec
CD62L	FITC	BD
CD62L	APC	BD
CD69	FITC	BD
CD69	Biotin	BD
CD103	FITC	BD
CD117 (c-kit)	PE-Cy7	Natutec
CD152 (CTLA-4)	Biotin	natutec
CTLA4	Biotin	
DX5	Biotin	BD
Foxp3	PE	natutec
Foxp3	APC	natutec
I-A/I-E	FITC	BD
I-A/I-E	PE	BD
IFN-g	PE	BD
IL-2	PE	BD
IL-17a	AlxFluor647	Natutec
Ly6C	Biotin	BD
Ly6C	FITC	BD
Ly6G+Ly6C (Gr-1)	FITC	BD
Ly-49A&D (sca-1)	APC	natutec
NK-1.1	APC	BD
NK-1.1	PerCP/Cy5.5	BD
NK-1.1	PE-Cy7	BD
TCR Vb11	PE	BD

The primary and secondary antibodies for Western blotting are listed below. Unless otherwise stated, they were purchased from Cell Signaling.

- Smad4 (rabbit)
- phospho-p44/42 MAP Kinase (Thr202/Tyr204)
- p42 MAP Kinase (3A7) mouse mAb
- p44/42 MAP Kinase rabbit antibody
- phospho-MEK1/2 (Ser221) rabbit
- MEK1/2 (rabbit)
- phospho-SAPK/JNK (Thr183/Tyr185) mouse mAb
- SAPK/JNK (rabbit)
- phospho-p38 MAPK (Thr180/Tyr182)(28B10) mouse mAb
- p38α MAP Kinase (L53F8) mouse mAb
- phospho-PKCθ (Thr538) Rabbit
- PKCθ (rabbit)
- phospho-Akt (Thr308)(C31E5) rabbit mAb
- phospho-IκB-α (Ser32/36)(5A5) mouse mAb
- IκB (L35A5) mouse mAb (aminoterminal Antigen)
- antibodies were obtained from Cell Signaling.
- Ras Activation Assay Kit was purchased from Upstate Biotechnology.
- Mouse IgG serum (Sigma and Meridian Bioscience)
- Goat anti-Mouse (Dianova)
- Goat anti-Rabbit (Dianova)

4.1.3 Microarrays

GeneChip Test3 Arrays (Affymetrix)

GeneChip Mouse Genome 430 2.0 Arrays (Affymetrix)

4.1.4 Cell lines

HEK 293T cell line

P815.K^b.B7 cell line

4.1.5 Buffers

4.1.5.1 Molecular Biology Buffers

TE:	100 mM Tris, 10 mM EDTA, pH 8.0
5x Fragmentation Buffer:	20mM Tris Acetate (pH : 8.2), 500mM Potassium Acetate, 150mM Magnesium Acetate
12x MES :	1.22M MES, 0.89M [Na+]
MES hybridization buffer :	Final 1X concentration is 100 mM MES, 1M [Na+], 20 mM EDTA, 0.01% Tween-20
Wash Buffer A :	6X SSPE, 0.01% Tween-20
Wash Buffer B :	100 mM MES, 0.1M [Na+], 0.01% Tween-20
2x Stain Buffer:	200 mM MES, 2M [Na+], 0.1% Tween-20
SAPE Stain solution:	1x Stain Buffer containing 2mg/ml BSA, 10µg/ml SAPE (Streptavidin Phycoerythrin)
Antibody Solution:	1x Stain Buffer containing 3mg/ml BSA, 0.1mg/ml Goat IgG and 3µg/ml biotynilated antibody

4.1.5.2 Protein Biochemistry Buffers

Lysis Buffer:	20mM Tris (pH 7.5), 5mM $MgCl_2$, 1% Novidet P40, protease inhibitor cocktail (Roche), phosphatase inhibitor cocktail (Calbiochem) and I-acetamide
SDS Running Buffer:	25 mM Tris, pH 8.3, 192 mM Glycin, 0.1 % SDS (w/v)
6x SDS sample Buffer:	62.5 mM Tris, pH 6.8, 20 % Glycerin, 2 % SDS (w/v), 714 mM β-Mercaptoethanol, 0.025 % Bromophenol blue (w/v)
Transfer Buffer:	48mM Tris, 39mM Glycine, SDS 1.3mM and 20% methanol. pH between 9-9,4
Stripping buffer:	62.5mM Tris/HCl (pH 6.7), 10mM β-Mercaptoethanol, 2% SDS
Blocking buffer:	PBS containing 0,1% Tween20 and 5% Skim Milk powder

4.1.5.3 Other Buffers

Phosphoate Buffered Saline (PBS):	130 mM NaCl, 2.6 mM KCl, 15 mM KH2PO4, 4 mM Na2HPO4
Dubelcco's PBS (dPBS):	PBS supplied with $MgCl_2$ and $CaCl_2$ was purchased by Invitrogen
dPBS-10:	dPBS containing 10% FCS
FACS Buffer:	
dPBS containing 0,5% FCS and 0.05% NaN_3	
Staining Buffer:	dPBS containing 1%FCS
Incubation Buffer:	PBS containing 0.5% (w/v) bovine serum albumin
MACS Buffer:	PBS pH 7.2 containing 2mM EDTA and 0.5% (v/v) FCS

4.1.6 Cell culture Media

T cell medium:	RPMI 1640 supplemented with 10% (v/v) heat-inactivated FCS, 10 mM Hepes, 2 mM L-glutamine, 0.05 mM 2-mercaptoethanol, 100 units/ml penicillin, and 100 mg/ml streptomycin
BMDC medium:	RPMI 1640 containing 10% (v/v) F1/16 cell supernatant containinig GM-CSF; 10% (v/v) heat-inactivated FCS, 10 mM Hepes, 2 mM L-glutamine, 0.05 mM 2-mercaptoethanol, 100 units/ml penicillin, and 100 mg/ml streptomycin
DMEM-full medium:	DMEM containing 10% heat-inactivated FCS, 10 mM Hepes, 2 mM L-glutamine, 1 mM sodium pyruvate, 0.05 mM 2-mercaptoethanol, 100 units/ml penicillin, and 100 mg/ml streptomycin
Cell-freezing medium:	heat inactivated FCS supplemented with 10%(v/v) DMSO:

4.2 Methods

4.2.1 Transfected Cell Lines

The murine mastocytoma cell line P815 (H-2K^d) transfected with the genes encoding for the murine MHC class I molecule H-2K^b and the B7-1 gene plus the neomycin resistance gene has been described (Alferink et al. 1995). Cells were cultured in full DMEM. For s.c. injection the cells were trypsinized (2 ml of 0.25% trypsin plus 2.5 mM EDTA for 5 min at room temperature) and washed twice with Dulbecco's PBS.

4.2.2 Mice

The Des-TCR mice (H-2K^k) carry a transgene for the K^b-specific TCR. The Des-TCRx2.4KerIV-K^b mice (H-2K^k or H-2K^d) additionally express the K^b molecule controlled by the 2.4KeratinIV-promoter (Alferink et al. 1995). The Des-TCR and Des-TCRx2.4KerIV-K^b transgenic mice were crossed to a recombination-activating gene 2-deficient (Rag2$^{-/-}$) background (H-2K^k). The Dickkopf-3 deficient (Dkk3$^{-/-}$) mice were kindly provided by professor C. Niehrs (Barrantes Idel et al. 2006). They were backcrossed to C57BL/6N mice at least 15 times. For the experiments Dkk3$^{+/+}$ littermates from Dkk3$^{+/-}$x Dkk3$^{+/-}$ breedings were used, unless stated otherwise. Dkk3$^{-/-}$ mice were crossed to Des-TCR mice (H-2K^k) and Der-TCRx2.4KerIV-K^b mice (H-2K^k or H-2K^d) and only the H-2K^k littermates were used for experiments. The C57BL/6 2D2-TCR (MOG_{35-55} specific TCR) strain is transgenic for the mouse T-cell receptor alpha and beta chain (TCRα and TCRβ) transgenes(Bettelli et al. 2003). The genotyping of the transgenic mice was performed by PCR or Flow Cytometry, as indicated in table 1. C57BL/6 mice were obtained from Charles River Breeding Laboratories (Sulzfeld, Germany). The experimental mice used were between six and twelve weeks of age. All mice were bred and maintained under specific pathogen-free conditions (SPF) at the animal facility of the German Cancer Research Center.

Mixed bone marrow chimeras were generated by irradiation of the recipient mice with 950cGray of γ-irradiation via a cesim isotope (^{127}Cs) source and subsequent intravenous transfer of 2-5x10^6 donor bone marrow cells 24 hours later. The chimeric mice were allowed to fully reconstitute the peripheral lymphoid tissue for eight weeks before use.

Transgene	Genotyping method	Reagents
Des-TCR	Flow Cytometry	anti-clonotypic mAb (Desire-1) binding to the H-2Kb-specific alloreactive cytolytic (CTL) clone KB5-C20 (Hua et al. 1986)
2.4KerIV-K^b	Southern Blot	
2D2-TCR	Flow Cytometry	anti-Vβ11 and anti-CD4 Abs
Dkk3 knockout	Triplex PCR	p1 (5'-GATAGCTTTCCGGGACACAC-3'), p2 (5'-TCCATCAGCTCCTCCACCTCT-3'), p3 (5'-TAAGTTGGGTAACGCCAGGGT-3') (Barrantes Idel et al. 2006)
Rag2 knockout	FACS	anti-CD45.R (B220) Ab, binding on B cells

Table 4-1. Mouse Genotyping

4.2.3 T cell and dendritic cell purification ex vivo

4.2.3.1 T cell isolation

T cells were isolated from the spleen or the subcutaneous (axilliary and inguinal) lymph nodes. A single cell suspension was made by cutting the spleen in two pieces with a scalpel and passing the cells through a sieve. Lymph nodes were smashed with frosted-end slides. Cells were washed with ice-cold dPBS and centrifuged at 4^{o}C at 1200rpm for 7min. Cell pellets were resuspended with dPBS. Lymphocyte numbers were determined by direct counting under the microscope using a Neubauer chamber, after suspending a cell aliquot in trypan blue (25% in dPBS (v/v)).

4.2.3.2 CD4 or CD8 T cell purification

Single-cell suspensions of T cells were washed with ice-cold dPBS and centrifuged at 4^{o}C at 1200rpm for 7min. For MACS positive selection cell pellets were resuspended with 90ul/10^7cells MACS buffer containing 10% (v/v) purified CD4 or CD8-specific microbeads (Miltenyi Biotec, Bergisch Gladbach, Germany). After 20min incubation at 4^{o}C cells were washed with ice-cold MACS buffer and centrifuged. Cell pellets were resuspended with 1ml MACS buffer and run over Miltenyi LS columns. Columns were washed 4 times with 3ml MACS buffer to eliminate non-specifically bound cells. CD4- or CD8-T cells were eluted from the column with 5ml MACS buffer and purity was checked with flow cytometry. For the microarray experiments, MACS isolated CD8 T cells were stained with Des-TCR- and CD8-specific antibodies and the Propidium Iodide negative cells were sorted on a FACSVantage (BD Biosciences).

For CD8 T cell purification with MACS CD8 isolation kit cell pellets were first incubated with the biotin-antibody cocktail at 4°C for 15min and additionally with the anti-biotin MACS beads for 10min prior to column purification. CD8 T cells were collected with the flow-through.

4.2.3.3 CNS-infiltrating T cell isolation

At day 20 or 29 after EAE induction, $Dkk3^{-/-}$ and $Dkk3^{+/+}$ mice were lethally anesthetized with injection of 0.7 ml of a ketanest (5mg/ml)/ rompun (0.2%) mix i.p.. Followingly, they were perfused with 20ml ice cold Hank's balanced salt solution (HBSS) each. Brain and spinal cord were removed and cell suspension was performed after 25min digestion at 37°C with 2.5mg/ml collagenase D and 1mg/ml deoxyribonuclease I (Sigma-Aldrich) in dPBS. T cells were isolated using Percoll gradient. For cytokine staining T cells were stimulated overnight with 5ug/ml anti-CD3 in full RPMI medium at 37°C. Six hours prior to flow cytometry stimulated T cells were given Protein Transport Inhibitor (BD GolgiPlug™) in a 1:1000 dilution.

4.2.3.4 Conventional dendritic cell isolation

Single spleen and lymph node cell suspension was made as described above. After washing cell pellets were resuspended with dPBS containing DNAse I and collagenase D. Digestion was performed at room temperature for 40min while stirring with a mini magnet. Cells were washed with dPBS containing 2mM EDTA to avoid the reassociation of dendritic cells with T cells. Where indicated, dendritic cells were further purified using the CD11c MACS beads. The protocol for MACS positive selection is described in paragraph 2.3.2.

4.2.3.5 Expansion of bone marrow derived dendritic cell (BMDC)

Bone marrow was extracted from the femur and tibiae bones with ice-cold dPBS. Cell suspension was made by gently pipetting. Cells were washed and resuspended with BMDC medium. $2x10^6$ cells were plated pro each 100mm Petri dish to a final volume of 10ml BMDC medium. At day 3 10ml of BMDC medium was added pro dish. At day 6 half of the medium was collected, centrifuged at 1200rpm and room temperature for 7 min. The cell pellet was resuspunded with fresh medium and replated. At day 10 the non-adherent cells (mostly dendritic cells) were collected by gently washing the bottom of the dishes. The resulting population was more than 75% CD11c positive, as confirmed by flow cytometry.

4.2.3.6 BMDC activation with CpG 1668

Ten days after BMDC expansion DCs were harvested, washed and resuspended with BMDC medium at $8x10^6$cells/ml in 15ml TPP tubes. DCs were then incubated with 0.5uM CpG 1668 for 1 hour at 37^{o}C with periodical mixing. Next they were washed with dPBS containing 2mM EDTA to avoid formation of cell clumps and cell pellets were frozen in BMDC medium plus 10%DMSO.

4.2.4 Flow Cytometry

4.2.4.1 Staining of surface antigens for Flow Cytometry

5-$10x10^6$ cells were suspended in 50ul FACS buffer containing fluorochrome-conjugated antibodies in a concentration of 2ug/ml each. Cells were incubated with the antibody mixture for 20min at 4^{o}C and then washed with FACS buffer. The antibodies that have been used for FACS are shown in table 2. Cell pellets were resuspended with 0.1ml FACS buffer. FACS buffer was always ice-cold. Flow cytometry was performed on a FACSCalibur with the CellQuest software or on a FACS Canto with the Diva software (BD Biosciences, San Diego, CA). The FACS data was analysed with the FlowJo software.

4.2.4.2 Staining of intracellular antigens for Flow Cytometry

Cells were stained for their surface markers, and then permeabilized using the cytofix/cytoperm kit (PharMingen). Briefly cells were gently resuspended in the cytofix/cytoperm solution for 20 min at 4^{o}C, washed with the cytoperm/wash buffer and stained with fluorochrome-conjugated antibodies for intracellular antigens diluted 1:50 in 0.1ml cytoperm/wash buffer for 30min at 4^{o}C. Cells were then washed with the cytoperm/wash buffer and resuspended in staining buffer.

To detect Foxp3 protein expression, cells stained with anti-CD4 and anti-CD25 Abs were fixed using Fix/Perm Buffer (eBioscience) for 30min at 4^{o}C, then incubated with APC-conjugated anti-mouse Foxp3 Ab (FJK-16; eBioscience) for 30 min at 4°C.

To detect phospho-ERK intracellularly, cells stained for surface markers were fixed with 1% formaldehyde for 10min at 37^{o}C and permeabilized with 90% ice-cold methanol for 30min at 4^{o}C. After washing with incubation buffer cells were stained with 10% anti-phospho-ERK-APC Ab in staining buffer for 30min at 4^{o}C.

4.2.5 Molecular Biology

4.2.5.1 RNA Isolation

0.3-0.5x10^6 Des-TCR CD8 T cells (purity >99%) were used for RNA isolation. Cell lysis and RNA isolation were performed with QIAshredder and Qiagen RNeasy Mini Kit. Up to ~260ng RNA was isolated from 0,5 x 10^6 CD8 T cells. RNA was precipitated with 3M NH_4OAc and pellet paint (dye which binds to RNA pellet, Novagen). RNA concentration was determined with Quant-iT RiboGreen RNA Assay kit (Invitrogen) – based on fluorescent dye that binds exclusively on RNA. RNA quality was controlled using Agilent RNA Nano Chips.

4.2.5.2 mRNA amplification

The mRNA contained in the isolated total RNA was isolated and amplified with two rounds of reverse transcription. Therefore the MessageAmp^{TM} mRNA amplification kit (Ambion) was used according to manufacturer's instructions. Briefly, the MessageAmp™ aRNA Amplification procedure is based on the RNA amplification protocol developed in the laboratory of Dr. James Eberwine (Van Gelder et al. 1990). The procedure consists of reverse transcription with an oligo(dT) primer bearing a T7 promoter and in vitro transcription of the resulting DNA with T7 RNA Polymerase to generate hundreds to thousands of antisense RNA copies of each mRNA in a sample. The antisense RNA is referred to as aRNA and the amplification method is referred to as the aRNA amplification procedure. Two rounds of amplification were performed. The starting amount of total RNA was 100-200ng in the first round and 2ug in the second round, so that a final amount of 20µg aRNA was obtained.

4.2.5.3 Determination of the RNA concentration by use of the RiboGreen kit

The RiboGreen® RNA quantification kit was used according to manufacturer's protocol for the low range assays. Briefly, the RiboGreen reagent was 2000-fold diluted with 1x TE buffer. Ribosomal RNA standard dilutions ranging from 1ng/ml to 50ng/ml were prepared. The isolated or amplified RNA was diluted 1:50 and the RiboGreen-TE solution was added in a 1:1 ratio to all samples. Upon 5min incubation in RT in the dark, the fluorescence of the samples at 525nm was determined in a fluorescence microplate reader. Blank values were extracted and RNA concentration was calculated based on the standard curve. All samples were always measured in duplicates.

4.2.5.4 aRNA hybridization, microarray scanning and analysis of the microarray results

The hybridization cocktail was prepared at room temperature and consisted of 50pM control oligonucleotide B2, 1x eukaryotic hybridization controls (affymetrix), 0.1mg/ml herring sperm DNA, 0.5mg/ml acetylated BSA, 1xMES hybridization buffer and 0.5mg/ml fragmented aRNA in total volume of 0.1ml. The cocktail was heated up in 99^{o}C for 5min and then incubated at 45^{o}C for 5min. After 5min centrifugation at 13000 rpm the supernatant was transferred to a fresh tube. The GeneChip was preincubated with 80ul 1xMES hybridization buffer for 10min at 45^{o}C while rotating with 60rpm. The buffer was then removed from the chip and the hybridization cocktail was added. The chip was left to hybridize at 45^{o}C, 60rpm for 16 hours. Prior to processing the mouse GeneChip 430 platforms, the hybridization cocktail was tested in test3 Chips for the aRNA integrity. After hybridization the cocktail was removed and the chip was washed with the non strigend Wash-Buffer A and the strigend Wash Buffer B and stained with the SAPE Stain Solution and Antibody Solution according to the following protocol.

Step	Procedure
Post Hyb Wash 1	10 cycles of 2mixes/cycle with Wash Buffer A at 25^{o}C
Post Hyb Wash 2	8 cycles of 15mixes/cycle with Wash Buffer B at 50^{o}C
Staining	Staining of the probe array in SAPE solution at 25^{o}C for 10min
Post Staining Wash	10 cycles of 4mixes/cycle with Wash Buffer A at 25^{o}C
Second Staining	Staining of the probe array in antibody solution at 25^{o}C for 10min
Third Staining	Staining of the probe array in SAPE solution at 25^{o}C for 10min
Final Wash	15 cycles of 4mixes/cycle with Wash Buffer A at 25^{o}C

4.2.5.5 Real time quantitative PCR

Isolated RNA was reverse transcribed into cDNA using Oligo(dT)12-18 primers () and Superscript II Reverse Transcriptase (Invitrogen). RT-PCR was performed in a Gene Amp

5700 Sequence Detection System (Applied Biosystems, Darmstadt, Germany). Relative mRNA frequencies were calculated and the experimental samples were normalized to the respective calibrator.

4.2.5.6 Triplex PCR for Dkk3$^{-/-}$ mouse genotyping

Mouse tails were digested for 2-3 hours at 56^{o}C in 20ul ProteinaseK Buffer (50mM Tris pH 8.0, 20mM NaCl, 1mM EDTA, 1% SDS and 2mg/ml Proteinase K (). Following digestion the tail-DNA was diluted 1:150 and 3ul were used for PCR with the primers p1 and p2 for the detection of the wild type gene and primers p1 and p3 for the detection of the knocked out gene (see table 1). PCR-Mix consisted of 10% (v/v) 10xPCR-Mix (Boehringer), 0.2mM dNTPs (Boehringer), 0.08U/ul Taq polymerase (Bioron) and 0.4pmol/ul each primer.
PCR reaction was conducted in total volume 50ul.

4.2.6 Protein Biochemistry

4.2.6.1 Dkk3 protein purification

Dkk3 protein was expressed in the eukaryotic HEK293T cells. Dkk3 expression was confirmed by flow cytometric and Western Blot analysis. The cell supernatant, which containted the secreted Dkk3 protein, was collected and protein purification was performed. Therefore, sepharose columns loaded with the monoclonal anti-Dkk3 antibobody were used. After washing with 1x PBS buffer, the HEK293T-Dkk3 supernatant was given through the anti-Dkk3 columns. Followingly the columns were washed with 1x PBS and the Dkk3 protein was eluted with elution buffer (0.1M glycine, 0.1M NaCl, pH: 3.2). Finaly, the protein was dialysed with 1xPBS and protein concentration was measured by photometry, in 280nm. The purity of the final protein solution was confirmed by Western Blot analysis.

4.2.6.2 Western Blotting

After stimulation the cell pellets were lysed with ice-cold lysis buffer for 20min on ice (30ul/10^{6} cells). Protein lysates were diluted with 6x SDS sample buffer, applied to 15% acrylamide SDS-PAGE gels, separated at 180 Volt and transferred to PVDF membranes (Millipore). The membranes had previously been incubated with methanol for 30sec, destilled water for 2 min and transfer buffer for 15min. For the transfer was used. After being blocked 4 hours with blocking buffer, the membranes were incubated with primary Ab (table 3) overnight at 4^{o}C. The protein band of interest were detected with secondary peroxidase-conjugated Ab-incubation for 1 hour at room temperature and imaged after 1min incubation with SuperSignal® WestDura Extended Duration Substrate (Pierce) in Lumi-imager (Roche

Boehriger Diagnostics). Membrane reprobing with different primary Ab was performed after membrane stripping at 50^{o}C with stripping buffer for 1 hour.

4.2.7 *In vitro* assessment of the T cell function

4.2.7.1 In vitro T cell stimulation for cell signalling studies

CD4 or CD8 T cells were purified from spleens and lymph nodes of 6-8-week-old mice, using MACS CD4 and CD8 beads or MACS CD8 isolation kit as described above. Flow cytometric analysis confirmed that the purity of the separated cells was consistently above 80%. CD4 or CD8 T cells were stimulated with PMA (250nM) for 15 min at 37^{o}C. Alternatively, purified T cells were incubated with 10ug/ml biotinylated anti-CD3ε (Clone 500A2, BD Bioscience) for 15min on ice, washed with dPBS-10 and cross-linked with prewarmed 20ug/ml streptavidin at 37^{o}C for the indicated time. Des-TCR CD8 T cells were stimulated in 24-well plates coated with 2ug/ml anti-clonotypic Désiré Ab at 37^{o}C for the indicated time. Following T cell activation T cells were washed with dPBS-10 and cell pellets were snap frozen with liquid nitrogen.

4.2.7.2 *In vitro* T cell proliferation assay

T cells were purified from spleens of 6-8-week-old mice. 200µl (1x10^{6}cells ml^{-1}) were cultured in 96.well (U-bottom) plate at 37^{o}C for 72 h. The plate was precoated with various concentrations of monoclonal mouse CD3ε and CD28 antibodies. ^{3}H (1µCi well^{-1}) was added at 72 h after stimulation and its incorporation was measured 24 hours later. For the CFSE proliferation assay cells were stained before stimulation with CFSE (20µM) for 15 min at 37^{o}C. At various time points cells were stained with color conjugated anti- mouse CD3, CD4 and CD8 antibodies and PI and analyzed in FACS.

4.2.7.3 IL-2 production assay (ELISA)

For IL-2 ELISA T cells were purified from spleens of 6-8-week-old mice. 200µl (1x10^{6}cells ml^{-1}) were cultured in 96.well (U-bottom) plate at 37^{o}C for 72 h. The plate was precoated with various concentrations of monoclonal mouse CD3ε and CD28 antibodies. Supernatants were collected 24 hours after stimulation with various concentrations of soluble monoclonal mouse CD3ε and CD28 antibodies and IL-2 in the culture media was determined using antibodies from. The results were obtained from triplicate samples.

4.2.8 *In vivo* experiments

4.2.8.1 Thymectomy

Up to 15-day-old mice were anesthetized with a mixture of ketamine (Fort Dodge Laboratories, Fort Dodge, IA) and xylazine (Abbott Laboratories, North Chicago, IL). A small incision of the upper thoracic region exposed the thymic lobes. The thymus was removed by the application of suction, and the wound was closed thereafter. Mice were kept under a heat lamp and observed after the procedure until they had regained consciousness. The complete extraction of both thymic lobes was controlled after the adult mice were sacrificed.

4.2.8.2 Tolerance Readout in Des-TCR x „2.4IVKerKb

Tolerance was assessed by injecting the mice with K^b and B7-positive P815 tumor cells (Alferink et al. 1995). P815.K^b.B7 tumors are rejected by single-transgenic Des-TCR mice and accepted by tolerant double-transgenic Des-TCRx2.4KerIV-K^b mice.

4.2.8.3 In vivo kill assay

Recipient mice were transferred with 2 x 10^6 BMDCs; activated with 0.5µM CpG-ODN 1668 i.v. Seven days after the first immunization, the specific *in vivo* kill was quantified as previously described (Reibke et al. 2006). Briefly, CBK spleen target cells (H-2^b) from naïve donor mice were loaded with a high CFSE concentration (1.5uM). CBA naïve splenocytes (H-2^k) labeled with a low CFSE concentration were used as nonspecific target cells. The two target cell populations were mixed in equal ratios, and 20 x 10^6 cells in total were transferred i.v. into effector mice. Four hours later the specific cytotoxic T lymphocyte activity was quantified in spleens of effector mice. The ratio between $CFSE^{hi}$ and $CFSE^{lo}$ cells recovered in nonimmunized Des-TCR mice indicated 0% specific kill activity.

4.2.8.4 Experimental Autoimmune Encephalitis (EAE)

Myelin oligodendrocyte glycoprotein (MOG) peptide 35–55 (sequence MEVGWYRSPFSRVVHLYRNGK) was synthesized in the Genomics and Proteomics core facility of the German Cancer Research center (Im Neuenheimer Feld 580, 69120 Heidelberg, Germany), and was ≥90% pure as assessed by HPLC and mass spectrometry. EAE was induced in 8- to 12-week-old mice. Briefly, $Dkk3^{-/-}$ and $Dkk3^{+/+}$ mice received in the flank a subcutaneous injection of 0.1 ml emulsion containing 200 µg MOG peptide in incomplete Freund's adjuvant, supplemented with 200 µg of heat-killed *Mycobacterium tuberculosis*.

Pertussis toxin (200 ng in 0.5 ml of dPBS) was injected intra-peritoneally (i.p.) after MOG immunization and 48 h later. The mice were observed for clinical signs and EAE scored on a scale of 0–5 with gradations of 0.5 for intermediate scores as follows: 0, no overt signs of disease; 1, limp tail or hind limb weakness (but not both); 2, limp tail and hind limb weakness; 3, partial hind limb paralysis; 4, complete hind limb paralysis and 5, moribund state or death by EAE. The average day of disease onset was calculated by averaging the first day of clinical signs for each mouse in one group. The average maximum disease score was determined by averaging the highest score achieved by each individual mouse.

5 RESULTS

5.1 Gene expression profile of regulatory Des-TCR CD8 T cells

CD8 T cell tolerance induction by parenchymal cells in the periphery contributes to the protection of the host tissues from autoaggressive T cells. The DesTCRxKerK^b transgenic mouse model used to study keratinocyte-induced CD8 T cell tolerance has already been thoroughly described (chapter 1.3.5.2). As mentioned before, the neonatally induced regulatory Des-TCR CD8 T cells are long-lived and control rejection of K^b-expressing skin or tumor grafts in adult mice. Thus, it was firstly investigated whether they express a specific tolerogenic genetic program, by the use of Affymetrix GeneChip microarrays.

GeneChip microarrays consist of small DNA fragments (probes), chemically synthesized at specific locations on a coated quartz surface. Each gene is represented by eleven 25mer probe pairs (11 perfect match & 11 mismatch probes, which serve as controls). The precise location where each probe is synthesized is called a feature, and millions of features are contained on one array. By hybridizing biotin-labeled amplified mRNA (aRNA) to the array, the amount of label can be monitored at each feature. The labeled aRNA is obtained upon *in vitro* reverse transcription of the isolated mRNA in the presence of UTP that is conjugated to biotin.

In this chapter the gene expression analysis of the tolerant CD8 T cell will be described. This involves the isolation of total RNA from naïve, activated and tolerant CD8 T cell samples, the amplification and labeling of mRNA prior to hybridization with the microarrays and the identification of differentially expressed genes by the use of Bioconductor and GCOS softwares.

5.1.1 Isolation of naïve, activated and tolerant CD8 T cells for gene expression analysis

In order to characterize their gene expression pattern naïve, activated and tolerant CD8 T cells were purified. The naïve CD8 T cells were derived from the spleen of thymectomised unimmunized Des-TCRxRAG2$^{-/-}$ mice. The activated CD8 T cells were obtained from K^b-reactive thymectomised Des-TCRxRAG2$^{-/-}$ mice, that had been subcutaneously injected with $2x10^5$ P815K^{b}B7 tumor cells and rejected the tumor. The tolerant CD8 T cells were isolated from P815K^{b}B7-immunized thymectomized Des-TCRxKerK^{b}xRAG2$^{-/-}$ mice that displayed tumor growth (Table 1). All mice were thymectomized at 2 weeks of age in order to enrich the long lived neonatally induced tolerant CD8 T cells. The RAG2$^{-/-}$ background assured isolation of K^b-specific CD8 T cells only. In Table 1 summarized statistics of tumor growth in reactive Des-TCR and tolerant Des-TCRxKerK^b mice are shown.

Experimental Model	Observation	ISOLATED CD8 T cells
Des-TCR mice	No tumor	Naïve CD8 T cells
Des-TCR mice injected s.c. with 2x10^5 P815 K^b B7 tumor cells	Tumor rejection (in 15/16 mice)	Activated CD8 T cells
Des-TCRxKer K^b injected s.c. with 2x10^5 P815 K^b B7 tumor cells	Tumor growth (in 12/15 mice)	Tolerant CD8 T cells

Table 5-1. Experimental model for the isolation of different CD8 T cell populations. The experimental protocol for the isolation of naïve, activated and tolerant Des-TCR CD8 T cells is presented. The summed statistics from the three experiments for the isolation of CD8 T cells for the microarray analysis are shown.

The isolation of CD8 T cells was performed 15 days after tumor injection with MACS purification, followed by CD8 T cell FACS sorting. First CD8 T cells underwent positive MACS selection by use of the anti-mouse CD8 magnetic microbeads. Then CD8 T cells were stained with fluorochrome-conjugated anti-CD8 antibody and sorted by flow cytometry. The dead cells were excluded by propidium iodide (PI) staining. The anti-clonotypic antibody for the Des-TCR was not used for the FACS sorting, since it has been shown that crosslinking of the TCR leads to CD8 T cell activation. With the above described procedure, the isolation of a more than 95% pure CD8 T cell population was achieved (Figure 1). As shown in Figure 1, the number of Des-TCR CD8 T cells in the thymectomised Des-TCRxRAG2$^{-/-}$ mice was very limited due to the thymectomy and the RAG2$^{-/-}$ background. In average, pooled spleens of four to five mice yielded 400.000 CD8 T cells upon MACS and FACS sorting.

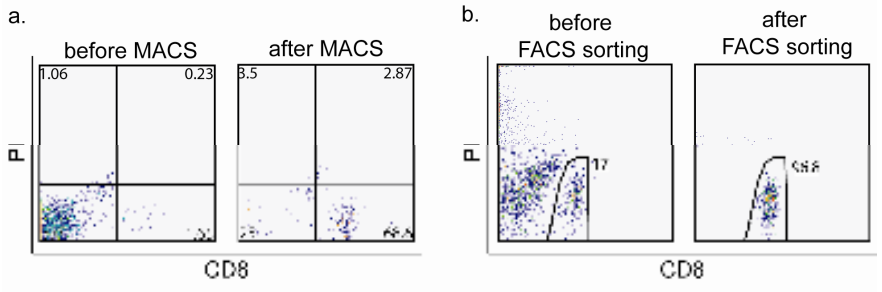

Figure 5-1 Isolation of a highly pure naïve Des-TCR CD8 T cell population. (a) Spleen cells were isolated and the percentage of CD8-positive T cells was estimated by flow cytometry before and after MACS CD8 T cell sorting. **(b)** Upon MACS purification, CD8-positive and PI-negative T cells were sorted by FACS and the final sample contained more than 95% CD8 T cells. The plots shown are representative for the activated and tolerant Des-TCR CD8 T cell samples as well.

5.1.2 Total-RNA isolation and mRNA amplification for the microarray analysis

Microarray analysis was performed with triplicate RNA samples derived from each CD8 T cell population. Every set of replicates was generated at the same time and comparable amounts of total RNA were used as templates for the mRNA amplification (Table 2). The

exact procedure of mRNA isolation and amplification is described in the material and methods chapter (paragraphs 2.5.1 and 2.5.2).

sample	sorted cell number	isolated RNA concentration_amount used for amplification	rna yield (1st round of amplification)	rna yield (2nd round of amplification)
Naive 1	$7x10^5$	29 ng/µl_176 ng	45 ng/µl	8 hrs_1.9 µg/µl
Naive 2	$9 x10^5$	18.8 ng/µl_112 ng	83.9 ng/µl	5 hrs_1.29 µg/µl
Naive 3	$4 x10^5$	60.6 ng/µl_121 ng	41.75 ng/µl	5 hrs_0.46 µg/µl
Activated 1	$4 x10^5$	30 ng/µl_100 ng	39.2 ng/µl	8 hrs_1.8 µg/µl
Activated 2	$5 x10^5$	43.5 ng/µl_100 ng	40.76 ng/µl	5 hrs_0.41 µg/µl
Activated 3	$4 x10^5$	39.7 ng/µl_198.6 ng	30.2 ng/µl	5 hrs_87.3 ng/µl
Tolerant 1	$4 x10^5$	19.6 ng/µl_160 ng	50 ng/µl	8 hrs 1.5 µg/µl
Tolerant 2	$5 x10^5$	29.7 ng/µl_105 mg	71.1 ng/µl	5 hrs_2.13 µg/µl
Tolerant 3	$4 x10^5$	73.2 ng/µl_198 ng	37.54ng/µl	5 hrs_2.15 µg/µl

Table 5-2. Summary of the total RNA isolation and mRNA amplification data.

Every total-RNA sample was isolated from pooled CD8 T cells of four to six mice. By doing this, enough RNA quantity for mRNA amplification procedure was obtained and the impact of biological variability on the gene expression analysis was minimized. The RNA concentration was defined with the RiboGreen kit for precise results, since it permits quantification of as little as 1ng/ml of RNA (Table 2). The quality of the isolated total RNA was checked using the Agilent RNA 6000 nano chip kit in the Agilent 2100 Bioanalyzer. The 28S:18S rRNA ratio has traditionally been viewed as the primary indicator of RNA quality, with a ratio of 2.0 considered to be indicative of high quality, intact RNA. However, with the widespread use of the Agilent 2100 bioanalyzer, it has become clear that the standard of a 2.0 rRNA ratio is difficult to meet, especially if the RNA is derived from *ex vivo* isolated samples (Schroeder et al. 2006). Therefore, the 28S:18S rRNA ratio, two highly structured and long-lived molecules, is not used as the sole measure of the quality of the underlying mRNA. According to manufacturer's recommendation total RNAs with 28S:18S rRNA ratios of 1.0 or greater were used as a starting material for mRNA amplification. Additionally, the RNA samples that displayed a high baseline between the 28S and 18S rRNA peaks were discarded, since the presence high amounts of middle-sized RNA peaks in the RNA plot is indicative or RNA degradation (figure 2).

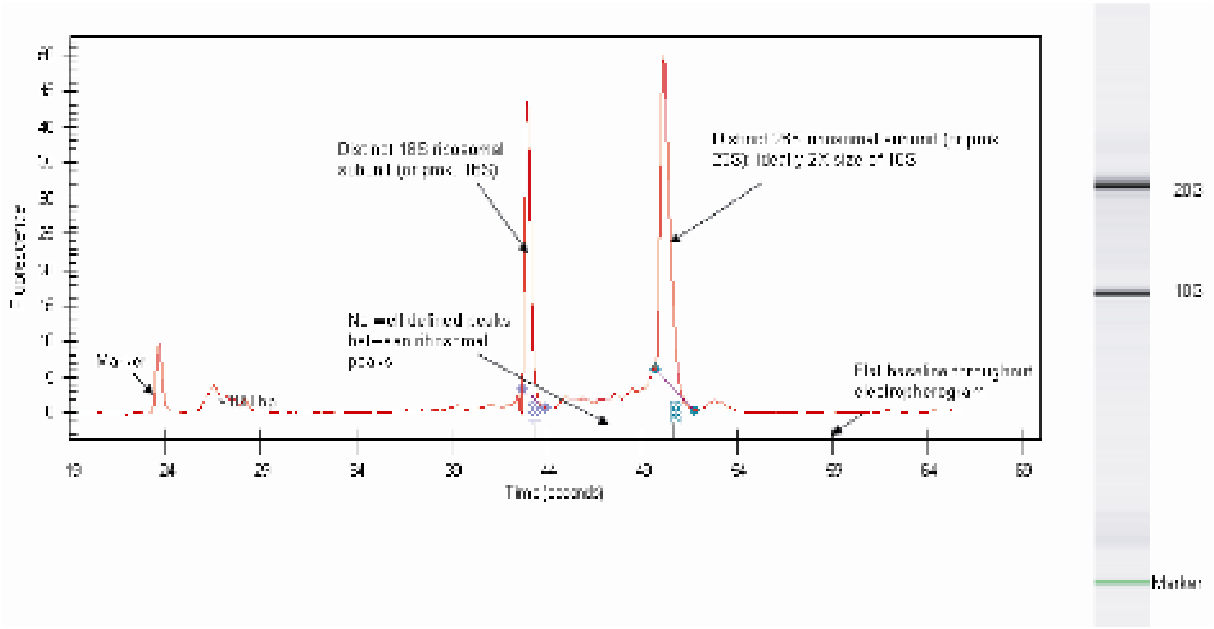

Figure 5-2. Quality control of the isolated total-RNA in Agilent Bioanalyzer 2100. A plot and the respective gel, which are representative of the nine RNA samples that were used as templates of mRNA amplification are shown.

The mRNA amplification protocol was established by optimizing a range of different parameters. This was done with control total-RNA, derived from MACS isolated CD8 T cells from C57.Bl/6 mice. The starting amount of total RNA was fixed at 150ng, due to the low RNA yield from the Rag2$^{-/-}$ derived Des-TCR CD8 T cells (see Table 2). The parameters that were changed to conclude for the final protocol were the number and the duration of the *in vitro* transcription cycles, as well as the amount of the amplified RNA (aRNA) template for the second round of amplification and biotin labeling. Two rounds of amplification were necessary to obtain the required amount of labeled aRNA. The best aRNA integrity and labeling resulted from the second *in vitro* transcription rounds that were of the shortest duration. The final protocol of the mRNA amplification is depicted in figure 3.

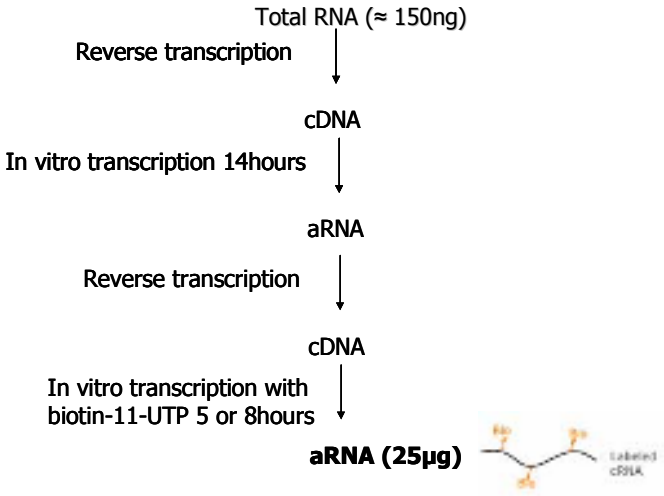

Figure 5-3. Summary of the mRNA amplification protocol.

The first series of samples were initially amplified by a round of 14 hours *in vitro* transcription. Then 1µg of aRNA was used as a template for a second round of 8 hours *in vitro* transcription. To optimize the labeling quality the next two sets of samples were generated with a first *in vitro* transcription round of 14 hours, followed by a second *in vitro* transcription round which lasted 5 hours. Since the duration of the second amplification round was shorter, the aRNA yield was maintained in the same level by increasing the amount of the template RNA to 2 µg.

Upon the first and the second amplification round, the mRNA integrity was assessed with the Agilent 2100 Bioanalyzer and in an agarose gel (Figure 4). Successfully amplified aRNA appears as a smear from 250 to 5000 nt. The average size of the aRNA is approximately 1500 nt. The aRNA quantity was calculated using the RiboGreen kit and verified by measurement of the optical density (OD) at a wavelength of 260nm. An absorbance value at 260nm (A260) of 1 is equivalent to 40µg/ml of RNA. Accordingly, the aRNA concentration (µg/ml) was calculated from the sample with the formula A260 x dilution factor x 40 µg/ml (Table 2).

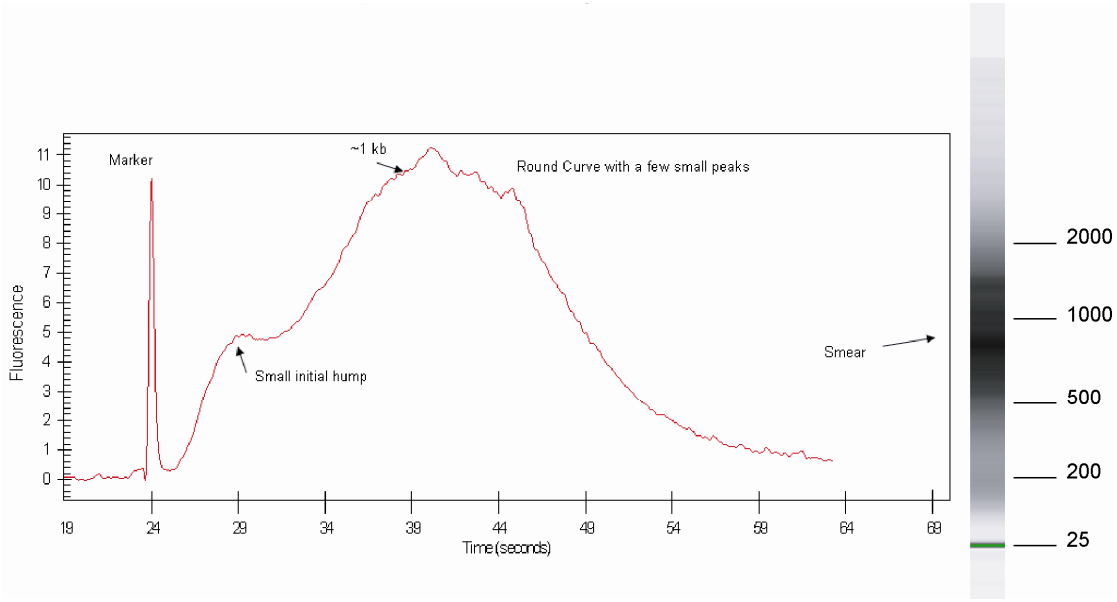

Figure 5-4. Estimation of the efficiency of the reverse transcription in Agilent Bioanalyser 2100. One representative plot and gel image of the nine samples that were used for the microarray experiment are shown.

Next, the amplified, labeled aRNA was then fragmented, so that the hybridization with the 25mer microarray probes is achieved. The quality of the fragmentation was again tested in the Agilent Bioanalyzer 2100 and in agarose gels. The mean size of the successfully fragmented aRNA is expected to be 100bp (figure 5).

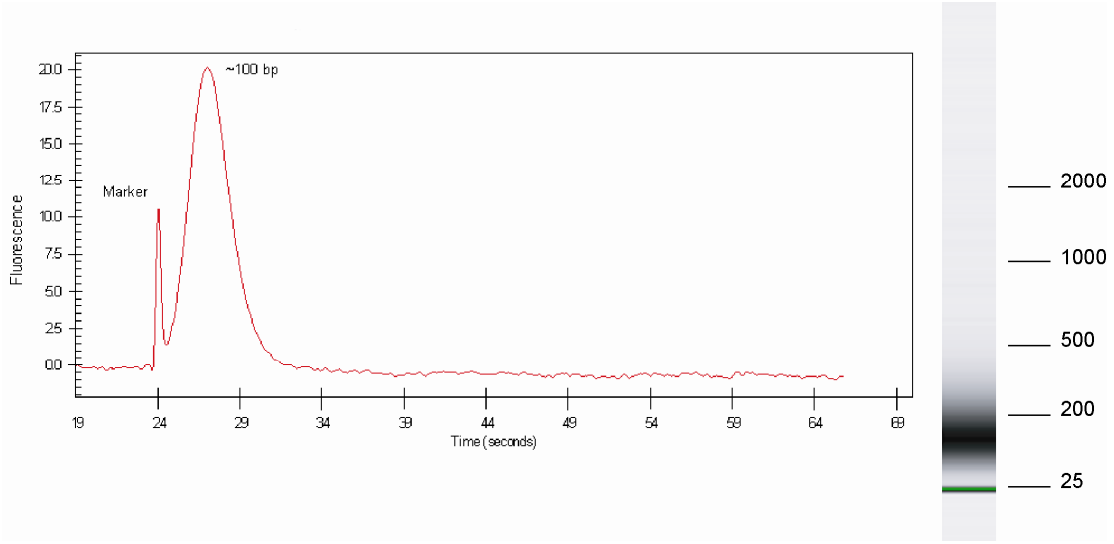

Figure 5-5. Quality control of the labelled fragmented aRNA. One representative plot and gel image of the nine samples that were used for the microarray experiment are shown.

5.1.3 Gene expression analysis with the Affymetrix mouse GeneChip 430.2 microarrays

5.1.3.1 Quality control and data normalization

The sample preparation, the mRNA amplification and labeling and the microarray hybridization and scanning procedures involve numerous steps, in which experimental errors and variation could occur. Therefore, before proceeding to gene expression analysis, quality control of the microarray experiment is essential, in order to exclude possible artifacts. The data normalization is equally important, since it eliminates the exogenous differences between the arrays to be compared.

A first step in the quality control is the performance of test microarrays in order to estimate the quality of the labeled fragmented aRNA samples. With the test microarrays, the presence or absence of aRNA hybridization to positive and negative controls respectively, provided a hint about the integrity of the aRNA and the hybridization efficiency. In detail, the hybridization intensity of the fragmented aRNA with the probes of the housekeeping genes beta-actin and glyceraldehyde 3-phosphate dehydrogonase was determined and compared among the different samples. Samples, where the mRNA of these housekeeping genes was not detectable or where the signal ratio was divergent from the mean range of values, were not used. Moreover, the average background value of the test arrays and the percentage of present and absent gene transcripts in the samples were analyzed. By this means, the good quality of the aRNA samples was validated. Samples with average background value that was higher than 40 or with a percentage of detectable mRNAs (P) lower than 40% were discarded and are not reported in table 2. Representative results of the test microarrays for each of the aRNA categories are attached as index tables 3, 4 and 5.

The results from the microarray experiment also underwent quality control. First, the CEL pictures, which result from the chip scanning, were checked for artifacts (such as scratches, air bubbles or other spatial inhomogeneities). The percentage of present aRNA fragments and the background values were also taken into consideration before concluding that the microarray results could further be normalized and analyzed.

Figure 5-6. CEL picture of the hybridized microarrays. One representative image out of the nine microarrays is shown. All scanned chips displayed no image artifacts or damage.

Following the image control, the dynamic range and the distribution of gene intensities in each array were analyzed. Since many experimental problems occur at the level of a whole array or the sample preparation, it was instructive to look at the histogram of intensities from every sample. A representative graph of one of the nine samples is shown (Figure 7a). Typically, for arrays that contain quasi-random gene selections, a characteristic distribution is observed with most of its mass at low intensities, corresponding to the majority of the sample genes, which are weakly transcribed or not expressed. The long tail to the right corresponds to genes that are transcribed at various levels.

The intensity distribution in all nine arrays is better summarized in the box plots for each sample (Figure 7b). Direct comparison of the gene intensity values of the nine arrays demonstrated that they were all in the same range, thus there was only limited experimental variation.

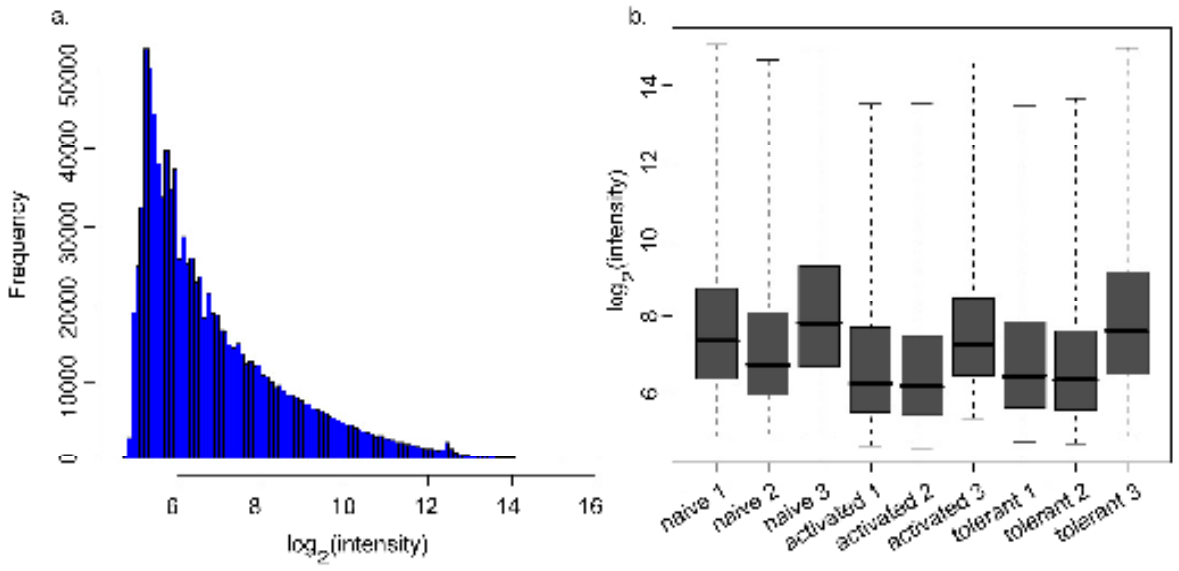

Figure 5-7. Quality control of the microarrays experiments based on probe intensity distribution. (**a**) Intensity distribution diagram for one representative sample. The plots of all nine samples display the same pattern. (**b**) Intensity box plots for the nine samles of the microarray experiment.

The second step of data processing prior to gene expression analysis is data normalization. The intensities of each microarray display variability, which does not allow direct comparison. Data normalization corrects for spatial or data bias and homogenizes the variability across arrays. This was performed by the quantile method, which is recommended for the affymetrix microarrays. The quantile normalization is a method to equalize the distribution of probe intensities for every chip, by averaging each quantile across chips. As a

result the gene intensities of all microarrays were corrected so that the independent experiments displayed the same intensity means (Figure 8b).

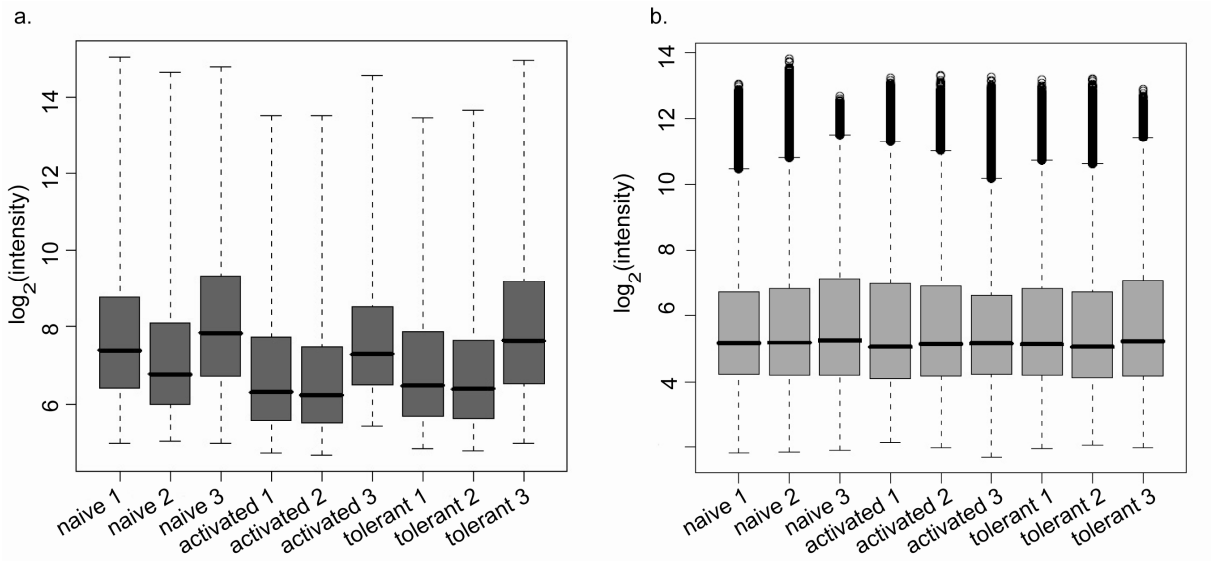

Figure 5-8. Box plots of gene intensity ranges in the nine arrays before and after data normalization. The array data were normalized with the quantile method using the rma command in the Bioconductor.

5.1.3.2 Gene expression data mining from the microarray results

A first insight into the results of the microarray experiments could be gained by cluster analysis of the samples. Hierarchical clustering is an algorithm used in microarray research to cluster samples. First, each object is assigned to its own cluster. The two most similar clusters are joined, representing a new node of the clustering tree. The same procedure is repeated until only one single cluster remains. The closer two nodes (samples) are, the higher is the similarity between them. The clustering of the nine independent aRNA samples was performed based on the 100 most variably expressed genes. Cluster analysis of the microarray results revealed that there were not any diverse expression patterns, characteristic for each of the naïve, activated and tolerant CD8 T cells (Figure 9a). This indicated that the tolerant status is not attributed to a specialized genetic program, comprising of differential expression of plenty of genes, but to differential expression of a limited number of genes which are shown as blue and red bars in Figure 9b.

The differentially expressed genes of tolerant CD8 T cells in comparison to the control samples were identified with both the Bioconductor and Affymetrix software tools. Bioconductor is an open source and open development software project for the analysis and comprehension of genomic data, comprising several R language packages for statistical analysis. The Affymetrix GCOS software is used for the scanning and the direct comparison of the gene intensities between the GeneChip microarrays. The Affymetrix Data Mining Tool

(DMT) software contains a variety of tools for filtering and sorting expression results, enabling rapid identification of the most significant results.

Microarray analysis performed with GCOS and Bioconductor analysis tools gave overlapping results. The most significantly up and down regulated genes arising from each analysis tools were essentially the same. The resulting genes that are overexpressed in the tolerant CD8 T cells as compared to the activated CD8 T cells are listed in appendix 1.

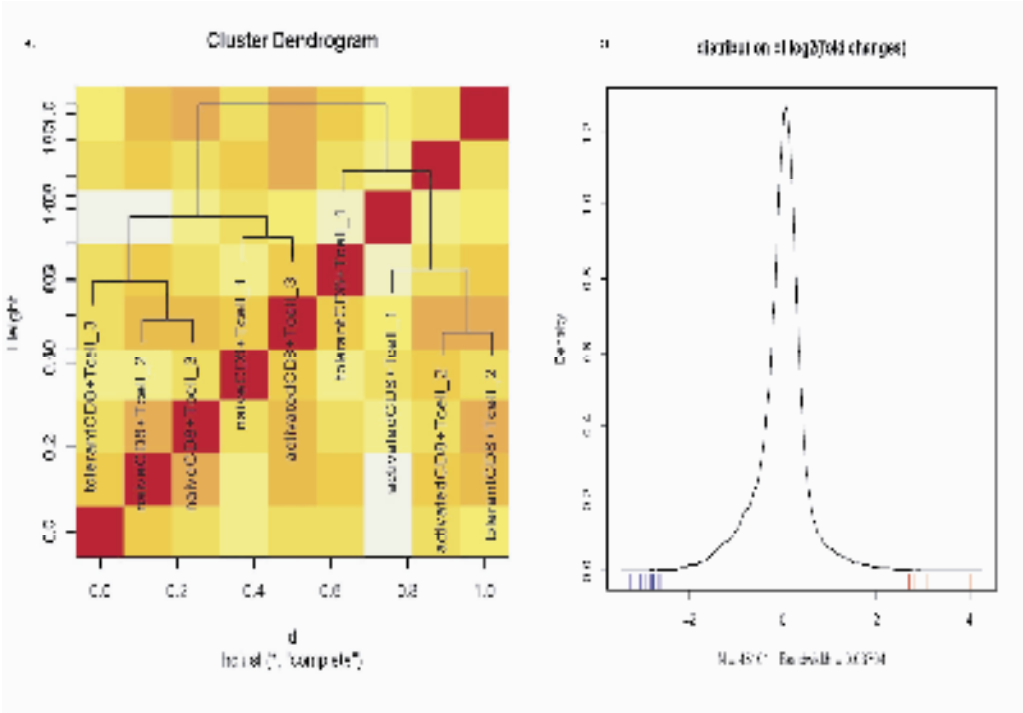

Figure 5-9. The naïve, activated and tolerant CD8 T cells display differential expression only of a limited number of genes. (**a**) Cluster analysis of the nine microarray experiments. The hierarchical clustering method was performed based on the 100 most variably expressed genes between the samples. (**b**) Distribution of the $\log_2$ of the fold change of every transcript between the tolerant and the naïve samples. The few upregulated and down regulated genes of the tolerant CD8 T cells are shown as blue and red bars respectively.

Interestingly, some genes to which the regulatory function of $CD4^+CD25^+FoxP3^+$ natural Treg cells has been attributed (see introduction) were found to be upregulated in the tolerant CD8 T cells (Figure 10). This observation confirmed that tolerant Des-TCR CD8 T cells share common molecular mechanisms of suppression with natural Treg cells.

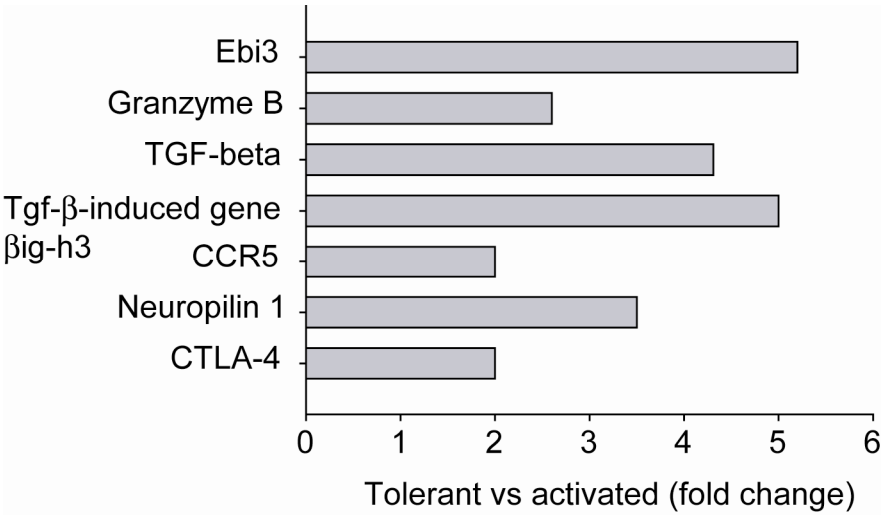

Figure 5-10. Upregulation of $CD4^+CD25^+FoxP3^+$ natural Treg associated molecules in the tolerant CD8 T cells. Triplicate comparisons of the tolerant and activated T cell microarrays were performed. The list of genes found to be more than two fold upregulated in the tolerant samples was scanned for the presence of Treg associated molecules. Molecules found to be upregulated in at least two independent comparisons are listed above and the mean fold change of upregulation is indicated. ($P<0.001$)

5.2 Dkk3 is upregulated in regulatory Des-TCR CD8 T cells and is crucial for their regulatory function

Having a long list of genes which were differentially expressed in the regulatory Des-TCR CD8 T cells, it was intriguing to identify some new molecules that could be related to CD8 T cell tolerance induction and maintenance. The attention was given to two categories of molecules: surface proteins that could be used as markers for the regulatory CD8 T cell population and secreted molecules, potential mediators of the T cell suppression. The list of secreted molecules was filtered for proteins that bind to cell surface receptors and are involved in signal transduction (see Appendix 2). Dkk3 is a secreted molecule that is upregulated in regulatory Des-TCR CD8 T cells and could mediate suppression of the proximate T cells. It had been shown to inhibit the ERK MAPK signaling (Lodygin et al. 2005), which is crucial for T cell proliferation and IL-2 production. Moreover, Dkk3 mRNA has been reported to be up-regulated in many immune privileged tissues, such as the brain, the embryo and the ovaries. All these clues indicated that Dkk3 could be a potential mediator of Des-TCR CD8 T cell regulation.

Therefore, it was further investigated whether the specific upregulation of Dkk3 in the tolerant CD8 T cells is connected with the regulatory phenotype of these cells. To address this, first Dkk3 upregulation in the regulatory Des-TCR CD8 T cells was confirmed on mRNA and protein level. Then the DesTCRxKerK^b transgenic mice were crossed to the

Dkk3$^{-/-}$ mice and several tolerance readout experimental systems were employed to clarify the effect of Dkk3 absence on CD8 T cell tolerance.

5.2.1 Upregulation of Dkk3 mRNA in the tolerant CD8 T cells

Microarray analysis identified Dkk3 to be specifically upregulated in the tolerant Des-TCR CD8 T cell population (Figure 11a). Dkk3 mRNA was present in all naïve and activated triplicates and in two out of three tolerant samples. Presumably the absence of Dkk3 mRNA hybridization in the one of the tolerant triplicates was due to experimental error. The comparison of the Dkk3 mRNA expression between the nine arrays was performed according to the scheme presented in table 3. Only the arrays of the samples that were generated with exactly the same mRNA amplification and labeling protocol were directly compared (see also Table 2).

	tolerant 1	tolerant 2	tolerant 3
naive 1	x	No Dkk3 mRNA signal	
naive 2			x
naive 3			x
activated 1	x		x
activated 2			x
activated 3			x

Table 5-3. Scheme of comparisons of Dkk3 expression performed between the tolerant and the naïve or the activated CD8 T cell samples. The (x) signs indicate the pairs of gene expression comparison.

Microarray analysis indicated that Dkk3 expression in tolerant CD8 T cells was on average 4.6 fold and 22.6 fold higher than in naïve and activated CD8 T cells respectively. The logarithmical ratios of Dkk3 mRNA in tolerant to naïve and activated CD8 T cells are depicted in figure 11a.

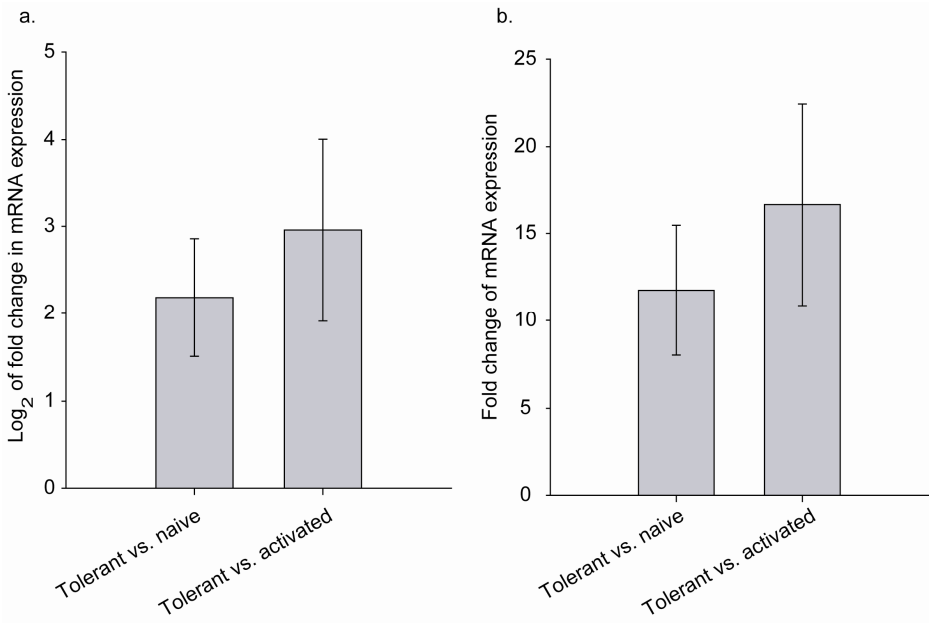

Figure 5-11. Upregulation of the Dkk3 mRNA in the tolerant CD8 T cells. (**a**) The log_2 signal ratio for the Dkk3 mRNA of the tolerant versus the naïve or activated samples was estimated and the mean +/-s.e.m of three independent comparisons is shown. (P< 0.001) (**b**) Total RNA was isolated from naïve, activated and tolerant Des-TCR CD8 T cells and the Dkk3 mRNA expression was measured by RT-PCR. The fold change of Dkk3 mRNA expression of tolerant samples in comparison to the naïve and activated samples was calculated. The mean +/- s.e.m of nine independent experiments is shown. (P< 0.01)

The microarray results concerning the transcription of the Dkk3 gene were confirmed by RT-PCR. Total RNA was isolated from triplicates of naïve, activated and tolerant Des-TCR CD8 T cells and mRNA was reversely transcribed to cDNA. Dkk3 mRNA was found to be upregulated in the regulatory Des-TCR CD8 T cells (Figure 11b). On average, Dkk3 expression was 11.7 fold higher in tolerant when compared to naïve CD8 T cells. Similarly, Dkk3 mRNA amount was 16.7 fold increased in tolerant versus activated CD8 T cells.

5.2.2 Generation of the molecular tools for the detection of Dkk3 protein in the tolerant CD8 T cells

In order to confirm the mRNA data on the protein level, a mouse Dkk3-specific monoclonal antibody was produced. For this, two Dkk3 cDNA constructs were generated. The first encoded for a Dkk3-GST fusion protein. The second consisted of the sequence for the mouse Dkk3 protein conjugated to the one of the mouse IgG2b. Additionally, HEK 293T cells were transfected with plasmids carrying the mouse Dkk3 and GFP genes.

For the antibody production, $Dkk3^{-/-}$ female mice were immunized with the purified Dkk3-IgG2b protein and hybridomas were generated, upon fusion of spleen cells that were derived from the immunized mice with the myeloma cell line X63-Ag8.653. The hybridomas-supernatant was first screened for recognition of the Dkk3-GST protein by ELISA. The whole

procedure of anti-Dkk3 antibody production was performed by Dr G. Moldenhauer. The purified anti-Dkk3 antibody could stain Dkk3 intracellularly in the GFP-positive Dkk3-transfected HEK 293T cells (Figure 12a). Moreover, the intracellular and secreted Dkk3, derived from HEK 293T cells, could be detected by western blot analysis with the newly produced anti-Dkk3 antibody (Figure 12b). The secreted and intracellular protein forms were found to have different size. Taking into account that there are four glycosylation sites in mouse Dkk3, this could be due to differential posttranslational modification.

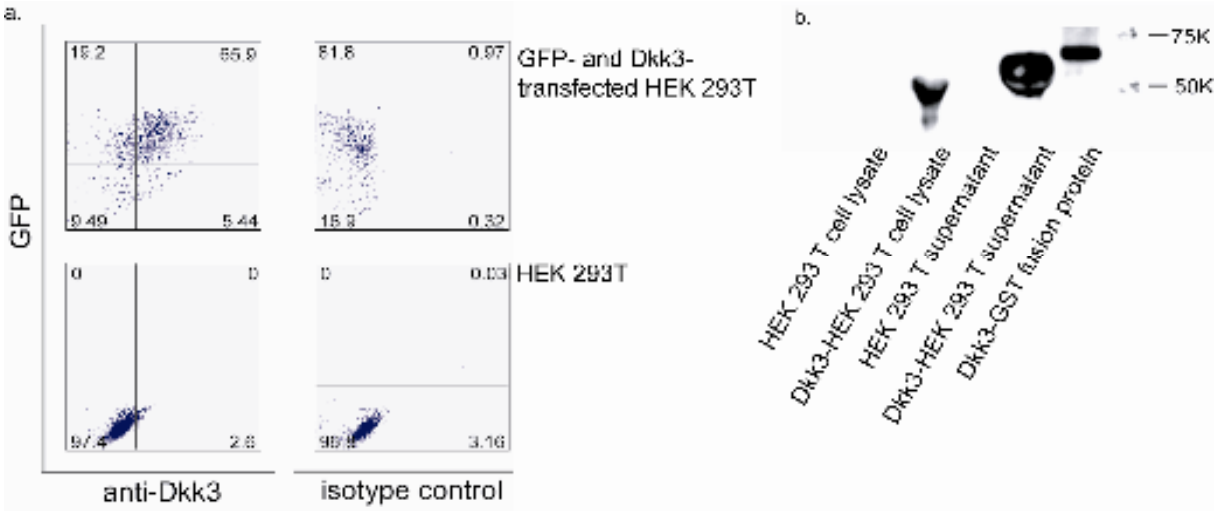

Figure 5-12. Characterization of the anti-mouse Dkk3 monoclonal antibody. (a) HEK 293T cells that were simultaneously transfected with GFP and Dkk3 cDNAs were stained intracellularly with the anti-Dkk3 antibody or the isotype control and screened by flow cytometry. Untransfected HEK293T cells were used as a negative control. (b) Total protein from supernatant or cell lysates derived from the HEK293T and the transfected Dkk3-HEK293T cells was analyzed by western blot for the presence of Dkk3 using the monoclonal anti-mouse Dkk3 antibody. The Dkk3-GST protein was used as a positive control.

5.2.3 Dkk3 protein expression by the tolerant CD8 T cells

After the development of a functional anti-Dkk3 antibody the Dkk3 protein level in CD8 T cells could be analyzed by flow cytometry. Naïve, activated and tolerant CD8 T cells were isolated from thymectomised Des-TCRxRAG2$^{-/-}$ and Des-TCRxKerK^{b}xRAG2$^{-/-}$ mice 15 days after subcutaneous P815.K^{b}.B7 tumor cell injection. Intracellular FACS analysis with the monoclonal anti-mouse Dkk3 antibody revealed the presence of Dkk3 in the tolerant Des-TCR CD8 T cell population on the single cell level (Figure 13). Since Dkk3 mRNA and protein are up-regulated in the tolerant CD8 T cells, Dkk3 could be a mediator of CD8 T cell regulation.

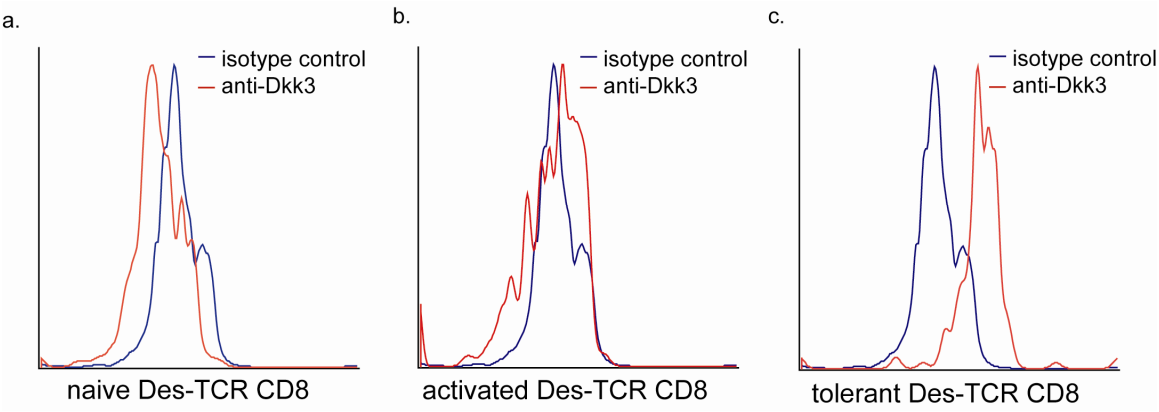

Figure 5-13. Dkk3 protein expression in tolerant Des-TCR CD8 T cells. Naïve (**a**), activated (**b**) and tolerant (**c**) Des-TCR CD8 T cells were isolated as described in paragraph 1.1, stained intracellularly for the Dkk3 protein and analyzed by FACS. Dkk3 expression in the Des-TCR CD8 populations is shown in histograms. Anti-human HD20 antibody was used as a negative isotype control.

5.2.4 The role of Dkk3 in the maintenance CD8 tolerance

K^b-positive tumor graft acceptance by DesTCR T cell-bearing mice was the first tolerance readout system used to investigate the contribution of Dkk3 in tolerance induction and maintenance. The Des-TCRxKerK^b mice were crossed with the Dkk3 knockout (Dkk3$^{-/-}$) mice to investigate whether lack of Dkk3 was sufficient to reverse tolerance against the K^b antigen. Briefly, 2x10^5 P815K^{b}B7 tumor cells were subcutaneously injected into mice and the tumor growth was assessed by measurement of the tumor surface (in cm^2). Contrary to the Des-TCRxKerK^b mice the Des-TCR as well the Des-TCRxKerK^{b}xDkk3$^{-/-}$ mice rejected the K^b-expressing tumor grafts (Figure 14a). The few tumors that had developed in Des-TCR and Des-TCRxKerK^{b}xDkk3$^{-/-}$ mice were significantly smaller than those that had grown in Des-TCRxKerK^b mice (Figure 14b).

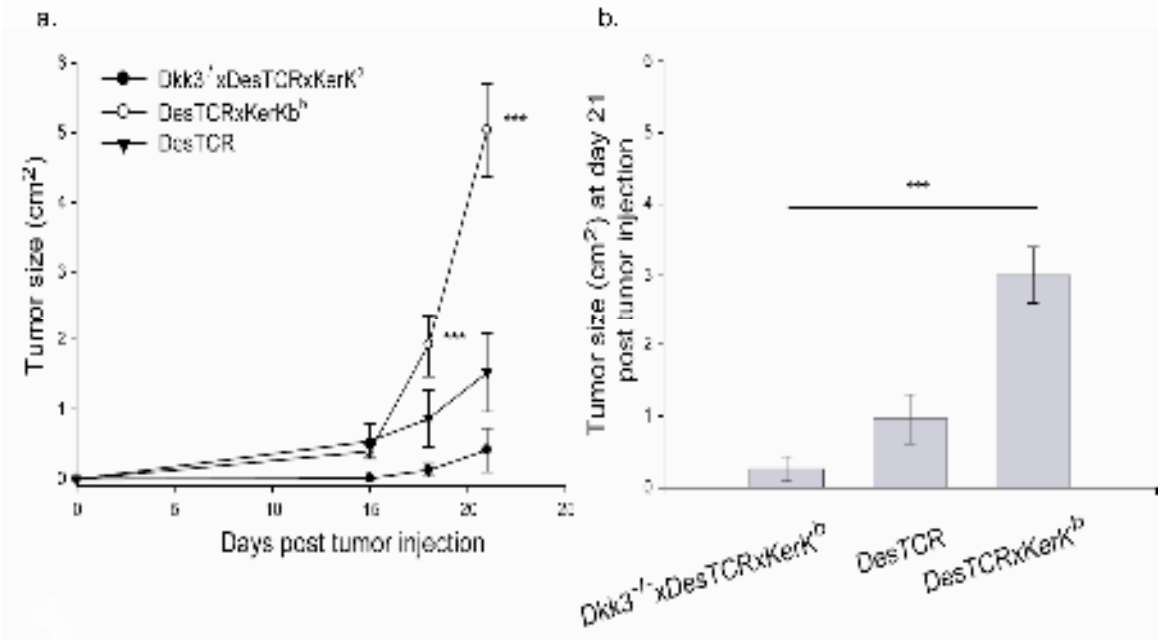

Figure 5-14. Dkk3 is essential for K^b – positive tumor graft acceptance mediated by the tolerant Des-TCR CD8 T cells. $2x10^5$ P815.K^b.B7 tumor cells were inoculated s.c. into Des-TCR, Des-TCR x $KerK^b$ and $Dkk3^{-/-}$ x Des-TCR x $KerK^b$ mice. Mice were assessed for tumor growth (cm^2). (**a**) The kinetics of tumor growth and (**b**) the tumor sizes at day 21 are indicated. Data represent the mean tumor size +/- s.e.m of two independent experiments. (***: P<0.001)

To strengthen this finding, a second tolerance readout system was used. Des-TCR, Des-TCRxKerK^b and Des-TCRxKerK^{b}xDkk3$^{-/-}$ mice were primed with activated K^b-positive dendritic cells, which were derived from B6 bone marrow (see Material and Methods, paragraphs 2.3.5 and 2.3.6). *In vivo* kill of K^b-positive target cells was measured 7 days after priming (see Materials and Methods, paragraph 2.8.3) to assess generation of K^b-specific cytotoxicity. Whereas the tolerant Des-TCRxKerK^b mice displayed less than 15% K^b-specific lysis, the Des-TCRxKerK^{b}xDkk3$^{-/-}$ mice showed T cell cytotoxicity comparable to Des-TCR mice (Figure 15). The assay was performed three times, twice with mice of the H2^{kxd} background and once with mice of the H2^{kxk} background and the pooled results of the three experiments are shown.

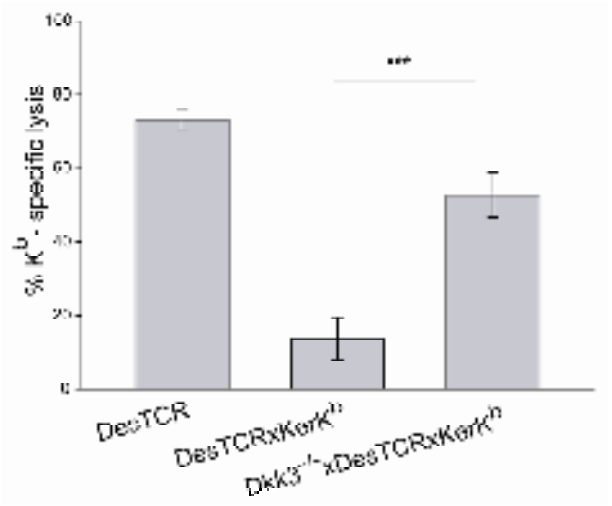

Figure 5-15. Dkk3 is indispensable for the suppression of anti-K^b reactivity of CD8 T cells in the DesTCR x KerK^b mice. Des-TCR, Des-TCRxKerK^b and Dkk3$^{-/-}$x Des-TCRxKerK^b mice were immunized with activated C57.Bl6 dendritic cells and after 7 days the percentage of specific killing of CFSE-labelled K^b-positive target cells *in vivo* was measured by FACS. The mean % lysis +/- s.e.m of three independent experiments is shown. (***: P<0.001)

Given that it is a secretory molecule it was interesting to clarify whether Dkk3 that is expressed by the tolerant CD8 T cells mediates tolerance by suppressing the proximate naive T cells. To address this, Des-TCRxKerK^b mice were tested for autologous skin graft acceptance after Dkk3 blockade by the anti-Dkk3 antibody. Two experimental groups were set. The first received the anti-Dkk3 antibody and the second the control mouse serum IgG. Each mouse was intraperitoneally injected with 1mg of anti-Dkk3 monoclonal antibody or mouse IgG at day 0 and with 0.5mg of antibody every second day. In total each mouse received 5mg of blocking or control antibody. Skin from the tail was transplanted to the back of the mice and skin graft and both groups were screened for long term skin graft acceptance. Interestingly, the Des-TCRxKerK^b mice that had received the Dkk3-blocking antibody rejected the autologous graft (Figure 16). This indicated that the Dkk3 protein that is secreted by the regulatory Des-TCR CD8 T cells is indeed essential for the maintenance of tolerance against self antigens and can suppress T cell responses.

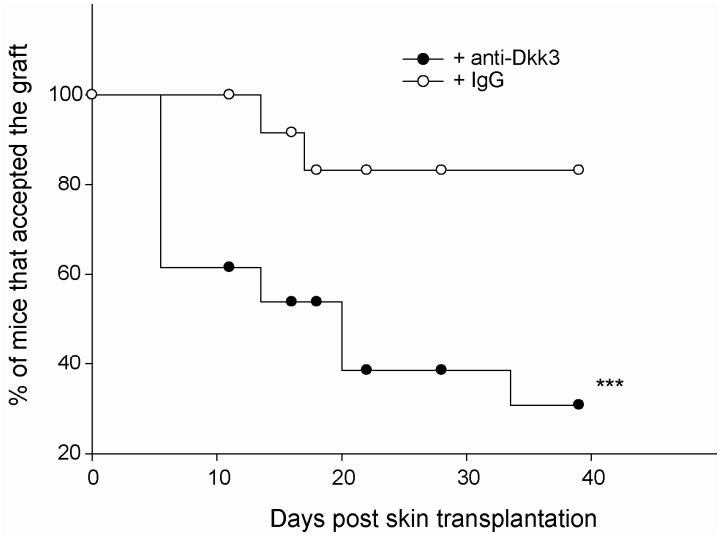

Figure 5-16. Blocking of the secreted Dkk3 protein abolishes T cell tolerance to autologous skin. Des-TCRxKerK^{b} mice underwent autologous skin transplantation. In one experimental group, each mouse received in total 5mg anti-Dkk3 blocking antibody and in the control group 5mg mouse IgG. Each group consisted of 12 mice. The mice were screened for skin graft acceptance for a time period of 45 days.. (**: P<0.01)

To exclude that Dkk3 also binds on the surface of the tolerant CD8 T cells and mediates tolerance by cell contact suppression, the Des-TCR CD8 T cells were tested in FACS for Dkk3 staining without fixation and permeabilization. However the cell-surface of the naïve, activated and tolerant Des-TCR CD8 T cells were all negative for Dkk3 staining (Figure 17). Hence, the secreted Dkk3 seems to be the mediator of the suppressive function of the regulatory DesTCR CD8 T cells.

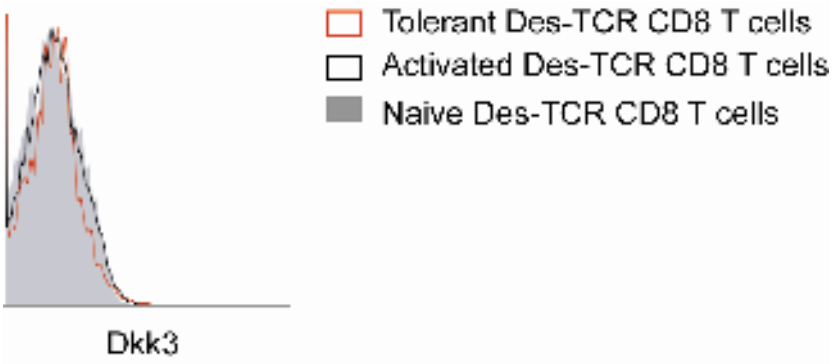

Figure 5-17. No presence of Dkk3 can be traced on the tolerant Des-TCR CD8 T cell-surface by flow cytometry. Naïve, activated and tolerant Des-TCR CD8 T cells have been isolated from Des-TCR and Des-TCRxKerK^{b} mice respectively and tested for binding of Dkk3 protein to their cell surface. Dkk3 staining was performed with the monoclonal mouse anti-Dkk3 antibody without cell fixation and permeabilization. With FACS analysis the CD8 Des-TCR population was gated and Dkk3 expression in each CD8 T cell population was depicted by histogram overlay.

5.3 Dkk3 affects polyclonal T cell reactivity

After identifying the regulatory effect of Dkk3 in the Des-TCRxKerK^{b} mouse model, it was examined whether Dkk3 is present in wild type regulatory T cell populations and whether it could also regulate polyclonal T cell reactivity. Therefore, Dkk3$^{-/-}$ and Dkk3$^{+/+}$ mice were used. First, Dkk3 expression analysis in lymphocytes was performed. Then, the effect of the absence of Dkk3 on T cell proliferation *in vitro* within a splenic cell population was addressed. Moreover, the CD4 and CD8 T cell populations were isolated from both mouse strains and their proliferation *in vitro* was measured in order to clarify whether the Dkk3 effect is T cell intrinsic or a result of the presence of Dkk3 in the splenic microenvironment.

5.3.1 Dkk3 expression in polyclonal T cells

It has been reported that the spleen, the lymph nodes and the thymus are negative for Dkk3 mRNA (Niehrs 2006). This has been confirmed by RT-PCR analysis of lymphatic organ-lysates that was performed in our lab. However, the Dkk3 mRNA and protein were traced in the tolerant Des-TCR CD8 T cells. Moreover, amplified mRNA from naïve and activated CD8 T cells were hybridized with the Dkk3 gene probes on the GeneChip microarrays. Consequently, it was asked whether a lymphocyte population expressing Dkk3 could be found in the spleen of wild type mice by flow cytometry. Therefore, splenocytes were isolated from Dkk3$^{+/+}$ C57.Bl/6 mice and Dkk3$^{-/-}$ mice and stained intracellularly with the monoclonal anti-mouse Dkk3 antibody. In each sample 2-4x10^{7} cells were analyzed by flow cytometry for the presence of Dkk3. B cells (data not shown) and T lymphocytes were found negative for Dkk3 protein. The same held true for NK cells and NK T cells (Figure 18). The above results were reproduced in three independent experiments. The observed difference in anti-Dkk3 binding in the CD8 and NK1.1 negative cell fraction was not reproducible and was attributed to unspecific staining, probably due to insufficient blocking of the Fc receptors on splenocytes.

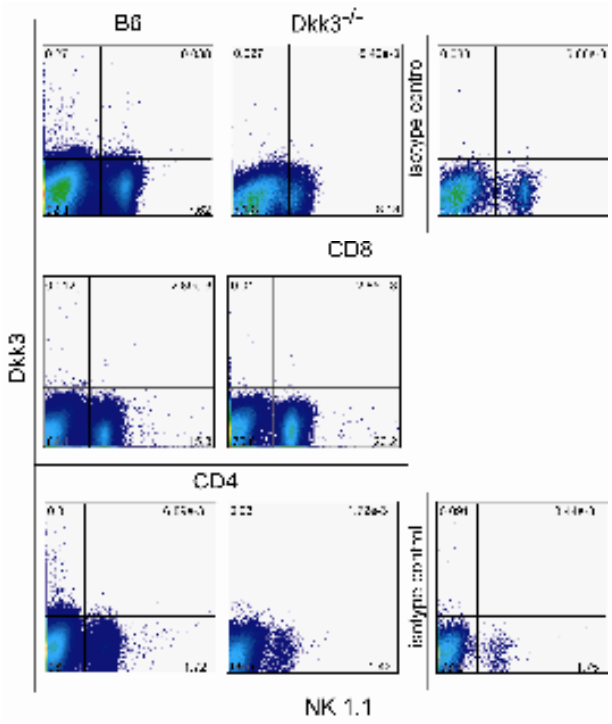

Figure 5-18. No Dkk3 protein expression can be traced in lymphocytes and NK cells by flow cytometry. Splenocytes from C57.Bl6 and Dkk3$^{-/-}$ mice were stained for surface cell markers and with the anti-Dkk3 or with the anti-HD-20 isotype control antibodies. 2x10^{7} cells from each spleen were analyzed by flow cytometry for Dkk3 expression. The CD8, CD4 T and NK cells were found to be negative for Dkk3.

In order to screen dendritic cells, monocytes and spleen stromal cells for Dkk3 protein expression, the spleens were first digested with DNAse I and collagenase IV in the presense of EDTA, so that cell clustering is avoided. In all cases 3-4x10^{7} spleen cells were acquired and analyzed by flow cytometry. The Gr1 and CD11b markers were used for the staining of the monocytes, whereas the dendritic cells were defined by positively gating the MHC class II^{+} CD11c^{+} or CD11b^{+} cells (Figure 19b). The splenic stromal cell gate resulted from exclusion of the CD3, CD19, CD11b and CD45.2 positive cells (Figure 19a). No Dkk3 protein expression was traced in any of the above mentioned populations.

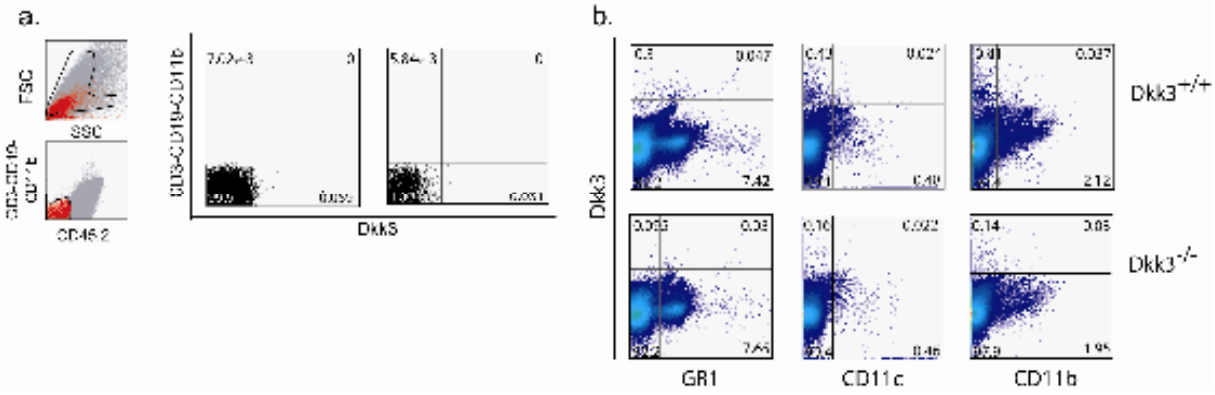

Figure 5-19. No Dkk3 expression can be traced in monocytes, dendritic cells and splenic stromal cells by flow cytometry. Spleens from C57.Bl6 and Dkk3$^{-/-}$ mice were enzymatically digested and the resulting cells were stained for cell surface markers and intracellular Dkk3 protein. 3-4x10^{7} cells per spleen were analyzed by

flow cytometry. The absence of Dkk3 expression from (**a**) splenic stromal cells, (**b**) monocytes and dendritic cells is shown.

5.3.2 Dkk3$^{-/-}$ splenocytes display increased proliferation *in vitro*

In order to investigate the impact of Dkk3 on T cell responses, splenocytes were isolated from Dkk3$^{+/+}$ and Dkk3$^{-/-}$ mice and stimulated with titrated amounts of anti-CD3 and anti-CD28 antibodies. The anti-CD3 and anti-CD28 antibodies provided the signals one and two for the T cell stimulation and costimulation. T cell proliferation was measured at day 4 by thymidine incorporation. Notably, Dkk3$^{-/-}$ T cell proliferation was increased as compared to wild-type T cells (Figure 20). Thus, the presence of Dkk3 in the wild type mice may set a limit to the T cell proliferation.

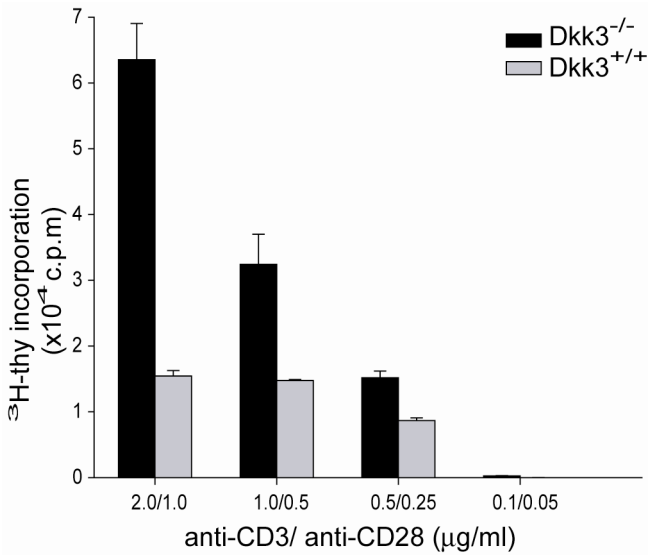

Figure 5-20. T cell proliferation *in vitro* is increased in the absence of Dkk3. Dkk3$^{-/-}$ and Dkk3$^{+/+}$ spleen cells were stimulated with varying concentrations of anti-CD3 and anti-CD28 antibodies. Proliferation was measured by thymidine incorporation at day 4. A representative of four independent experiments +/- s.e.m is shown.

To analyze the kinetics of T cell proliferation, splenocytes isolated from Dkk3$^{+/+}$ and Dkk3$^{-/-}$ mice were stained with CFSE, before being stimulated *in vitro* as described above. Proliferation of the CD4 and CD8 T cell subpopulations was screened by FACS at days 4, 5 and 6 (figure 21). The CD4 and predominantly the CD8 T cell population indicated higher proliferation rates in the absence of Dkk3 at days 4 and 5 after stimulation.

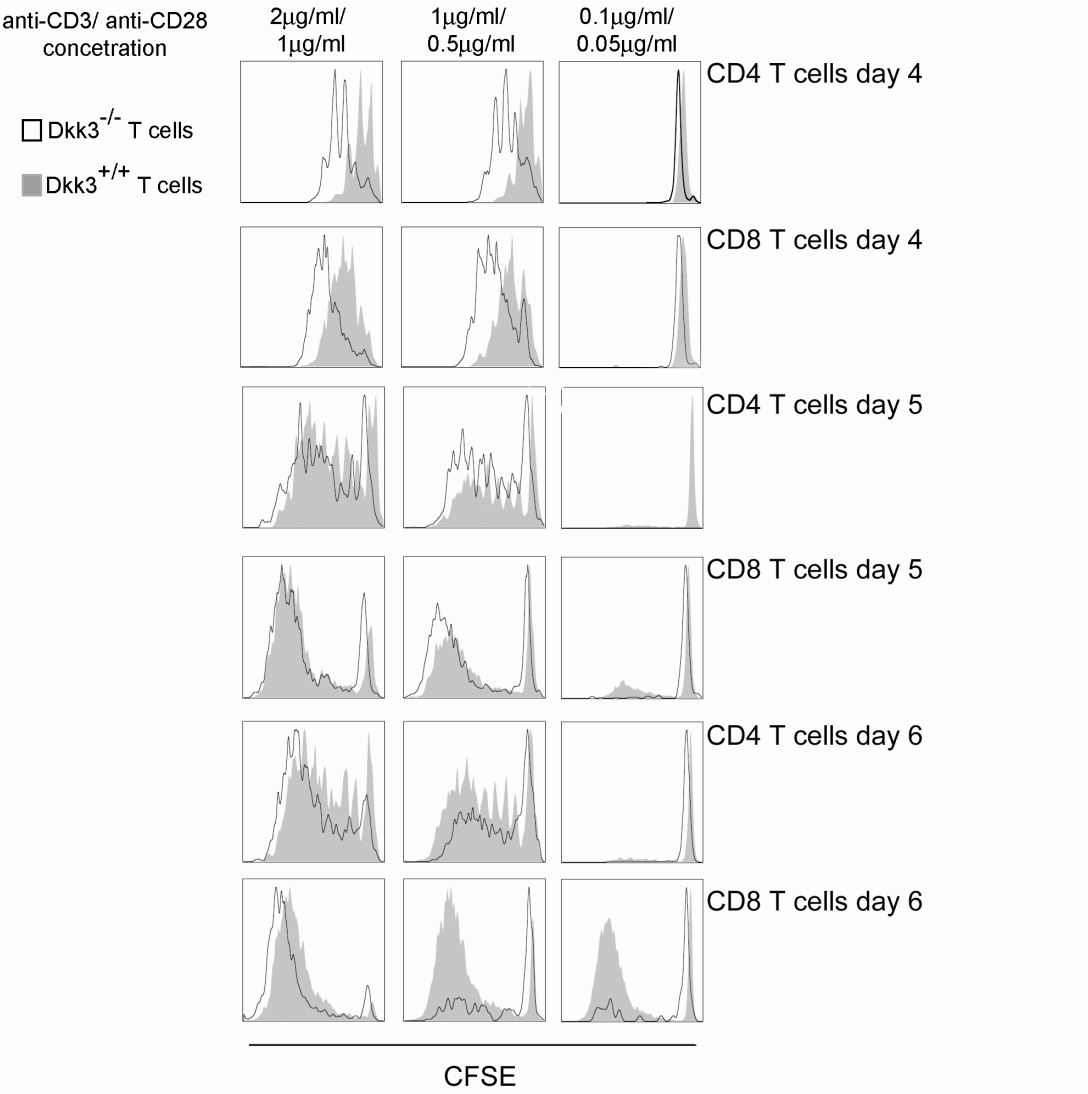

Figure 5-21. Absence of Dkk3 expression in the spleen results in increased CD4 and CD8 T cell proliferation. CFSE labeled Dkk3$^{-/-}$ and Dkk3$^{+/+}$ spleen cells were stimulated with titrated amounts of anti-CD3 and anti-CD28 and CFSE-dilution in the CD4 and CD8 T cell subpopulations was determined by flow cytometry at days 4, 5 and 6 upon T cell stimulation.

The CFSE histograms show that the Dkk3$^{-/-}$ CD4 and CD8 T cells proliferate faster than the wild type control. The Dkk3$^{-/-}$ T cell proliferation at day 4 was much higher than in wild type. This may be attributed to earlier initiation of the T cell proliferation or accelerated cell cycle. At day 5, the Dkk3$^{-/-}$ T cells that had been stimulated with lower dose of anti-CD3 and anti-CD28 still display increased proliferation in comparison to the Dkk3$^{+/+}$. The wild type T cell proliferation level reaches the one Dkk3$^{-/-}$ T cell proliferation at high doses of T cell stimulation at day 5 and at low doses of T cell stimulation at day 6. This implies that on later time points Dkk3$^{-/-}$ T cell proliferation slows down, possible due to activation induced cell death and nutrients' exhaustion.

5.3.3 Dkk3$^{-/-}$ T cell hyperproliferation is not an effect of increased T cell activation status or natural Treg deficiency

In order to clarify the cause of Dkk3$^{-/-}$ T cell hyperproliferation, some control experiments were performed. It could be argued that Dkk3$^{-/-}$ T cells are already pre-activated before in vitro stimulation and therefore start to proliferate earlier. To exclude this, the proliferation of naïve (CD62L^{high}) Dkk3$^{+/+}$ and Dkk3$^{-/-}$ T cells was compared. Naïve spleen T cells were purified from Dkk3$^{+/+}$ and Dkk3$^{-/-}$ mice by MACS CD62L microbead positive selection. The CD62L^{high} Dkk3$^{-/-}$ T cells were stimulated with anti-CD3 (2 μg/ml) and anti-CD28 (1 μg/ml) and T cell proliferation was measured four days after stimulation by thymidine incorporation. The CD62L^{high} Dkk3$^{-/-}$ T cells proliferated better than the wild type control, suggesting that the observed effect is not due to the pre-activation of the Dkk3$^{-/-}$ T cells in the mouse (Figure 22). At this point, it is worth mentioning that previous studies in the lab had revealed no significant up-regulation of T cell activation markers (CD69, CD44, and CD25) on Dkk3$^{-/-}$ CD4 and CD8 T cells.

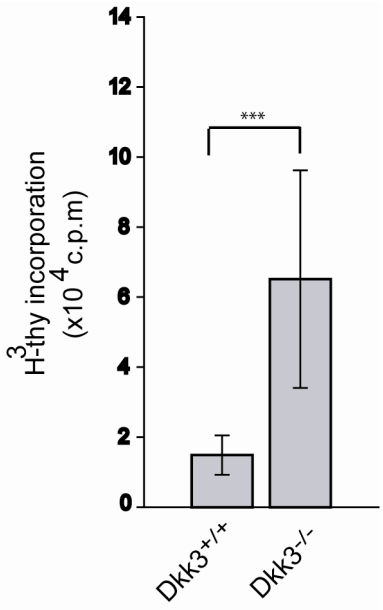

Figure 5-22. Increased Dkk3-/- T cell proliferation *in vitro* is not a result of pre-activation *in vivo*. MACS sorted CD62L ^{high} T cells from Dkk3-/- and Dkk3+/+ spleens were stimulated with anti-CD3 (2 ug/ml) and anti-CD28 (1 ug/ml) and T cell proliferation *in vitro* was assessed at day 4 by thymidine incorporation. The mean+/- s.e.m from 2 independent experiments is shown.

It is also possible that the difference in T cell proliferation described above is a result of a malfunction of the Dkk3$^{-/-}$ natural Treg cells. However, Treg cells were found to be negative for Dkk3 in the mRNA (data not shown) and protein level (Figure 23a). Additionally, the Dkk3$^{-/-}$ CD4^{+}CD25^{+}FoxP3^{+} Tregs were as efficient as the wild type controls in *in vitro* suppression assays (Figure 23b).

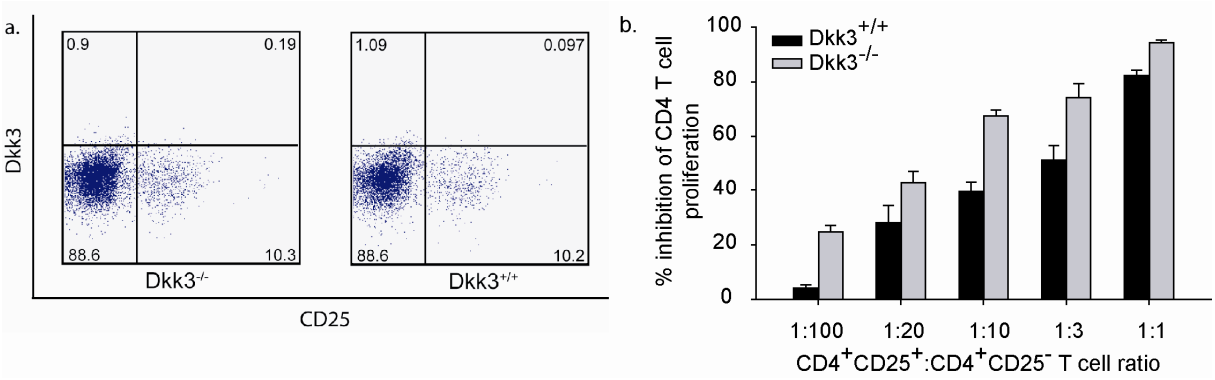

Figure 5-23. Increased Dkk3$^{-/-}$ T cell proliferation cannot be attributed to a malfunction of the Dkk3$^{-/-}$ CD4^{+}CD25^{+}FoxP3^{+} regulatory T cells. (**a**) CD4^{+}CD25^{+} positive T cells were analyzed for Dkk3 expression by flow cytometry and found negative. (**b**) CD4^{+}CD25^{-} T cells were cocultured with Dkk3$^{+/+}$ or Dkk3$^{-/-}$CD4^{+}CD25^{+} in different ratios and CD4 T cell proliferation was measured by thymidine incorporation at day 4. The mean+/- s.e.m of two independent experiments is shown.

5.3.4 Isolated Dkk3$^{-/-}$ CD8 but not CD4 T cells display increased proliferation in comparison to wild type control T cells

In the previous paragraph it was shown that the absence of Dkk3 from the spleen results in stronger CD4 and CD8 T cell proliferation in the total splenocyte cultures. It was then reasonable to investigate whether T cell proliferation was influenced by the lack of Dkk3 expression from the CD4 and CD8 T cells themselves or from the splenic microenvironment. To investigate this, CD4 or CD8 T cells were isolated using the respective MACS negative selection kits with over 87% purity and were stimulated with anti-CD3 (2μg/ml) and anti-CD28 (1μg/ml) in the absence of any other spleen cell population. Isolated CD4 T cells derived from the Dkk3$^{-/-}$ mice displayed the same proliferation degree as the Dkk3$^{+/+}$ control CD4 T cells. This can be easily explained, since no Dkk3 mRNA or protein expression was found in the CD4 T cells (Figure 24a). Unexpectedly, the isolated CD8 T cells showed a slightly higher but significant proliferation rate in the absence of Dkk3 (Figure 24b).

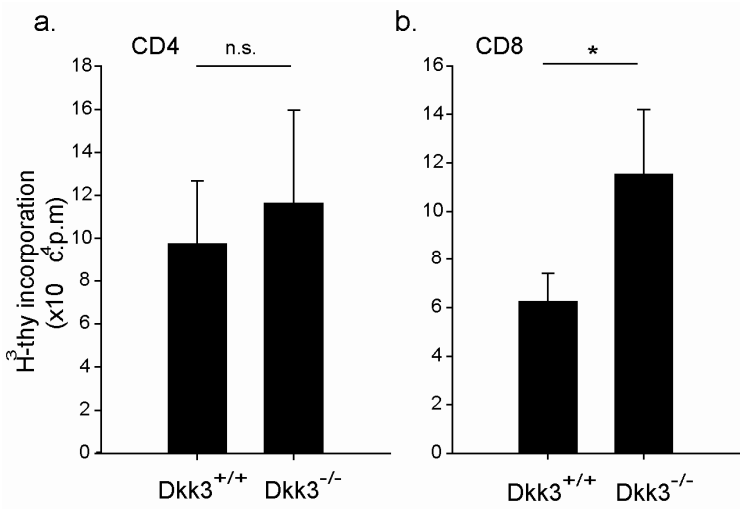

Figure 5-24. Isolated CD4 but not CD8 T cells derived from Dkk3$^{-/-}$ mice proliferate as much as the wild type controls. MACS sorted (**a**) CD4 and (**b**) CD8 T cells from Dkk3$^{-/-}$ and Dkk3$^{+/+}$ spleens were stimulated with anti-CD3 (2 ug/ml) and anti-CD28 (1 ug/ml) and T cell proliferation *in vitro* was assessed at day 4 by thymidine incorporation. The mean+/- s.e.m from five independent experiments is shown. (* P< 0.05)

This finding could be explained by two arguments. It is possible that there is a regulatory CD8 T cell subpopulation that expresses Dkk3, exactly like the tolerant CD8 T cells in the transgenic Des-TCRxKerK^b mouse system. This subpopulation could be so small that no Dkk3 expression can be traced in the total spleen, or in the CD8 T cell fraction. On the other hand, the probability that the presence of Dkk3, which is secreted by peripheral tissues in the mouse influences permanently the reactivity of the CD8 T cells and temporalily the reactivity of the CD4 T cells cannot be excluded. A direct identification of Dkk3-expressing CD8 T cells with RT-PCR flow cytometry, ELISA, western blot analysis and histology was not feasible. In the next chapter, some experimental approaches that indirectly address this point will be described.

5.4 Attributes of Dkk3$^{-/-}$ T cell hyperproliferation

5.4.1 Thymic selection is unaltered in Dkk3$^{-/-}$ mice

The previously described differences in T cell reactivity between the Dkk3$^{-/-}$ and Dkk3$^{+/+}$ mice could have different explanations. First, it could be argued that Dkk3 deficiency results in altered thymic selection. In other words, the observed Dkk3$^{-/-}$ T cell hyperproliferation could be attributed to a bias of the positive selection towards more reactive T cell clones. To address this, bone marrow chimeras were constructed. Wild type mice were irradiated and reconstituted with bone marrow from either Dkk3$^{-/-}$ or Dkk3$^{+/+}$ donor mice. Thus, the thymic epithelium of the chimeric mice is Dkk3$^{+/+}$ and the positively selected T cells are Dkk3$^{-/-}$ and Dkk3$^{+/+}$ respectively. Additionally, Dkk3$^{-/-}$ recipient mice were chimerized with bone marrow

from Dkk3$^{+/+}$ donor mice. The percentages of T cells expressing a spectrum of TCR Vβ chains (Vβ8.1, Vβ8.2, Vβ5.1, Vβ5.2, Vβ6, Vβ11, Vβ9, Vβ13, Vβ3, Vβ17A, Vβ14, Vβ7, Vβ2, Vβ10B, Vβ12, Vβ4, Vβ8.3) were defined in the chimeric and control Dkk3$^{-/-}$ and Dkk3$^{+/+}$ mice. As shown in table 3, there are no differences in the TCR repertoire derived from Dkk3-sufficient or deficient thymic epithelium.

Thymus CD4	**8.1 & 8.2**	**5.1 & 5.2**	**6**	**11**	**9**	**13**	**3**	**17a**	**7**	**14**	**2**	**10b**	**12**	**4**	**8.3**
Dkk3 -/-	10.6	2.78	4.56	5.78	6.75	0.95	3.91	3.26	1.1	3.32	0.51	5.11	0.66	4.29	0.33
B6	8.62	2.78	6.23	4.94	8.02	1.31	4.52	2.97	1.32	3.8	0.47	3.69	1.15	2.43	0.55
Thymus CD8	**8.1 & 8.2**	**5.1 & 5.2**	**6**	**11**	**9**	**13**	**3**	**17a**	**7**	**14**	**2**	**10b**	**12**	**4**	**8.30**
Dkk3 -/-	9.47	4.62	9.48	1.19	6.14	0.21	4.29	1.6	1.62	2.5	0.1	1.56	0.21	3.32	0.36
B6	8.35	5.84	11.5	0.85	5.82	0.51	5.48	2.11	1.74	1.97	0.14	0.96	0.45	1.37	0.15
Thymus CD4	**8.1 & 8.2**	**5.1 & 5.2**	**6**	**11**	**9**	**13**	**3**	**17a**	**7**	**14**	**2**	**10b**	**12**	**4**	**8.30**
B6 in B6	11.8	5.66	5.49	6.18	7.87	1.33	5.02	3.3	1.24	3.48	0.43	5.88	1.7	4.73	0.3
B6 in Dkk3	10.7	2.89	3.82	6.16	7.22	1.44	4.54	3.67	1.09	3.43	0.32	4.99	1.75	5.58	0.24
Dkk3 -/- in B6	11	2.75	5.75	5.64	7.9	1.58	5.01	3.56	1.1	4.48	0.65	4.89	1.69	3.92	0.49
Thymus CD8	**8.1 & 8.2**	**5.1 & 5.2**	**6**	**11**	**9**	**13**	**3**	**17a**	**7**	**14**	**2**	**10b**	**12**	**4**	**8.30**
B6 in B6	8.33	5.39	9.67	1.62	5.47	0.71	3.26	2.59	1.71	2.23	0.23	1.5	0.62	2.15	0.59
B6 in Dkk3-/-	5.91	5.3	6.47	1.47	4.75	0.49	3.7	1.51	1.12	1.29	0.62	1.62	1.15	5.61	0.28
Dkk3 -/- in B6	9.33	4.57	12	1.34	6.92	0.31	4.75	2.85	1.52	2.65	0.3	1.62	0.51	0.7	0.28
Spleen CD4	**8.1 & 8.2**	**5.1 & 5.2**	**6**	**11**	**9**	**13**	**3**	**17a**	**7**	**14**	**2**	**10b**	**12**	**4**	**8.3**
Dkk3 -/-	6.92	2.23	3.43	3.32	6.26	1	3.61	2.34	1.67	2.15	0.65	4.45	2.94	1.81	0.87
B6	7.48	2.34	3.07	3.47	8.71	0.95	4.9	2.47	1	3.61	0.62	0.56	0.74	2.62	0.58
Spleen CD8	**8.1 & 8.2**	**5.1 & 5.2**	**6**	**11**	**9**	**13**	**3**	**17a**	**7**	**14**	**2**	**10b**	**12**	**4**	**8.30**
Dkk3 -/-	5.49	5.24	7.95	0.87	4.26	0.64	4.17	0.53	0.64	1.14	0.29	1.05	1.52	0.69	0.56
B6	6.23	4.69	11.7	0.57	6.71	0.28	5.67	0.94	0.86	1.86	0.16	0.21	0.52	1.6	0.17
Spleen CD4	**8.1 & 8.2**	**5.1 & 5.2**	**6**	**11**	**9**	**13**	**3**	**17a**	**7**	**14**	**2**	**10b**	**12**	**4**	**8.3**
B6 in B6	9.65	2	3.62	4.58	7.04	1.36	4.33	3.39	1.35	3.54	0.72	4.88	1.38	4.97	0.7
B6 in Dkk3	9.59	1.82	3.02	6	6.52	1.46	3.99	3.65	0.94	3.71	6.45	2.11	0	1.58	0.78
Dkk3 -/- in B6	10	1.72	2.66	5.16	7.02	1.12	4.74	3.93	0.87	3.43	0.62	1.51	1.92	4.57	0.62
Spleen CD8	**8.1 & 8.2**	**5.1 & 5.2**	**6**	**11**	**9**	**13**	**3**	**17a**	**7**	**14**	**2**	**10b**	**12**	**4**	**8.3**
B6 in B6	7.94	5.81	13.2	0.64	5.3	0.48	3.66	1.47	1.55	2.37	0.15	1.22	0.35	3.72	0.37
B6 in Dkk3	8.12	5.37	15	0.86	5.32	0.19	3.91	2.05	1.45	2.33	0	0.51	□	0.59	0.16
Dkk3 -/- in B6	7.83	4.59	14.1	0.78	4.99	0.31	4.86	1.31	1.46	2.5	0.14	0.31	0.49	3.65	0.23

Table 5-4. Absence of Dkk3 from the thymus does not result in altered positive selection. The thymic and splenic CD4 and CD8 T cells from Dkk3$^{-/-}$, Dkk3$^{+/+}$ mice and Dkk3$^{-/-}$ in Dkk3$^{+/+}$, Dkk3$^{+/+}$ in Dkk3$^{-/-}$ and Dkk3$^{+/+}$ in Dkk3$^{+/+}$ chimeras were screened for the percentage of different Vβ chain populations.

5.4.2 T cell-extrinsic factors predominantly contribute to Dkk3$^{-/-}$ T cell hyperproliferation

The Dkk3$^{-/-}$ T cell hyperproliferation could be explained in two ways. One possibility is that CD8 T cells or another splenic cell population produce Dkk3. Thus, the absence of local Dkk3 production in Dkk3$^{-/-}$ spleen leads to impaired control of T cell proliferation. On the

other hand, it cannot be excluded that non-hematopoietic tissue-derived Dkk3 somehow influences the proliferative capacity of naïve T cells. In other words, $Dkk3^{-/-}$ T cell hyperproliferation could result either from lack of splenocyte-derived Dkk3 or tissue-derived Dkk3. To further analyze this point bone marrow chimeras were used, which carried both donor-derived and host-derived T cells, due to partial host T cell depletion by irradiation. By this means, the proliferation of $Dkk3^{+/+}$ and $Dkk3^{-/-}$ T cells that are both derived from either a Dkk3 deficient or a Dkk3 sufficient mouse could be compared in one host.

Moreover, if Dkk3 was secreted in a non-detectable amount within in the lymphoid organs, or as suggested above by a subpopulation of CD8 T cells, the presence of Dkk3-blocking monoclonal anti-mouse Dkk3 antibody during the *in vitro* T cell stimulation would result in increased T cell proliferation, resembling the phenotype of $Dkk3^{-/-}$ T cell. The results of the above described experimental approaches will be presented below.

5.4.2.1 The hyperproliferation of $Dkk3^{-/-}$ T cells is controlled in a $Dkk3^{+/+}$ mouse

Wild type mice carrying the CD45.2 congenic marker on lymphocytes or CD45.1 mice having the CD45.1 congenic marker were sublethally irradiated. In some mice 40-50 % of the host lymphocytes survived upon irradiation and these were chosen as recipients for the generation of mixed bone marrow chimeras. The recipient mice were then injected with CD45.1 or $Dkk3^{-/-}$ (carrying the CD45.2 congenic marker) bone marrow cells respectively ($Dkk3^{+/+}$→$Dkk3^{+/+}$ and $Dkk3^{-/-}$→$Dkk3^{+/+}$ chimeric mice). After reconstitution, splenocytes were isolated from the chimeric mice, labeled with CFSE and let to proliferate *in vitro* in the presence of anti-CD3 (2µg/ml) and anti-CD28 (1µg/ml) antibodies. The proliferation of the host- and donor-derived T cells was then compared by flow cytometry (Figure 25). As shown, the two populations displayed around 50 % chimerism in the radioresistant CD8 T cell compartment and 70 % chimerism in the more radiosensitive CD4 T cell compartment. However, both donor derived CD4 and CD8 T cells proliferated as strong as the host CD4 and CD8 T cells. More specifically, the proliferation of the $Dkk3^{-/-}$ T cells was not increased in comparison to this of the wild type T cells, when the $Dkk3^{-/-}$ T cells had developed in a Dkk3 sufficient environment. Since it has been already shown that there are no differences in the intrathymic selection between the knockout and control mice, the observed differences indicate that external (T cell- or non T cell-derived) Dkk3 can control the T cell reactivity (Figure 27a).

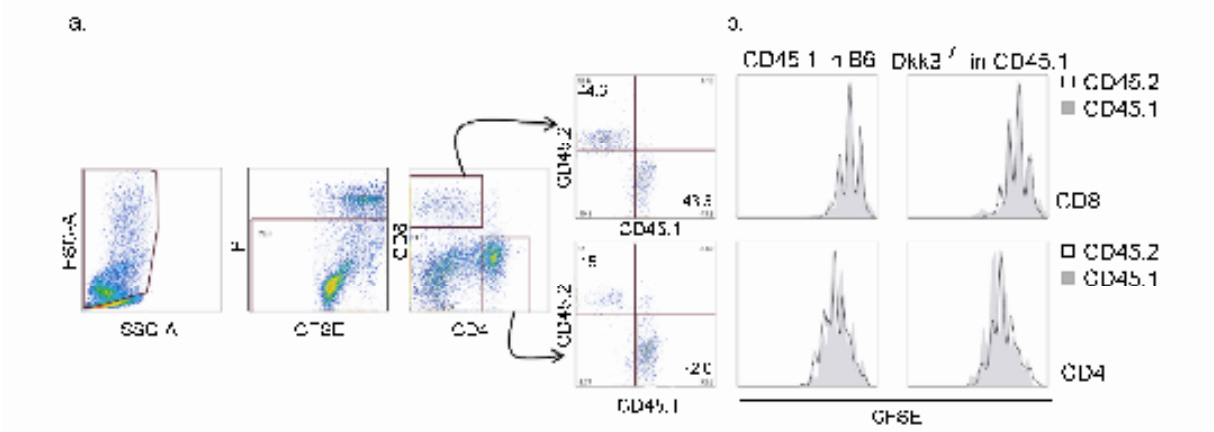

Figure 5-25. Dkk3 deficient T cells are regulated in chimeric Dkk3$^{-/-}$ → Dkk3$^{+/+}$ mice carrying host Dkk3$^{+/+}$ T cells. Spleen cells were isolated from the Dkk3$^{-/-}$ → Dkk3$^{+/+}$ (CD45.1) and control Dkk3$^{+/+}$ (CD45.1) → Dkk3$^{+/+}$ (CD45.2) chimeric mice and labeled with CFSE prior to T cell stimulation with anti-CD3 (2µg/ml) and anti-CD28 (1µg/ml). Four days upon stimulation T cell proliferation was assessed by the dilution of the CFSE dye. (**a**) Donor and recipient derived T cells from the Dkk3$^{-/-}$ → Dkk3$^{+/+}$ chimeric mice were gated according to the surface CD45.2 and CD45.1 marker. The dot plots are representative of the Dkk3$^{+/+}$ → Dkk3$^{+/+}$ chimeric mice as well. (**b**) CD4 and CD8 T cell proliferation in Dkk3$^{-/-}$ → Dkk3$^{+/+}$ and Dkk3$^{+/+}$ → Dkk3$^{+/+}$ spleens was measured by flow cytometry. One representative of four independent experiments is shown.

5.4.2.2 Dkk3$^{+/+}$ T cells reach the Dkk3$^{-/-}$ T cell proliferation rate in a Dkk3$^{-/-}$ mouse

Dkk3$^{+/+}$ CD45.1 bone marrow was then transferred into irradiated Dkk3$^{+/+}$ or Dkk3$^{-/-}$ CD45.2 recipient mice (Dkk3$^{+/+}$→Dkk3$^{+/+}$ and Dkk3$^{+/+}$ → Dkk3$^{-/-}$ chimeric mice). Like in the experimental setting described before, the chimerism ranged between 30-50%, so the *in vitro* T cell proliferation of both Dkk3$^{+/+}$ and Dkk3$^{-/-}$ T cells derived from the same mouse could be compared. Interestingly, the Dkk3$^{+/+}$ T cells in the Dkk3$^{-/-}$ host proliferated as much as the remaining Dkk3$^{-/-}$ host T cells (Figure 26a). This proliferation rate was increased in comparison to Dkk3$^{+/+}$ T cells derived from a Dkk3 sufficient environment (Figure 26b). Thus the production of Dkk3 in the non-hematopoietic tissues is essential for the prevention of T cell hyperproliferation (Figure 27b and c).

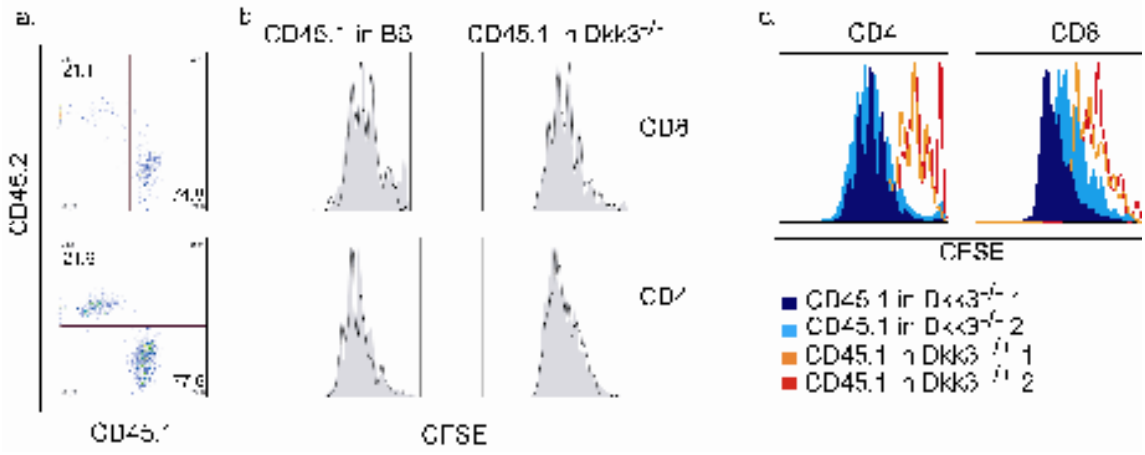

Figure 5-26. Wild type T cells in chimeric Dkk3$^{+/+}$ → Dkk3$^{-/-}$ mice carrying Dkk3$^{-/-}$ T cells display elevated proliferation rate. Spleen cells were isolated from the Dkk3$^{+/+}$ (CD45.1) → Dkk3$^{-/-}$ and control Dkk3$^{+/+}$ (CD45.1) → Dkk3$^{+/+}$ chimeric mice and labeled with CFSE prior to T cell stimulation with anti-CD3 (2µg/ml) and anti-CD28 (1µg/ml). Four days upon stimulation, T cell proliferation was assessed by the dilution of the CFSE dye. (**a**) Donor and recipient derived T cells from the Dkk3$^{+/+}$ → Dkk3$^{-/-}$ chimeric mice were gated according to the surface CD45.2 and CD45.1 marker. The dot plots are representative of the Dkk3$^{+/+}$ → Dkk3$^{+/+}$ chimeric mice as well. (**b**) CD4 and CD8 T cell proliferation in Dkk3$^{+/+}$ → Dkk3$^{-/-}$ and Dkk3$^{+/+}$ → Dkk3$^{+/+}$ spleens was measured by flow cytometry. One representative of four independent experiments is shown. (**c**) The proliferation rate of the Dkk3$^{+/+}$ (CD45.1) → Dkk3$^{-/-}$ chimeras-derived wild type CD4 and CD8 T cells was compared to the one of Dkk3$^{+/+}$ (CD45.1) → Dkk3$^{+/+}$ chimeras-derived wild type CD4 and CD8 T cells by histogram analysis. The results of two independent experiments are shown.

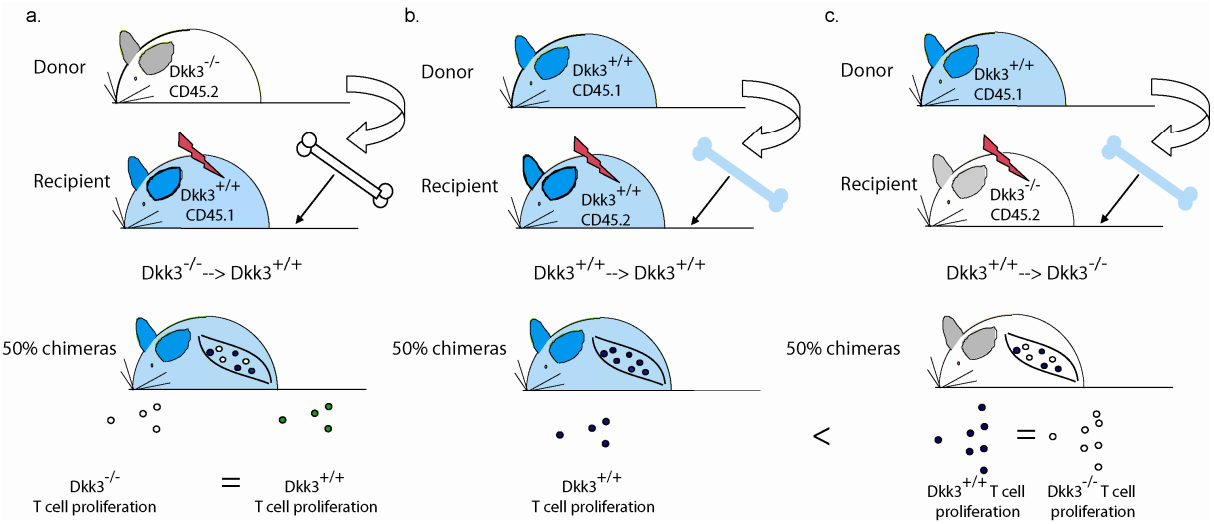

Figure 5-27. Overview of the experiments with the 50% bone marrow chimeric mice. (**a**) In order to prove that Dkk3$^{-/-}$ T cell proliferation is not a permanent T cell-intrinsic attribute, 50% Dkk3$^{-/-}$→Dkk3$^{+/+}$ chimeric mice were generated so that Dkk3$^{-/-}$ and Dkk3$^{+/+}$ T cell proliferation could be compared in the same Dkk3 sufficient host. In the presence of host non-hematopoietic tissue- or T cell-derived Dkk3 protein, Dkk3$^{-/-}$ T cells did not proliferate stronger that Dkk3$^{+/+}$ T cells. (**b**) Dkk3$^{+/+}$ T cell proliferation in Dkk3$^{+/+}$→Dkk3$^{+/+}$ chimeric mice was used as a control. (**c**) In order to investigate the contribution of non-hematopoietic tissue-derived Dkk3 protein 50% Dkk3$^{+/+}$→Dkk3$^{-/-}$ chimeric mice were generated so that the proliferation of Dkk3$^{+/+}$ T cells that were

derived from Dkk3 deficient host could be compared with the proliferation of $Dkk3^{+/+}$ T cells that were derived from Dkk3 sufficient host. $Dkk3^{+/+}$ T cells that had developed in a $Dkk3^{-/-}$ environment proliferated stronger than the control.

5.4.2.3 *In vitro* Dkk3 blockade is not sufficient for induction of *in vitro* T cell hyperproliferation

In order to confirm that, unlike tissue-derived Dkk3, potential splenocyte-derived Dkk3 is not crucial for the control of T cell responses, *in vitro* T cell proliferation assays were performed in the presence of the anti-Dkk3 blocking antibody. In detail, $Dkk3^{+/+}$ splenocytes were stimulated with titrated amounts of anti-CD3 and anti-CD28 antibodies in the presence of the Dkk3-blocking monoclonal anti-Dkk3 antibody (10μg/ml) or the control mouse serum derived IgG. T cell proliferation was assessed by thymidine incorporation at day 4 upon T cell stimulation. In the presence of the anti-Dkk3 antibody the proliferation of the isolated CD4 and CD8 T cells was similar to the control (Figure 28). It was not increased as one would expect if the anti-Dkk3 antibody would have neutralized spleen cell derived Dkk3. The blocking ability of the anti-Dkk3 monoclonal antibody has been shown in *in vivo* experiments presented in this thesis (Figures 16 and 46). Its inability to induce increased T cell proliferation suggests that if any Dkk3 is secreted in the spleen, its amount is not enough to regulate T cell responsiveness. It is thus likely that tissue derived Dkk3 is responsible for the regulation of T cell proliferation.

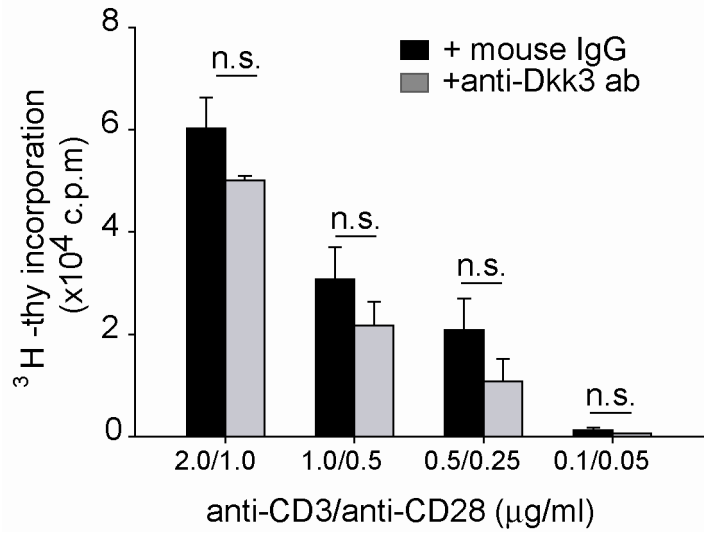

Figure 5-28. T cell proliferation is not increased in the presence of the anti-Dkk3 monoclonal antibody. Wild type T cells were stimulated with titrated amounts of anti-CD3 and anti-CD28 antibody in the presence of 10 μg/ml anti-Dkk3 antibody or mouse serum-derived IgG. T cell proliferation was measured at day 4 upon stimulation by thymidine incorporation. The mean+/-s.e.m of triplicate values of one experiment are shown. (P>0.1)

5.5 Molecular mechanisms of Dkk3$^{-/-}$ T cell hyperproliferation

In summary, lack of Dkk3 leads to increased T cell proliferation. Very low Dkk3 production by splenocytes and its contribution to the observed effect cannot be excluded, but tissue-derived Dkk3 seems to definitely play a role in the control of T cell proliferation. Since isolated Dkk3$^{-/-}$ CD8 T cells display increased proliferation it could be proposed that the absence of Dkk3 permanently alters the biochemistry of T cell stimulation and proliferation. In this chapter the changes in CD8 T cell signaling pathways resulting from the lack of Dkk3 will be investigated.

5.5.1 Dkk3 does not interfere with the TGF-β pathway in T cells

The TGF-β signaling pathway is known to restrain T cell proliferation. Upon binding of TGF-β to its receptor on the T cell membrane, the Smad2 and Smad3 proteins are phosphorylated. This leads to the formation of the Smad2/3 complex, which in turn binds to the cytoplasmic protein Smad4. The Smad2/3/4 complex translocates to the nucleus, where it regulates gene transcription (Nakao et al. 1997; Derynck et al. 2003). The induced genes limit T cell proliferation.

Smad4 has been shown to be degraded by ubiquitination upon Ras activation (Saha et al. 2001). It should be noted that T cell stimulation involves Ras activation and therefore Smad4 degradation. At this point it is interesting to mention that Dkk3 was reported to be required for TGF-β signaling in the Xenopus laevis embryo since it stabilizes Smad4 by downregulating the ubiquitin ligase ectodermin (Pinho et al. 2007).

Therefore, it was analyzed whether the increase of T cell proliferation in the absence of Dkk3 could be attributed to unresponsiveness of T cells to TGF-β due to Smad4 proteolytic degradation. First, TGF-β was added to *in vitro* proliferating Dkk3$^{+/+}$ and Dkk3$^{-/-}$ T cells and the percentage of inhibition of T cell proliferation was calculated. Both at high and low TGF-β doses there was no decrease in the percentage of inhibition (Figure 29). In detail, the mean Dkk3$^{-/-}$ T cell proliferation was decreased from 120,020 to 5,555 thymidine counts by the presence of 5ng/ml TGF-β. Similarly, the mean Dkk3$^{+/+}$ T cel proliferation was decreased from 67,561 to 2,175 counts by TGF-β. Therefore it seems unlikely that absence of Dkk3 leads to Smad4 degradation and TGF-β unresponsiveness.

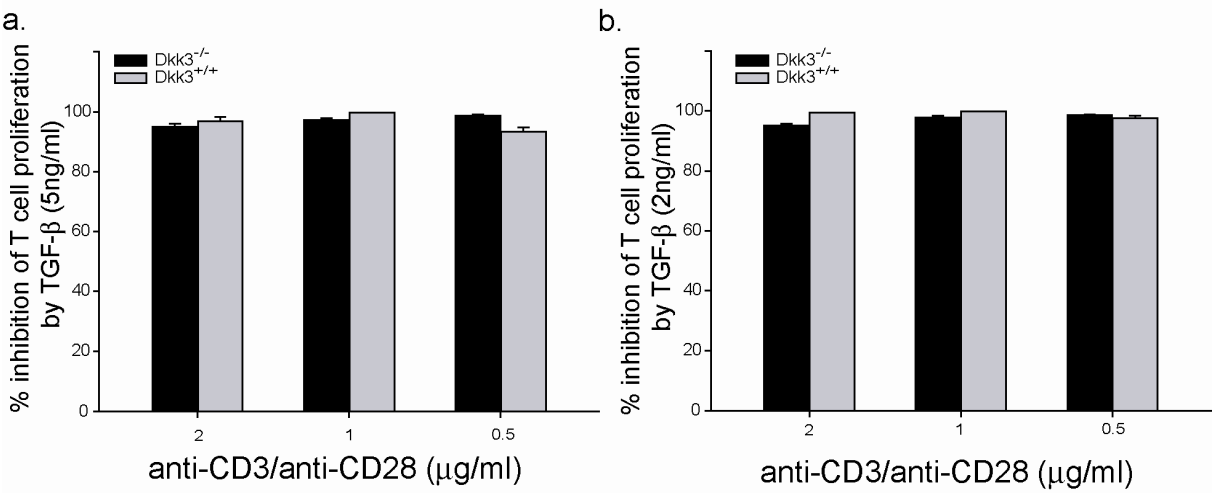

Figure 5-29. TGF-β signaling is not deficient in the absence of Dkk3. Dkk3$^{+/+}$ and Dkk3$^{-/-}$ T cells were stimulated with anti-CD3 (2 µg/ml) and anti-CD28(1 µg/ml) in the presence of TGF-β and T cell proliferation was measured at day 4 upon stimulation by thymidine incorporation. The percentage of TGF-β-mediated inhibition of T cell proliferation was calculated as the difference of thymidine counts in the absence and the presence of TGF-β divided by the counts in the absence of TGF-β. (**a**) A high dose (5 ng/ml) of TGF-β was added to the T cell proliferation assay. Mean+/-s.e.m of two independent experiments are shown. (**b**) a low dose (2 ng/ml) of TGF-β was added to the T cell proliferation assay. Mean+/- of triplicates of one experiment are shown.

Moreover, Western Blot analysis of the cytoplasmic levels of Smad4 in CD8 T cells derived from Dkk3$^{-/-}$ and Dkk3$^{+/+}$ mice was performed. CD8 T cells were stimulated with anti-CD3 (2µg/ml) and anti-CD28 (1µg/ml) for the indicated time, varying from 2 to 48 hours (Figure 30). The CD8 T cell protein lysates were analyzed for the relative amount of Smad4 by western blot analysis. The levels of the calnexin protein were used as a reference, since it is not newly synthesized or degraded during T cell stimulation. There was no increase in Smad4 degradation noticed in the Dkk3$^{-/-}$ CD8 T cells.

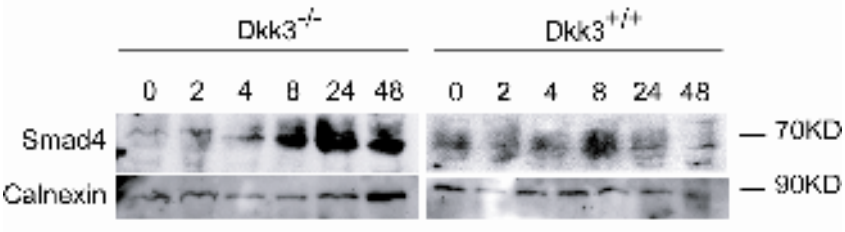

Figure 5-30. Smad4 degradation is not decreased in the absence of Dkk3 from CD8 T cells. MACS isolated Dkk3$^{-/-}$ and Dkk3$^{+/+}$ CD8 T cells were stimulated with anti-CD3 (2µg/ml) and anti-CD28 (1µg/ml) for the indicated times. The stimulated CD8 T cell protein lysates were then tested for the levels of Smad4 protein by western blot analysis. The levels of calnexin were used as a control for the protein loading amount. One representative of three independent experiments is shown.

5.5.2 Lack of Dkk3 leads to an altered ERK pathway activity upon CD8 T cell stimulation

The next CD8 T cell signaling pathway to be examined was the ERK MAPK pathway. TCR triggering leads to the activation in the one hand of the Src-type tyrosine kinases Lck and Fyn, followed by ZAP-70 and on the other hand the activation of phospholipase C-γ (PLCγ) (Noh et al. 1995; Pacholczyk et al. 2007). The tyrosine kinases are responsible for the phosphorylation and recruitment of the LAT adaptor protein (Pitkanen et al. 2003). PLC-γ mediates the generation of DAG (Crabtree 1989). The LAT adaptor protein and the DAG messenger initiate two independent signaling pathways that both lead to the activation of Ras GTPase (van Leeuwen et al. 1999; Stone 2006). The active Ras-GTP in turn phosphorylates the c-Raf kinase, thus initiating the ERK pathway. Activated c-Raf catalyses MEK phosphorylation. Phosphorylated MEK then activates ERK1 and ERK2. ERK activation upon T cell stimulation leads to Fos protein activation which together with c-Jun forms the AP-1 transcription factor. AP-1 nuclear translocation and transcriptional function are essential for T cell proliferation. Thereby, the transcription of IL-2 is induced, which in turn leads to the survival and proliferation of T cells (Cantrell 1996). Since ERK inhibition is a feature of T cell anergy and tolerance, it was reasonable to study the effect of the absence of Dkk3 on this particular signaling pathway.

5.5.2.1 In the absence of Dkk3 IL-2 production upon T cell stimulation is increased

The first hint that the activation of the ERK pathway could be altered in the absence of Dkk3 was the fact that $Dkk3^{-/-}$ T cells not only proliferated stronger, but that they also produced higher levels of IL-2. The supernatants of the proliferating $Dkk3^{-/-}$ and $Dkk3^{+/+}$ T cells was tested for IL-2 at day 1 upon stimulation. The increased proliferative capacity of the $Dkk3^{-/-}$ splenocytes was found to be accompanied by an increase in IL-2 production (Figure 31)

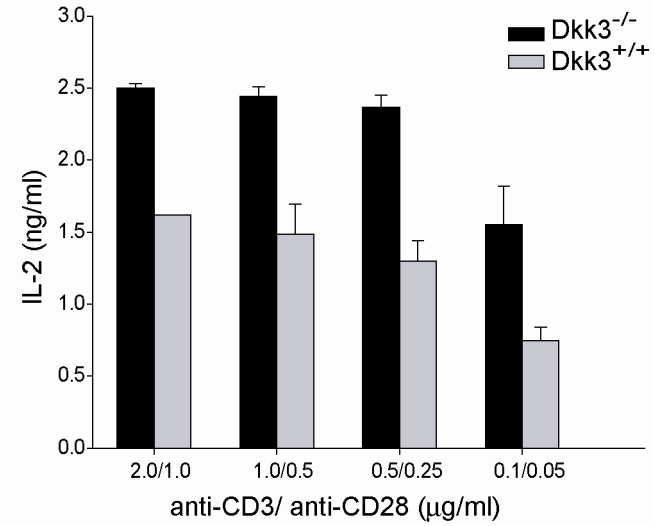

Figure 5-31. In the absence of Dkk3 splenocyte IL-2 production is increased. Dkk3$^{-/-}$ and Dkk3$^{+/+}$ spleen cells were stimulated with varying concentrations of anti-CD3 and anti-CD28 antibodies. IL-2 production was measured by ELISA 24 hours upon stimulation. A representative of three independent experiments +/- s.e.m is shown.

5.5.2.2 In the absence of Dkk3 the ERK MAPK pathway activity is increased

Knowing that Dkk3$^{-/-}$ T cells produce higher amounts of IL-2, the activation state of the upstream p42 and p44 kinases, following Dkk3$^{-/-}$ and wild type CD8 T cell stimulation was examined. MACS purified CD8 T cells were stimulated with the DAG analogue PMA (250nM) for 15min at 37˚C. Alternatively, TCR signaling was simulated by CD8 T cell incubation with anti-CD3ε-biotin followed by streptavidin cross-linking for 1, 3 and 5 minutes at 37˚C. Western blot analysis showed that lack of Dkk3 in CD8 T cells leads in higher ERK activation (Figure 32a, 32b).

MEK phosphorylation was also increased in Dkk3$^{-/-}$ CD8 T cells, indicating that the phospho-ERK inhibition takes place upstream of MEK. On the other hand, Ras-GTP levels remained unchanged in the absence of Dkk3 (Figure 31b). This data suggest that Dkk3 specifically inhibits ERK activation by acting on the level of the c-Raf kinase. It inhibits either the phosphorylation of MEK by the activated c-Raf kinase of the phosphorylation of c-Raf itself. However, the analysis of the phospho c-Raf kinase levels in *ex-vivo* isolated CD8 T cells by immune precipitation and western blotting was technically difficult with the available antibodies.

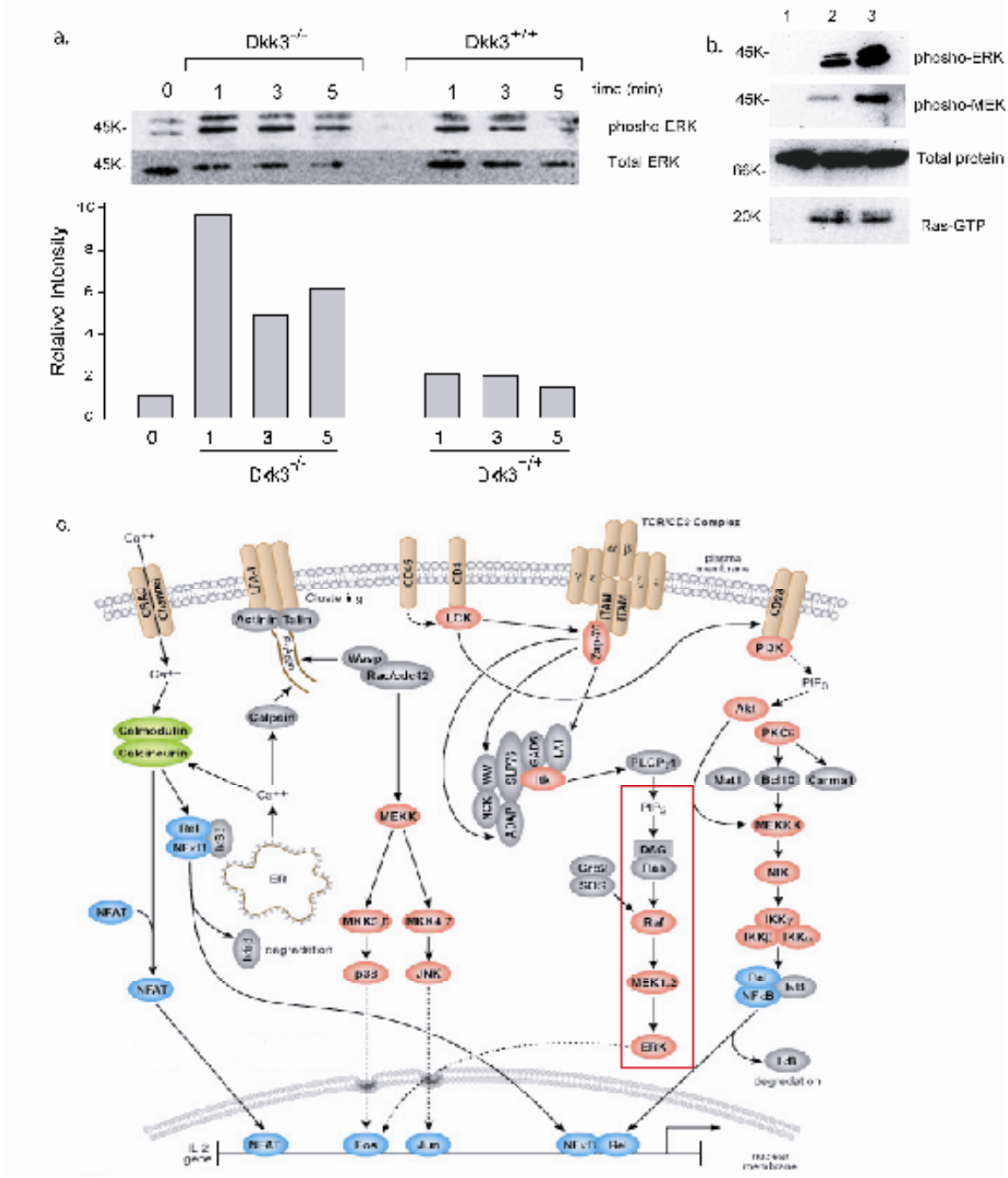

Figure 5-32. Dkk3 specifically inhibits the ERK-MAPK signaling pathway. (**a**) MACS isolated Dkk3$^{+/+}$ and Dkk3$^{-/-}$ CD8 T cells were stimulated with biotynilated anti-CD3 which was crosslinked to streptavidin for the indicated time and the levels of phosphorylated and total ERK-MAPK were detected by Western Blot analysis. The blot and the quantitative results of one out of 3 independent experiments are shown. (**b**) MACS isolated (2) Dkk3$^{+/+}$ and (3) Dkk3$^{-/-}$ CD8 T cells were stimulated with PMA 250nM for 15min and the activation levels of ERK, MEK and Ras were detected by Western Blot analysis. In series (1) non-stimulated control CD8 T cells were analyzed. Representative results of three independent experiments are shown. (**c**) Schematic representation of the signalling events that are initiated after TCR triggering. The central role of ERK MAPK pathway in TCR signal transduction is highlighted.

5.5.3 Dkk3$^{-/-}$ CD8 T cells display no changes in the p38 MAPK and PKCθ/NF-κB signaling

Next, it was investigated whether the lack of Dkk3 affected other signaling molecules apart from the ERK pathway. In detail, the p38, JNK, phospho-Akt and NF-κB signaling pathway activities were examined. The p38 MAPK is induced upon TCR stimulation and costimulation. Additionally, some cytokine receptors, such as IL-12R, IL-18R and TNFR, can activate p38 MAPK. In CD8 T cells, p38 MAPK phosphorylation has been reported to induce increased IFNγ production and caspase-mediated apoptosis. However, p38 triggering upon TCR stimulation of isolated CD8 T cells in the absence of Dkk3 was not altered (Figure 33).

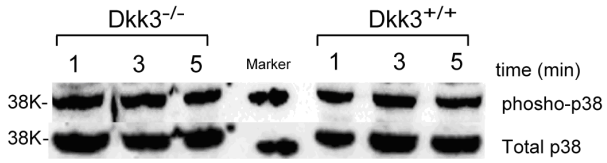

Figure 5-33. Dkk3 deficiency does not influence the p38-MAPK signaling pathway. MACS isolated Dkk3$^{+/+}$ and Dkk3$^{-/-}$ CD8 T cells were stimulated with PMA (250nM) and ionomycin (10μM) for the indicated time at 37˚C and the levels of phosphorylated and total p38-MAPK protein were assessed by Western Blot analysis. One representative of two independent experiments is shown.

The IκBα phosphorylation status was then investigated, since IκBα is a specific inhibitor of the nuclear factor NF-κB. NF-κB activation is induced upon TCR stimulation accompanied by costimulatory signals. TCR triggering leads to the activation of the PKCθ, which cooperates with Akt1 to induce IKK activity. IKK is the complex of two catalytic subunits (IKKα and IKKβ) and the regulatory IKKγ (NEMO) protein. The IKK complex phosphorylates the IκB proteins, thus allowing their subsequent polyubiquitination and proteasomal degradation. Upon IκB degradation, NF-κB is released and phosphorylated and translocates to the nucleus, where it regulates gene expression. To test whether the absence of Dkk3 affects the NF-κB pathway, the IκBα phosphorylation status and integrity was analyzed by western blot analysis. If Dkk3$^{-/-}$ CD8 T cells display NF-κB hyperactivation, IκBα phosphorylation upon TCR triggering should be increased and the total IκBα levels should be reduced due to its proteolytic degradation. However, the lack of Dkk3 does not seem to affect the NF-κB pathway (Figure 34).

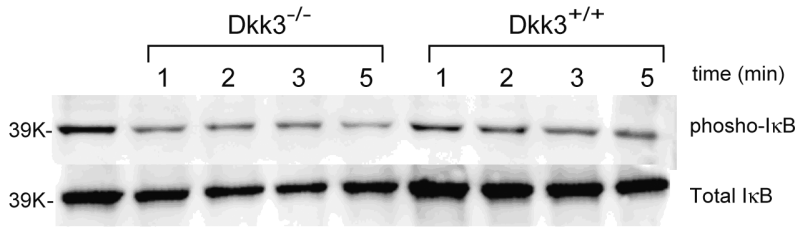

Figure 5-34. Dkk3 deficiency does not influence the NF-κB signaling pathway. MACS isolated Dkk3$^{+/+}$ and Dkk3$^{-/-}$ CD8 T cells were stimulated with biotynilated anti-CD3 which was crosslinked to streptavidin for the indicated times. The levels of phosphorylated and total IκB protein were assessed by Western Blot analysis. One representative of two independent experiments is shown.

5.6 Dkk3 is secreted by immune privileged tissues and contributes to the control of T cell reactivity

In the previous paragraphs Dkk3 was shown to be involved in the maintenance of peripheral tolerance in the Des-TCR transgenic mouse model and to regulate polyclonal T cell reactivity. As mentioned in the introduction though, apart from the mechanisms of systemic peripheral T cell tolerance, immune homeostasis is preserved by the establishment of a local immunosuppressive microenvironment in non-regenerative tissues that are vital for host survival. Therefore it was interesting to investigate whether Dkk3 expression also contributes to the immunosuppressive environment detected in immune privileged organs.

5.6.1 Dkk3 is expressed by immune privileged tissues

It has been reported that Dkk3 mRNA is present in peripheral tissues, including the brain, spinal cord, eye, heart, ovary, uterus and liver (Niehrs 2006). By using the monoclonal anti-Dkk3 antibody in ELISA Dkk3 protein could be traced in the tissues of two different inbred mouse strains. It is worth mentioning that Dkk3 protein was found to be present in the brain, the spinal cord and the eye. Additionally, the lung and the heart also expressed a significant level of Dkk3 (Table 5). The liver produced Dkk3 protein as well (Table 5). Finally, the embryo and the ovary, uterus and placenta all contained Dkk3 (Table 5). On the other hand, Dkk3 was absent from the skin, spleen, lymph nodes, thymus and serum. These results were confirmed by histological analysis.

	B6 mouse			CBA mouse		
Organ	1:5	1:10	1:100	1:5	1:10	1:100
Brain	1.2	1.2	0.6	1.4	1.4	0.5
Eye	1.2	1.0	0.2	1.4	1.3	0.2
Lung	0.5	0.3	0	1.0	0.6	0
Heart	1.0	0.8	0	1.3	1.0	0
Liver	0.7	0.4	0	1.2	0.2	0
Thymus	0	0	0	0.2	0.1	0
Spleen	0	0	0	0.1	0	0
Lymph node	0	0	0	0.3	0.1	0
Serum	0	0	0	0	0	0
Skin	0	0	0	0	0	0
Pancreas	0.3	0.1	0	0	0	0
Uterus	0.9	0.7	0.1	1.0	0.6	0
Embryo	1.34	1.32	1.21			
Placenta	1.32	1.29	0.44			
Control:						
Dkk3-GST	1.3	1.3	1.3			

Values expressed as OD at 492 nm

Table 5-5. Dkk3 protein expression in peripheral tissues. Organs were isolated from C57.Bl6 and CBA mice and the protein lysates were titrated and screened for Dkk3 by ELISA. Organ lysates from Dkk3$^{-/-}$ mice displayed no Dkk3 antibody binding (data not shown). A representative of three independent experiments is shown for the C57.Bl6 mouse. The CBA mouse organs were tested in ELISA in a single experiment.

In order to define the cell type in the central nervous system that expresses Dkk3, brain sections were analyzed for Dkk3 expression pattern using the markers Neurofilament N and Glial fibrillary acidic protein (GFAP). Neurofilament N is a specific marker for the neuronal cells and was found to be co-localized with Dkk3 protein (Figure 35). On the other hand, GFAP positive cells, which are the astrocytes, were not found to express Dkk3 in the steady state or during EAE. However, astrocytes isolated from the neonatal brain and expanded by *in vitro* culture were found to be positive for Dkk3 mRNA in RT-PCR. Apparently, the cell activation upon culture, which resembles strong inflammatory signals, induced the expression of Dkk3 in astrocytes.

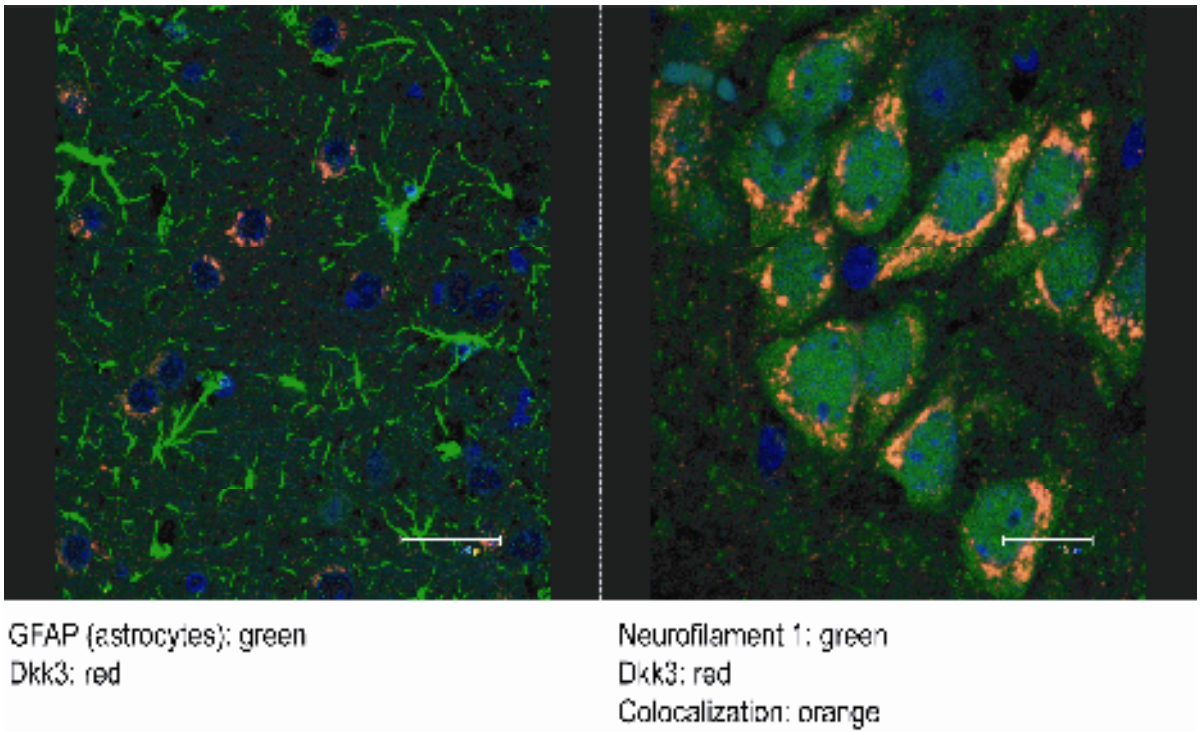

Figure 5-35. Dkk3 expression in the brain is to neurons but not to astrocytes. The brain of C57Bl6 mice that had been perfused with formaldehyde was analyzed for Dkk3 expression by confocal microscopy. The cell markers Neurofilament N for neuronal cells and GFAP for astrocytes were also used for the determination of the Dkk3-producing cell type.

5.6.2 Secretory Dkk3 protein suppresses CD4 and CD8 T cell proliferation

It was shown that lack of Dkk3 leads to increased T cell proliferation. Dkk3 expression was found to be prevalent in the immune privileged tissues. The reasonable question was then whether the presence of Dkk3 in peripheral tissues is important for the control of T cell responses. To address this, the direct effect of secreted Dkk3 on T cells was investigated with a series of *in vitro* assays.

5.6.2.1 Dkk3 protein has a direct effect on CD4 and CD8 T cell proliferation

In order to study the direct effect of Dkk3 on T cell proliferation, the Dkk3-secreting HEK 293T-Dkk3 cells were used (see also paragraph 5.2.2). The HEK 293T-Dkk3 and the control HEK 293T cells were irradiated with 300 Gray and plated in 96-well plates in a concentration of 10^5cells/well. After irradiation the HEK 293T cells were living, thus expressed and secreted Dkk3, but were not able to proliferate. Either splenocytes or MACS-isolated CD8 T cells were added to the plate, at a final concentration of 10^5cells/well. The T cell proliferation was measured by thymidine incorporation at day 4 and the results of 3 independent experiments are shown in figures 36 and 37.

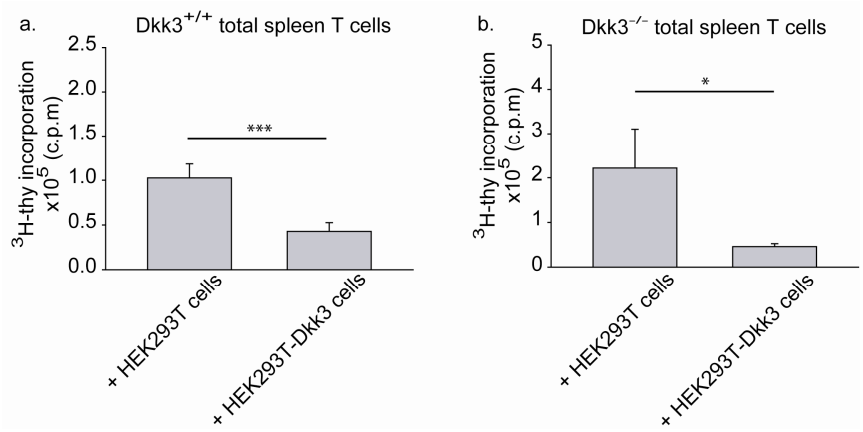

Figure 5-36. Dkk3 protein secreted by the HEK293T-Dkk3 cells suppresses T cell proliferation in vitro. **S**pleenocytes from Dkk3$^{+/+}$ (a) and Dkk3$^{-/-}$ (b) mice were stimulated with anti-CD3 (2μg/ml) and anti-CD28 (1μg/ml) in the presence of irradiated HEK293T or HEK293T-Dkk3 T cells. T cell proliferation was measured by thymidine incorporation at day 4 upon stimulation. Mean+/- s.e.m from three independent experiments is shown. (* P<0.05, *** P<0.001)

The secreted Dkk3 could down-regulate total spleen T cell proliferation as well as CD8 T cell proliferation. The effect was observed in both Dkk3$^{+/+}$ and Dkk3$^{-/-}$ groups, but was more pronounced with the knockout T cells (Figures 36b and 37b). It seems that the secreted Dkk3 can bind to a yet unknown receptor on the T cells and directly suppress their proliferation.

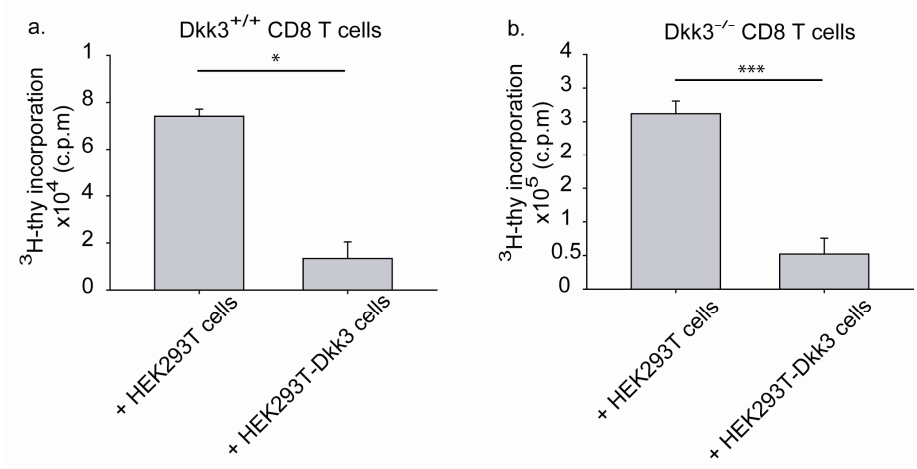

Figure 5-37. Dkk3 protein secreted by the HEK293T-Dkk3 cells suppresses CD8 T cell proliferation in vitro. MACS isolated CD8 T cells from Dkk3$^{+/+}$ (a) and Dkk3$^{-/-}$ (b) mice were stimulated with anti-CD3 (2μg/ml) and anti-CD28 (1μg/ml) in the presence of irradiated HEK23T or HEK293T-Dkk3 T cells. T cell proliferation was measured by thymidine incorporation at day 4 upon stimulation. Mean+/- s.e.m from three independent experiments is shown. (* P<0.05, *** P<0.001)

Furthermore, it was tested whether the observed effect of Dkk3-HEK 293T cells on T cell proliferation was exclusively due to the presence of secreted Dkk3. Purified recombinant mouse Dkk3 protein was added to *in vitro* proliferating T cells. The recombinant mouse Dkk3 inhibited CD4 and CD8 T proliferation in a concentration dependent manner (Figure 38).

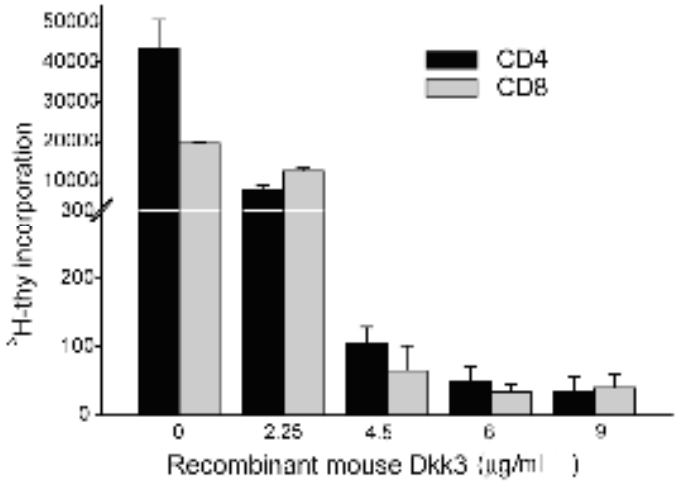

Figure 5-38. Recombinant mouse Dkk3 protein suppresses CD4 and CD8 T cell proliferation *in vitro*. The proliferation of MACS isolated wild type CD4 and CD8 T cells in the presence of titrated concentrations of recombinant mouse Dkk3 protein was measured by thymidine incorporation at day 4 after anti-CD3 (2µg/ml) and anti-CD28 (1µg/ml) stimulation. One representative of three independent experiments +/-s.e.m is shown.

5.6.2.2 Dkk3 protein regulates activated T cells by suppressing their proliferation *in vitro*

Up to this point the effect of Dkk3 protein on T cell proliferation was studied by administration of the recombinant mouse Dkk3 to naïve T cells. Nonetheless, it was intriguing to investigate whether the suppressive function of Dkk3 could also be exerted on pre-activated T cells. Therefore, recombinant mouse Dkk3 protein (3.5µg/ml) was added to activated CD4 or CD8 T cells, that had been stimulated *in vitro* with anti-CD3 (2µg/ml) and anti-CD28 (1µg/ml) for two days. T cell proliferation was measured 4 days upon T cell stimulation and 2 days upon addition of recombinant mouse Dkk3 protein to the proliferating T cell medium. Indeed, Dkk3 protein could inhibit further proliferation of the pre-activated CD4 and CD8 T cells (Figure 39).

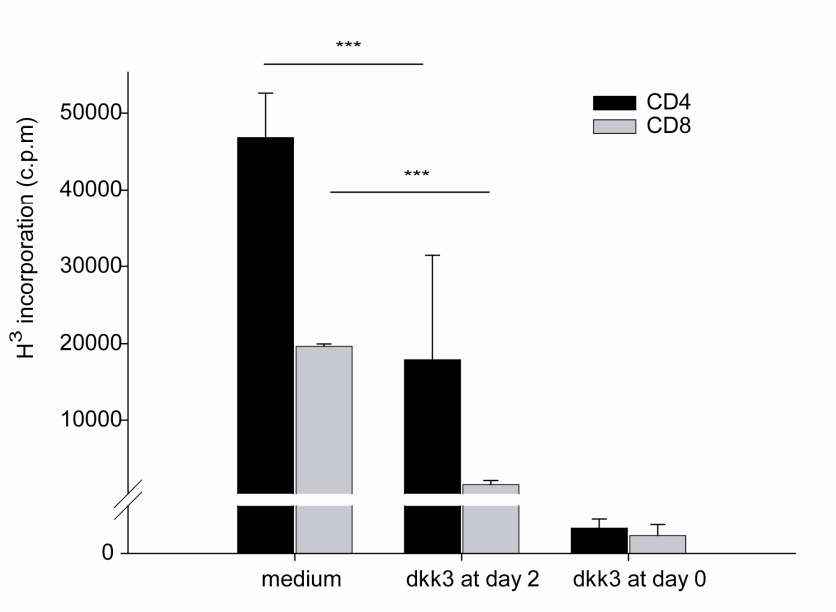

Figure 5-39. Recombinant mouse Dkk3 protein can inhibit activated T cells from proliferating. MACS isolated CD4 or CD8 T cells were stimulated with anti-CD3 (2µg/ml) and anti-CD28 (1µg/ml). Recombinant mouse Dkk3 was added to the T cell medium at day two upon stimulation and T cell proliferation was assessed at day 4 after T cell stimulation by thymidine incorporation. Means of triplicates +/- s.e.m of one experiment are shown (*** P<0.001)

5.6.2.3 Dkk3-mediated regulation of T cell proliferation involves an increase in T cell apoptosis

Various mechanisms may lie behind the observed inhibitory effect of Dkk3 on T cell proliferation. One possibility is that Dkk3 induces early apoptosis of the activated T cells. To address this, C57.Bl/6 splenocytes or MACS isolated CD8 T cells were stimulated with anti-CD3 (2µg/ml) and anti-CD28 (1µg/ml) antibodies in the absence or the presence of 3.5µg/ml Dkk3 protein. It has been reported that Dkk3 induces tumor cell apoptosis in a cell-density dependent manner (Hsieh et al. 2004). Therefore, titrated cell numbers were stimulated in the presence of Dkk3 in a constant volume of 0.2ml in a 96-well plate.

In order to screen T cell apoptosis, the binding of annexin V to the cell surface was used as an early apoptotic marker. One of the earliest indications of apoptosis is the translocation of the membrane phospholipid phosphatidylserine (PS) from the inner to the outer leaflet of the plasma membrane. Once exposed to the extracellular environment, binding sites on PS become available for Annexin V, a 35-36 kDa, Ca^{2+}-dependent, phospholipid binding protein with a high affinity for PS. Annexin V-binding cells can then be detected by flow cytometry. The proapoptotic cells are the annexin V positive, propidium iodide (PI) negative fraction and the late apoptotic or dead cells are within the annexin V positive PI positive fraction.

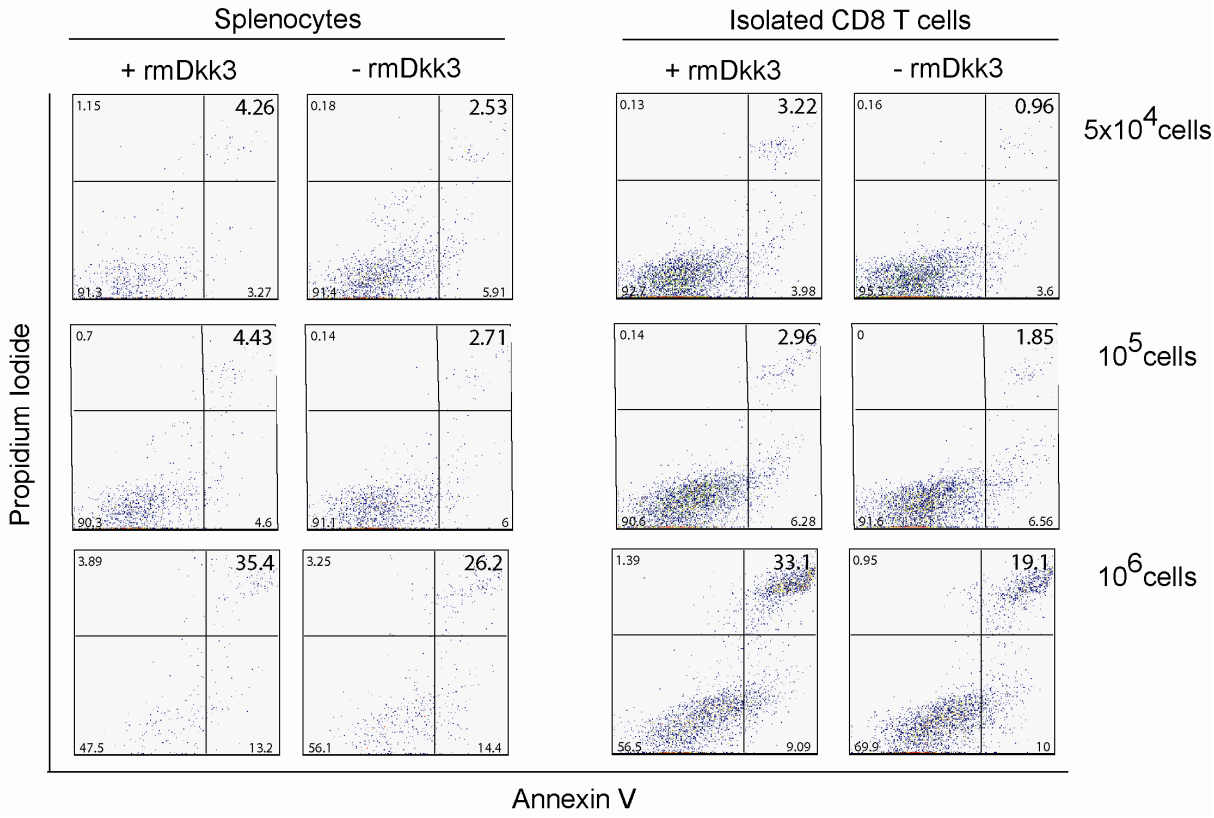

Figure 5-40. Activation induced cell death is increased in the presence of recombinant mouse Dkk3 protein. Titrated densities of Splenocytes or MACS isolated CD8 T cells from C57.Bl6 mice were stimulated with anti-CD3 (2μg/ml) and anti-CD28 (1μg/ml) in the presence or absence of recombinant mouse Dkk3 protein (3.5μg/ml). The percentage of apoptotic (annexin and propidium iodide positive) T cells was assessed by flow cytometry 24 hours upon stimulation.

As shown in Figure 40, rmDkk3 protein resulted in increased percentages of apoptotic T cells. In detail, in CD4 and CD8 T cells in total spleen recombinant mouse Dkk3 induced a mean 1.6 fold upregulation of apoptosis. The effect of rmDkk3 on the isolated CD8 T cells was more pronounced, with an average 2.2 fold increase in the percentage of apoptotic cells.

5.7 Dkk3 regulates T cell responses in Experimental Autoimmune Encephalitis

Up to this point, it has been shown that Dkk3 protein is secreted by immune privileged tissues and can control T cell reactivity *in vitro*, partially through the induction of T cell apoptosis. Obviously, it was intriguing to investigate the role of tissue-secreted Dkk3 in the regulation of T cell responses *in vivo*. Knowing that high amounts of Dkk3 are produced in the brain, the model of EAE was the ideal experimental system to address this point.

5.7.1 Dkk3$^{-/-}$ mice display more severe and persistent EAE

To determine whether the clinical course of EAE was altered in the absence of Dkk3, Dkk3$^{-/-}$ and Dkk3$^{+/+}$ mice were immunized with MOG_{35-55} peptide in CFA and additionally received two doses of pertussis toxin at days 0 and 2.

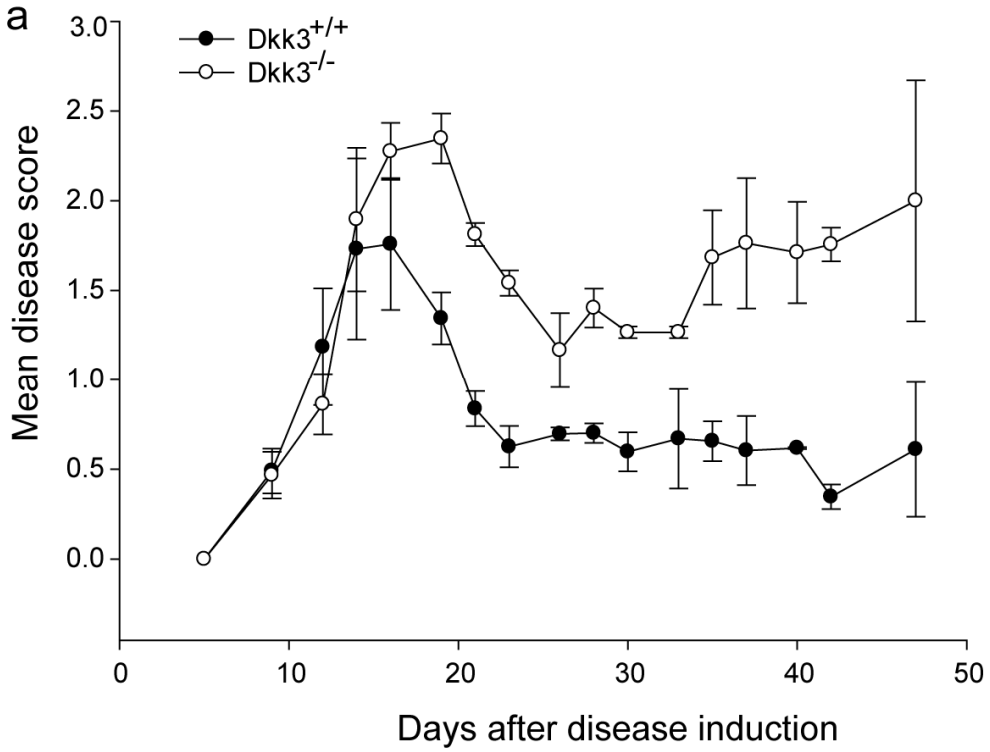

Figure 5-41. Absence of Dkk3 results in more severe and persistent EAE. Dkk3$^{+/+}$ and Dkk3$^{-/-}$ mice were immunized with MOG_{33-55} in CFA plus pertussis toxin and the EAE symptoms were assessed every second day. Mean +/- s.e.m of three independent experiments are shown.

The clinical data from more than 60 days of observation of three independent experiments (Figure 41 and Table 6) indicated that lack of Dkk3 leads to more severe and persistent EAE. The disease onset (days 10-14) was similar in wild type and Dkk3$^{-/-}$ animals. At the peak of the disease, however, at day 15, the Dkk3$^{-/-}$ mice displayed more severe symptoms. The mean maximum disease score remained higher for the Dkk3$^{-/-}$ group throughout the 60 days of observation. As shown in table 6 four Dkk3$^{-/-}$ mice and only one wild type mouse died from severe EAE.

	Incidence	Mean Onset (Day)	Mean Maximum score	Dead mice
DKK3 $^{+/+}$	24/26	11.1+/-2.6	2.4+/-1.1	1
DKK3 $^{-/-}$	25/25	10.8+/-2.3	3.1+/-1.1 (P<0.05)	4

Table 5-6. Clinical data from three independent EAE experiments. The mean onset refers to the mean+/-s.e.m day upon immunization that the first symptoms were observed. The mean maximum score refers to the mean+/-s.e.m disease maximum of each mouse.

The EAE graph shows that the wild type mice recovered from the disease after day 22, but the mice lacking Dkk3 remained ill and their clinical state did not ameliorate during the observation time. The increased disease chronicity in the Dkk3$^{-/-}$ group is more apparent in figure 42, where the mice that have died from the disease are excluded from the analysis. The disease duration in the living mice is shown.

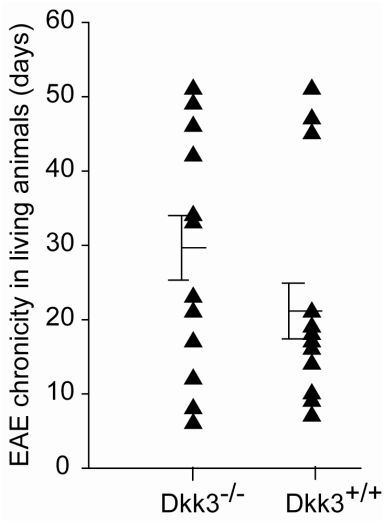

Figure 5-42. EAE diseased Dkk3$^{-/-}$ mice display increased EAE disease chronicity. The disease duration of each Dkk3$^{+/+}$ and Dkk3$^{-/-}$ mouse in two independent EAE experiments is shown. The mice that died from the disease were excluded from the analysis.

5.7.2

5.7.3

5.7.4 The increased EAE chronicity in the Dkk3$^{-/-}$ mice is accompanied by persistence of activated CD8 T cells in the CNS.

In order to clarify why Dkk3$^{-/-}$ mice do not recover from EAE, CNS-infiltrating T cells were isolated from the brain and spinal cord of the mice at days 20 and 29. FACS analysis suggested that the severe disease phenotype of Dkk3$^{-/-}$ mice was due to persistence of IFNγ-producing activated CD8 T cells in the CNS (Figure 43). The percentage of TNF-α and IL-17 producing CD4 T cells in the Dkk3$^{-/-}$ mice suffering from EAE were comparable with the ones found in recovered Dkk3$^{+/+}$ mice. Moreover, there was no difference in the cell number and representation of the CNS infiltrating leukocyte types.

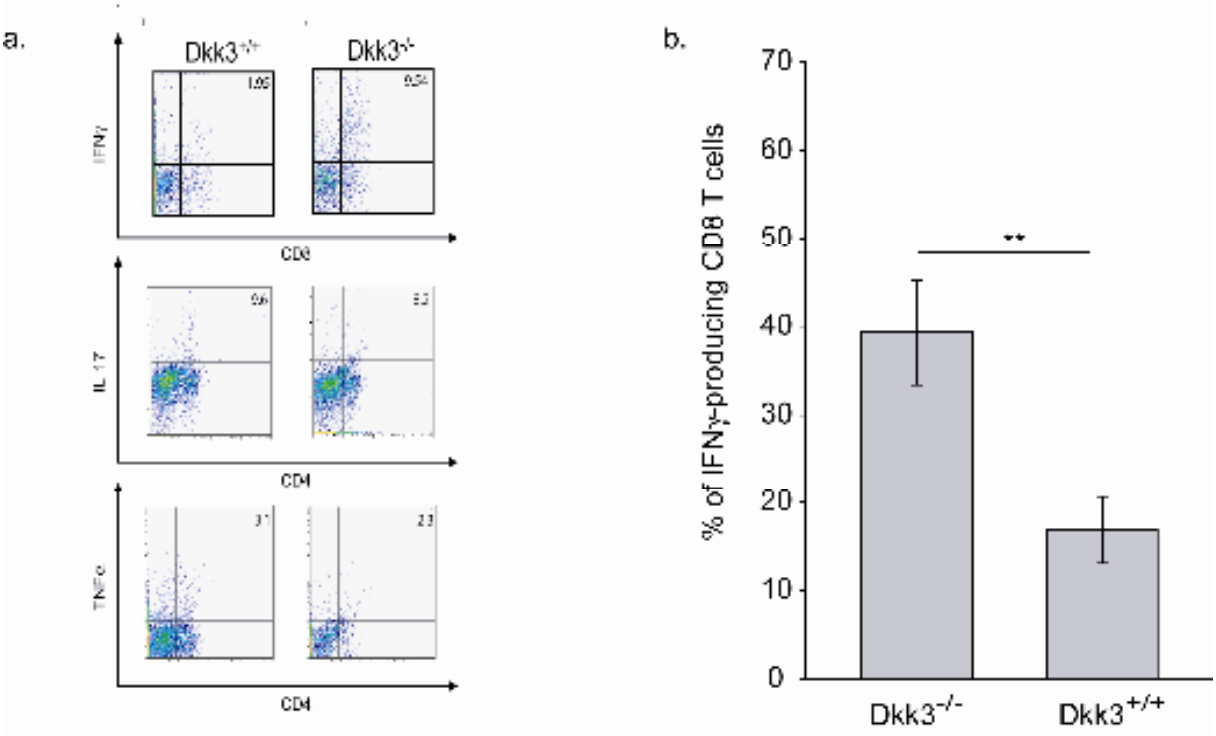

Figure 5-43. In the absence of Dkk3 IFNγ-producing CD8 T cells persist in the CNS of mice suffering from EAE. (**a**) CNS-infiltrating T cells were isolated from EAE-diseased mice and stained intracellularly for the IFNγ,IL-17, TNFα cytokine expression. Representative results of five independent experiments are shown. (**b**) The mean +/- s.e.m of the percentage of IFNγ-producing CD8 T cells in the CNS of EAE diseased mice, at day 29 upon EAE immunization. (**P<0.01)

5.7.5 Neuron-derived Dkk3 is crucial for the control of EAE

As already mentioned, Dkk3 production by T cells could not be proven, neither in this thesis nor by others (Krupnik et al. 1999; Niehrs 2006). However, it can not be formally excluded that T cells express undetectable amounts of Dkk3, which modify their function, or that T cell development in a $Dkk3^{-/-}$ host has an effect on T cell reactivity. Thus, the last question asked was whether the observed severe EAE phenotype in $Dkk3^{-/-}$ mice was strictly a T cell-intrinsic effect or due to the absence of the neuron-derived Dkk3.

To address this point, bone marrow chimeras were constructed. Bone marrow from wild type mice was transferred to irradiated $Dkk3^{-/-}$ mice and conversely $Dkk3^{-/-}$ bone marrow was injected to wild type recipients. A control group of irradiated wild type mice that received $Dkk3^{+/+}$ bone marrow was also included in the experimental setup. Eight weeks after the reconstitution of the mice, the chimerism was checked by defining the percentage of donor derived B and T cells in the blood and EAE was induced as described. All mice developed very severe symptoms (all displayed an EAE score of 4 or higher), probably because of the

damage induced in the CNS by the extended inflammation caused by the irradiation (Zehntner et al. 2004).

However, there was a difference in the onset of the disease. The Dkk3$^{+/+}$→ Dkk3$^{-/-}$ chimeras developed EAE symptoms earlier, indicating that absence of Dkk3 from the tissues is the main cause of severe EAE. Indeed, the presence of neuron-derived Dkk3 in the brain could partially control T cell responses in the Dkk3$^{-/-}$→ Dkk3$^{+/+}$ and Dkk3$^{+/+}$→ Dkk3$^{+/+}$ chimeric mice (Figure 44).

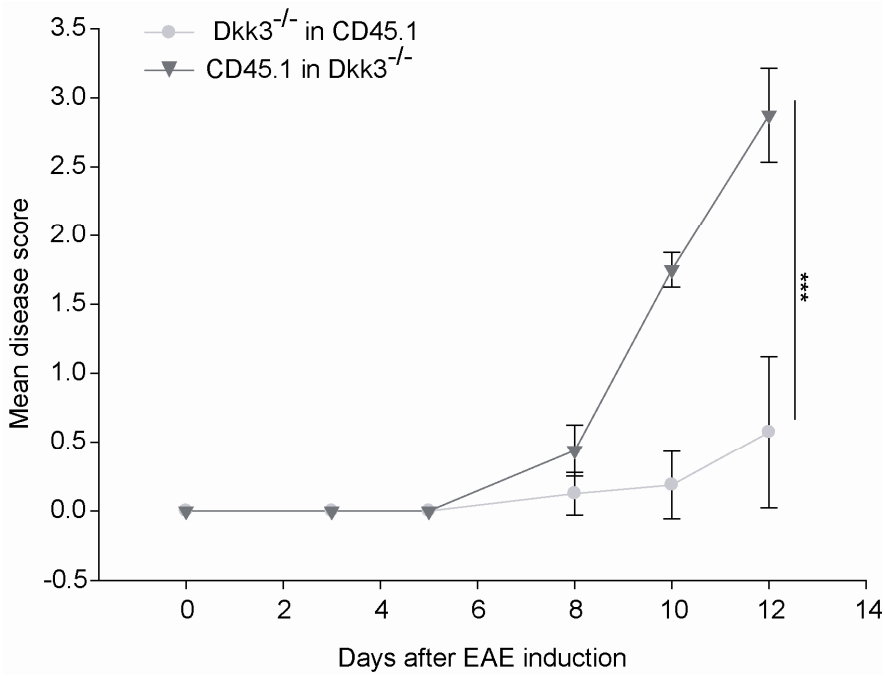

Figure 5-44. Lack of Dkk3 in the brain rather than in T cells leads to more severe EAE. Lethally irradiated Dkk3$^{-/-}$ and Dkk3$^{+/+}$ mice were injected with Dkk3$^{+/+}$ and Dkk3$^{-/-}$ bone marrow cells respectively. Additionally control Dkk3$^{+/+}$ → Dkk3$^{+/+}$ chimeric mice were generated. The chimeras were immunized with MOG_{33-55} in CFA and received two doses of pertussis toxin i.p. The EAE onset is depicted in the graph. The mean+/-s.e.m from each group is shown. All experimental groups consisted of eight mice.

The result obtained in the bone marrow chimeras EAE experiment was confirmed using T cell transfer studies. The aim was to induce passive EAE in Dkk3$^{+/+}$ and Dkk3$^{-/-}$ donor mice by adoptive transfer of pre-activated MOG-specific T cells. Donor Dkk3$^{+/+}$ and Dkk3$^{-/-}$ mice were immunized with MOG_{33-55} peptide (200µg/mouse) in CFA (500ng *M. tuberculosis*/mouse) in the presence of pertussis toxin (250ng/mouse). Ten days upon immunization T cells were isolated from the spleen and the draining lymph nodes of the diseased mice and cultured for 4 days *in vitro* in the presence of the MOG_{33-55} peptide (10µg/ml) and IL-12 (2.5ng/ml), or the MOG_{33-55} peptide (10µg/ml) and IL-12 (25ng/ml) plus IL-2 (0.5ng/ml and upon day 2 of culture 2.5ng/ml) and IL-18 (25ng/ml). After their *in vitro* expansion, MOG_{33-55}-specific T cells were intravenously injected to the recipient mice (1-

$2x10^7$/mouse), which also received pertussis toxin (250ng/mouse) intraperitoneally. Unfortunately, the mice displayed only weak disease symptoms (EAE sores ranged from 0.5 to 1.5) (Figure 45). Therefore, it was not possible to draw a conclusion concerning the role of $Dkk3^{-/-}$ T cells in EAE severity and persistence from this experiment.

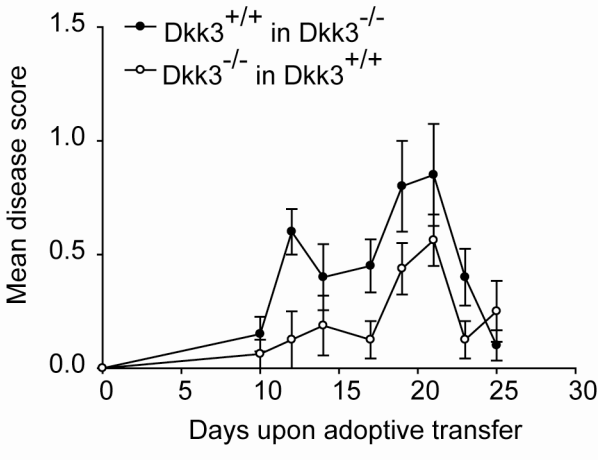

Figure 5-45. Passive EAE induction by adoptive transfer. Activated MOG-specific $Dkk3^{+/+}$ and $Dkk3^{-/-}$ T cells were isolated from immunized donors and expanded *in vitro* in the presence of MOG peptide (10µg/ml) and IL-12 (2.5µg/ml). $Dkk3^{-/-}$ and $Dkk3^{+/+}$ mice received $2x10^7$ activated MOG-specific $Dkk3^{+/+}$ and $Dkk3^{-/-}$ T cells respectively. The disease course was followed. The mean EAE score+/- s.e.m of eight mice per group is shown.

Additionally, transgenic 2D2 mice, carrying the MOG_{33-55}-specific Vβ11 TCR chain, were used as donor mice. However, there was again only slight disease occurrence. The passive immunization was also attempted with simultaneous subcutaneous administration of DCs, which had previously been activated with CpG and loaded with the MOG_{33-35} peptide. $2x10^7$ activated and peptide-loaded DCs were intraperitoneally and subcutaneously injected to the recipient mice. However, again the mice only developed mild EAE symptoms.

It was then considered that adoptive transfer of pre-activated MOG-specific T cells could induce high disease score, when combined with host immunization. Since the simultaneous activation of host T cells by the immunization was not desired, $Rag1^{-/-}$ mice were used as recipient mice. The MOG-specific activated T cells were obtained as described above. The $Rag1^{-/-}$ were transferred with $2x10^7$ T cells and at the same time received pertussis toxin (250ng/mouse) intraperitoneally. One day after the adoptive transfer, the recipient mice were immunized with MOG_{33-55} peptide in CFA. At day two the mice received an extra dose of pertussis toxin. The disease symptoms started at day 4, as the MOG specific T cells were already activated. The disease course mediated by $Dkk3^{-/-}$ T cells was comparable with the one induced by $Dkk3^{+/+}$ T cells (Figure 46). This strongly suggests that the presence or absence of Dkk3 in T cells is not the decisive factor for the protection against autoimmunity.

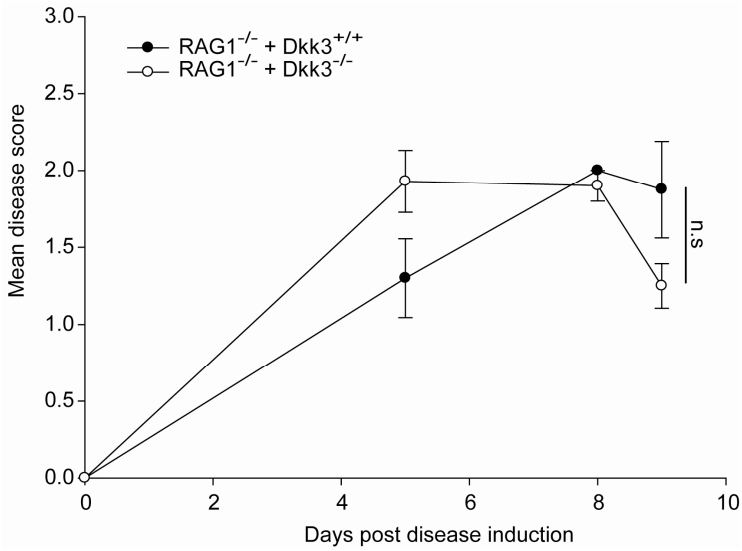

Figure 5-46. Dkk3$^{-/-}$ and Dkk3$^{+/+}$ T cells cause equally severe EAE symptoms in Rag1$^{-/-}$ host mice. Activated MOG-specific Dkk3$^{+/+}$ and Dkk3$^{-/-}$ T cells were isolated from immunized donors and expanded *in vitro* in the presence of MOG peptide (10µg/ml) and IL-12 (2.5µg/ml). Rag1$^{-/-}$ mice received 2x10^{7} activated MOG-specific Dkk3$^{+/+}$ and Dkk3$^{-/-}$ T cells and pertussis toxin. One day after transfer the mice were immunized with MOG in CFA. At day 2 upon adoptive T cell transfer the Rag1$^{-/-}$ were injected with pertussis toxin. The disease course was followed. The mean EAE score+/- s.e.m of five mice per group is shown.

Finally, the Dkk3-blocking monoclonal antibody was employed to prove that the presence of secreted Dkk3 in CNS is important for the regulation of the autoimmune response. Additionally by this approach it was possible to confirm that the altered EAE phenotype of the Dkk3$^{-/-}$ mice cannot be attributed to different thymic selection of the developing T cells or to another yet undefined T cell-intrinsic effect of Dkk3.

EAE was induced in wild type mice by immunization with the MOG_{33-55} peptide in CFA and injection of pertussis toxin (250ng/mouse) as described above. Additionally the mice received intraperitoneally 1 mg of anti-Dkk3 monoclonal antibody or control mouse IgG at day 7. Administration of 0.5mg of antibody per mouse was repeated at days 10, 15, 20, 25, 35 and 50.

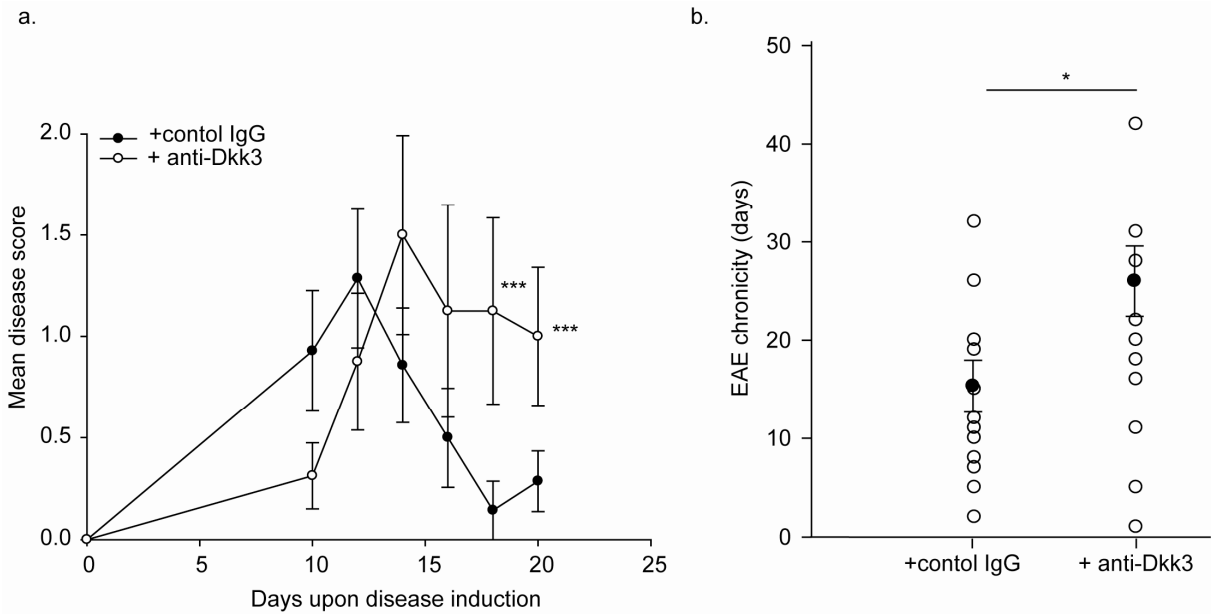

Figure 5-47. Dkk3 blockade by the monoclonal anti-Dkk3 antibody leads to increased EAE chronicity. C57.Bl/6 mice were immunized with MOG peptide in CFA and pertussis toxin. Additionally, one experimental group received anti-Dkk3 and the other control mouse IgG at days 7 (1mg/mouse), 10, 15, 20, 25 and 35 (0.5mg/mouse). (**a**) The mean disease score+/-s.e.m of seven mice pro group is shown. The results are from one representative out of three independent experiments. (***P<0.001). (**b**) The disease duration of each EAE-immunized mouse is shown. Pooled data from two independent experiments are presented. (*P<0.05)

Blockade of the secreted Dkk3 by the anti-Dkk3 monoclonal antibody resulted in slightly elevated and longer lasting EAE scores in C57.Bl/6 mice (Figure 47a and 47b). The disease onset was similar in both groups. Importantly, the disease chronicity was significantly increased in mice that received the anti-Dkk3 antibody in each of the three experiments.

6 DISCUSSION

The main point of the current thesis is the identification of Dickkopf 3 protein as a universal immune regulator. Briefly, Dkk3 was shown to be expressed and secreted by tolerant CD8 T cells in a transgenic mouse model of parenchymal cell-induced CD8 T cell tolerance. In this mouse model, secretory Dkk3 was proved to be essential for the mediation of T cell suppression in a paracrine function. Moreover, studies carried out with polyclonal T cells of the C57.BL/6 background indicated the crucial role of Dkk3 in controlling T cell reactivity. Last but not least, Dkk3 was shown to contribute to the protection of immune privileged organs from the devastating consequences of extended immune responses. The characterization of Dkk3 as a mediator of immune suppression in more than one contexts, e.g. in the Des-TCR CD8 T cell tolerance, in T cell responses in the secondary lymphoid organs and in immune privileged organs, is of importance, considering that there are not many molecules reported to have such a wide spectrum of function. The detailed aspects of Dkk3 function as well as the significance of these findings will be discussed below.

6.1 Characterization of the gene expression profile of the Des-TCR regulatory CD8 T cells

The characterization of the gene expression profile of the tolerant CD8 T cells could give insight into novel molecular mechanisms of immune suppression. Indeed, gene expression analysis of the regulatory Des-TCR CD8 T cells has revealed the upregulation of genes, which encode either for markers of the CD4+CD25+FoxP3$^+$ natural Treg cells, or for mediators of the regulatory function of natural Treg cells. The pronounced expression of TGF-β, CTLA-4, CCR5, neuropilin-1, Epstein-Barr virus-induced gene 3 (EBI3) and granzyme B indicates that regulatory Des-TCR CD8 T cells display common markers and suppressive mechanisms with natural Treg cells (Figure 5-10).

TGF-β is a well characterized immune suppressive cytokine. It has been shown to induce the differentiation of adaptive Treg cells and is crucial for the suppressive function of both natural and induced Tregs (Wan et al. 2007). Moreover, TGF-β has been shown to contribute to the immunosuppressive microenvironment of the immune privileged tissues (Niederkorn 2006). The expression of TGF-β underlies the observed regulatory function of Des-TCR CD8 T cells in the tolerant Des-TCRxKerK^b mice.

CTLA-4 is a surface molecule, expressed by all activated T cells but not by the naïve T cells. Like CD28, CTLA-4 is a receptor for the B7 costimulatory molecules that are expressed on APCs and provide the signal 2 for T cell stimulation. However, unlike CD28, its ligation leads

to the suppression of T cell activation and proliferation (Greenwald et al. 2005). CTLA-4 was also found to be expressed by natural Treg cells and was shown to be indispensible for their suppressive function (Itoh et al. 1999; Kingsley et al. 2002; Read et al. 2006). CTLA-4 has been found to mediate Treg suppressive function, by stimulating the APCs to upregulate the immunosuppressive enzyme IDO (Puccetti et al. 2007). Notably, CTLA-4, together with TGF-β, are the sole Treg-related genes whose disruption results in a severe phenotype, similar to the phenotype of Treg deficient mice (Tang et al. 2008). Thus CTLA-4 might also contribute to the regulatory function of the Des-TCR CD8 T cells.

The chemokine receptor CCR5 is expressed on activated CD4 and CD8 T cells, NK cells, macrophages, and dendritic cells (Murphy et al. 2000). The ligands for this receptor, CCL3, CCL4, and CCL5, are expressed at sites of inflammation. Thus, CCR5 may play a role in the migration of effector cells to the tissues (Huffnagle et al. 1999; Glass et al. 2001; Murai et al. 2003; Deaglio et al. 2007). Interestingly however, multiple studies in CCR5-deficient mice demonstrate enhanced cell-mediated immune responses during pathogen infection (Sato et al. 1999; Algood et al. 2004), delayed-type hypersensitivity (Liu et al. 2007), and tumor vaccination (Ng-Cashin et al. 2003) suggesting an immunoregulatory role for CCR5. Expression of CCR5 by Treg cell is critical for the suppression of immune responses *in vivo*, since it directs Treg cells to the sites of inflammation (Wysocki et al. 2005; Yurchenko et al. 2006). Subsequently, CCR5 may be of importance for the suppressive capacity of the tolerant Des-TCR CD8 T cells, by enabling their migration to the inflamed tumor or skin grafts.

Neuropilin 1 (Nrp1) was first identified as a receptor for the class 3 semaphorins and members of the vascular endothelial growth factor (VEGF) family (Romeo et al. 2002). It has been shown to be constitutively expressed by the natural Treg cells and to promote regulatory T cell activity (Bruder et al. 2004). In detail, Nrp1 has been reported to bind the latency-associated peptide (LAP)-TGF-β, which is the latent form of TGF-β, as well as free LAP and active TGF-β (Glinka et al. 2008). Moreover, Nrp1 was demonstrated to prolong the contact between Treg cells and immature DCs in steady state conditions (Sarris et al. 2008). Importantly, increased expression of Nrp1 in the tolerant CD8 T cells is an additional hint for their regulatory role. In the future Nrp1 could be studied as a marker for the regulatory CD8 T cells, since it is a surface molecule that is not expressed on naïve and activated CD8 T cells.

EBI-3 molecule is a member of the IL-12 family of proteins. It is homologous to the p40 subunit of the IL-12 cytokine and until recently it was only known to heterodimerize with p28 subunit to form the cytokine IL-27 (Holscher 2004). Interestingly, it was lately shown to form a heterodimer with the p35 subunit of IL-12, which was given the name IL-35. EBI-3 and p35

are both expressed by natural Treg cells and IL-35 has been reported to contribute to their regulatory function *in vitro* and *in vivo* (Collison et al. 2007). Moreover, EBI-3 has been shown to be expressed by the placenta, where it has been suggested to exert an immune suppressive role (Devergne et al. 1997). Interestingly, EBI-3, but not p35 or p40, is expressed by the regulatory Des-TCR CD8 T cells. This indicates that it may be a mediator of immune regulation upon binding to an unknown subunit of the IL-12 family or by forming homodimers.

Granzyme B is a caspase-like serine protease released from cytotoxic CD8 T cells and NK cells within granules against virus-infected host cells and tumor cells (Andrade et al. 2004). Once in the target cells, it activates the caspases and the proapoptotic molecule Bid by proteolytic cleavage, thereby inducing apoptosis (Lord et al. 2003). Its upregulation in the tolerant Des-TCR CD8 T cells, which are not able to reject the P815 tumor carrying their cognate K^b antigen, is however not a paradox, since granzyme B has been lately reported to be expressed by natural Treg and to mediate their suppressive function. Interestingly, granzyme B has been shown to be upregulated in natural Treg cells and to mediate cell contact-dependent suppression *in vitro*, by inducing apoptosis of effector CD4 T cells (Gondek et al. 2005). Additionally, in *in vivo* studies Treg cells have been reported to suppress tumor clearance in a granzyme B-dependent fashion, which involves the death of NK and CD8 T cells (Cao et al. 2007). Granzyme B has also been implied to mediate the suppressive function of CD4 and CD8 double positive $CD25^+$ regulatory T cells that are isolated from the lymph nodes of diabetic NOD mice (Qin et al. 2006). Importantly, granzyme B has been demonstrated to be expressed by other CD8 regulatory T cell populations (Mahic et al. 2008). Thus, it is reasonable to suggest that granzyme B upregulation in the Des-TCR tolerant CD8 T cells it may contribute to their suppressive function.

Interestingly, FoxP3, the transcription factor that is crucial for natural Treg differentiation and function is not upregulated in the tolerant CD8 T cells. This finding differentiates the regulatory Des-TCR CD8 T cells from other $FoxP3^+$CD8 T cell regulatory populations which are either induced *in vitro* (Kapp et al. 2006) or *in vivo*, during ACAID (Jiang et al. 2007) or murine lupus (Sharabi et al. 2008). This suggests that the development of self antigen-specific tolerant CD8 T cells in the neonatal mouse follows distinct molecular proccess from the development of $FoxP3^+$ regulatory T cells in the thymus (natural Treg cells) or in the periphery (adaptive Treg cells). However, the occurring suppressive T cells may employ

common mechanisms of regulatory function, such as expression of TGF-β, CTLA-4, EBI-3, Nrp1 and granzyme B.

6.2 Dkk3 is up-regulated in tolerant CD8 T cells and is crucial for their regulatory function

Having identified numerous genes that are differentially regulated in the Des-TCR regulatory CD8 T cells, a decision had to be made, which candidate gene product should be studied in detail to establish a causal link between enhanced gene expression and the observed *in vivo* tolerance. Among the differentially expressed genes Dickkopf 3 was chosen for further investigation. Importantly Dkk3 is a secreted molecule that could mediate regulation of the proximate T cells. Moreover, it had been shown to inhibit the ERK MAPK signaling (Lodygin et al. 2005), which is crucial for T cell proliferation and IL-2 production. Finaly, Dkk3 mRNA has been reported to be up-regulated in many immune privileged tissues, such as the brain, the embryo and the ovaries. All these clues indicated that Dkk3 could be a potential mediator of Des-TCR CD8 T cell regulation.

Dkk3, mRNA was found to be induced in the tolerant CD8 T cell population by RT-PCR (Figure 5-11). Interestingly, Dkk3 protein was also traced by intracellular staining of tolerant CD8 T cells by flow cytometry (Figure 5-13). In summary, tolerant CD8 T cells express the secretory molecule Dkk3 on the mRNA and protein level.

Studies using Des-TCRxKerK^b mice lacking Dkk3 expression (Dkk3$^{-/-}$xDes-TCRxKerK^b mice) revealed that Dkk3 is not just an intracellular marker of tolerant Des-TCR CD8 T cells but also contributes to their function. In the absence of Dkk3, the Des-TCR CD8 T cells that develop in a mouse expressing the K^b cognate antigen in the skin are not suppressive. K^b-positive P815 tumor cells tumor grafts were rejected with the same kinetics as in the Des-TCR control mice (Figure 5-14).

The role of Dkk3 in Des-TCR CD8 T cell tolerance was also tested upon priming of the Dkk3$^{-/-}$xDes-TCRxKerK^b mice with CpG-activated K^b-positive dendritic cells. The cytotoxic T cells were challenged 7 days after with K^b-positive target cells and the cytotoxicity was measured by FACS. The tolerant Des-TCRx KerK^b mice exhibited no effector cell responses. On the contrary, the Dkk3$^{-/-}$xDes-TCRxKerK^b mice displayed elevated cytotoxicity as compared to the control Des-TCRxKerK^b mice (Figure 5-15).

Thus, Dkk3 is thus indispensable for CD8 T cell tolerance as shown in two independent test systems. From the findings mentioned above it does not become clear whether the presence of Dkk3 is essential for the induction of tolerance by parenchymal cells in the neonatal mice or for the mediation of tolerance during an immune response in the adult individuals. To

examine this, Des-TCRxKerK^{b} mice, which have been shown to develop tolerant CD8 T cells during the neonatal phase, were tested for autologous skin graft acceptance in the presence of Dkk3-blocking antibody. Interestingly, administration of Dkk3-blocking antibody resulted in the rejection of the transplants (Figure 5-16). This indicates that Dkk3 mediates CD8 T cell tolerance upon secretion, therefore blocking of the secreted molecule inhibits immune suppression. Additionally, it is apparent that absence of tolerance is not an artifact of the Dkk3$^{-/-}$xDes-TCRxKerK^{b} mice but it is essential for CD8 T cell tolerance maintenance during the adult phase of wild type Des-TCRxKerK^{b} mice.

Dkk3 is suggested to mediate tolerance upon secretion and binding on target cells rather than by a cell contact-dependent manner. FACS analysis after extracellular staining of Dkk3 on naïve, activated and tolerant Des-TCR CD8 T cells revealed that there is no Dkk3 protein bound on their membrane (Figure 5-17). Since the amounts of membrane-bound Dkk3 were under the detection limit, it is reasonable to propose that the mechanism of Dkk3-dependent tolerance is the secretion of Dkk3 and the paracrine suppression of non-tolerant CD8 T cells.

In summary, Dkk3 protein is expressed by the tolerant Des-TCR CD8 T cells and is indispensable for their suppressive function. Lack of Dkk3 from the Des-TCRxKerK^{b} mice results in the activation of naïve Des-TCR CD8 T cells after encountering their cognate antigen. It is suggestive that the suppressive function of the tolerant Des-TCR CD8 T cell is mediated by the secreted Dkk3, since administration of the blocking anti-Dkk3 antibody in adult mice is sufficient to reverse tolerance against K^{b}-expressing autologous skin grafts. It seems that Dkk3 does not mediate cell-contact dependent suppression, since surface-bound Dkk3 cannot be traced on tolerant Des-TCR CD8 T cells by FACS.

6.3 Dkk3 affects polyclonal T cell reactivity

Dkk3 apparently plays a major role in the establishment of peripheral Des-TCR CD8 T cell tolerance in the transgenic mouse model carrying a single T cell receptor. However, its regulatory role is not limited to this transgenic model of peripheral CD8 T cell tolerance. Dkk3 affects polyclonal T cell reactivity as well. This was shown by a series of experiments with mice of C57.Bl/6 background lacking Dkk3 (Dkk3$^{-/-}$) and in studies of the direct effect of Dkk3 protein on T cell proliferation, which are discussed in paragraph 6.6.

Comparison of the *in vitro* proliferation of Dkk3$^{+/+}$ and Dkk3$^{-/-}$ splenocytes showed that Dkk3$^{-/-}$ CD4 and CD8 T cells proliferate significantly more than the control Dkk3$^{+/+}$ T cells (Figure 5-20). Analysis of the kinetics of Dkk3$^{-/-}$ T cell proliferation by FACS revealed that in the absence of Dkk3, T cells had undergone more proliferation rounds on day 4 (Figure 5-21).

Wild type T cell proliferation reached the Dkk3$^{-/-}$ T cell proliferation level at later time points. This could mean that Dkk3$^{-/-}$ T cells started proliferating earlier or that in the absence of Dkk3 the rate of T cell proliferation was increased. Therefore Dkk3$^{-/-}$ T cells may have died by day 5, due to activation induced cell death and nutrient exhaustion. In general, it seems that Dkk3 expression in mice with polyclonal repertoire sets a limit to T cell reactivity.

The observed hyperproliferation of Dkk3$^{-/-}$ T cells was not an effect of T cell *in vivo* pre-activation. Unpublished work in our lab had shown that the levels of the activation markers on T cells derived from naïve Dkk3$^{-/-}$ are comparably low with these of wild type naïve T cells. Moreover, it was here shown that isolated CD62L^{high} Dkk3$^{-/-}$ naïve T cell proliferation was stronger than the proliferation of Dkk3$^{+/+}$ controls (Figure 5-22), thereby confirming the assumption that the presence of Dkk3 in the wild type mice suppresses the proliferation of T cells upon their stimulation.

The Dkk3-mediated suppression is not related to CD4^{+}CD25^{+}FoxP3^{+} regulatory T cells. It could be possible that such a hyperproliferative Dkk3$^{-/-}$ T cell phenotype was due to Treg malfunction, since Treg cells have been reported to play a major role in the control of T cell reactivity. However, neither was Dkk3 expression found in CD4^{+}CD25^{+}FoxP3^{+} regulatory T cells, nor was the suppressive function of Dkk3$^{-/-}$ Treg cells compromised (Figure 5-23).

To summarize, Dkk3 is indispensable for the control of T cell reactivity in mice with polyclonal TCR repertoire. Absence of Dkk3 leads to T cell hyperproliferation upon stimulation of naïve T cells through T cell receptor. Expression analysis accompanied by functional studies suggests that Dkk3 is not a mediator of natural Treg function, but controls activated T cell proliferation via a Treg-independent mechanism.

The observed effect of Dkk3 on polyclonal T cell reactivity contradicts the reports, according to which Dkk3 is not expressed by lymphoid organs, e.g. spleen, lymph nodes and thymus. These data were validated in our lab both by RT-PCR and ELISA (Table 5-5). However, Dkk3 mRNA and protein were traced in the tolerant Des-TCR CD8 T cells (Figures 5-11 and 5-13). Moreover, only after mRNA amplification naïve and activated Des-TCR CD8 T cell samples displayed hybridization with the Dkk3 gene probes on the GeneChip microarrays. Similarly, in a microarray study done by Kaech *et al.*, it was reported that Dkk3 expression levels in P14 transgenic CD8 T cells were decreased during the peak as well as the late phase of the immune response (days 8-22 post LCMV viral infection) and then increased as the memory CD8 T cell population was stabilized (Kaech et al. 2002). This suggests that in the particular study Dkk3 mRNA was also present in the naïve, activated and memory CD8 T cell samples in tiny amounts that could be traced only upon mRNA amplification.

FACS analysis of the Dkk3 protein levels in lymphocytes from wild type mice was not efficient in detecting a CD8 T cell population expressing the Dkk3 protein. Similarly, CD4 T cells, NK cells, dendritic cells, monocytes and stromal spleen cells were also negative for Dkk3 (Figures 5-18 and 5-19).

Generally, it cannot be excluded by the FACS analysis that a tiny undetectable spleen cell population expresses Dkk3. Indeed, considering the consequences of the extended expression of a negative regulator of T cell responses in the spleen of naïve mice, it is reasonable to suggest that if there is any Dkk3 expression in spleen or in other lymphoid organs, it is so limited that it cannot be traced by RT-PCR, FACS and ELISA analysis of the total organ. Based on the Des-TCRxKerK^{b} transgenic model it could be hypothesized that only few self antigen-specific T cells may upregulate Dkk3 expression upon encountering their cognate antigen in the periphery under steady state conditions, probably during the neonatal phase, when they have access to peripheral tissues.

However, it is possible to prove Dkk3 expression by T cells indirectly, through functional assays. Moreover, in future studies single cell RT-PCR could be employed to trace the few spleen cells that could possibly express Dkk3 mRNA.

6.4 Cellular mechanisms of Dkk3$^{-/-}$ T cell hyperproliferation

In total spleen proliferation assays both CD4 and CD8 T cells were hyperproliferative in the absence of Dkk3 when compared to wild type controls. However, isolated Dkk3$^{-/-}$ CD4 T cells proliferated as much as isolated Dkk3$^{+/+}$ CD4 T cells (Figure 5-24). This suggests that the difference observed in the proliferation of Dkk3$^{-/-}$ and Dkk3$^{+/+}$ CD4 T cell in total spleen cultures can be attributed to the role of CD4 T cell-extrinsic Dkk3 protein. Apparently, CD4 T cells can respond to the presence of Dkk3 but do not produce Dkk3 themselves.

On the contrary, isolated Dkk3$^{-/-}$ CD8 T cells displayed hyperproliferation, exactly like in total spleen assays (Figure 5-24). This suggests that CD8 T cells not only are able to respond to Dkk3 but they also are influenced by its absence. One hypothesis is that Dkk3 is expressed by a small regulatory CD8 T cell population that is untraceable by FACS analysis. Thereby, CD8-derived Dkk3 can further regulate CD8 T cell proliferation and its absence results in CD8 T cell hyperproliferation. However, it cannot be excluded that tissue-derived Dkk3 affects permanently CD8 T cell reactivity and CD8 T cells that develop in a Dkk3 deficient environment are hyperproliferative.

For example, the differential Dkk3$^{-/-}$ CD8 T cell reactivity could be a consequence of altered thymic selection in the absence of Dkk3, which could favor more reactive T cell clones.

Analysis of the TCR repertoire in Dkk3$^{-/-}$ and Dkk3$^{+/+}$ mice as well as in Dkk3$^{-/-}$→Dkk3$^{+/+}$, Dkk3$^{+/+}$→Dkk3$^{-/-}$ and control Dkk3$^{+/+}$→Dkk3$^{+/+}$ chimeras revealed that the absence of Dkk3 from the thymic epithelium or from cells of hematopoietic origin that play a role in thymic selection does not affect T cell development in the thymus (Table 5-4).

However, studies carried out with Dkk3$^{-/-}$→Dkk3$^{+/+}$ and Dkk3$^{+/+}$→Dkk3$^{-/-}$ chimeras revealed the importance of tissue-derived Dkk3 for the control of T cell reactivity. Wild type T cells that developed in Dkk3$^{-/-}$ host displayed increased proliferation when compared to wild type T cells that developed in Dkk3 sufficient environment (Figure 5-27). Consequently, although Dkk3 expression in a CD8 T cell subpopulation cannot be excluded, it is undisputable that Dkk3 production by cells of non-hematopoietic origin influences T cell reactivity.

6.5 Molecular mechanisms of Dkk3$^{-/-}$ T cell hyperproliferation

Taking into account that Dkk3$^{-/-}$ T cell responses are different from the wild type ones, it was intriguing to investigate which signaling pathways are modified in the absence of Dkk3 molecule. Dkk3 belongs to the Dickkopf family of mediators of the Wnt signaling pathway. However, it is widely accepted that it does not interact with the known receptors that initiate Wnt signaling (Krupnik et al. 1999; Mao et al. 2002; Wu et al. 2006). Interestingly, no receptor has been identified to bind secretory Dkk3.

Although Dkk3 is involved in the TGF-β pathway by maintaining normal levels of Smad4 in the *Xenopus laevis* embryo (Pinho et al. 2007), there is no evidence that it affects the TGF-β pathway in T cells. TGF-β exerted the same suppressive effect on both Dkk3$^{-/-}$ and Dkk3$^{+/+}$ T cells (Figure 5-29). Additionally, the levels of intracellular Smad4 protein were not found to be decreased despite the absence of Dkk3 from activated T cells (Figure 5-30).

The activation of the ERK pathway is essential for T cell survival and proliferation since it leads to IL-2 production by T cells. Inhibition of ERK phosphorylation leads to T cell anergy. It is characteristic that in tolerant Des-TCR CD8 T cells that were obtained from thymectomized Des-TCRxKerK^{b}xRAG2$^{-/-}$ mice the levels of phosphorylated ERK upon T cell stimulation were highly decreased in comparison to activated Des-TCR CD8 T cells.

In the absence of Dkk3, polyclonal T cells display an increased proliferation rate and elevated IL-2 production (Figures 5-31 and 5-32). The molecular mechanism lying behind this effect seems to be the increased activity of the ERK pathway. TCR stimulation as well as direct signaling via the DAG analogue PMA led to increased ERK activation in the Dkk3$^{-/-}$ CD8 T cells.

This suggests that Dkk3 is an inhibitor of the ERK pathway. It seems that it inhibits downstream of Ras and upstream of the MEK kinase, most possibly at the level of the c-Raf kinase. The conclusion that Dkk3 is an inhibitor of the ERK pathway is also consistent with the observation that Dkk3 overexpression in the prostate cancer cell line PC3 prevents ERK phosphorylation (Lodygin et al. 2005).

The observed effect of the lack of Dkk3 on the ERK pathway in CD8 T cells could explain $Dkk3^{-/-}$ T cell hypereactivity. However, what remains to be investigated is whether the presence of secreted Dkk3 inhibits directly the ERK pathway, since the above experiments cannot exclude the possibility that lack of Dkk3 indirectly affects the ERK signaling in T cells.

6.6 Dkk3 is secreted by immune privileged tissues and contributes to the control of T cell reactivity

6.6.1 Dkk3 is expressed by immune privileged tissues

It has previously been reported that Dkk3 mRNA is present in peripheral tissues, including the brain, the spinal cord, the eye, the heart, the ovary, the uterus and the liver. By using the monoclonal anti-Dkk3 antibody in ELISA and histology staining, Dkk3 could indeed be detected in those tissues (Table 5-5 and Figure 5-35). Interestingly, Dkk3 is present in the brain, the spinal cord and the eye, which are characterized as immune privileged organs. As mentioned before, immune privileged organs are known to express the immune suppressive molecules Fas, IDO and the TGF-β cytokine. Thus, the presence of Dkk3 secretory molecule in the CNS and the eye could be an additional mechanism of active control of the immune responses in these tissues, where aberrant immunity and extended inflammation are detrimental for the host.

The exact cell type producing Dkk3 in the brain and the spinal cord was investigated by histological studies. In the steady state the neurons were shown to express considerable amounts of Dkk3. On the contrary, the astrocytes and the microglia were negative for Dkk3 protein. However, Dkk3 mRNA was traced in primary astrocyte cultures. It is suggested that the *in vitro* culture conditions, which resemble the *in vivo* inflammatory conditions, activate the astrocytes and possibly then induce Dkk3 expression. Accordingly, brain sections derived from diseased EAE C57.Bl/6 mice were also tested for Dkk3 expression by histology. The neuronal cells were found positive, displaying no apparent up-regulation of Dkk3 expression. However, Dkk3 expression was not traced in the astrocytes. Thus the induction of Dkk3 expression in activated astrocytes *in vitro* does not reflect the *in vivo* EAE situation.

Additionally, the lung and the heart, where even transient autoimmunity, such as pulmonary fibrosis and rheumatic fever, might be of a severe risk for the individual, also express a significant level of Dkk3. The liver, an organ important for the induction of T cell tolerance, produces Dkk3 protein as well. Finally, the embryo and the ovary, uterus and placenta, where a tolerogenic milieu is needed, all secrete Dkk3. On the other hand, it is interesting that all the lymphoid tissues, such as the thymus, the spleen and the lymph nodes do not express Dkk3 protein. This observation is meaningful, since the presence of high amounts of a potent suppressor of T cell responses in the above lymphoid organs would be deleterious for the protection of the host against infections.

6.6.2 Secretory Dkk3 protein suppresses CD4 and CD8 T cell proliferation

The *in vivo* effect of the Dkk3, which is secreted by the immune privileged tissues, on T cell responses was investigated by using cells that secreted Dkk3 protein in *in vitro* proliferation assays. HEK 293T cells, transfected with Dkk3, were shown to express Dkk3 by RT-PCR. Moreover, they were demonstrated to secrete Dkk3 protein by ELISA and Western blot analysis of their supernatant. Thus these cells were employed to reproduce the model of Dkk3 secretion by neuronal cells in the brain. Interestingly, secreted Dkk3 could down regulate total spleen T cell proliferation as well as CD8 T cell proliferation. The effect was observed in both $Dkk3^{+/+}$ and $Dkk3^{-/-}$ groups, but was more pronounced with the knockout T cells (Figures 5-36 and 5-37).

The direct proof for the regulatory capacity of Dkk3 came from the use of purified recombinant mouse Dkk3 protein in the *in vitro* T cell proliferation assays. Indeed, recombinant mouse Dkk3 inhibited CD4 and CD8 T cell proliferation in a concentration dependent manner (Figure 5-38).

The main hypothesis is that activated T cells express the receptor for Dkk3 on their surface and thereby respond to secreted Dkk3. To verify this hypothesis, Dkk3 was administered to proliferating T cells two days after their stimulation. The suppressive effect on their proliferation was as potent as in the case of Dkk3 being present in the proliferation assay from the first day of stimulation (Figure 5-39). Thus, the activated T cells respond to the presence of soluble Dkk3, possibly via a specific Dkk3 receptor, and loose their proliferative capacity. In more detail, preliminary experiments indicated that Dkk3 acts on activated T cells by inducing early apoptosis.

6.7 Dkk3 regulates T cell responses in Experimental Autoimmune Encephalitis (EAE)

EAE is an autoimmune disease resembling human demyelinating diseases and in particular multiple sclerosis. It is initiated upon the priming of T cells with CNS-derived antigens in the presence of potent adjuvants. Like in multiple sclerosis, EAE is accompanied by the presence of multiple CNS lesions, which are distributed by time and in the site of occurence. Most pronounced lesions are found in the brain stem and the spinal cord.

The inflammatory process involves the disruption of the blood-brain barrier and the recruitment of blood-born macrophages and microglia. Additionally, cytokines are locally up-regulated and released. The CNS tissue-cells and the infiltrating lymphocytes release IFN-γ, IL-23, TNF-α, as well as the death ligands TRAIL and Fas. As a consequence, oligodendrocytes and neurons within the lesions undergo cell death. Furthermore, axons become demyelinated and dissected, leading to the blockade of nerve conduction and thus the clinical symptoms of paresis and paralysis (Aktas et al. 2006). However, EAE in mice is reversible. Inflammation is controlled and gradually recedes, permitting partial remyelination and recovery from the EAE symptoms.

6.7.1 Dkk3$^{-/-}$ mice display more severe and persistent EAE

Here, it was demonstrated that Dkk3 contributes to the control of the immune response which occurs during the course of EAE. Lack of Dkk3 does not affect the onset of the disease, but importantly the later stages, thus resulting in more severe and persistent EAE symptoms (Figure 5-41).

The MOG_{33-55}-specific naïve CD4 and CD8 T cells are normally primed in the absence of Dkk3. They then pass through the blood-brain barrier, thus initiating the inflammation in the CNS. Apparently their priming and migration to the brain and spinal cord are independent of Dkk3.

Nevertheless, the mean maximum score of the disease is higher and the severe symptoms are more persistent in the absence of Dkk3 (Table 5-6). This leads to the hypothesis that secretory Dkk3 may bind on activated CNS-infiltrating T cells, thereby suppressing them. Consequently, the effect of Dkk3-mediated suppression is seen during the recovery phase. Therefore, absence of the suppressor Dkk3 leads to increased EAE chronicity.

Histological analyses revealed that Dkk3 expression in the brain is unaltered during the course of the disease. Thus, it is possible that the observed relevance of Dkk3 for the control of the disease during the recovery phase is not due to protein-overexpression at this stage but might be due to up-regulation of the respective Dkk3-receptor on T cells. The possibility that

T cell-derived Dkk3 contributes to the control of inflammation at late stages of EAE is partially excluded by experiments that will be addressed later. At this point, it is important to stress out that the observed difference between the EAE Dkk3$^{+/+}$ and Dkk3$^{-/-}$ mice cannot be attributed to altered thymic selection, since the MOG-specific CD4 and CD8 T cells, carrying the TCR-$V_{\beta 11}$ chain, are present in the same percentages in both mouse strains (Table 5-4).

Interestingly, Dkk3 is expressed in the brain and other immune privileged sites and can control immune responses, possibly by inducing apoptosis (Figure 4-40), without harming the nervous tissues. Noticeably, other molecules expressed in the brain and known to induce apoptosis in T cells, such as Fas and its ligand have a dual role in EAE and multiple sclerosis. They have been shown to exacerbate the disease symptoms, because they do not specifically induce apoptosis of activated T cells, but also of oligodendrocytes, thereby contributing to the demyelination (Aktas et al. 2006). Additionally, the immunosuppressive enzyme IDO, which is also expressed by the tissue cells during EAE, suppresses T cell proliferation, but also induces the production of side products of the kyanourine pathway, which are toxic for the nervous system (Kwidzinski et al. 2007). It seems that Dkk3 suppresses T cell responses without damaging the CNS tissue. However it remains to be clarified whether Dkk3-receptor is induced on CNS tissue cells upon inflammation.

6.7.2 The increased EAE chronicity in the Dkk3$^{-/-}$ mice is accompanied by activated CD8 T cell-persistence in the CNS.

A more detailed investigation of the effect of Dkk3 deficiency on EAE was achieved by analyzing the CNS-infiltrating T cell populations shortly after the disease peak (day 20) and during the recovery phase (day 29). At day 20 both Dkk3$^{+/+}$ and Dkk3$^{-/-}$ experimental groups exhibited severe EAE symptoms. On the contrary, at day 29 the Dkk3$^{+/+}$ mice had already recovered from EAE, whereas the Dkk3$^{-/-}$ mice still suffered from high EAE score (Figure 5-43).

Strikingly, the absolute numbers and percentages of activated CD4 and CD8 T cells in the CNS of EAE-diseased Dkk3$^{-/-}$ and Dkk3$^{+/+}$ were comparable. However, it is possible that Dkk3 regulates CNS-infiltrating T cell subsets with characteristic cytokine profile that are responsible for the persistence of inflammation during EAE. Therefore CD4 and CD8 T cells derived from the brain and spinal cord of diseased Dkk3$^{+/+}$ and Dkk3$^{-/-}$ mice were analyzed by flow cytometry for their cytokine profile. Interestingly, there were no differences between the EAE-diseased Dkk3$^{+/+}$ and Dkk3$^{-/-}$ mice in the percentages of TNF-α, IL-17 and IFN-γ producing CD4 T cells.

IL-17 mRNA has been shown to be induced on day 6 after immunization of C57.Bl/6 mice with MOG_{33-55} peptide. IL-17 expression by CD4 T cells is increased at the EAE onset and declines upon the peak of the disease. IFN-γ expression by CD4 T cells displays the same pattern (Sonobe et al. 2007). Both IL-17- and IFN-γ-producing CD4 T cell subsets have been implied to play a crucial role in the induction of EAE (Langrish et al. 2005; Sonobe et al. 2007). Thus, it is expectable that these particular CD4 T cell populations are not involved in the chronic disease phase that is observed in the $Dkk3^{-/-}$ experimental group. On the contrary, TNF-α production by CD4 and CD8 T cells is intensified during the late disease stages (Sonobe et al. 2007) and has been suggested to contribute to the pathophysiology of the disease, by inducing apoptosis of oligodendrocytes and neuronal degeneration (reviewed in (Aktas et al. 2006)). However, Dkk3 does not seem to regulate CD4 T cells, which are the main producers of TNF-α during the late EAE stages.

On the other hand, the subpopulation of CD8 T cells expressing IFN-γ appears to be much more expanded in $Dkk3^{-/-}$ mice when compared to $Dkk3^{+/+}$ mice. CD8 T cells have been reported to produce IFN-γ later on in the disease course than CD4 T cells and have been suggested to play a role in the maintenance of the EAE late stages (Sonobe et al. 2007).

This finding contradicts former reports concerning the regulatory role of CD8 T cells and IFN-γ in the EAE. It has previously been shown that CD8 T cells isolated from EAE-recovered mice specifically inhibited MBP-activated CD4 T cell clones *in vitro* and their depletion was followed by recurrence of EAE. Additionally, mice reconstituted with EAE-experienced CD8 T cells were resistant to MBP vaccination-induced EAE (Jiang et al. 2003). The proposed mechanism of CD8 T cell-suppression involved the non-classical MHC I molecules Qa-1, shown to be expressed by some pathogenic CD4 T cells. It was suggested that suppressor CD8 T cells recognize a peptide from the auto-reactive CD4 T cell-TCR, presented by the Qa-1 molecules (Madakamutil et al. 2003; Kumar 2004). Therefore the auto-reactive CD4 T cells are depleted by the suppressor CD8 T cells in wild type but not in Qa-1 deficient mice (Hu et al. 2004). Nonetheless, Qa-1 mediated suppression is controversial, since it was observed during secondary, but not primary responses (Friese et al. 2005).

Furthermore, another study has identified a distinct population of suppressor CD8 T cells that lack CD28 expression and render the APCs tolerogenic (Najafian et al. 2003). However, the exact function of these CD8 T cells *in vivo* is not clear. In general, it cannot be excluded that a regulatory CD8 T cell population can be identified in EAE diseased mice. The same holds true for CD4 regulatory T cells.

Actually, during the last few years many reports concerning the effector function of CD8 T cells during EAE have been published. It has been shown that MBP and MOG immunizations lead to the expansion of CD8 T cells which are specific for the MBP and MOG peptides respectively, when presented by the MHC I molecules (Huseby et al. 1999; Huseby et al. 2001; Sun et al. 2001). Isolation of the expanded CD8 T cells followed by their adoptive transfer into naïve recipients induced EAE. The severe clinical symptoms were accompanied by extended lesion formation in the brain and to a lesser extend in the spinal cord, massive CD8 T cell infiltration, increased demyelination and perivascular cell death. In general, the disease profile resembled more to multiple sclerosis than conventional EAE with a relapsing-remitting course. Interestingly, co-injection of anti-IFN-γ antibodies markedly reduced the disease severity, whereas blocking TNF with a TNF receptor-Fc fusion did not have such an effect (Huseby et al. 2001). These results contradict the previously suggested regulatory role of IFN-γ in EAE, which was based on the observation that IFN-$\gamma^{-/-}$ mice displayed EAE of increased severity (Krakowski et al. 1996; Willenborg et al. 1996). This discrepancy remains yet to be clarified. However, this study points out the contribution of IFN-γ, which is produced by CD8 T cells only, at the late stages of the disease course, to the persistence of the EAE symptoms.

In conclusion, it seems that the presence of Dkk3 in the brain during EAE has a suppressive effect on the disease course, and more particularly it contributes to the recovery from the disease. Lack of Dkk3 leads to the increase of IFN-γ-producing CD8 T cells, which may be responsible for the inhibition of EAE recovery. Potential mechanisms of IFN-γ mediated disease chronicity are the induction of blood brain barrier permeability (Oshima et al. 2001) and the up-regulation of MHC I and II molecules in the CNS (Neumann et al. 2002; Horwitz et al. 2003). Moreover, IFN-γ promotes the cytotoxic function of T cells (Horwitz et al. 2003), activates the macrophages, astrocytes (Nikcevich et al. 1997) and microglia (Takeuchi et al. 2006) and directly induces the cell death of oligodendrocytes (Popko et al. 1999).

6.7.3 Neuron-derived but not T cell-derived Dkk3 is crucial for the control of EAE

Having shown that Dkk3 contributes to the immune regulation of EAE by suppressing the IFN-γ-producing CD8 T cells, it was challenging to investigate whether the main source of Dkk3 were the neurons or the CNS-infiltrating T cells. As already mentioned, Dkk3 is secreted in considerable amounts by neuronal cells in steady state and in inflammation. On the contrary, Dkk3 expression by T cells is not detectable in the polyclonal repertoire. However, it cannot be excluded that a small subpopulation of CD8 regulatory T cells secretes Dkk3.

The contribution of CNS- and T cell-derived Dkk3 to EAE recovery was studied in bone marrow chimeras. On one hand, $Dkk3^{-/-}$ recipient mice were reconstituted with $Dkk3^{+/+}$ bone marrow, in order to study the contribution of the brain to the Dkk3-mediated control of EAE. On the other hand, $Dkk3^{+/+}$ irradiated mice received $Dkk3^{-/-}$ bone marrow and it was investigated whether the lack of Dkk3 from T cells is sufficient to lead to more severe EAE symptoms.

It has been reported that the extended inflammation, which is induced upon lethal irradiation of the recipient mice, results in severe and non-reversible EAE in chimeric mice (Zehntner et al. 2004). This effect was also observed after active immunization of $Dkk3^{+/+} \rightarrow Dkk3^{-/-}$ and $Dkk3^{-/-} \rightarrow Dkk3^{+/+}$ chimeric mice. However, the kinetics of the disease onset could give a hint about the differential control of autoimmune disease. More specifically, it could be investigated whether an earlier disease onset is mediated by wild type T cells in a $Dkk3^{-/-}$ CNS microenvironment or by $Dkk3^{-/-}$ T cells in a Dkk3-sufficient CNS background. T cells that develop in the previously irradiated chimeric mice have an activated phenotype. Thus, since it suppresses activated T cells, the expected suppressive effect of Dkk3 during EAE can theoretically be observed from the first days upon disease induction.

Dkk3 was indeed shown to exert a suppressive effect on activated T cells during the disease onset. In chimeric mice lacking Dkk3 expression in the brain and spinal cord, activated CD4 and CD8 T cells, which passed through the permeabilized blood-brain barrier, induced the disease earlier (Figure 5-44). Possibly, on days 6-12 the amount of Dkk3 secreted by the neurons is sufficient to suppress the already activated CNS-infiltrating T cells. Nonetheless, after day 12 the influx of activated T cells may be so increased that the amount of Dkk3 present in the CNS is not sufficient to suppress their inflammatory capacity. Moreover, the induced cytokine expression by tissue cells may also contribute to demyelination and to occurrence of severe clinical symptoms.

In the $Dkk3^{-/-} \rightarrow Dkk3^{+/+}$ chimeras, lack of Dkk3 from T cells did not result in early disease onset. Apparently, the presence of Dkk3 that is secreted by the neurons is sufficient to inhibit early disease onset.

The results obtained upon the induction of EAE in the chimeric mice could be used to draw conclusions concerning the importance of the brain-derived Dkk3 for the control of autoimmune encephalitis. However, in order to directly exclude the thymic influence from the experimental system, an alternative approach was used. In this approach, Dkk3 was blocked in C57.Bl/6 mice with the monoclonal anti-Dkk3 antibody, after the induction of the disease. Dkk3 blockade resulted in increased disease chronicity, thereby confirming the initial

hypothesis that Dkk3 is crucial for T cell suppression during the late stages of EAE (Figure 5-47). The anti-Dkk3 and control IgG antibodies were administered intraperitoneally and are thought to access the brain, since the blood-brain barrier was permeabilized upon administration of pertussis toxin. IgG has been also previously described to access the CNS during EAE and has been shown to inhibit the disease course, as indicated by milder clinical symptoms (Jorgensen et al. 2005; Jorgensen et al. 2007). In the case of the anti-Dkk3 mouse IgG administration, it neither ameliorated the disease course nor increased the mean disease duration.

The suppressive role of Dkk3 during EAE recovery was shown by the use of the blocking antibody. Thus, combining the results obtained from the analysis of the cytokine profile of CNS-infiltrating T cells, it could be argued that blocking of secreted Dkk3 by the monoclonal anti-Dkk3 antibody inhibits binding of Dkk3 on effector CD8 T cells and thereby increases the chronicity of the disease.

6.8 Conclusions and Outlook

Dkk3 is a newly identified modulator of the immune responses. It is expressed by transgenic regulatory Des-TCR CD8 T cells and is the mediator of their function. Regulatory Des-TCR CD8 T cells were shown to secrete the suppressive Dkk3 molecule, which then presumably binds to an unknown receptor on target T cells.

The immune regulatory function of Dkk3 was not found to be limited to the Des-TCR transgenic mouse model. Lack of Dkk3 from polyclonal T cells results in hyperproliferation and increased IL-2 production. This effect could be explained by the fact that the ERK MAPK is over activated in the absence of Dkk3. It seems that Dkk3 specifically inhibits the ERK pathway activation on the level of the Raf kinase in CD8 T cells.

Dkk3 expression could not be detected in the lymphoid organs. Yet, it is unclear whether a limited CD8 T cell population secretes Dkk3, but tissue-derived Dkk3 was shown to permanently affect CD8 T cell reactivity. Thymic selection does not seem to be altered in the absence of Dkk3.

Among the tissues that express Dkk3 in high amounts are all immune privileged organs (CNS, ovaries, placenta), the liver, which is a crucial site for the establishment of T cell tolerance to oral antigens, the heart and the lung. It seems that Dkk3 secreted by the above organs can control potentially harmful T cell responses by inducing T cell apoptosis.

Specifically, the immune regulatory role of Dkk3 in the CNS is apparent in the context of EAE. Absence of neuron-derived Dkk3 leads to severe and persistent EAE, due to lack of

suppression of activated CD8 T cells. Interestingly, blockade of the secreted Dkk3 at the site of inflammation results in increased disease chronicity as well.

In conclusion, Dkk3 is an immune regulator, employed by both transgenic regulatory CD8 T cells and immune privileged tissues. The above finding is of importance, since except from its assumed role in embryonic development no other function has been assigned to Dkk3. It seems that Dkk3's primary function is unrelated to the immune system, since genes, with great homology to Dkk3 first appeared in invertebrates such as the cnidaria, before the evolution of the adaptive immune system (Fedders et al. 2004). However, Dkk3, like other molecules which are vital for the functionality of the adaptive immune system, may have acquired a second function throughout evolution, which is this of an immune modulator.

Taking the immune regulatory role of Dkk3 into consideration, future research investigating the role of Dkk3 in antiviral responses and autoimmune diseases would be fascinating. Most intriguing is the role of Dkk3 in anti-tumor immunity, since it has been recently shown that it is strongly expressed by endothelial cells on the tumor blood vessels (Hermann et al. 2007). It is thus possible that blockade of Dkk3 by the monoclonal anti-Dkk3 antibody may inhibit not only tumor angiogenesis but also the suppression of anti-tumor immune responses. On the other hand, the importance of the identification of the Dkk3 specific receptor is not to be overseen.

7 REFERENCES

Abarzua, F., M. Sakaguchi, M. Takaishi, Y. Nasu, K. Kurose, S. Ebara, M. Miyazaki, M. Namba, H. Kumon and N. H. Huh (2005). "Adenovirus-mediated overexpression of REIC/Dkk-3 selectively induces apoptosis in human prostate cancer cells through activation of c-Jun-NH2-kinase." Cancer Res **65**(21): 9617-22.

Abarzua, F., M. Sakaguchi, R. Tanimoto, H. Sonegawa, D. W. Li, K. Edamura, T. Kobayashi, M. Watanabe, Y. Kashiwakura, H. Kaku, T. Saika, K. Nakamura, Y. Nasu, H. Kumon and N. H. Huh (2007). "Heat shock proteins play a crucial role in tumor-specific apoptosis by REIC/Dkk-3." Int J Mol Med **20**(1): 37-43.

Abi-Hanna, D., D. Wakefield and S. Watkins (1988). "HLA antigens in ocular tissues. I. In vivo expression in human eyes." Transplantation **45**(3): 610-3.

Aktas, O., T. Prozorovski and F. Zipp (2006). "Death ligands and autoimmune demyelination." Neuroscientist **12**(4): 305-16.

Albert, M. L., B. Sauter and N. Bhardwaj (1998). "Dendritic cells acquire antigen from apoptotic cells and induce class I-restricted CTLs." Nature **392**(6671): 86-9.

Alderson, M. R., T. W. Tough, T. Davis-Smith, S. Braddy, B. Falk, K. A. Schooley, R. G. Goodwin, C. A. Smith, F. Ramsdell and D. H. Lynch (1995). "Fas ligand mediates activation-induced cell death in human T lymphocytes." J Exp Med **181**(1): 71-7.

Alferink, J., B. Schittek, G. Schonrich, G. J. Hammerling and B. Arnold (1995). "Long life span of tolerant T cells and the role of antigen in maintenance of peripheral tolerance." Int Immunol **7**(2): 331-6.

Alferink, J., A. Tafuri, D. Vestweber, R. Hallmann, G. J. Hammerling and B. Arnold (1998). "Control of neonatal tolerance to tissue antigens by peripheral T cell trafficking." Science **282**(5392): 1338-41.

Algood, H. M. and J. L. Flynn (2004). "CCR5-deficient mice control Mycobacterium tuberculosis infection despite increased pulmonary lymphocytic infiltration." J Immunol **173**(5): 3287-96.

Anderson, G., J. J. Owen, N. C. Moore and E. J. Jenkinson (1994). "Thymic epithelial cells provide unique signals for positive selection of CD4+CD8+ thymocytes in vitro." J Exp Med **179**(6): 2027-31.

Andrade, F., L. A. Casciola-Rosen and A. Rosen (2004). "Granzyme B-induced cell death." Acta Haematol **111**(1-2): 28-41.

Apostolou, I., A. Sarukhan, L. Klein and H. von Boehmer (2002). "Origin of regulatory T cells with known specificity for antigen." Nat Immunol **3**(8): 756-63.

Apostolou, I. and H. von Boehmer (2004). "In vivo instruction of suppressor commitment in naive T cells." J Exp Med **199**(10): 1401-8.

Aranami, T. and T. Yamamura (2008). "Th17 Cells and Autoimmune Encephalomyelitis (EAE/MS)." Allergol Int **57**(2): 115-20.

Askenasy, N., E. S. Yolcu, I. Yaniv and H. Shirwan (2005). "Induction of tolerance using Fas ligand: a double-edged immunomodulator." Blood **105**(4): 1396-404.

Azuma, M., M. Cayabyab, D. Buck, J. H. Phillips and L. L. Lanier (1992). "CD28 interaction with B7 costimulates primary allogeneic proliferative responses and cytotoxicity mediated by small, resting T lymphocytes." J Exp Med **175**(2): 353-60.

Banchereau, J. and R. M. Steinman (1998). "Dendritic cells and the control of immunity." Nature **392**(6673): 245-52.

Barrantes Idel, B., A. Montero-Pedrazuela, A. Guadano-Ferraz, M. J. Obregon, R. Martinez de Mena, V. Gailus-Durner, H. Fuchs, T. J. Franz, S. Kalaydjiev, M. Klempt, S. Holter, B. Rathkolb, C. Reinhard, G. Morreale de Escobar, J. Bernal, D. H. Busch, W. Wurst, E. Wolf, H. Schulz, S. Shtrom, E. Greiner, M. Hrabe de Angelis, H. Westphal

and C. Niehrs (2006). "Generation and characterization of dickkopf3 mutant mice." Mol Cell Biol **26**(6): 2317-26.

Belkaid, Y., C. A. Piccirillo, S. Mendez, E. M. Shevach and D. L. Sacks (2002). "CD4+CD25+ regulatory T cells control Leishmania major persistence and immunity." Nature **420**(6915): 502-7.

Bennett, C. L., J. Christie, F. Ramsdell, M. E. Brunkow, P. J. Ferguson, L. Whitesell, T. E. Kelly, F. T. Saulsbury, P. F. Chance and H. D. Ochs (2001). "The immune dysregulation, polyendocrinopathy, enteropathy, X-linked syndrome (IPEX) is caused by mutations of FOXP3." Nat Genet **27**(1): 20-1.

Bettelli, E., M. Pagany, H. L. Weiner, C. Linington, R. A. Sobel and V. K. Kuchroo (2003). "Myelin oligodendrocyte glycoprotein-specific T cell receptor transgenic mice develop spontaneous autoimmune optic neuritis." J Exp Med **197**(9): 1073-81.

Bluestone, J. A. and A. K. Abbas (2003). "Natural versus adaptive regulatory T cells." Nat Rev Immunol **3**(3): 253-7.

Bopp, T., C. Becker, M. Klein, S. Klein-Hessling, A. Palmetshofer, E. Serfling, V. Heib, M. Becker, J. Kubach, S. Schmitt, S. Stoll, H. Schild, M. S. Staege, M. Stassen, H. Jonuleit and E. Schmitt (2007). "Cyclic adenosine monophosphate is a key component of regulatory T cell-mediated suppression." J Exp Med **204**(6): 1303-10.

Bouneaud, C., P. Kourilsky and P. Bousso (2000). "Impact of negative selection on the T cell repertoire reactive to a self-peptide: a large fraction of T cell clones escapes clonal deletion." Immunity **13**(6): 829-40.

Brocker, T., M. Riedinger and K. Karjalainen (1997). "Targeted expression of major histocompatibility complex (MHC) class II molecules demonstrates that dendritic cells can induce negative but not positive selection of thymocytes in vivo." J Exp Med **185**(3): 541-50.

Bruder, D., M. Probst-Kepper, A. M. Westendorf, R. Geffers, S. Beissert, K. Loser, H. von Boehmer, J. Buer and W. Hansen (2004). "Neuropilin-1: a surface marker of regulatory T cells." Eur J Immunol **34**(3): 623-30.

Burkly, L. C., S. Degermann, J. Longley, J. Hagman, R. L. Brinster, D. Lo and R. A. Flavell (1993). "Clonal deletion of V beta 5+ T cells by transgenic I-E restricted to thymic medullary epithelium." J Immunol **151**(8): 3954-60.

Cadigan, K. M. and Y. I. Liu (2006). "Wnt signaling: complexity at the surface." J Cell Sci **119**(Pt 3): 395-402.

Calne, R. Y., H. J. White, R. M. Binns, B. M. Herbertson, P. R. Millard, J. Pena, J. R. Salaman, J. R. Samuel and D. R. Davis (1969). "Immunosuppressive effects of the orthotopically transplanted porcine liver." Transplant Proc **1**(1): 321-4.

Cantrell, D. (1996). "T cell antigen receptor signal transduction pathways." Annu Rev Immunol **14**: 259-74.

Cao, X., S. F. Cai, T. A. Fehniger, J. Song, L. I. Collins, D. R. Piwnica-Worms and T. J. Ley (2007). "Granzyme B and perforin are important for regulatory T cell-mediated suppression of tumor clearance." Immunity **27**(4): 635-46.

Cardell, S., B. Sander and G. Moller (1992). "Primary stimulation of CD4+ cells in the presence of IL-4 or IFN-gamma alters the frequencies of cytokine-producing cells at restimulation." Scand J Immunol **36**(6): 769-77.

Chatila, T. A., F. Blaeser, N. Ho, H. M. Lederman, C. Voulgaropoulos, C. Helms and A. M. Bowcock (2000). "JM2, encoding a fork head-related protein, is mutated in X-linked autoimmunity-allergic disregulation syndrome." J Clin Invest **106**(12): R75-81.

Chen, W., M. S. Ford, K. J. Young and L. Zhang (2004). "The role and mechanisms of double negative regulatory T cells in the suppression of immune responses." Cell Mol Immunol **1**(5): 328-35.

Chen, W., W. Jin, N. Hardegen, K. J. Lei, L. Li, N. Marinos, G. McGrady and S. M. Wahl (2003). "Conversion of peripheral CD4+CD25- naive T cells to CD4+CD25+ regulatory T cells by TGF-beta induction of transcription factor Foxp3." J Exp Med **198**(12): 1875-86.

Chen, Y., V. K. Kuchroo, J. Inobe, D. A. Hafler and H. L. Weiner (1994). "Regulatory T cell clones induced by oral tolerance: suppression of autoimmune encephalomyelitis." Science **265**(5176): 1237-40.

Collison, L. W., C. J. Workman, T. T. Kuo, K. Boyd, Y. Wang, K. M. Vignali, R. Cross, D. Sehy, R. S. Blumberg and D. A. Vignali (2007). "The inhibitory cytokine IL-35 contributes to regulatory T-cell function." Nature **450**(7169): 566-9.

Crabtree, G. R. (1989). "Contingent genetic regulatory events in T lymphocyte activation." Science **243**(4889): 355-61.

Crispe, I. N., M. Giannandrea, I. Klein, B. John, B. Sampson and S. Wuensch (2006). "Cellular and molecular mechanisms of liver tolerance." Immunol Rev **213**: 101-18.

Deaglio, S., K. M. Dwyer, W. Gao, D. Friedman, A. Usheva, A. Erat, J. F. Chen, K. Enjyoji, J. Linden, M. Oukka, V. K. Kuchroo, T. B. Strom and S. C. Robson (2007). "Adenosine generation catalyzed by CD39 and CD73 expressed on regulatory T cells mediates immune suppression." J Exp Med **204**(6): 1257-65.

Derbinski, J., A. Schulte, B. Kyewski and L. Klein (2001). "Promiscuous gene expression in medullary thymic epithelial cells mirrors the peripheral self." Nat Immunol **2**(11): 1032-9.

Derynck, R. and Y. E. Zhang (2003). "Smad-dependent and Smad-independent pathways in TGF-beta family signalling." Nature **425**(6958): 577-84.

Devergne, O., M. Birkenbach and E. Kieff (1997). "Epstein-Barr virus-induced gene 3 and the p35 subunit of interleukin 12 form a novel heterodimeric hematopoietin." Proc Natl Acad Sci U S A **94**(22): 12041-6.

Dorr, J., I. Bechmann, S. Waiczies, O. Aktas, H. Walczak, P. H. Krammer, R. Nitsch and F. Zipp (2002). "Lack of tumor necrosis factor-related apoptosis-inducing ligand but presence of its receptors in the human brain." J Neurosci **22**(4): RC209.

Dubois, P. M., M. Pihlgren, M. Tomkowiak, M. Van Mechelen and J. Marvel (1998). "Tolerant CD8 T cells induced by multiple injections of peptide antigen show impaired TCR signaling and altered proliferative responses in vitro and in vivo." J Immunol **161**(10): 5260-7.

Edamura, K., Y. Nasu, M. Takaishi, T. Kobayashi, F. Abarzua, M. Sakaguchi, Y. Kashiwakura, S. Ebara, T. Saika, M. Watanabe, N. H. Huh and H. Kumon (2007). "Adenovirus-mediated REIC/Dkk-3 gene transfer inhibits tumor growth and metastasis in an orthotopic prostate cancer model." Cancer Gene Ther **14**(9): 765-72.

Endharti, A. T., I. M. s. Rifa, Z. Shi, Y. Fukuoka, Y. Nakahara, Y. Kawamoto, K. Takeda, K. Isobe and H. Suzuki (2005). "Cutting edge: CD8+CD122+ regulatory T cells produce IL-10 to suppress IFN-gamma production and proliferation of CD8+ T cells." J Immunol **175**(11): 7093-7.

Etheridge, S. L., G. J. Spencer, D. J. Heath and P. G. Genever (2004). "Expression profiling and functional analysis of wnt signaling mechanisms in mesenchymal stem cells." Stem Cells **22**(5): 849-60.

Fathman, C. G. and N. B. Lineberry (2007). "Molecular mechanisms of CD4+ T-cell anergy." Nat Rev Immunol **7**(8): 599-609.

Fedders, H., R. Augustin and T. C. Bosch (2004). "A Dickkopf- 3-related gene is expressed in differentiating nematocytes in the basal metazoan Hydra." Dev Genes Evol **214**(2): 72-80.

Ferber, I., G. Schonrich, J. Schenkel, A. L. Mellor, G. J. Hammerling and B. Arnold (1994). "Levels of peripheral T cell tolerance induced by different doses of tolerogen." Science **263**(5147): 674-6.

Fields, P. E., T. F. Gajewski and F. W. Fitch (1996). "Blocked Ras activation in anergic CD4+ T cells." Science **271**(5253): 1276-8.

Filaci, G., M. Fravega, D. Fenoglio, M. Rizzi, S. Negrini, R. Viggiani and F. Indiveri (2004). "Non-antigen specific CD8+ T suppressor lymphocytes." Clin Exp Med **4**(2): 86-92.

Floess, S., J. Freyer, C. Siewert, U. Baron, S. Olek, J. Polansky, K. Schlawe, H. D. Chang, T. Bopp, E. Schmitt, S. Klein-Hessling, E. Serfling, A. Hamann and J. Huehn (2007). "Epigenetic control of the foxp3 locus in regulatory T cells." PLoS Biol **5**(2): e38.

Fontenot, J. D., M. A. Gavin and A. Y. Rudensky (2003). "Foxp3 programs the development and function of CD4+CD25+ regulatory T cells." Nat Immunol **4**(4): 330-6.

Friese, M. A. and L. Fugger (2005). "Autoreactive CD8+ T cells in multiple sclerosis: a new target for therapy?" Brain **128**(Pt 8): 1747-63.

Gallegos, A. M. and M. J. Bevan (2004). "Central tolerance to tissue-specific antigens mediated by direct and indirect antigen presentation." J Exp Med **200**(8): 1039-49.

Glass, W. G., M. T. Liu, W. A. Kuziel and T. E. Lane (2001). "Reduced macrophage infiltration and demyelination in mice lacking the chemokine receptor CCR5 following infection with a neurotropic coronavirus." Virology **288**(1): 8-17.

Glinka, A., W. Wu, H. Delius, A. P. Monaghan, C. Blumenstock and C. Niehrs (1998). "Dickkopf-1 is a member of a new family of secreted proteins and functions in head induction." Nature **391**(6665): 357-62.

Glinka, Y. and G. J. Prud'homme (2008). "Neuropilin-1 is a receptor for transforming growth factor beta-1, activates its latent form, and promotes regulatory T cell activity." J Leukoc Biol **84**(1): 302-10.

Gondek, D. C., L. F. Lu, S. A. Quezada, S. Sakaguchi and R. J. Noelle (2005). "Cutting edge: contact-mediated suppression by CD4+CD25+ regulatory cells involves a granzyme B-dependent, perforin-independent mechanism." J Immunol **174**(4): 1783-6.

Gordon, L. B., P. M. Knopf and H. F. Cserr (1992). "Ovalbumin is more immunogenic when introduced into brain or cerebrospinal fluid than into extracerebral sites." J Neuroimmunol **40**(1): 81-7.

Greenwald, R. J., G. J. Freeman and A. H. Sharpe (2005). "The B7 family revisited." Annu Rev Immunol **23**: 515-48.

Griffiths, G. M. (1995). "The cell biology of CTL killing." Curr Opin Immunol **7**(3): 343-8.

Grossman, W. J., J. W. Verbsky, W. Barchet, M. Colonna, J. P. Atkinson and T. J. Ley (2004). "Human T regulatory cells can use the perforin pathway to cause autologous target cell death." Immunity **21**(4): 589-601.

Groux, H. (2001). "An overview of regulatory T cells." Microbes Infect **3**(11): 883-9.

Groux, H., A. O'Garra, M. Bigler, M. Rouleau, S. Antonenko, J. E. de Vries and M. G. Roncarolo (1997). "A CD4+ T-cell subset inhibits antigen-specific T-cell responses and prevents colitis." Nature **389**(6652): 737-42.

Guder, C., S. Pinho, T. G. Nacak, H. A. Schmidt, B. Hobmayer, C. Niehrs and T. W. Holstein (2006). "An ancient Wnt-Dickkopf antagonism in Hydra." Development **133**(5): 901-11.

Harling-Berg, C., P. M. Knopf, J. Merriam and H. F. Cserr (1989). "Role of cervical lymph nodes in the systemic humoral immune response to human serum albumin microinfused into rat cerebrospinal fluid." J Neuroimmunol **25**(2-3): 185-93.

Harling-Berg, C. J., P. M. Knopf and H. F. Cserr (1991). "Myelin basic protein infused into cerebrospinal fluid suppresses experimental autoimmune encephalomyelitis." J Neuroimmunol **35**(1-3): 45-51.

Harrington, L. E., P. R. Mangan and C. T. Weaver (2006). "Expanding the effector CD4 T-cell repertoire: the Th17 lineage." Curr Opin Immunol **18**(3): 349-56.

Harris, J. E., K. D. Bishop, N. E. Phillips, J. P. Mordes, D. L. Greiner, A. A. Rossini and M. P. Czech (2004). "Early growth response gene-2, a zinc-finger transcription factor, is required for full induction of clonal anergy in CD4+ T cells." J Immunol **173**(12): 7331-8.

Hayday, A. and R. Tigelaar (2003). "Immunoregulation in the tissues by gammadelta T cells." Nat Rev Immunol **3**(3): 233-42.

Heath, W. R., C. Kurts, J. F. Miller and F. R. Carbone (1998). "Cross-tolerance: a pathway for inducing tolerance to peripheral tissue antigens." J Exp Med **187**(10): 1549-53.

Heissmeyer, V. and A. Rao (2004). "E3 ligases in T cell anergy--turning immune responses into tolerance." Sci STKE **2004**(241): pe29.

Hermann, M., D. Pirkebner, A. Draxl, P. Berger, G. Untergasser, R. Margreiter and P. Hengster (2007). "Dickkopf-3 is expressed in a subset of adult human pancreatic beta cells." Histochem Cell Biol **127**(5): 513-21.

Holscher, C. (2004). "The power of combinatorial immunology: IL-12 and IL-12-related dimeric cytokines in infectious diseases." Med Microbiol Immunol **193**(1): 1-17.

Hori, S., T. Nomura and S. Sakaguchi (2003). "Control of regulatory T cell development by the transcription factor Foxp3." Science **299**(5609): 1057-61.

Horwitz, D. A., S. G. Zheng and J. D. Gray (2003). "The role of the combination of IL-2 and TGF-beta or IL-10 in the generation and function of CD4+ CD25+ and CD8+ regulatory T cell subsets." J Leukoc Biol **74**(4): 471-8.

Hsieh, C. S., Y. Zheng, Y. Liang, J. D. Fontenot and A. Y. Rudensky (2006). "An intersection between the self-reactive regulatory and nonregulatory T cell receptor repertoires." Nat Immunol **7**(4): 401-10.

Hsieh, S. Y., P. S. Hsieh, C. T. Chiu and W. Y. Chen (2004). "Dickkopf-3/REIC functions as a suppressor gene of tumor growth." Oncogene **23**(57): 9183-9.

Hu, D., K. Ikizawa, L. Lu, M. E. Sanchirico, M. L. Shinohara and H. Cantor (2004). "Analysis of regulatory CD8 T cells in Qa-1-deficient mice." Nat Immunol **5**(5): 516-23.

Hua, C., C. Boyer, M. Buferne and A. M. Schmitt-Verhulst (1986). "Monoclonal antibodies against an H-2Kb-specific cytotoxic T cell clone detect several clone-specific molecules." J Immunol **136**(6): 1937-44.

Huesmann, M., B. Scott, P. Kisielow and H. von Boehmer (1991). "Kinetics and efficacy of positive selection in the thymus of normal and T cell receptor transgenic mice." Cell **66**(3): 533-40.

Huffnagle, G. B., L. K. McNeil, R. A. McDonald, J. W. Murphy, G. B. Toews, N. Maeda and W. A. Kuziel (1999). "Cutting edge: Role of C-C chemokine receptor 5 in organ-specific and innate immunity to Cryptococcus neoformans." J Immunol **163**(9): 4642-6.

Huseby, E. S., D. Liggitt, T. Brabb, B. Schnabel, C. Ohlen and J. Goverman (2001). "A pathogenic role for myelin-specific CD8(+) T cells in a model for multiple sclerosis." J Exp Med **194**(5): 669-76.

Huseby, E. S., C. Ohlen and J. Goverman (1999). "Cutting edge: myelin basic protein-specific cytotoxic T cell tolerance is maintained in vivo by a single dominant epitope in H-2k mice." J Immunol **163**(3): 1115-8.

Itoh, M., T. Takahashi, N. Sakaguchi, Y. Kuniyasu, J. Shimizu, F. Otsuka and S. Sakaguchi (1999). "Thymus and autoimmunity: production of CD25+CD4+ naturally anergic and suppressive T cells as a key function of the thymus in maintaining immunologic self-tolerance." J Immunol **162**(9): 5317-26.

Jenkins, M. K., D. M. Pardoll, J. Mizuguchi, H. Quill and R. H. Schwartz (1987). "T-cell unresponsiveness in vivo and in vitro: fine specificity of induction and molecular characterization of the unresponsive state." Immunol Rev **95**: 113-35.

Jeremias, I., I. Herr, T. Boehler and K. M. Debatin (1998). "TRAIL/Apo-2-ligand-induced apoptosis in human T cells." Eur J Immunol **28**(1): 143-52.

Ji, Q. and J. Goverman (2007). "Experimental autoimmune encephalomyelitis mediated by CD8+ T cells." Ann N Y Acad Sci **1103**: 157-66.

Jiang, H., S. Curran, E. Ruiz-Vazquez, B. Liang, R. Winchester and L. Chess (2003). "Regulatory CD8+ T cells fine-tune the myelin basic protein-reactive T cell receptor V beta repertoire during experimental autoimmune encephalomyelitis." Proc Natl Acad Sci U S A **100**(14): 8378-83.

Jiang, L., P. Yang, H. He, B. Li, X. Lin, S. Hou, H. Zhou, X. Huang and K. Aize (2007). "Increased expression of Foxp3 in splenic CD8+ T cells from mice with anterior chamber-associated immune deviation." Mol Vis **13**: 968-74.

Jordan, M. S., A. Boesteanu, A. J. Reed, A. L. Petrone, A. E. Holenbeck, M. A. Lerman, A. Naji and A. J. Caton (2001). "Thymic selection of CD4+CD25+ regulatory T cells induced by an agonist self-peptide." Nat Immunol **2**(4): 301-6.

Jorgensen, S. H., P. E. Jensen, H. Laursen and P. S. Sorensen (2005). "Intravenous immunoglobulin ameliorates experimental autoimmune encephalomyelitis and reduces neuropathological abnormalities when administered prophylactically." Neurol Res **27**(6): 591-7.

Jorgensen, S. H., N. Storm, P. E. Jensen, H. Laursen and P. S. Sorensen (2007). "IVIG enters the central nervous system during treatment of experimental autoimmune encephalomyelitis and is localised to inflammatory lesions." Exp Brain Res **178**(4): 462-9.

June, C. H., J. A. Bluestone, L. M. Nadler and C. B. Thompson (1994). "The B7 and CD28 receptor families." Immunol Today **15**(7): 321-31.

Kaech, S. M., S. Hemby, E. Kersh and R. Ahmed (2002). "Molecular and functional profiling of memory CD8 T cell differentiation." Cell **111**(6): 837-51.

Kang, S. M., B. Beverly, A. C. Tran, K. Brorson, R. H. Schwartz and M. J. Lenardo (1992). "Transactivation by AP-1 is a molecular target of T cell clonal anergy." Science **257**(5073): 1134-8.

Kaplan, H. J. and J. W. Streilein (1977). "Immune response to immunization via the anterior chamber of the eye. I. F. lymphocyte-induced immune deviation." J Immunol **118**(3): 809-14.

Kapp, J. A., K. Honjo, L. M. Kapp, X. Xu, A. Cozier and R. P. Bucy (2006). "TCR transgenic CD8+ T cells activated in the presence of TGFbeta express FoxP3 and mediate linked suppression of primary immune responses and cardiac allograft rejection." Int Immunol **18**(11): 1549-62.

Kappler, J. W., N. Roehm and P. Marrack (1987). "T cell tolerance by clonal elimination in the thymus." Cell **49**(2): 273-80.

Kawabe, Y. and A. Ochi (1990). "Selective anergy of V beta 8+,CD4+ T cells in Staphylococcus enterotoxin B-primed mice." J Exp Med **172**(4): 1065-70.

Kawahata, K., Y. Misaki, M. Yamauchi, S. Tsunekawa, K. Setoguchi, J. Miyazaki and K. Yamamoto (2002). "Generation of CD4(+)CD25(+) regulatory T cells from autoreactive T cells simultaneously with their negative selection in the thymus and from nonautoreactive T cells by endogenous TCR expression." J Immunol **168**(9): 4399-405.

Kawano, Y., M. Kitaoka, Y. Hamada, M. M. Walker, J. Waxman and R. M. Kypta (2006). "Regulation of prostate cell growth and morphogenesis by Dickkopf-3." Oncogene **25**(49): 6528-37.

Kearney, E. R., K. A. Pape, D. Y. Loh and M. K. Jenkins (1994). "Visualization of peptide-specific T cell immunity and peripheral tolerance induction in vivo." Immunity **1**(4): 327-39.

Kim, J. M., J. P. Rasmussen and A. Y. Rudensky (2007). "Regulatory T cells prevent catastrophic autoimmunity throughout the lifespan of mice." Nat Immunol **8**(2): 191-7.

Kimpton, W. G., E. A. Washington and R. N. Cahill (1995). "Virgin alpha beta and gamma delta T cells recirculate extensively through peripheral tissues and skin during normal development of the fetal immune system." Int Immunol **7**(10): 1567-77.

Kingsley, C. I., M. Karim, A. R. Bushell and K. J. Wood (2002). "CD25+CD4+ regulatory T cells prevent graft rejection: CTLA-4- and IL-10-dependent immunoregulation of alloresponses." J Immunol **168**(3): 1080-6.

Kisielow, P. (1988). "The true function of the thymus." Immunol Today **9**(12): 367.

Knolle, P. A., E. Schmitt, S. Jin, T. Germann, R. Duchmann, S. Hegenbarth, G. Gerken and A. W. Lohse (1999). "Induction of cytokine production in naive CD4(+) T cells by antigen-presenting murine liver sinusoidal endothelial cells but failure to induce differentiation toward Th1 cells." Gastroenterology **116**(6): 1428-40.

Kobayashi, K., M. Ouchida, T. Tsuji, H. Hanafusa, M. Miyazaki, M. Namba, N. Shimizu and K. Shimizu (2002). "Reduced expression of the REIC/Dkk-3 gene by promoter-hypermethylation in human tumor cells." Gene **282**(1-2): 151-8.

Kohn, A. D. and R. T. Moon (2005). "Wnt and calcium signaling: beta-catenin-independent pathways." Cell Calcium **38**(3-4): 439-46.

Korn, T., M. Oukka, V. Kuchroo and E. Bettelli (2007). "Th17 cells: effector T cells with inflammatory properties." Semin Immunol **19**(6): 362-71.

Krakowski, M. and T. Owens (1996). "Interferon-gamma confers resistance to experimental allergic encephalomyelitis." Eur J Immunol **26**(7): 1641-6.

Kretschmer, K., I. Apostolou, D. Hawiger, K. Khazaie, M. C. Nussenzweig and H. von Boehmer (2005). "Inducing and expanding regulatory T cell populations by foreign antigen." Nat Immunol **6**(12): 1219-27.

Krupnik, V. E., J. D. Sharp, C. Jiang, K. Robison, T. W. Chickering, L. Amaravadi, D. E. Brown, D. Guyot, G. Mays, K. Leiby, B. Chang, T. Duong, A. D. Goodearl, D. P. Gearing, S. Y. Sokol and S. A. McCarthy (1999). "Functional and structural diversity of the human Dickkopf gene family." Gene **238**(2): 301-13.

Kumar, V. (2004). "Homeostatic control of immunity by TCR peptide-specific Tregs." J Clin Invest **114**(9): 1222-6.

Kuphal, S., S. Lodermeyer, F. Bataille, M. Schuierer, B. H. Hoang and A. K. Bosserhoff (2006). "Expression of Dickkopf genes is strongly reduced in malignant melanoma." Oncogene **25**(36): 5027-36.

Kurts, C., W. R. Heath, H. Kosaka, J. F. Miller and F. R. Carbone (1998). "The peripheral deletion of autoreactive CD8+ T cells induced by cross-presentation of self-antigens involves signaling through CD95 (Fas, Apo-1)." J Exp Med **188**(2): 415-20.

Kwidzinski, E. and I. Bechmann (2007). "IDO expression in the brain: a double-edged sword." J Mol Med **85**(12): 1351-9.

Lampson, L. A. and C. A. Fisher (1984). "Weak HLA and beta 2-microglobulin expression of neuronal cell lines can be modulated by interferon." Proc Natl Acad Sci U S A **81**(20): 6476-80.

Langrish, C. L., Y. Chen, W. M. Blumenschein, J. Mattson, B. Basham, J. D. Sedgwick, T. McClanahan, R. A. Kastelein and D. J. Cua (2005). "IL-23 drives a pathogenic T cell population that induces autoimmune inflammation." J Exp Med **201**(2): 233-40.

Leifeld, L., C. Trautwein, F. L. Dumoulin, M. P. Manns, T. Sauerbruch and U. Spengler (1999). "Enhanced expression of CD80 (B7-1), CD86 (B7-2), and CD40 and their ligands CD28 and CD154 in fulminant hepatic failure." Am J Pathol **154**(6): 1711-20.

Lenardo, M., K. M. Chan, F. Hornung, H. McFarland, R. Siegel, J. Wang and L. Zheng (1999). "Mature T lymphocyte apoptosis--immune regulation in a dynamic and unpredictable antigenic environment." Annu Rev Immunol **17**: 221-53.

Li, M. O., Y. Y. Wan and R. A. Flavell (2007). "T cell-produced transforming growth factor-beta1 controls T cell tolerance and regulates Th1- and Th17-cell differentiation." Immunity **26**(5): 579-91.

Li, W., C. D. Whaley, A. Mondino and D. L. Mueller (1996). "Blocked signal transduction to the ERK and JNK protein kinases in anergic CD4+ T cells." Science **271**(5253): 1272-6.

Limmer, A., J. Ohl, C. Kurts, H. G. Ljunggren, Y. Reiss, M. Groettrup, F. Momburg, B. Arnold and P. A. Knolle (2000). "Efficient presentation of exogenous antigen by liver endothelial cells to CD8+ T cells results in antigen-specific T-cell tolerance." Nat Med **6**(12): 1348-54.

Liu, Y. J., V. Soumelis, N. Watanabe, T. Ito, Y. H. Wang, W. Malefyt Rde, M. Omori, B. Zhou and S. F. Ziegler (2007). "TSLP: an epithelial cell cytokine that regulates T cell differentiation by conditioning dendritic cell maturation." Annu Rev Immunol **25**: 193-219.

Lodygin, D., A. Epanchintsev, A. Menssen, J. Diebold and H. Hermeking (2005). "Functional epigenomics identifies genes frequently silenced in prostate cancer." Cancer Res **65**(10): 4218-27.

Loeser, S. and J. M. Penninger (2007). "Regulation of peripheral T cell tolerance by the E3 ubiquitin ligase Cbl-b." Semin Immunol **19**(3): 206-14.

Lohse, A. W., P. A. Knolle, K. Bilo, A. Uhrig, C. Waldmann, M. Ibe, E. Schmitt, G. Gerken and K. H. Meyer Zum Buschenfelde (1996). "Antigen-presenting function and B7 expression of murine sinusoidal endothelial cells and Kupffer cells." Gastroenterology **110**(4): 1175-81.

Lord, S. J., R. V. Rajotte, G. S. Korbutt and R. C. Bleackley (2003). "Granzyme B: a natural born killer." Immunol Rev **193**: 31-8.

Lutz, M. B. and G. Schuler (2002). "Immature, semi-mature and fully mature dendritic cells: which signals induce tolerance or immunity?" Trends Immunol **23**(9): 445-9.

Lyakh, L., P. Ghosh and N. R. Rice (1997). "Expression of NFAT-family proteins in normal human T cells." Mol Cell Biol **17**(5): 2475-84.

Macian, F., F. Garcia-Cozar, S. H. Im, H. F. Horton, M. C. Byrne and A. Rao (2002). "Transcriptional mechanisms underlying lymphocyte tolerance." Cell **109**(6): 719-31.

Madakamutil, L. T., I. Maricic, E. Sercarz and V. Kumar (2003). "Regulatory T cells control autoimmunity in vivo by inducing apoptotic depletion of activated pathogenic lymphocytes." J Immunol **170**(6): 2985-92.

Mahic, M., K. Henjum, S. Yaqub, B. A. Bjornbeth, K. M. Torgersen, K. Tasken and E. M. Aandahl (2008). "Generation of highly suppressive adaptive CD8(+)CD25(+)FOXP3(+) regulatory T cells by continuous antigen stimulation." Eur J Immunol **38**(3): 640-6.

Maloy, K. J. and F. Powrie (2001). "Regulatory T cells in the control of immune pathology." Nat Immunol **2**(9): 816-22.

Maloy, K. J., L. Salaun, R. Cahill, G. Dougan, N. J. Saunders and F. Powrie (2003). "CD4+CD25+ T(R) cells suppress innate immune pathology through cytokine-dependent mechanisms." J Exp Med **197**(1): 111-9.

Mao, B., W. Wu, G. Davidson, J. Marhold, M. Li, B. M. Mechler, H. Delius, D. Hoppe, P. Stannek, C. Walter, A. Glinka and C. Niehrs (2002). "Kremen proteins are Dickkopf receptors that regulate Wnt/beta-catenin signalling." Nature **417**(6889): 664-7.

Mao, B., W. Wu, Y. Li, D. Hoppe, P. Stannek, A. Glinka and C. Niehrs (2001). "LDL-receptor-related protein 6 is a receptor for Dickkopf proteins." Nature **411**(6835): 321-5.

Mariani, S. M. and P. H. Krammer (1998). "Surface expression of TRAIL/Apo-2 ligand in activated mouse T and B cells." Eur J Immunol **28**(5): 1492-8.

McLean, J. M. and R. J. Scothorne (1970). "The lymphatics of the endometrium in the rabbit." J Anat **107**(Pt 1): 39-48.

Medawar (1948). "Immunity to homologous skin grafting III. The fate of skin homografts transplanted to the brain and to the anterior chamber of the eye." Br J Exp Path **29**: 58-69.

Micklem, H. S., C. E. Ford, E. P. Evans and J. Gray (1966). "Interrelationships of myeloid and lymphoid cells: studies with chromosome-marked cells transfused into lethally irradiated mice." Proc R Soc Lond B Biol Sci **165**(998): 78-102.

Micsenyi, A., X. Tan, T. Sneddon, J. H. Luo, G. K. Michalopoulos and S. P. Monga (2004). "Beta-catenin is temporally regulated during normal liver development." Gastroenterology **126**(4): 1134-46.

Modigliani, Y., A. Coutinho, P. Pereira, N. Le Douarin, V. Thomas-Vaslin, O. Burlen-Defranoux, J. Salaun and A. Bandeira (1996). "Establishment of tissue-specific tolerance is driven by regulatory T cells selected by thymic epithelium." Eur J Immunol **26**(8): 1807-15.

Mogil, R. J., L. Radvanyi, R. Gonzalez-Quintial, R. Miller, G. Mills, A. N. Theofilopoulos and D. R. Green (1995). "Fas (CD95) participates in peripheral T cell deletion and associated apoptosis in vivo." Int Immunol **7**(9): 1451-8.

Moore, M. A. and J. J. Owen (1965). "Chromosome marker studies on the development of the haemopoietic system in the chick embryo." Nature **208**(5014): 956 passim.

Moore, M. A. and J. J. Owen (1967). "Experimental studies on the development of the thymus." J Exp Med **126**(4): 715-26.

Morelli, A. E. and A. W. Thomson (2003). "Dendritic cells: regulators of alloimmunity and opportunities for tolerance induction." Immunol Rev **196**: 125-46.

Murai, M., H. Yoneyama, T. Ezaki, M. Suematsu, Y. Terashima, A. Harada, H. Hamada, H. Asakura, H. Ishikawa and K. Matsushima (2003). "Peyer's patch is the essential site in initiating murine acute and lethal graft-versus-host reaction." Nat Immunol **4**(2): 154-60.

Murphy, P. M., M. Baggiolini, I. F. Charo, C. A. Hebert, R. Horuk, K. Matsushima, L. H. Miller, J. J. Oppenheim and C. A. Power (2000). "International union of pharmacology. XXII. Nomenclature for chemokine receptors." Pharmacol Rev **52**(1): 145-76.

Nagata, S. (1997). "Apoptosis by death factor." Cell **88**(3): 355-65.

Najafian, N., T. Chitnis, A. D. Salama, B. Zhu, C. Benou, X. Yuan, M. R. Clarkson, M. H. Sayegh and S. J. Khoury (2003). "Regulatory functions of CD8+CD28- T cells in an autoimmune disease model." J Clin Invest **112**(7): 1037-48.

Nakao, A., T. Imamura, S. Souchelnytskyi, M. Kawabata, A. Ishisaki, E. Oeda, K. Tamaki, J. Hanai, C. H. Heldin, K. Miyazono and P. ten Dijke (1997). "TGF-beta receptor-mediated signalling through Smad2, Smad3 and Smad4." Embo J **16**(17): 5353-62.

Nelson, W. J. and R. Nusse (2004). "Convergence of Wnt, beta-catenin, and cadherin pathways." Science **303**(5663): 1483-7.

Neumann, H., I. M. Medana, J. Bauer and H. Lassmann (2002). "Cytotoxic T lymphocytes in autoimmune and degenerative CNS diseases." Trends Neurosci **25**(6): 313-9.

Ng-Cashin, J., J. J. Kuhns, S. E. Burkett, J. D. Powderly, R. R. Craven, H. W. van Deventer, S. L. Kirby and J. S. Serody (2003). "Host absence of CCR5 potentiates dendritic cell vaccination." J Immunol **170**(8): 4201-8.

Niederkorn, J. Y. (2006). "See no evil, hear no evil, do no evil: the lessons of immune privilege." Nat Immunol **7**(4): 354-9.

Niehrs, C. (2006). "Function and biological roles of the Dickkopf family of Wnt modulators." Oncogene **25**(57): 7469-81.

Nikcevich, K. M., K. B. Gordon, L. Tan, S. D. Hurst, J. F. Kroepfl, M. Gardinier, T. A. Barrett and S. D. Miller (1997). "IFN-gamma-activated primary murine astrocytes express B7 costimulatory molecules and prime naive antigen-specific T cells." J Immunol **158**(2): 614-21.

Noh, D. Y., S. H. Shin and S. G. Rhee (1995). "Phosphoinositide-specific phospholipase C and mitogenic signaling." Biochim Biophys Acta **1242**(2): 99-113.

Ono, M., H. Yaguchi, N. Ohkura, I. Kitabayashi, Y. Nagamura, T. Nomura, Y. Miyachi, T. Tsukada and S. Sakaguchi (2007). "Foxp3 controls regulatory T-cell function by interacting with AML1/Runx1." Nature **446**(7136): 685-9.

Oshima, T., F. S. Laroux, L. L. Coe, Z. Morise, S. Kawachi, P. Bauer, M. B. Grisham, R. D. Specian, P. Carter, S. Jennings, D. N. Granger, T. Joh and J. S. Alexander (2001). "Interferon-gamma and interleukin-10 reciprocally regulate endothelial junction integrity and barrier function." Microvasc Res **61**(1): 130-43.

Ouyang, W., J. K. Kolls and Y. Zheng (2008). "The biological functions of T helper 17 cell effector cytokines in inflammation." Immunity **28**(4): 454-67.

Pacholczyk, R., J. Kern, N. Singh, M. Iwashima, P. Kraj and L. Ignatowicz (2007). "Nonself-antigens are the cognate specificities of Foxp3+ regulatory T cells." Immunity **27**(3): 493-504.

Pandiyan, P., L. Zheng, S. Ishihara, J. Reed and M. J. Lenardo (2007). "CD4+CD25+Foxp3+ regulatory T cells induce cytokine deprivation-mediated apoptosis of effector CD4+ T cells." Nat Immunol **8**(12): 1353-62.

Phillips, T. A., J. Ni, G. Pan, S. M. Ruben, Y. F. Wei, J. L. Pace and J. S. Hunt (1999). "TRAIL (Apo-2L) and TRAIL receptors in human placentas: implications for immune privilege." J Immunol **162**(10): 6053-9.

Pickart, C. M. and D. Fushman (2004). "Polyubiquitin chains: polymeric protein signals." Curr Opin Chem Biol **8**(6): 610-6.

Pinho, S. and C. Niehrs (2007). "Dkk3 is required for TGF-beta signaling during Xenopus mesoderm induction." Differentiation **75**(10): 957-67.

Pitkanen, J. and P. Peterson (2003). "Autoimmune regulator: from loss of function to autoimmunity." Genes Immun **4**(1): 12-21.

Pollard, S. L. and P. W. Holland (2000). "Evidence for 14 homeobox gene clusters in human genome ancestry." Curr Biol **10**(17): 1059-62.

Popko, B. and K. D. Baerwald (1999). "Oligodendroglial response to the immune cytokine interferon gamma." Neurochem Res **24**(2): 331-8.

Praseedom, R. K., K. D. McNeil, C. J. Watson, G. J. Alexander, R. Y. Calne, J. Wallwork and P. J. Friend (2001). "Combined transplantation of the heart, lung, and liver." Lancet **358**(9284): 812-3.

Puccetti, P. and U. Grohmann (2007). "IDO and regulatory T cells: a role for reverse signalling and non-canonical NF-kappaB activation." Nat Rev Immunol **7**(10): 817-23.

Qin, H. Y., R. Mukherjee, E. Lee-Chan, C. Ewen, R. C. Bleackley and B. Singh (2006). "A novel mechanism of regulatory T cell-mediated down-regulation of autoimmunity." Int Immunol **18**(7): 1001-15.

Quill, H. and R. H. Schwartz (1987). "Stimulation of normal inducer T cell clones with antigen presented by purified Ia molecules in planar lipid membranes: specific induction of a long-lived state of proliferative nonresponsiveness." J Immunol **138**(11): 3704-12.

Read, S., R. Greenwald, A. Izcue, N. Robinson, D. Mandelbrot, L. Francisco, A. H. Sharpe and F. Powrie (2006). "Blockade of CTLA-4 on CD4+CD25+ regulatory T cells abrogates their function in vivo." J Immunol **177**(7): 4376-83.

Refaeli, Y., L. Van Parijs, C. A. London, J. Tschopp and A. K. Abbas (1998). "Biochemical mechanisms of IL-2-regulated Fas-mediated T cell apoptosis." Immunity **8**(5): 615-23.

Reibke, R., N. Garbi, R. Ganss, G. J. Hammerling, B. Arnold and T. Oelert (2006). "CD8+ regulatory T cells generated by neonatal recognition of peripheral self-antigen." Proc Natl Acad Sci U S A **103**(41): 15142-7.

Reinke, E. and Z. Fabry (2006). "Breaking or making immunological privilege in the central nervous system: the regulation of immunity by neuropeptides." Immunol Lett **104**(1-2): 102-9.

Roman-Gomez, J., A. Jimenez-Velasco, X. Agirre, J. A. Castillejo, G. Navarro, M. Barrios, E. J. Andreu, F. Prosper, A. Heiniger and A. Torres (2004). "Transcriptional silencing of the Dickkopfs-3 (Dkk-3) gene by CpG hypermethylation in acute lymphoblastic leukaemia." Br J Cancer **91**(4): 707-13.

Romeo, P. H., V. Lemarchandel and R. Tordjman (2002). "Neuropilin-1 in the immune system." Adv Exp Med Biol **515**: 49-54.

Safford, M., S. Collins, M. A. Lutz, A. Allen, C. T. Huang, J. Kowalski, A. Blackford, M. R. Horton, C. Drake, R. H. Schwartz and J. D. Powell (2005). "Egr-2 and Egr-3 are negative regulators of T cell activation." Nat Immunol **6**(5): 472-80.

Saha, D., P. K. Datta and R. D. Beauchamp (2001). "Oncogenic ras represses transforming growth factor-beta /Smad signaling by degrading tumor suppressor Smad4." J Biol Chem **276**(31): 29531-7.

Sakaguchi, S., T. Yamaguchi, T. Nomura and M. Ono (2008). "Regulatory T cells and immune tolerance." Cell **133**(5): 775-87.

Sarris, M., K. G. Andersen, F. Randow, L. Mayr and A. G. Betz (2008). "Neuropilin-1 expression on regulatory T cells enhances their interactions with dendritic cells during antigen recognition." Immunity **28**(3): 402-13.

Sato, N., W. A. Kuziel, P. C. Melby, R. L. Reddick, V. Kostecki, W. Zhao, N. Maeda, S. K. Ahuja and S. S. Ahuja (1999). "Defects in the generation of IFN-gamma are overcome to control infection with Leishmania donovani in CC chemokine receptor (CCR) 5-, macrophage inflammatory protein-1 alpha-, or CCR2-deficient mice." J Immunol **163**(10): 5519-25.

Schartner, J. M., C. G. Fathman and C. M. Seroogy (2007). "Preservation of self: an overview of E3 ubiquitin ligases and T cell tolerance." Semin Immunol **19**(3): 188-96.

Schmitt, E., P. Hoehn, C. Huels, S. Goedert, N. Palm, E. Rude and T. Germann (1994). "T helper type 1 development of naive CD4+ T cells requires the coordinate action of interleukin-12 and interferon-gamma and is inhibited by transforming growth factor-beta." Eur J Immunol **24**(4): 793-8.

Schroeder, A., O. Mueller, S. Stocker, R. Salowsky, M. Leiber, M. Gassmann, S. Lightfoot, W. Menzel, M. Granzow and T. Ragg (2006). "The RIN: an RNA integrity number for assigning integrity values to RNA measurements." BMC Mol Biol **7**: 3.

Schwartz, R. H. (2003). "T cell anergy." Annu Rev Immunol **21**: 305-34.

Seddon, B. and D. Mason (2000). "The third function of the thymus." Immunol Today **21**(2): 95-9.

Sharabi, A. and E. Mozes (2008). "The suppression of murine lupus by a tolerogenic peptide involves foxp3-expressing CD8 cells that are required for the optimal induction and function of foxp3-expressing CD4 cells." J Immunol **181**(5): 3243-51.

Shevach, E. M., R. S. McHugh, C. A. Piccirillo and A. M. Thornton (2001). "Control of T-cell activation by CD4+ CD25+ suppressor T cells." Immunol Rev **182**: 58-67.

Sloan-Lancaster, J., B. D. Evavold and P. M. Allen (1993). "Induction of T-cell anergy by altered T-cell-receptor ligand on live antigen-presenting cells." Nature **363**(6425): 156-9.

Sonobe, Y., S. Jin, J. Wang, J. Kawanokuchi, H. Takeuchi, T. Mizuno and A. Suzumura (2007). "Chronological changes of CD4(+) and CD8(+) T cell subsets in the experimental autoimmune encephalomyelitis, a mouse model of multiple sclerosis." Tohoku J Exp Med **213**(4): 329-39.

Steinman, L. (2001). "Myelin-specific CD8 T cells in the pathogenesis of experimental allergic encephalitis and multiple sclerosis." J Exp Med **194**(5): F27-30.

Steinman, R. M., D. Hawiger and M. C. Nussenzweig (2003). "Tolerogenic dendritic cells." Annu Rev Immunol **21**: 685-711.

Steinman, R. M. and M. C. Nussenzweig (2002). "Avoiding horror autotoxicus: the importance of dendritic cells in peripheral T cell tolerance." Proc Natl Acad Sci U S A **99**(1): 351-8.

Steinman, R. M. and M. D. Witmer (1978). "Lymphoid dendritic cells are potent stimulators of the primary mixed leukocyte reaction in mice." Proc Natl Acad Sci U S A **75**(10): 5132-6.

Stephens, G. L. and E. M. Shevach (2007). "Foxp3+ regulatory T cells: selfishness under scrutiny." Immunity **27**(3): 417-9.

Stockinger, B. and M. Veldhoen (2007). "Differentiation and function of Th17 T cells." Curr Opin Immunol **19**(3): 281-6.

Stone, J. C. (2006). "Regulation of Ras in lymphocytes: get a GRP." Biochem Soc Trans **34**(Pt 5): 858-61.

Street, N. E. and T. R. Mosmann (1991). "Functional diversity of T lymphocytes due to secretion of different cytokine patterns." Faseb J **5**(2): 171-7.

Streilein, J. W. (2003). "Ocular immune privilege: therapeutic opportunities from an experiment of nature." Nat Rev Immunol **3**(11): 879-89.

Sun, C. M., J. A. Hall, R. B. Blank, N. Bouladoux, M. Oukka, J. R. Mora and Y. Belkaid (2007). "Small intestine lamina propria dendritic cells promote de novo generation of Foxp3 T reg cells via retinoic acid." J Exp Med **204**(8): 1775-85.

Sun, D., J. N. Whitaker, Z. Huang, D. Liu, C. Coleclough, H. Wekerle and C. S. Raine (2001). "Myelin antigen-specific CD8+ T cells are encephalitogenic and produce severe disease in C57BL/6 mice." J Immunol **166**(12): 7579-87.

Suwa, T., M. Chen, C. L. Hawks and P. J. Hornsby (2003). "Zonal expression of dickkopf-3 and components of the Wnt signalling pathways in the human adrenal cortex." J Endocrinol **178**(1): 149-58.

Takeuchi, H., J. Wang, J. Kawanokuchi, N. Mitsuma, T. Mizuno and A. Suzumura (2006). "Interferon-gamma induces microglial-activation-induced cell death: a hypothetical mechanism of relapse and remission in multiple sclerosis." Neurobiol Dis **22**(1): 33-9.

Tang, Q. and J. A. Bluestone (2008). "The Foxp3+ regulatory T cell: a jack of all trades, master of regulation." Nat Immunol **9**(3): 239-44.

Thakker, P., M. W. Leach, W. Kuang, S. E. Benoit, J. P. Leonard and S. Marusic (2007). "IL-23 is critical in the induction but not in the effector phase of experimental autoimmune encephalomyelitis." J Immunol **178**(4): 2589-98.

van Leeuwen, J. E. and L. E. Samelson (1999). "T cell antigen-receptor signal transduction." Curr Opin Immunol **11**(3): 242-8.

van Meerwijk, J. P., S. Marguerat, R. K. Lees, R. N. Germain, B. J. Fowlkes and H. R. MacDonald (1997). "Quantitative impact of thymic clonal deletion on the T cell repertoire." J Exp Med **185**(3): 377-83.

Volkmann, A., T. Zal and B. Stockinger (1997). "Antigen-presenting cells in the thymus that can negatively select MHC class II-restricted T cells recognizing a circulating self antigen." J Immunol **158**(2): 693-706.

Wagner, D. H., Jr. (2007). "Re-shaping the T cell repertoire: TCR editing and TCR revision for good and for bad." Clin Immunol **123**(1): 1-6.

Wan, Y. Y. and R. A. Flavell (2007). "Regulatory T cells, transforming growth factor-beta, and immune suppression." Proc Am Thorac Soc **4**(3): 271-6.

Wang, S., Z. F. Boonman, H. C. Li, Y. He, M. J. Jager, R. E. Toes and J. Y. Niederkorn (2003). "Role of TRAIL and IFN-gamma in CD4+ T cell-dependent tumor rejection in the anterior chamber of the eye." J Immunol **171**(6): 2789-96.

Wenkel, H., J. W. Streilein and M. J. Young (2000). "Systemic immune deviation in the brain that does not depend on the integrity of the blood-brain barrier." J Immunol **164**(10): 5125-31.

Willenborg, D. O., S. Fordham, C. C. Bernard, W. B. Cowden and I. A. Ramshaw (1996). "IFN-gamma plays a critical down-regulatory role in the induction and effector phase of myelin oligodendrocyte glycoprotein-induced autoimmune encephalomyelitis." J Immunol **157**(8): 3223-7.

Wu, Y., M. Borde, V. Heissmeyer, M. Feuerer, A. D. Lapan, J. C. Stroud, D. L. Bates, L. Guo, A. Han, S. F. Ziegler, D. Mathis, C. Benoist, L. Chen and A. Rao (2006). "FOXP3 controls regulatory T cell function through cooperation with NFAT." Cell **126**(2): 375-87.

Wysocki, C. A., Q. Jiang, A. Panoskaltsis-Mortari, P. A. Taylor, K. P. McKinnon, L. Su, B. R. Blazar and J. S. Serody (2005). "Critical role for CCR5 in the function of donor CD4+CD25+ regulatory T cells during acute graft-versus-host disease." Blood **106**(9): 3300-7.

Yue, W., Q. Sun, S. Dacic, R. J. Landreneau, J. M. Siegfried, J. Yu and L. Zhang (2008). "Downregulation of Dkk3 activates beta-catenin/TCF-4 signaling in lung cancer." Carcinogenesis **29**(1): 84-92.

Yurchenko, E., M. Tritt, V. Hay, E. M. Shevach, Y. Belkaid and C. A. Piccirillo (2006). "CCR5-dependent homing of naturally occurring CD4+ regulatory T cells to sites of Leishmania major infection favors pathogen persistence." J Exp Med **203**(11): 2451-60.

Zehntner, S. P., L. Bourbonniere, M. Hassan-Zahraee, E. Tran and T. Owens (2004). "Bone marrow-derived versus parenchymal sources of inducible nitric oxide synthase in experimental autoimmune encephalomyelitis." J Neuroimmunol **150**(1-2): 70-9.

Zinkernagel, R. M., M. F. Bachmann, T. M. Kundig, S. Oehen, H. Pirchet and H. Hengartner (1996). "On immunological memory." Annu Rev Immunol **14**: 333-67.

Zinkernagel, R. M. and P. C. Doherty (1974). "Restriction of in vitro T cell-mediated cytotoxicity in lymphocytic choriomeningitis within a syngeneic or semiallogeneic system." Nature **248**(450): 701-2.

Zinkernagel, R. M. and P. C. Doherty (1979). "MHC-restricted cytotoxic T cells: studies on the biological role of polymorphic major transplantation antigens determining T-cell restriction-specificity, function, and responsiveness." Adv Immunol **27**: 51-177.

Appendix 1: The 1000 first most up-regulated genes in regulatory Des-TCR CD8 T cells as compared to activated Des-TCR CD8 T cells

Probe Set Name	Signal Log Ratio	Change p-value	Gene Symbol
1447096_at	8.64	0.00002	---
1455986_at	8.33	0.001651	Zdhhc17
1449603_at	7.72	0.00002	AI594671
1451463_at	6.48	0.000046	Arhgap8
1438945_x_at	6.35	0.001077	Gja1
1441630_at	6.34	0.00003	Ep400
1439397_at	6.33	0.000241	Fmn1
1429943_at	6.28	0.000052	Ctbs
1437707_at	6.13	0.001077	Slmo1
1415855_at	6.11	0.000346	Kitl
1441964_at	5.94	0.000552	1110003F05Rik
1458103_at	5.94	0.00004	Ncor1
1456940_at	5.84	0.000214	Slc43a2
1450037_at	5.76	0.000692	Usp9x
1421173_at	5.75	0.00002	Irf4
1452388_at	5.71	0.000046	Hspa1a
1427127_x_at	5.62	0.00002	Hspa1b
1423842_a_at	5.59	0.000068	Rnf41
1454232_at	5.55	0.000147	9430027B09Rik
1416579_a_at	5.44	0.000052	Tacstd1
1416687_at	5.42	0.001486	Plod2
1427126_at	5.4	0.00002	Hspa1b
1452318_a_at	5.31	0.00002	Hspa1b
1434559_at	5.25	0.00002	Stx3
1423700_at	5.23	0.000865	Rfc3
1428749_at	5.22	0.001336	Dmxl2
1442463_at	5.22	0.001336	---
1443153_at	5.22	0.00002	---
1457247_at	5.13	0.000101	---
1438377_x_at	5.09	0.000147	Slc13a3
1428609_at	5.07	0.000346	LOC100048581 /// LOC621579 /// Mylc2b
1423178_at	5.05	0.000774	Abi1
1420549_at	4.99	0.00003	Gbp1
1425380_at	4.96	0.000774	Rasgrp4

1436690_at	4.93	0.001651	Lrba
1448943_at	4.92	0.000147	Nrp1
1433496_at	4.77	0.001201	Glt25d1
1436672_at	4.75	0.000389	Grk5
1440325_at	4.73	0.00002	---
1445749_at	4.73	0.001832	---
1435128_at	4.72	0.000865	Baiap2
1437445_at	4.72	0.000052	Trpm1
1459810_at	4.71	0.000273	1110008F13Rik
1436916_at	4.66	0.000692	Tmem108
1434572_at	4.65	0.00002	Hdac9
1431133_at	4.63	0.000492	Arhgap18
1422252_a_at	4.61	0.001077	Cdc25c
1417704_a_at	4.58	0.000147	Arhgap6
1451013_at	4.56	0.000189	Slc29a3
1428578_s_at	4.52	0.000035	Ppfia4
1419094_at	4.51	0.000307	Cyp2c37
1418455_at	4.5	0.000865	Copz2
1455970_at	4.5	0.00002	---
1457295_at	4.49	0.001832	Tnrc6a
1431867_a_at	4.47	0.000618	1700007B13Rik
1422160_at	4.33	0.000692	H2-T24
1422781_at	4.32	0.00002	Tlr3
1438349_at	4.32	0.00002	BC043476
1434599_a_at	4.3	0.00002	Tjp2
1437950_at	4.27	0.000023	BC035537
1455180_at	4.27	0.000389	AA407270
1454803_a_at	4.26	0.000692	Hdac11
1437762_at	4.24	0.000027	Rab39
1442971_at	4.24	0.000046	Baz2b
1458399_at	4.24	0.000189	Lrrc3
1437186_at	4.23	0.000023	BC055324
1427376_a_at	4.21	0.000438	Map4k5
1429427_s_at	4.2	0.00003	Tcf7l2
1432472_a_at	4.2	0.001201	Mccc2
1441887_x_at	4.2	0.00002	EG622976
1430955_at	4.18	0.000273	2810403A07Rik
1449310_at	4.18	0.00002	Ptger2
1417073_a_at	4.17	0.00002	Qk
1418086_at	4.16	0.00002	Ppp1r14a
1439214_a_at	4.15	0.00003	Api5

1417172_at	4.13	0.001486	Ube2l6
1419821_s_at	4.13	0.00002	Idh1
1435542_s_at	4.13	0.00002	Cttnbp2nl
1435771_at	4.12	0.00002	Plcb4
1448944_at	4.12	0.00004	Nrp1
1416467_at	4.09	0.000492	Ddx3x
1458662_at	4.07	0.000552	Daam1
1441423_at	4.06	0.00013	Ece1
1425878_at	4.03	0.000147	Cabp4
1429466_s_at	4.02	0.00002	Aph1b /// Aph1c
1428856_at	4.01	0.000167	H13
1429527_a_at	4	0.000492	Plscr1
1422411_s_at	3.99	0.00002	Ear1 /// Ear12 /// Ear2 /// Ear3
1441344_at	3.98	0.000346	Erlin1
1453985_at	3.98	0.000692	0610007P08Rik
1416188_at	3.96	0.000035	Gm2a
1422964_at	3.96	0.000027	Rad23a
1416236_a_at	3.94	0.00003	Mpzl2
1439127_at	3.94	0.00002	AI314180
1448627_s_at	3.94	0.001201	Pbk
1450883_a_at	3.93	0.00002	Cd36
1452487_x_at	3.93	0.000552	Pira2
1460329_at	3.93	0.001077	B4galt6 /// LOC675709
1422824_s_at	3.92	0.00002	Eps8
1443336_at	3.92	0.001486	---
1425513_at	3.91	0.000774	Map2k7
1434277_a_at	3.9	0.00002	Ypel2
1437502_x_at	3.9	0.000023	Cd24a /// EG621324
1426301_at	3.88	0.001201	Alcam
1457753_at	3.87	0.000114	Tlr13
1429332_at	3.86	0.000273	4632427E13Rik
1436329_at	3.86	0.00002	Egr3
1428034_a_at	3.85	0.000552	Tnfrsf9
1434955_at	3.84	0.00002	1-Mar
1435679_at	3.84	0.000167	Optn
1427170_at	3.83	0.000552	Psma8
1430439_at	3.83	0.000027	Mctp1
1431645_a_at	3.83	0.001201	Gdi2
1439790_at	3.83	0.00002	Serpinb9
1455796_x_at	3.83	0.00002	Olfm1
1453135_at	3.82	0.00002	Fndc5

1455621_at	3.82	0.001201	BC066107
1421955_a_at	3.81	0.00002	Nedd4
1447914_x_at	3.8	0.00002	2600010E01Rik
1436080_at	3.79	0.000618	AW011738
1448460_at	3.79	0.00002	Acvr1
1451243_at	3.79	0.00002	Rnpep
1428260_at	3.78	0.00002	Spg3a
1428517_at	3.78	0.000046	Wdfy3
1429428_at	3.78	0.00002	Tcf7l2
1449858_at	3.78	0.00002	Cd86
1451867_x_at	3.78	0.000088	Arhgap6
1422294_at	3.77	0.000027	Xcr1
1438030_at	3.77	0.00002	Rasgrp3
1456174_x_at	3.76	0.00002	Ndrg1
1429656_at	3.75	0.000774	Rhobtb1
1449670_x_at	3.75	0.000023	Gpr137b /// LOC100044979
1423319_at	3.74	0.000241	Hhex
1450070_s_at	3.74	0.00002	Pak1
1436397_at	3.73	0.000167	Tifab
1437921_x_at	3.73	0.00002	Zfp516
1423569_at	3.71	0.00002	Gatm
1434442_at	3.71	0.00002	Stbd1
1438463_x_at	3.71	0.000438	Zdhhc6
1421137_a_at	3.69	0.00002	Pkib
1438306_at	3.69	0.00002	Rnf180
1432466_a_at	3.68	0.00003	Apoe
1433452_at	3.68	0.00002	B630019K06Rik
1451386_at	3.68	0.00002	Blvrb
1452411_at	3.68	0.00002	Lrrc1
1455009_at	3.68	0.00013	Cpd
1434061_at	3.67	0.00002	Rp2h
1438068_at	3.67	0.00002	---
1453181_x_at	3.67	0.00002	Plscr1
1452301_at	3.66	0.00003	Aldh3b1
1424902_at	3.65	0.00002	Plxdc1
1435064_a_at	3.65	0.00002	Tmem27
1438313_at	3.65	0.000692	---
1419627_s_at	3.63	0.00002	Clec4n
1424413_at	3.63	0.00002	Ogfrl1
1438169_a_at	3.63	0.00002	Frmd4b
1452458_s_at	3.63	0.000147	Ppil5

1416034_at	3.62	0.00002	Cd24a /// EG621324
1423378_at	3.62	0.00002	Adam23 /// LOC100046035
1428097_at	3.62	0.000241	2510009E07Rik
1447040_at	3.62	0.00002	---
1458802_at	3.62	0.00002	Hivep3
1416120_at	3.61	0.000618	Rrm2
1423166_at	3.61	0.00002	Cd36
1426775_s_at	3.61	0.00002	Scamp1
1449846_at	3.61	0.00002	Ear2
1425951_a_at	3.6	0.00003	Clec4n
1427081_at	3.6	0.00002	A630072M18Rik
1435029_at	3.6	0.00002	---
1416645_a_at	3.59	0.00002	Afp
1424367_a_at	3.59	0.000023	Homer2
1429775_a_at	3.59	0.00002	Gpr137b /// Gpr137b-ps /// LOC100044979
1429909_at	3.59	0.00002	2600010E01Rik
1437467_at	3.59	0.000035	Alcam
1439622_at	3.59	0.00002	Rassf4
1459804_at	3.59	0.000068	Crebbp
1416165_at	3.58	0.00002	Rab31
1418084_at	3.58	0.000552	Nrp1
1419829_a_at	3.58	0.000023	---
1425597_a_at	3.58	0.001336	Qk
1430886_at	3.58	0.00003	1700112E06Rik
1434695_at	3.58	0.00004	Dtl
1456574_at	3.57	0.000618	Zfp800
1458438_at	3.57	0.00002	Ccdc122
1429228_at	3.55	0.00002	4930534B04Rik
1448233_at	3.55	0.00002	Prnp
1439833_at	3.54	0.00002	3-Sep
1449348_at	3.54	0.00002	Mpp6
1458406_at	3.54	0.00002	---
1419853_a_at	3.53	0.00003	P2rx7
1424124_at	3.53	0.00002	Mospd2
1429520_a_at	3.53	0.00002	Phca
1453069_at	3.53	0.00002	Pik3cb
1457307_at	3.53	0.000346	Apol11b
1427996_at	3.52	0.000346	BC028528
1429417_at	3.52	0.000147	Chsy3
1453416_at	3.52	0.00002	Gas2l3
1415973_at	3.51	0.00002	Marcks

1421855_at	3.5	0.00002	Fgl2
1422468_at	3.5	0.00002	Ppt1
1428574_a_at	3.5	0.000027	Chn2
1434447_at	3.5	0.00002	Met
1425214_at	3.49	0.000241	P2ry6
1433908_a_at	3.49	0.00002	Cttn
1428385_at	3.48	0.000189	8-Mar
1425496_at	3.47	0.00004	Abca3
1431394_a_at	3.47	0.000068	Lrrk2
1438672_at	3.47	0.001486	Parvb
1440209_at	3.47	0.00002	1-Mar
1451623_at	3.47	0.000438	Mrpl15
1424046_at	3.46	0.000023	Bub1
1425583_at	3.46	0.00003	---
1435517_x_at	3.46	0.00002	Ralb
1436265_at	3.46	0.00004	ENSMUSG00000072769
1439489_at	3.46	0.000101	Gpr120
1422499_at	3.45	0.00002	Lima1
1422823_at	3.45	0.00002	Eps8 /// LOC632638
1429055_at	3.45	0.00002	4930506M07Rik
1435372_a_at	3.45	0.000068	Pa2g4
1435939_s_at	3.45	0.000023	AI987662
1436519_a_at	3.45	0.00002	1110057K04Rik
1448788_at	3.45	0.000023	Cd200
1451604_a_at	3.45	0.00002	Acvrl1
1424292_at	3.44	0.000068	Depdc1a
1440799_s_at	3.44	0.00002	Farp2
1424356_a_at	3.43	0.00002	Metrnl
1427456_at	3.43	0.000214	Wdfy3
1440927_x_at	3.43	0.000114	Apol11b
1451416_a_at	3.43	0.000552	Tgm1
1451929_a_at	3.43	0.000052	Vrk2
1447363_s_at	3.42	0.00003	Bub1b
1450496_a_at	3.42	0.000966	2810433K01Rik
1422412_x_at	3.41	0.000068	Ear3
1425315_at	3.41	0.00003	Dock7
1435490_at	3.41	0.000023	Hk3
1436913_at	3.41	0.00002	Cdc14a
1451451_at	3.41	0.000035	Gca
1428167_a_at	3.4	0.000027	Mpzl1
1437378_x_at	3.4	0.00002	Scarb1

1439153_at	3.4	0.00002	Rnf144b
1448558_a_at	3.4	0.001832	Pla2g4a
1422011_s_at	3.39	0.000023	3830403N18Rik /// Xlr
1425530_a_at	3.39	0.00002	Stx3
1457662_x_at	3.39	0.000774	Tpk1
1426952_at	3.38	0.00002	Arhgap18
1427912_at	3.38	0.00013	Cbr3
1433735_a_at	3.38	0.00002	Tmem64
1434437_x_at	3.38	0.00002	Rrm2
1443245_at	3.38	0.001832	---
1416431_at	3.37	0.00002	Tubb6
1418379_s_at	3.37	0.00002	Gpr124
1425477_x_at	3.37	0.000023	H2-Ab1 /// Rmcs2 /// Rmcs5
1435664_at	3.37	0.000214	Zfp397
1416441_at	3.36	0.00002	Pgcp
1416558_at	3.36	0.000046	Melk
1420980_at	3.36	0.00002	Pak1
1424733_at	3.36	0.00002	P2ry14
1426260_a_at	3.36	0.00002	LOC632297 /// Ugt1a1 /// Ugt1a10 /// Ugt1a2 /// Ugt1a5 /// Ugt1a6a /// Ugt1a6b /// Ugt1a7c /// Ugt1a9
1426530_a_at	3.36	0.00002	Klhl5
1448265_x_at	3.36	0.001832	Mpzl2
1454838_s_at	3.36	0.00002	AW548124 /// LOC100048505
1454884_at	3.36	0.00002	Zbtb46
1456475_s_at	3.36	0.00002	Prkar2b
1417938_at	3.35	0.00002	Rad51ap1
1422620_s_at	3.35	0.00002	Ppap2a
1423596_at	3.35	0.00002	Nek6
1435386_at	3.35	0.000035	Vwf
1439787_at	3.35	0.00002	P2rx7
1449453_at	3.35	0.00002	Bst1
1460431_at	3.35	0.000147	Gcnt1
1425536_at	3.34	0.000147	Stx3
1428568_at	3.34	0.000088	B230217C12Rik
1435332_at	3.34	0.000088	Htr7
1437466_at	3.34	0.000052	Alcam
1448732_at	3.34	0.00002	Ctsb
1449309_at	3.34	0.001651	Cyp8b1
1450884_at	3.34	0.000035	Cd36
1452410_a_at	3.34	0.00002	Fes
1422782_s_at	3.33	0.00002	Tlr3

1428573_at	3.33	0.00002	Chn2
1435703_at	3.33	0.00004	LOC677224
1438893_at	3.33	0.000966	5530601H04Rik
1448213_at	3.33	0.00006	Anxa1
1448600_s_at	3.33	0.00002	Vav3
1451708_at	3.33	0.000088	Gpr33
1451721_a_at	3.33	0.00002	H2-Ab1 /// Rmcs2 /// Rmcs5
1453361_at	3.33	0.001651	Hells
1455333_at	3.33	0.00002	Tns3
1419249_at	3.32	0.00004	Pftk1
1425053_at	3.32	0.00004	Isoc1
1430570_at	3.32	0.00002	Kynu
1434705_at	3.32	0.000023	Ctbp2
1434929_at	3.32	0.00002	BC035044
1435477_s_at	3.32	0.000052	Fcgr2b
1441667_s_at	3.32	0.001077	Smyd1
1447106_at	3.32	0.00013	---
1450702_at	3.32	0.000068	Hfe
1451716_at	3.32	0.000492	Mafb
1454875_a_at	3.32	0.00002	Rbbp4
1421813_a_at	3.31	0.00002	Psap
1422789_at	3.31	0.000088	Aldh1a2
1426501_a_at	3.31	0.00002	LOC637082 /// Tifa
1427311_at	3.31	0.000307	Bptf
1448226_at	3.31	0.000023	Rrm2
1424698_s_at	3.3	0.00002	Gca
1428369_s_at	3.3	0.00002	Arhgap21
1436633_at	3.3	0.00003	---
1438664_at	3.3	0.00002	Prkar2b
1455260_at	3.3	0.00002	Lcorl
1434781_at	3.29	0.000189	Dnajc16
1450896_at	3.29	0.00002	Arhgap5
1453317_a_at	3.29	0.00002	Khdrbs3
1434171_at	3.28	0.000774	C330011K17Rik
1435825_at	3.28	0.00002	Acvrl1
1437831_at	3.28	0.000167	Zcchc4
1442320_at	3.28	0.00002	LOC553096
1444884_at	3.28	0.000189	Ppt1
1416537_at	3.27	0.000389	Creld1
1420544_at	3.27	0.00003	Gcet2
1425294_at	3.27	0.00003	Slamf8

1425544_at	3.27	0.00002	Plekha5
1425784_a_at	3.27	0.00002	Olfm1
1428069_at	3.27	0.000966	Cdca7
1440790_x_at	3.27	0.00002	---
1451986_s_at	3.27	0.00002	Lrrk1
1454966_at	3.27	0.000078	Itga8
1416167_at	3.26	0.00002	Prdx4
1418258_s_at	3.26	0.000189	Dynll2
1419144_at	3.26	0.000052	Cd163
1422430_at	3.26	0.00002	Fignl1
1434089_at	3.26	0.00002	Synpo
1451043_at	3.26	0.00002	Nek6
1455843_at	3.26	0.000046	Fut4
1422601_at	3.25	0.00002	Serpinb9
1427151_at	3.25	0.000034	Qser1
1427682_a_at	3.25	0.000088	Egr2
1428577_at	3.25	0.000147	Ppfia4
1428579_at	3.25	0.00002	Fmnl2
1429831_at	3.25	0.00002	Pik3ap1
1434945_at	3.25	0.00002	Lpcat2
1454816_at	3.25	0.000147	Rp2h
1416309_at	3.24	0.00002	Nusap1
1422671_s_at	3.24	0.000273	Naalad2
1430598_at	3.24	0.001201	Crem
1435748_at	3.24	0.001832	Gda
1437306_at	3.24	0.000346	C130092O11Rik
1442582_at	3.24	0.00002	Gcet2
1448316_at	3.24	0.00002	Cmtm3 /// LOC100046883
1449580_s_at	3.24	0.00002	H2-DMb1 /// H2-DMb2
1452398_at	3.24	0.000147	Plce1
1460304_a_at	3.24	0.000774	Ubtf
1426452_a_at	3.23	0.00002	Rab30
1451246_s_at	3.23	0.000023	Aurkb
1419470_at	3.22	0.000035	Gnb4
1419587_s_at	3.22	0.000167	Rp2h
1435115_at	3.22	0.001336	Fndc5
1435330_at	3.22	0.00002	BC094916 /// LOC100048304 /// LOC637605 /// Pyhin1
1452074_at	3.22	0.000114	Tmem135
1418776_at	3.21	0.000035	5830443L24Rik
1438434_at	3.21	0.00002	Arhgap11a
1450939_at	3.21	0.000273	Entpd1

1417695_a_at	3.2	0.00002	Soat1
1419838_s_at	3.2	0.00002	Plk4
1433716_x_at	3.2	0.00004	Gfra2
1434272_at	3.2	0.000035	Cpeb2
1447458_at	3.2	0.000774	---
1448923_at	3.2	0.000078	Prkra
1449308_at	3.2	0.000389	C6
1455849_at	3.2	0.00002	Nav1
1457035_at	3.2	0.00003	AI607873
1415971_at	3.19	0.00002	Marcks
1417162_at	3.19	0.00002	Tmbim1
1418057_at	3.19	0.00002	Tiam1
1418365_at	3.19	0.00002	Ctsh
1435727_s_at	3.19	0.00002	Lima1
1448176_a_at	3.19	0.00002	Hnrpk
1455162_at	3.19	0.00002	4922503N01Rik
1416527_at	3.18	0.000052	Rab32
1420522_at	3.18	0.00002	Ccdc50
1422645_at	3.18	0.00002	Hfe
1423557_at	3.18	0.00002	Ifngr2
1426915_at	3.18	0.000101	Dapk1
1438610_a_at	3.18	0.00002	Cryz
1448761_a_at	3.18	0.00002	Copg2
1416418_at	3.17	0.000052	Gabarapl1
1417392_a_at	3.17	0.00002	Slc7a7
1417932_at	3.17	0.00002	Il18
1418123_at	3.17	0.00002	Unc119
1423889_at	3.17	0.000189	EG434402
1427488_a_at	3.17	0.000078	Birc6
1434369_a_at	3.17	0.000035	Cryab
1434988_x_at	3.17	0.000389	Aldh2
1437154_at	3.17	0.00003	Cep170
1440037_at	3.17	0.000027	Pbx1
1448892_at	3.17	0.00002	Dock7
1450744_at	3.17	0.00002	Ell2
1455761_at	3.17	0.000552	2310009B15Rik
1455820_x_at	3.17	0.00002	Scarb1
1459316_at	3.17	0.000023	---
1460341_at	3.17	0.00002	Plekhb2
1416111_at	3.16	0.00002	Cd83
1417312_at	3.16	0.00004	Dkk3

1422619_at	3.16	0.00002	Ppap2a
1437119_at	3.16	0.000035	Ern1
1437208_at	3.16	0.001486	10-Sep
1442798_x_at	3.16	0.00002	Hk3
1455665_at	3.16	0.001651	LOC631639 /// Lonrf1
1415922_s_at	3.15	0.00002	Marcksl1
1428603_at	3.15	0.00002	LOC100036521
1436025_at	3.15	0.000552	Ccdc88a
1447360_at	3.15	0.00002	Tsc22d1
1447640_s_at	3.15	0.00002	Pbx3
1450731_s_at	3.15	0.00002	Tnfrsf21
1416968_a_at	3.14	0.00002	Hsd3b7
1419586_at	3.14	0.000214	Rp2h
1420463_at	3.14	0.00002	Clnk
1422881_s_at	3.14	0.000273	Sypl
1427683_at	3.14	0.000046	Egr2
1429954_at	3.14	0.00002	Clec4a3
1439555_at	3.14	0.000023	Rlf
1448143_at	3.14	0.000035	Aldh2
1449164_at	3.14	0.00002	Cd68
1415677_at	3.13	0.00002	Dhrs1
1425108_a_at	3.13	0.000052	BC004728
1426914_at	3.13	0.00002	Marveld2
1429649_at	3.13	0.000035	Slc35a3
1438834_at	3.13	0.000023	Mospd2
1452279_at	3.13	0.00002	Cfp
1453299_a_at	3.13	0.00002	LOC100045567 /// Pnp1 /// Pnp2
1458341_x_at	3.13	0.00004	---
1417019_a_at	3.12	0.00002	Cdc6
1419081_at	3.12	0.000023	Atg10
1422535_at	3.12	0.000078	Ccne2
1426794_at	3.12	0.00002	Ptprs
1436907_at	3.12	0.00002	Nav1
1441075_at	3.12	0.00002	Nostrin
1441974_at	3.12	0.000068	Camk4
1452700_s_at	3.12	0.00002	Kbtbd7
1455425_at	3.12	0.00002	BB001228
1455901_at	3.12	0.00006	Chpt1
1421818_at	3.11	0.00002	Bcl6
1423621_a_at	3.11	0.00002	Slc33a1
1424650_at	3.11	0.00002	Pdia5

1435244_at	3.11	0.00002	Vav2
1440490_at	3.11	0.000046	---
1452514_a_at	3.11	0.00002	Kit
1455418_at	3.11	0.00002	---
1456772_at	3.11	0.00002	Ncf1
1415948_at	3.1	0.00002	Creg1
1415972_at	3.1	0.00002	Marcks
1419907_s_at	3.1	0.00002	Fcrla
1423170_at	3.1	0.000088	Taf7
1427345_a_at	3.1	0.00002	Sult1a1
1429468_at	3.1	0.00002	1110018F16Rik
1430419_at	3.1	0.00002	2310031A07Rik
1448669_at	3.1	0.000114	Dkk3
1449947_s_at	3.1	0.000046	Zfhx3
1416735_at	3.09	0.00006	Asah1
1418774_a_at	3.09	0.000023	Atp7a
1419883_s_at	3.09	0.00013	Atp6v1b2
1427161_at	3.09	0.00002	Cenpf
1435306_a_at	3.09	0.00004	Kif11
1436508_at	3.09	0.000273	2410014A08Rik
1438750_at	3.09	0.00002	Atrx
1444367_at	3.09	0.000035	Fndc7
1451318_a_at	3.09	0.00002	LOC676654 /// Lyn
1454736_at	3.09	0.000088	Ankrd57
1415897_a_at	3.08	0.000023	Mgst1
1416304_at	3.08	0.000023	Litaf
1424766_at	3.08	0.000167	Ercc6l
1432606_at	3.08	0.000346	2610012C04Rik
1435774_at	3.08	0.00002	AV024533
1437215_at	3.08	0.001201	LOC100047504 /// Nudt15
1460231_at	3.08	0.00002	Irf5
1422542_at	3.07	0.000273	Gpr34
1429206_at	3.07	0.000027	Rhobtb1
1444778_at	3.07	0.00002	3-Sep
1449454_at	3.07	0.00003	Bst1
1458159_at	3.07	0.00003	---
1416934_at	3.06	0.00002	Mtm1
1422804_at	3.06	0.000023	Serpinb6b
1429189_at	3.06	0.00002	Arsb
1439189_at	3.06	0.00002	Fnip2
1452858_at	3.06	0.001832	Elavl1

1460014_at	3.06	0.00002	Treml4
1418506_a_at	3.05	0.00002	Prdx2
1423160_at	3.05	0.000389	Spred1
1428468_at	3.05	0.00002	3110043O21Rik
1436826_at	3.05	0.000774	Tmtc3
1436921_at	3.05	0.00002	Atp7a
1440883_at	3.05	0.00002	Usp6nl
1457682_at	3.05	0.00002	9030420J04Rik
1457824_at	3.05	0.00002	Plscr1
1416046_a_at	3.04	0.00002	Fuca2
1416299_at	3.04	0.000078	Shcbp1
1426356_at	3.04	0.00002	6330578E17Rik
1427040_at	3.04	0.00002	Mdfic
1434014_at	3.04	0.00006	Atg4c
1434789_at	3.04	0.001486	Depdc1b
1438855_x_at	3.04	0.00002	Tnfaip2
1447946_at	3.04	0.000023	Adam23
1449976_a_at	3.04	0.00002	Gpr35
1420898_at	3.03	0.00003	Snap23
1435129_at	3.03	0.00002	---
1437401_at	3.03	0.001201	Igf1
1438435_at	3.03	0.00002	Phca
1443104_at	3.03	0.00004	---
1449590_a_at	3.03	0.000052	Mras
1453573_at	3.03	0.00002	Hist1h3b /// Hist1h3c /// Hist1h3d /// Hist1h3e /// Hist1h3f /// Hist2h3b /// Hist2h3c1 /// Hist2h3c2
1455102_at	3.03	0.00002	Larp4
1418715_at	3.02	0.00003	Pank1
1435644_at	3.02	0.00003	Sh3pxd2b
1436915_x_at	3.02	0.00002	Laptm4b
1460006_at	3.02	0.00002	Zfhx3
1416258_at	3.01	0.00002	Tk1
1419538_at	3.01	0.000023	Flt3
1420760_s_at	3.01	0.000307	Ndrg1
1430073_at	3.01	0.000035	2900016B01Rik
1431182_at	3.01	0.00013	Hspa8 /// LOC624853 /// LOC641192 /// LOC666031
1433568_at	3.01	0.00004	Papd4
1433853_at	3.01	0.000052	Mib1
1435564_at	3.01	0.000052	C230078M08Rik
1443141_at	3.01	0.00002	---
1454783_at	3.01	0.00004	Il13ra1

1415871_at	3	0.00002	Tgfbi
1419585_at	3	0.000052	Rp2h
1420664_s_at	3	0.000114	Procr
1420979_at	3	0.00002	Pak1
1421534_at	3	0.00002	LOC14210
1422755_at	3	0.00002	Btk
1430291_at	3	0.00002	Dock5
1431146_a_at	3	0.000046	Cpne8
1434911_s_at	3	0.000046	Arhgap19
1436853_a_at	3	0.000023	Snca
1438609_x_at	3	0.000114	Tnni2
1451133_s_at	3	0.000088	Tmem168
1454701_at	3	0.00002	4930503L19Rik
1419905_s_at	2.99	0.00002	Hpgd
1420398_at	2.99	0.00002	Rgs18
1424303_at	2.99	0.000966	Depdc7
1424412_at	2.99	0.00002	Ogfrl1
1427442_a_at	2.99	0.000035	App
1429347_at	2.99	0.00002	Bcl2l14
1437286_x_at	2.99	0.000273	1110020G09Rik
1443777_at	2.99	0.00003	---
1448405_a_at	2.99	0.000023	Eid1
1455885_at	2.99	0.00002	Amz1
1418243_at	2.98	0.000307	Fcna
1421223_a_at	2.98	0.00002	Anxa4
1424588_at	2.98	0.000068	Srgap3
1424603_at	2.98	0.00002	Sumf1
1428562_at	2.98	0.000241	2210403K04Rik
1437187_at	2.98	0.000438	E2f7
1440615_at	2.98	0.00002	Dusp16
1445440_at	2.98	0.000438	Ccdc88a
1448698_at	2.98	0.000078	Ccnd1
1422891_at	2.97	0.000167	H2-Ea
1424987_at	2.97	0.000346	5430435G22Rik
1430386_at	2.97	0.000101	E030024N20Rik
1431323_at	2.97	0.00002	Lztfl1
1434310_at	2.97	0.000023	Bmpr2
1446497_at	2.97	0.00002	---
1448205_at	2.97	0.000023	Ccnb1 /// Ccnb1-rs1
1456599_at	2.97	0.000023	Nxt2
1415789_a_at	2.96	0.000189	LOC100045709 /// Ublcp1

1415904_at	2.96	0.00002	Lpl
1419171_at	2.96	0.000023	Tmem157
1422612_at	2.96	0.00002	Hk2
1426552_a_at	2.96	0.000189	Bcl11a
1430534_at	2.96	0.000167	Rnase6
1430557_at	2.96	0.000167	4930434J08Rik
1433696_at	2.96	0.000035	Hn1l
1433741_at	2.96	0.00002	Cd38
1439234_a_at	2.96	0.00002	Tm2d2
1444546_at	2.96	0.00002	Tifab
1460597_at	2.96	0.00002	Asxl2
1417122_at	2.95	0.000035	Vav3
1419469_at	2.95	0.000023	Gnb4
1420132_s_at	2.95	0.000167	Pttg1ip
1422743_at	2.95	0.000068	Phka1
1427368_x_at	2.95	0.00002	Fes
1436759_x_at	2.95	0.00002	Cnn3 /// LOC100047856
1440911_at	2.95	0.00004	Col23a1
1452473_at	2.95	0.000389	Prr15
1453748_a_at	2.95	0.000189	Kif23
1456700_x_at	2.95	0.00002	Marcks
1423555_a_at	2.94	0.00002	Ifi44
1428284_at	2.94	0.00004	8430427H17Rik
1435777_at	2.94	0.00003	E030018N11Rik
1437854_at	2.94	0.000023	---
1437956_at	2.94	0.000068	Pik3r6
1448566_at	2.94	0.000492	Slc40a1
1452123_s_at	2.94	0.00002	Frmd4b
1454740_at	2.94	0.00002	Mib1
1454896_at	2.94	0.00002	Rbpj
1455053_a_at	2.94	0.000023	Dcun1d1
1456210_at	2.94	0.000389	5430407P10Rik
1417124_at	2.93	0.00004	Dstn
1418638_at	2.93	0.000147	H2-DMb1
1419153_at	2.93	0.00002	2810417H13Rik
1421221_at	2.93	0.000027	Bco2
1421410_a_at	2.93	0.000023	Pstpip2
1422141_s_at	2.93	0.000214	Csprs
1423702_at	2.93	0.000027	H1f0
1428572_at	2.93	0.00002	Basp1 /// LOC100045716
1433623_at	2.93	0.00002	Zfp367

1436999_at	2.93	0.00002	5033414K04Rik
1449645_s_at	2.93	0.000088	Cct3
1454728_s_at	2.93	0.00002	Atp8a1
1456886_at	2.93	0.000027	---
1417716_at	2.92	0.001077	Got2
1419453_at	2.92	0.00002	Uchl5
1424923_at	2.92	0.00002	Serpina3g
1425546_a_at	2.92	0.00002	Trf
1426594_at	2.92	0.000241	Frmd4b
1426716_at	2.92	0.000147	Tdrd7
1434549_at	2.92	0.00002	Rab11a
1434875_a_at	2.92	0.00002	Hmgn3
1438310_at	2.92	0.000114	---
1441546_at	2.92	0.00002	LOC624524
1447277_s_at	2.92	0.000027	Pcyox1
1452011_a_at	2.92	0.00002	Uxs1
1456712_at	2.92	0.00003	Lcorl
1416166_a_at	2.91	0.000078	Prdx4
1417266_at	2.91	0.000618	Ccl6
1424615_at	2.91	0.00002	Frag1
1426817_at	2.91	0.00002	Mki67
1427084_a_at	2.91	0.000052	Map4k5
1439775_at	2.91	0.000114	Brwd3
1444516_at	2.91	0.000438	---
1448318_at	2.91	0.00004	Adfp
1452203_at	2.91	0.00002	Obfc2a
1452210_at	2.91	0.00013	Dna2
1452912_at	2.91	0.000078	Dscc1
1453122_at	2.91	0.000114	4921533L14Rik
1455468_at	2.91	0.00013	---
1416021_a_at	2.9	0.00003	Fabp5 /// LOC620603
1419565_a_at	2.9	0.001832	Zfx
1420064_s_at	2.9	0.000023	Tktl1
1422567_at	2.9	0.00002	Niban
1423597_at	2.9	0.00002	Atp8a1
1428938_at	2.9	0.000027	Gnaq
1435702_s_at	2.9	0.00002	Ywhae
1443814_x_at	2.9	0.00002	Ctsh
1449216_at	2.9	0.00002	Itgae
1449585_at	2.9	0.000966	Il1rap
1454938_at	2.9	0.000068	Snx13

1460359_at	2.9	0.00002	Armcx3 /// LOC100044266
1419123_a_at	2.89	0.000023	Pdgfc
1428450_at	2.89	0.001486	2610034B18Rik
1429190_at	2.89	0.00013	Arsb
1432042_a_at	2.89	0.00002	Smu1
1440736_at	2.89	0.000027	AI131651
1446861_at	2.89	0.00002	Gns
1448770_a_at	2.89	0.00002	Atpif1
1449195_s_at	2.89	0.000027	Cxcl16
1451667_at	2.89	0.00004	C530043G21Rik
1452655_at	2.89	0.000774	Zdhhc2
1455292_x_at	2.89	0.00003	---
1456790_at	2.89	0.000618	Zfp800
1460623_at	2.89	0.00002	Skap2
1419456_at	2.88	0.00002	Dcxr
1419754_at	2.88	0.00006	Myo5a
1420920_a_at	2.88	0.00002	Arf1
1421210_at	2.88	0.000114	Ciita
1422892_s_at	2.88	0.00002	H2-Ea
1427306_at	2.88	0.000052	Ryr1
1428323_at	2.88	0.00002	Gpd2
1430163_at	2.88	0.00002	Rab43
1435240_at	2.88	0.000027	Baz2b
1435467_at	2.88	0.000346	Fgd6
1448670_at	2.88	0.00002	LOC100047012 /// Ube2e3
1449401_at	2.88	0.00002	C1qc
1450036_at	2.88	0.000241	Sgk3
1450882_s_at	2.88	0.00002	Gpr137b /// Gpr137b-ps /// LOC100044979
1417588_at	2.87	0.000273	Galnt3
1417925_at	2.87	0.000035	Ccl22
1421274_at	2.87	0.000101	Socs4
1426580_at	2.87	0.000046	Plk4
1428374_at	2.87	0.00002	Glce
1428939_s_at	2.87	0.000027	Gnaq
1429761_at	2.87	0.000114	Rtn1
1430125_s_at	2.87	0.00002	Pqlc1
1433847_at	2.87	0.000147	D330017J20Rik
1434860_at	2.87	0.00002	Narg3
1435665_at	2.87	0.00006	AI451617
1441892_x_at	2.87	0.000023	---
1442059_at	2.87	0.00002	Fxr1

1449193_at	2.87	0.000101	Cd5l
1451563_at	2.87	0.00002	Emr4
1452408_at	2.87	0.00002	---
1455729_at	2.87	0.00002	Gnaq
1459682_at	2.87	0.00002	EG434249
1416168_at	2.86	0.00002	Serpinf1
1416303_at	2.86	0.000046	Litaf
1416412_at	2.86	0.00002	Nsmaf
1417541_at	2.86	0.00002	Hells
1427619_a_at	2.86	0.000189	Sh3tc1
1429172_a_at	2.86	0.000692	Ncapg
1429642_at	2.86	0.001336	Anubl1
1434285_at	2.86	0.00002	Frmd4a
1434828_at	2.86	0.000101	B430201A12Rik
1435058_x_at	2.86	0.000035	Stxbp3a
1435914_at	2.86	0.000088	Ncor1
1439256_x_at	2.86	0.00002	Gpr137b-ps
1448123_s_at	2.86	0.00002	Tgfbi
1448182_a_at	2.86	0.00002	Cd24a /// EG621324
1448720_at	2.86	0.00002	Lrrc40
1448839_at	2.86	0.001336	Kank3
1452016_at	2.86	0.000027	Alox5ap
1415834_at	2.85	0.00002	Dusp6
1430038_at	2.85	0.00002	---
1430077_at	2.85	0.00002	Sfrs11
1437989_at	2.85	0.00002	Pde8b
1447849_s_at	2.85	0.00002	Maf
1418895_at	2.84	0.000114	Skap2
1419097_a_at	2.84	0.00002	Stom
1422013_at	2.84	0.000189	Clec4a2
1423774_a_at	2.84	0.000214	Prc1
1425229_a_at	2.84	0.000774	Tcf7l2
1428259_at	2.84	0.000114	Pxdn
1434502_x_at	2.84	0.000552	Slc4a1
1435745_at	2.84	0.00002	5031439G07Rik
1436330_x_at	2.84	0.00002	EG631624
1437226_x_at	2.84	0.00002	Marcksl1
1438910_a_at	2.84	0.00002	Stom
1448314_at	2.84	0.00002	Cdc2a
1449874_at	2.84	0.001832	Ly96
1450876_at	2.84	0.001486	Cfh /// LOC100048018

1452759_s_at	2.84	0.000438	Ppfibp1
1458077_at	2.84	0.00002	---
1418736_at	2.83	0.000618	B3galnt1
1430981_s_at	2.83	0.00004	Gpbp1
1435597_at	2.83	0.00002	Atad5
1439235_x_at	2.83	0.000035	Tm2d2
1440179_x_at	2.83	0.000865	Rnf217
1441556_at	2.83	0.00002	---
1443858_at	2.83	0.00003	EG667823
1447873_x_at	2.83	0.000966	Bid
1452190_at	2.83	0.000189	Prcp
1452445_at	2.83	0.000438	Slc41a2
1416330_at	2.82	0.00002	Cd81
1416419_s_at	2.82	0.000023	Gabarapl1
1417376_a_at	2.82	0.000023	Cadm1
1417462_at	2.82	0.001651	Cap1
1417980_a_at	2.82	0.00002	Insig2
1418301_at	2.82	0.001651	Irf6
1418512_at	2.82	0.000052	Stk3
1420908_at	2.82	0.00002	Cd2ap
1424604_s_at	2.82	0.00002	Sumf1
1428192_at	2.82	0.00002	Kbtbd7
1436686_at	2.82	0.000068	LOC100046449 /// Zfp706
1437611_x_at	2.82	0.000273	Kif2c
1439255_s_at	2.82	0.00002	Gpr137b /// Gpr137b-ps /// LOC100044979
1449049_at	2.82	0.00002	Tlr1
1449429_at	2.82	0.000078	Fkbp1b
1452061_s_at	2.82	0.00002	Strbp
1452191_at	2.82	0.000068	LOC100048391 /// Prcp
1453076_at	2.82	0.00002	Batf3
1454086_a_at	2.82	0.00004	Lmo2 /// LOC100048263
1417508_at	2.81	0.00002	Rnf19a
1424574_at	2.81	0.00002	LOC100046567 /// Tmed5
1429436_at	2.81	0.00002	Prpf40a
1432478_a_at	2.81	0.000046	Rnf19b
1433965_at	2.81	0.000035	Atp8a1
1438329_at	2.81	0.00002	Tlr12
1445984_at	2.81	0.00002	---
1452352_at	2.81	0.001486	Ctla2b
1453228_at	2.81	0.000023	Stx11
1453783_at	2.81	0.00003	6330411E07Rik

1459888_at	2.81	0.000241	LOC545261
1415822_at	2.8	0.00002	Scd2
1416337_at	2.8	0.000035	Uqcrb
1417045_at	2.8	0.00002	Bid
1417061_at	2.8	0.00002	Slc40a1
1417910_at	2.8	0.00002	Ccna2
1420693_at	2.8	0.00013	Myom1
1423608_at	2.8	0.000023	Itm2a
1425028_a_at	2.8	0.00013	Tpm2
1431777_a_at	2.8	0.00002	Hmgn3
1433920_at	2.8	0.001077	Sema4c
1433995_s_at	2.8	0.00002	Ccdc50
1440201_at	2.8	0.000189	C130026L21Rik /// Slc8a1
1452054_at	2.8	0.000023	Ube2w
1418150_at	2.79	0.000346	Mtmr4
1422491_a_at	2.79	0.000114	Bnip2
1423306_at	2.79	0.000346	2010002N04Rik
1426221_at	2.79	0.00002	Loh11cr2a
1426649_at	2.79	0.000692	LOC100045217 /// Tmeff1
1429270_a_at	2.79	0.000189	Syce2
1433750_at	2.79	0.000023	Slc31a1
1433894_at	2.79	0.000068	Jazf1
1435327_at	2.79	0.00002	AW112037 /// Lpgat1
1438606_a_at	2.79	0.00002	Clic4
1442739_at	2.79	0.00002	BC031441
1460639_a_at	2.79	0.00002	Atox1
1416109_at	2.78	0.00002	Fuca1
1417377_at	2.78	0.00002	Cadm1
1418209_a_at	2.78	0.000101	Pfn2
1419513_a_at	2.78	0.00002	Ect2
1424438_a_at	2.78	0.00002	Leprot
1428484_at	2.78	0.00002	Osbpl3
1434260_at	2.78	0.00002	Fchsd2
1438796_at	2.78	0.00002	Nr4a3
1439426_x_at	2.78	0.00002	Lyz1
1448731_at	2.78	0.00002	Il10ra
1449043_at	2.78	0.00002	Naga
1457671_at	2.78	0.00003	9330120H11Rik
1418436_at	2.77	0.00002	Stx7
1418747_at	2.77	0.00003	Sfpi1
1421211_a_at	2.77	0.00002	Ciita

1422449_s_at	2.77	0.00002	Rcn2
1430569_at	2.77	0.00004	Ttc9c
1448149_at	2.77	0.00002	Ctnna1
1449661_at	2.77	0.000492	Suz12
1457676_at	2.77	0.00002	Tirap
1460203_at	2.77	0.000027	Itpr1
1417170_at	2.76	0.00002	Lztfl1
1426774_at	2.76	0.00002	Parp12
1433751_at	2.76	0.00002	Slc39a10
1437807_x_at	2.76	0.00002	Ctnna1
1449602_at	2.76	0.00002	---
1450044_at	2.76	0.00002	Fzd7
1456898_at	2.76	0.00003	---
1459906_at	2.76	0.000492	---
1416525_at	2.75	0.00002	Spop
1417622_at	2.75	0.000101	Slc12a2
1423613_at	2.75	0.000167	Ssfa2
1424926_at	2.75	0.000035	Sec63
1425705_a_at	2.75	0.000078	Ero1lb
1428094_at	2.75	0.00002	Lamp2
1429209_at	2.75	0.00002	Col23a1
1434547_at	2.75	0.000438	Cpd
1437111_at	2.75	0.00002	Zc3h12c
1438379_x_at	2.75	0.000023	2310007F21Rik
1442465_s_at	2.75	0.000241	Strbp
1442865_at	2.75	0.000101	Dgkk
1449198_a_at	2.75	0.00002	St3gal5
1449268_at	2.75	0.000078	Gfpt1
1449746_s_at	2.75	0.000027	Glipr1
1451161_a_at	2.75	0.000307	Emr1
1455241_at	2.75	0.000023	BC037703
1460076_x_at	2.75	0.000307	---
1460335_at	2.75	0.00002	Lysmd3
1416666_at	2.74	0.00004	Serpine2
1417190_at	2.74	0.00002	Nampt
1417378_at	2.74	0.000552	Cadm1
1418652_at	2.74	0.000241	Cxcl9
1426461_at	2.74	0.00002	Ugp2
1435492_at	2.74	0.000101	Socs6
1436991_x_at	2.74	0.00002	Gsn
1437404_at	2.74	0.000273	Mast4

1443629_at	2.74	0.000147	Nav1
1444559_at	2.74	0.001651	Phtf2
1446104_at	2.74	0.000273	---
1449187_at	2.74	0.000147	Pdgfa
1450792_at	2.74	0.000046	Tyrobp
1452092_at	2.74	0.00002	4631426J05Rik
1452717_at	2.74	0.00002	Slc25a24
1459991_at	2.74	0.001486	Myo9a
1416094_at	2.73	0.00002	Adam9
1417898_a_at	2.73	0.00002	Gzma
1418585_at	2.73	0.000346	Ccnh
1419254_at	2.73	0.00002	Mthfd2
1422573_at	2.73	0.00002	Ampd3
1426850_a_at	2.73	0.000114	Map2k6
1428480_at	2.73	0.000865	Cdca8
1434339_at	2.73	0.000101	Fnbp1l
1434557_at	2.73	0.00004	Hip1
1436509_at	2.73	0.000023	2410014A08Rik
1437495_at	2.73	0.000966	LOC100047187 /// Mbtps2 /// Yy2
1441600_at	2.73	0.000027	C920021A13
1443184_at	2.73	0.000068	Cdc14a /// LOC100047731
1447593_x_at	2.73	0.000307	Gnaq
1448339_at	2.73	0.00002	Tmem30a
1456592_at	2.73	0.00003	---
1415788_at	2.72	0.00002	Ublcp1
1417811_at	2.72	0.000023	Slc24a6
1426687_at	2.72	0.000552	Map3k3
1428481_s_at	2.72	0.00002	Cdca8
1428930_at	2.72	0.00002	Tmem29
1429295_s_at	2.72	0.000027	Trip13
1430700_a_at	2.72	0.000078	Pla2g7
1435069_at	2.72	0.001486	BC064078
1436890_at	2.72	0.000241	Uap1l1
1436997_x_at	2.72	0.00002	Sh3bgrl
1437033_a_at	2.72	0.00002	Skp2
1438511_a_at	2.72	0.000088	1190002H23Rik
1439845_at	2.72	0.000438	Hp1bp3
1444437_at	2.72	0.001077	Usp34
1452213_at	2.72	0.00006	Tex2
1452242_at	2.72	0.00002	Cep55
1452598_at	2.72	0.000046	Gins1

1455101_at	2.72	0.00002	Phactr2
1455618_x_at	2.72	0.000101	Tspan33
1420507_a_at	2.71	0.000023	Sfrs12ip1
1423804_a_at	2.71	0.00002	Idi1
1424852_at	2.71	0.000078	Mef2c
1427144_at	2.71	0.00002	Hnrpll
1429432_at	2.71	0.000078	Bat2d
1433655_at	2.71	0.00002	Rnf141
1436911_at	2.71	0.000078	Ss18l1
1440954_at	2.71	0.000618	---
1449221_a_at	2.71	0.000035	Rrbp1
1452885_at	2.71	0.000035	Sfrs2ip
1456533_at	2.71	0.000023	Dpy19l1
1456936_at	2.71	0.000214	Cabp4
1459874_s_at	2.71	0.00002	Mtmr4
1417590_at	2.7	0.00002	Cyp27a1
1419300_at	2.7	0.000027	Flt1
1420814_at	2.7	0.00002	Gdi2
1421525_a_at	2.7	0.000307	Naip5
1423543_at	2.7	0.000023	Swap70
1425019_at	2.7	0.000114	Ubxd4
1428194_at	2.7	0.00002	Usp9x
1433678_at	2.7	0.000088	Pld4
1433985_at	2.7	0.00002	Abi2
1438930_s_at	2.7	0.00002	Mecp2
1442560_at	2.7	0.001336	---
1451608_a_at	2.7	0.000692	Tspan33
1454809_at	2.7	0.000167	Ncoa7
1454880_s_at	2.7	0.000189	Bmf
1458630_at	2.7	0.00002	---
1416066_at	2.69	0.00002	Cd9
1417744_a_at	2.69	0.000114	Ralb
1418100_at	2.69	0.000023	A030009H04Rik
1419253_at	2.69	0.00002	Mthfd2
1423195_at	2.69	0.00002	Hiat1
1424128_x_at	2.69	0.000046	Aurkb
1428018_a_at	2.69	0.000492	AF251705
1430530_s_at	2.69	0.00002	Nmral1
1433159_at	2.69	0.000088	Kif13b
1434687_at	2.69	0.000068	C730026J16
1437009_a_at	2.69	0.00002	Zfp364

1447985_s_at	2.69	0.000023	Ankib1
1448162_at	2.69	0.00002	Vcam1
1449014_at	2.69	0.00002	Lactb /// LOC677144
1449116_a_at	2.69	0.000241	Dtymk
1449708_s_at	2.69	0.00002	Chek1
1454947_a_at	2.69	0.00002	Ublcp1
1416062_at	2.68	0.000241	Tbc1d15
1416514_a_at	2.68	0.00002	Fscn1
1417381_at	2.68	0.00002	C1qa
1420404_at	2.68	0.00002	Cd86
1420618_at	2.68	0.00002	Cpeb4
1420650_at	2.68	0.000307	Zfhx3
1420907_at	2.68	0.00002	Cd2ap
1420915_at	2.68	0.00002	Stat1
1420989_at	2.68	0.000214	4933411K20Rik
1421056_at	2.68	0.000027	Dnase1l3
1422467_at	2.68	0.00002	Ppt1
1423266_at	2.68	0.00003	2810405K02Rik
1423326_at	2.68	0.000046	Entpd1
1424383_at	2.68	0.000023	Tmem51
1428700_at	2.68	0.000618	P2ry13
1429171_a_at	2.68	0.000307	Ncapg
1430332_a_at	2.68	0.00002	Gusb
1433796_at	2.68	0.00002	Endod1
1448620_at	2.68	0.000068	Fcgr3
1448960_at	2.68	0.000046	Cxxc5
1451730_at	2.68	0.000101	Zfp62
1452115_a_at	2.68	0.001651	Plk4
1455852_at	2.68	0.001486	Nsl1
1456435_at	2.68	0.000023	Morn1
1460586_at	2.68	0.000147	Megf8
1416344_at	2.67	0.000027	Lamp2
1416802_a_at	2.67	0.00002	Cdca5
1416957_at	2.67	0.00002	Pou2af1
1419519_at	2.67	0.000389	Igf1
1419603_at	2.67	0.000438	Ifi204
1420819_at	2.67	0.00002	Sla
1420919_at	2.67	0.000114	Sgk3
1421871_at	2.67	0.00002	Sh3bgrl
1422201_at	2.67	0.000088	H2-Ob
1422476_at	2.67	0.000114	Ifi30

1424210_at	2.67	0.000035	Erlin1
1428653_x_at	2.67	0.000241	Elavl1
1433592_at	2.67	0.00002	Calm1
1436186_at	2.67	0.000189	E2f8
1437461_s_at	2.67	0.00002	Rnpc3
1447694_x_at	2.67	0.000774	Neo1
1448075_at	2.67	0.000438	AA408251
1451584_at	2.67	0.00002	Havcr2
1453595_at	2.67	0.00003	2900064B18Rik
1456312_x_at	2.67	0.00002	Gsn
1416728_at	2.66	0.00002	Csnk2b
1417870_x_at	2.66	0.00002	Ctsz
1418681_at	2.66	0.000241	Alg13
1420072_s_at	2.66	0.000101	---
1422433_s_at	2.66	0.00002	Idh1
1423796_at	2.66	0.00002	Sfpq
1427434_at	2.66	0.00002	Birc1f
1427567_a_at	2.66	0.000046	Tpm3
1430460_at	2.66	0.00006	2310047O13Rik
1434767_at	2.66	0.000214	C79407
1434835_at	2.66	0.00002	Wapal
1435632_at	2.66	0.00002	Nufip2
1441727_s_at	2.66	0.00003	Zfp467
1443136_at	2.66	0.000046	LOC432459
1449360_at	2.66	0.00002	Csf2rb2
1450350_a_at	2.66	0.000147	Jdp2
1450386_at	2.66	0.00002	Kpna3
1451313_a_at	2.66	0.00002	1110067D22Rik
1452504_s_at	2.66	0.000068	Ctbs
1454901_at	2.66	0.000492	Ypel2
1456236_s_at	2.66	0.00002	Commd10
1415995_at	2.65	0.00002	Casp6
1418219_at	2.65	0.000046	Il15
1419130_at	2.65	0.00002	Adat2
1421968_a_at	2.65	0.00002	Nipa2
1424389_at	2.65	0.000307	Nupl1
1442606_at	2.65	0.00002	---
1449345_at	2.65	0.000167	Ccdc34
1451134_a_at	2.65	0.00002	Tm2d2
1455130_at	2.65	0.00002	Spty2d1
1456822_at	2.65	0.000438	Rad23b

1416035_at	2.64	0.00003	Hif1a
1416964_at	2.64	0.000046	Eefsec
1417668_at	2.64	0.000774	Rtn4ip1
1417878_at	2.64	0.00002	E2f1
1418483_a_at	2.64	0.00002	Ggta1
1420475_at	2.64	0.00002	Mtpn
1423568_at	2.64	0.00002	Psma7
1424095_at	2.64	0.00002	Rtcd1
1428107_at	2.64	0.00002	Sh3bgrl
1430088_at	2.64	0.001336	Zfp619
1438385_s_at	2.64	0.00002	Gpt2
1447757_x_at	2.64	0.000167	Inpp5f
1454942_at	2.64	0.00002	Niban
1457672_at	2.64	0.00002	Chd9
1417450_a_at	2.63	0.00002	Tacc3
1418204_s_at	2.63	0.000027	Aif1
1420361_at	2.63	0.00002	Slc11a1
1421679_a_at	2.63	0.000966	Cdkn1a
1422527_at	2.63	0.000027	H2-DMa
1426398_at	2.63	0.000046	Ube2w
1426936_at	2.63	0.00002	BC005512 /// EG641366 /// LOC215866 /// LOC629242
1428715_at	2.63	0.00002	2810423A18Rik /// Gfpt1
1434714_at	2.63	0.00003	Ero1lb
1435059_at	2.63	0.000492	---
1435554_at	2.63	0.00002	Tmcc3
1436303_at	2.63	0.00004	Mllt4
1439520_at	2.63	0.00003	Dtl
1441867_x_at	2.63	0.000027	4930534B04Rik
1448148_at	2.63	0.00002	Grn
1452007_at	2.63	0.00002	Vamp7
1455054_a_at	2.63	0.000167	Dcun1d1
1455089_at	2.63	0.000865	Gng12
1456060_at	2.63	0.000046	Maf
1457434_s_at	2.63	0.00002	Ptpla
1416076_at	2.62	0.001336	Ccnb1 /// Ccnb1-rs1 /// EG434175 /// LOC667005
1418188_a_at	2.62	0.000046	Malat1
1421936_at	2.62	0.00002	Dapp1
1422948_s_at	2.62	0.00002	Hist1h4a /// Hist1h4b /// Hist1h4c /// Hist1h4d /// Hist1h4f /// Hist1h4h /// Hist1h4i /// Hist1h4j /// Hist1h4k /// Hist1h4m /// Hist2h4 /// Hist4h4 /// LOC100041230
1423775_s_at	2.62	0.000035	Prc1

1424431_at	2.62	0.00002	Csgalnact2
1426785_s_at	2.62	0.000068	Mgll
1441972_at	2.62	0.000307	6230424C14Rik
1449222_at	2.62	0.00004	Ebi3
1450430_at	2.62	0.00002	Mrc1

Appendix 2: Overrepresentation analysis of the genes that are upregulated in the tolerant Des-TCR CD8 T cells as compared to the activated Des-TCR CD8 T cells

System	Gene Category	Population Hits	Population Total	Official Gene Symbol
GO Cellular Component	cytoplasm	874	1672	ABCB7; ABCD1; ABL1; ABR; ACAA2; ACADL; ACADVL; ACAT1; ACO1; ACOX1; ACP1; ACP2; ACTB; ACTR10; ACTR8; ADA; ADAR; ADD1; ADD3; ADFP; ADK; AHCYL1; AIF1; AIM1; AK2; AK3; AKAP9; ALDH1A2; ALDH2; ALDH3A2; ALDH9A1; ALDOC; ALS2; AMD1; ANP32A; ANP32E; ANXA4; ANXA5; ANXA6; ANXA7; AP1G1; AP1GBP1; AP1S2; AP3B1; AP3D1; AP3M1; AP3S1; AP3S2; APAF1; APC; APOE; APP; APPBP2; ARF1; ARF3; ARF4; ARFGAP3; ARFRP1; ARHGAP5; ARHGAP6; ARHGEF10; ARHGEF7; ARIH2; ARL1; ARL3; ARL6; ARPC4; ARPC5; ARRB1; ASAH1; ASAH2; ASL; ASNA1; ATF6; ATP2A2; ATP5A1; ATP5C1; ATP5E; ATP6V0D1; ATP6V1A; ATP6V1B2; ATP6V1D; ATP6V1H; ATP7A; ATPIF1; AUH; AXIN1; B4GALT4; B4GALT6; BAD; BAG5; BAIAP2; BASP1; BBX; BECN1; BID; BIRC5; BLMH; BMI1; BNIP3L; BTK; BUB1; BZW1; BZW2; CALM1; CALM2; CAMTA2; CANX; CAPZA1; CAPZA2; CAPZB; CARD10; CARHSP1; CASK; CASP7; CAT; CBFA2T3; CBR3; CCNA2; CCNB1; CCNB2; CCND1; CCND2; CCR5; CCT3; CCT7; CD2AP; CD68; CDC16; CDC20; CDC6; CDK2AP1; CDK4; CDK5; CDK8; CENPE; CENPF; CETN2; CFL2; CHFR; CHUK; CKB; CLASP1; CLK1; CLN3; CLN8; CLPP; CLTA; CLTB; CLTC; CNN3; COPZ2; COQ3; CORO2A; COX15; COX5B; COX7C; CRK; CROT; CRYAB; CRYZ; CS; CSK; CSNK1D; CSNK1G1; CSRP1; CSRP2; CTBS; CTDP1; CTNNA1; CTPS; CTSB; CTSC; CTSH; CTSL; CTSS; CTSZ; CUGBP2; CXCR3; CYBA; CYC1; CYCS; CYP27A1; CYP8B1; DAPK1; DAPK3; DBI; DBN1; DBT; DCK; DCXR; DDX6; DEK; DFFA; DFFB; DGUOK; DLG1; DMXL1; DNAJB11; DNAJB4; DNAJB6; DNAJB9; DNMT3A; DNPEP; DPAGT1; DPM1; DPP8; DRG1; DSTN; DTYMK; DUSP1; DUSP16; DUSP22; DUSP6; DUSP7; DUT; DYRK1A; EBP; ECT2; EGLN1; EHD1; EHD2; EHD4; EHHADH; EIF1A; EIF1AY; EIF2AK3; EIF2B2; EIF2B4; EIF4B; EIF4E; EIF4G1; EIF4G2; EIF4G3; ELAC1; ENO2; EPC1; EPHX1; EPRS; EPS15; EPS8; ERBB2IP; ERO1L; ESD; ETF1; EVL; EXTL2; EXTL3; FABP5; FECH; FEM1B; FEN1; FES; FGD2; FIGNL1; FKBP1A; FKBP1B; FKBP2; FKBP4; FKBP9; FLII; FLNB; FNTA; FPR1; FRAP1; FSCN1; FUCA1; FUCA2; FUSIP1; FXC1; FXR1; FYCO1; GABARAPL2; GADD45B; GADD45G; GALC; GALNT1; GALNT11; GALNT3; GATM; GBA; GBP1; GBP2; GBP3; GCA; GCH1; GCSH; GDI1; GDI2; GLG1; GLRX; GLRX2; GLUD1; GM2A; GNAI3; GNPAT; GNS; GOLGA4; GOLPH3; GOT1; GOT2; GPD2; GPHN; GPX4; GRPEL1; GSN; GSPT1; GUSB; GZMA; GZMB; GZMK; HABP4; HADHB; HARS; HARS2; HAT1; HCCS; HCK; HDAC11; HDAC2; HDAC5; HERPUD1; HEXA; HEXB; HFE; HIBADH; HIP1; HK2; HLCS; HMGCL; HMGCR; HMGCS1; HMOX1; HOMER2; HRBL; HSD17B4; HSPA1A; HSPA1B; HSPA4; HSPA5; HSPA8; HSPH1; HUS1; IARS; ICMT; IDH1; IDH2; IDI1; IDS; IER5; IFI30; IFI35; IFI44; IFIT1; IFIT2; IGF2R; IKBKG; IL15; ILK; INPP1; INPP4A; INPP5D; INPPL1; IPO7; IQGAP1; IREB2; IRF3; IRF4; IRF5; IRF6; IRF7; ITGA4; ITGA8; ITGA9; ITGAE; ITGAV; ITGAX; ITGB1; ITGB2; ITPR1; ITPR2; JAK1; JAK2; JAK3; KARS; KATNA1; KHK; KIF11; KIF1B; KIF1C; KIF20A; KIF23; KIF2C; KIF3B; KIF5B; KLHL2; KLHL5; KPNA1; KPNA2; KPNB1; KRT17; KTN1; LACTB; LAMP2; LAMP3; LANCL2; LAP3; LARGE; LASP1; LCMT1; LCP1; LGMN; LIMK1; LIPA; LMAN1;

				LRMP; LRRFIP1; LRRFIP2; LSP1; LYN; LYPLA1; LZTFL1; M6PR; MAD2L1; MADD; MAN1A2; MAN2A1; MAN2B1; MANBA; MAP3K3; MAP3K4; MAP3K8; MAP4K5; MAPK14; MAPRE2; MARCKS; MBP; MCL1; MDH1; MELK; METAP2; MFHAS1; MGAT2; MGLL; MGST1; MKI67IP; MKLN1; MLF2; MLH3; MMAA; MRPL1; MRPL11; MRPL15; MRPL16; MRPL17; MRPL22; MRPL27; MRPL3; MRPL46; MRPL48; MRPL49; MRPL50; MRPS14; MRPS15; MRPS2; MRPS21; MRPS25; MRPS28; MRPS9; MTAP; MTHFD2; MTHFS; MTM1; MTMR1; MTMR6; MTX2; MVP; MX1; MYCBP; MYL6; MYO1C; MYO5A; MYO6; MYO9A; MYOM1; NAGA; NAGLU; NARS; NCBP2; NCF1; NCOA1; NDRG1; NDST1; NDST2; NDUFA5; NDUFA9; NDUFAB1; NDUFB4; NDUFB7; NDUFC2; NDUFS4; NDUFS5; NDUFV1; NEDD9; NFAT5; NFATC1; NFIX; NFKB1; NFKBIE; NGLY1; NMI; NNT; NOLA2; NOLC1; NPEPPS; NR3C1; NSF; NSMAF; NT5C2; NUCB2; NUDT1; NUMB; NUP50; NUP54; NUTF2; OAT; ODC1; OGT; OLFM1; OSGEP; P4HA1; P4HB; PA2G4; PACSIN1; PAFAH1B2; PAFAH1B3; PAPOLG; PAPSS1; PCCA; PCM1; PCMT1; PDCL; PDK1; PDK3; PDLIM2; PDPK1; PEX11A; PEX13; PEX3; PEX6; PEX7; PFDN2; PFKFB3; PFKL; PFKP; PFN2; PFTK1; PGD; PGLS; PHYH; PIGC; PIGF; PIGH; PIGS; PIK3C2A; PIK3CD; PLA2G4A; PLCE1; PLCG2; PLDN; PLEC1; PLEK; PLEKHA1; PLEKHA2; PLEKHF2; PLOD2; PLP2; PLS3; PMAIP1; PMM2; PMPCB; PMVK; PNN; PPAT; PPFIA4; PPID; PPIF; PPP1R2; PPP1R7; PPP2R1B; PPP4R2; PPT1; PPT2; PRC1; PRCP; PRDX2; PRKAG2; PRKCB1; PRKCD; PRKCH; PRKRA; PRNP; PSAP; PSEN1; PSMA4; PSMA6; PSMA7; PSMB3; PSMB4; PSMB5; PSMB7; PSMB8; PSMB9; PSMC1; PSMC2; PSMC6; PSMD10; PSMD13; PSMD14; PSMD2; PSMD4; PSMD8; PSME3; PTEN; PTGIS; PTPN11; PTPN6; PTPRE; PTTG1IP; PUM1; PUM2; PURA; PVR; PXN; PYGB; QARS; RAB24; RAB2B; RAB30; RAB31; RAB32; RAB33B; RAB5A; RAB6B; RAB7; RAD51; RAD51L1; RAD51L3; RANBP2; RANBP9; RAP1GDS1; RASSF5; RBBP8; RBM4; RCN2; RDBP; RDH11; RDX; RERE; REV3L; RFC3; RFC4; RFX5; RGS18; RGS19; RGS2; RGS3; RNASEH1; RNF14; RNF7; ROCK1; ROCK2; RPL11; RPL13; RPL14; RPL15; RPL23; RPL30; RPL31; RPL5; RPN1; RPS10; RPS13; RPS24; RPS6; RPS6KA2; RPS6KB1; RPS6KB2; RPS9; RRAS2; RRBP1; RREB1; RRM2; RTN1; RTN3; RTN4; RUNX1; RYR1; SC4MOL; SCARB2; SCP2; SDCBP; SDCCAG3; SDCCAG8; SDHA; SDHC; SEC14L1; SEC23A; SEC24B; SEC24C; SEC24D; SEC63; SERPINB9; SERPINF1; SF1; SFXN2; SGCB; SGPL1; SH3BGRL; SH3GLB1; SHMT1; SHOC2; SIAH2; SIRT2; SLC25A11; SLC25A13; SLC25A14; SLC25A20; SLC25A5; SLC30A4; SLC33A1; SLC35A1; SLC35B1; SLC37A3; SLMAP; SNCA; SNX10; SNX2; SNX3; SNX4; SNX5; SNX6; SOAT1; SOCS4; SOCS5; SOLH; SPIB; SPTLC1; SPTLC2; SQSTM1; SREBF2; SRI; SRP14; SSR2; SSR3; SSR4; SSX2IP; STAM2; STARD3; STAT1; STAT3; STAT5A; STAT6; STK17B; STK3; STK39; STMN1; STOM; STRBP; STRN; STRN3; STX18; STX5A; STX6; STX7; STX8; SUCLG1; SULT1A1; SUOX; SURF4; SYK; SYNJ2BP; SYPL; SYT11; TACC3; TALDO1; TANK; TAP2; TAPBP; TAX1BP1; TBCD; TBK1; TCF19; TEC; TES; TGOLN2; TIA1; TIAL1; TIMM17B; TIMM22; TK1; TLR1; TM9SF2; TMEM1; TMOD3; TNIP2; TNNI2; TOMM70A; TOP1; TOR3A; TPI1; TPM1; TPM2; TPM3; TPM4; TPP2; TPR; TPST1; TRAF3; TRAM1; TRIM17; TRIM3; TRIM32; TRIM33; TRIM34; TRIP12; TRIP13; TRNT1; TSG101; TTK; TUBGCP5; TUFM; TXK; TXN2; TXNDC4; TXNRD1; TYK2; UAP1; UCHL5; UCP2; UGCGL1; UGP2; UGT1A5; ULK1; UMPS; UNC119; UQCRB; UQCRFS1; USP4; UXT; VAMP4; VAMP8; VASP; VAV1; VAV3; VCL; VDAC1; VDAC3; VPS35; VPS4B; WASF2; WASL; WDR1; XPO1; XPO7; YME1L1; YWHAB; YWHAQ; YWHAZ; ZAP70; ZDHHC3; ZFP36L1; ZFYVE16; ZFYVE21
GO Cellular	membrane	599	1672	ABCA3; ABCB7; ABCD1; ABCF1; ABCF3; ABHD3; ACP2; ACVR1; ACVRL1; ADAM10; ADAM17; ADAM19; ADAM23; ADAM8; ADAM9; ADCY7; ADD1; ADD3; ADFP; ADK; AGPAT3; ALCAM; ALDH3A2; ALOX5AP; AMD1; AMPD3; ANPEP; AP1G1; AP1S2; APOE; APP; ARF1; ARHGAP12; ARHGAP5; ARHGAP9; ARRB1; ASB13; ASNA1; ATF6; ATOX1; ATP11A; ATP11B; ATP1B1; ATP2A2; ATP2C1; ATP5A1;

Component				ATP5C1; ATP5E; ATP6V0A2; ATP6V0B; ATP6V0D1; ATP6V1A; ATP6V1B2; ATP6V1C1; ATP6V1D; ATP6V1H; ATP7A; ATP8A1; AXL; B4GALT4; B4GALT6; BAD; BAIAP2; BASP1; BCL11A; BCL11B; BCL2L11; BECN1; BFAR; BNIP2; BNIP3L; BRI3; BST1; C6; CABP4; CACNA1S; CACNB3; CALCRL; CALM1; CALM2; CANX; CASK; CAST; CCR5; CCR9; CD14; CD163; CD36; CD38; CD44; CD48; CD5; CD5L; CD68; CD74; CD80; CD81; CD83; CD86; CD8A; CD9; CD96; CD97; CD99L2; CDC42; CDCA7; CEBPG; CHD6; CHN2; CHPT1; CHRNB1; CKLF; CLCN3; CLDN1; CLIC4; CLN3; CLN8; CLTA; CLTB; CLTC; CNOT2; CNP; CNR2; COPZ2; COX15; COX5B; CPD; CPNE1; CPNE3; CRAMP1L; CRIM1; CRLF2; CRLF3; CSF1R; CSF2RA; CSF2RB; CSNK2A1; CTNNA1; CXCL16; CXCR3; CYB561; CYBA; CYC1; CYCS; CYP27A1; CYP8B1; CYSLTR1; DDEF1; DDR1; DEK; DGCR2; DLG1; DLG3; DNAJA1; DNAJC5; DPAGT1; DPP4; DPP8; DSCR3; EBI3; EBP; ECE1; EEF1E1; EIF2AK3; EIF2AK4; ELF1; ELK3; EMD; EMR1; ENPP4; ENTPD1; EPHX1; ERBB2IP; ERO1L; ETS2; ETV3; ETV6; EVI2A; EVI2B; EVI5; EVL; EXTL2; EXTL3; EZH2; FADS1; FCGR2B; FCGRT; FLI1; FLNB; FLT1; FLT3; FMO5; FPR1; FTH1; FXC1; FZD7; GABARAPL1; GABBR1; GABPA; GALNT1; GALNT3; GBA; GCA; GHITM; GIT2; GJA1; GLG1; GMFB; GNA13; GNAI3; GNB2; GNB4; GNG10; GNG12; GNG2; GNPAT; GP2; GPR124; GPR34; GPR35; GPR65; GPRC5B; GPSN2; GTPBP2; GYPC; HABP4; HADHB; HCCS; HERPUD1; HFE; HK2; HMGCR; HRB; HRBL; HRH2; HS2ST1; HS6ST1; ICAM1; ICMT; ICOS; IFITM3; IFNAR1; IFNAR2; IFNGR2; IGF2R; IL10RA; IL13RA1; IL15; IL15RA; IL1RAP; IL2RG; IL6ST; ILK; INPP5B; IPO7; IRAK1; IRAK4; ITGA4; ITGA8; ITGA9; ITGAE; ITGAV; ITGAX; ITGB1; ITGB2; ITM2A; ITM2B; ITM2C; ITPR1; ITPR2; JAG2; JTB; KATNA1; KCNJ10; KCNN4; KHDRBS1; KHDRBS3; KHK; KIF1B; KIT; KLRC1; KMO; KPNA1; KPNA3; KPNB1; KTN1; LAMP2; LAMP3; LANCL2; LAPTM4A; LAPTM4B; LARGE; LEPROTL1; LGALS3; LGALS3BP; LIFR; LILRB3; LIMD1; LIMS1; LIN7C; LITAF; LMAN1; LPP; LRMP; LRP4; LRRC1; LST1; LY75; LY86; LY96; M6PR; MADD; MAN1A2; MAN2A1; MARCKS; MCL1; MDM2; MDM4; MERTK; METAP1; MGAT2; MGST1; MKRN1; MPP6; MRAS; MRC1; MS4A1; MTX2; MYCL1; MYD88; NAALAD2; NDFIP1; NDFIP2; NDST1; NDST2; NDUFV1; NNT; NOTCH1; NOTCH2; NOTCH4; NRP1; NUCB2; NUDT4; NUFIP1; NUMB; NUP153; NUP50; NUP54; NUP62; NUTF2; ODC1; OLFM1; ORMDL2; P2RX4; P2RY6; PAK1; PAK2; PCNX; PCNXL3; PDGFA; PDGFC; PDPK1; PEPD; PEX11A; PEX13; PEX3; PIGC; PIGF; PIGM; PIGN; PIGQ; PIGS; PIP5K1C; PITPNM1; PLA2G4A; PLCE1; PLEC1; PLOD2; PLP2; PLSCR1; PLSCR3; PLXNB2; PLXNC1; PNN; PPAP2A; PPAP2B; PPAP2C; PPP2R1B; PREB; PRKCB1; PRKCD; PRKCI; PRKRIR; PRNP; PROCR; PRRG2; PSAP; PSCD2; PSEN1; PSME4; PTDSS1; PTGER1; PTGER2; PTGER4; PTGIS; PTGS1; PTPN6; PTPN9; PTPRE; PTPRJ; PTPRS; PTTG1IP; PVR; RAB6IP1; RAC1; RALA; RALB; RAMP1; RANBP2; RAP1B; RAP2A; RASGRP4; RDH11; RDX; RECQL; RGS19; RNF121; RNF44; RNMT; RPN1; RRAS2; RRBP1; RTN1; RTN3; RTN4; RYR1; SACM1L; SC4MOL; SCAMP1; SCAMP2; SCARB1; SCARB2; SDC3; SDCBP; SDHC; SEC14L1; SEC24B; SEC63; SEMA4D; SEMA4F; SFRS1; SFRS9; SFXN2; SGCB; SGPL1; SGPP1; SH3GLB1; SIN3B; SLC11A1; SLC12A2; SLC13A3; SLC14A1; SLC15A2; SLC1A5; SLC22A5; SLC25A11; SLC25A13; SLC25A14; SLC25A20; SLC25A5; SLC2A9; SLC30A4; SLC30A5; SLC30A7; SLC31A1; SLC31A2; SLC33A1; SLC35A1; SLC35A5; SLC35B1; SLC35E1; SLC4A1; SLC4A7; SLC6A6; SLC7A6; SLC7A7; SLC8A1; SLC9A3R2; SLMAP; SNAP23; SOAT1; SON; SPAG5; SPINT2; SPTLC1; SPTLC2; SQLE; SREBF2; SRF; SSFA2; SSR2; SSR3; SSR4; STARD3; STARD3NL; STOM; STX12; STX17; STX18; STX5A; STX6; STX7; STX8; SURF4; SYNGR2; SYNJ2BP; SYPL; SYT11; TACSTD1; TAP1; TAP2; TAPBP; TBC1D8; TBXAS1; TCIRG1; TGFBR1; TGFBR2; TGM1; TGOLN2; TIAM1; TIMM17B; TIMM22; TJP2; TLE3; TLR1; TLR2; TLR3; TLR4; TM6SF1; TM9SF2; TMEFF1; TMEM1; TMEM8; TMPO; TNFAIP1; TNFRSF1A; TNFRSF21; TNFRSF9; TOMM70A; TPD52; TPR; TPST1; TRAM1; TREX1; TRIM37; TRIO; TRIP6; TRPM7; TRPV2; TULP3; TXNDC4; TYROBP; UBE2J1; UBE3A; UCP2;

				UGT1A1; UGT1A10; UGT1A5; UGT1A9; UNC93B1; UPF2; UQCRB; UQCRFS1; UTX; VAMP3; VAMP4; VAPB; VCAM1; VCL; VDAC1; VDAC3; VPS18; VPS41; VRK2; WASF2; XBP1; XCR1; XPNPEP1; XPO1; XPO7; YME1L1; ZDHHC14; ZDHHC2; ZDHHC3; ZDHHC6; ZDHHC9; ZFYVE21; ZFYVE26; ZYX
GO Cellular Component	nucleus	506	1672	ABL1; ADAR; ADNP; AHR; AIF1; ANAPC11; ANP32A; ANP32E; AP3D1; API5; ARFGAP3; ARHGAP6; ARIH2; ASF1B; ASNA1; ASXL1; ATF1; ATF2; ATF3; ATF6; ATF7IP; ATM; ATRX; BACH1; BAD; BASP1; BAZ1B; BAZ2A; BAZ2B; BCAS2; BCL3; BCL6; BCL9; BLMH; BMI1; BRD8; BUB1; BUB3; BXDC1; CAPN7; CBFA2T3; CBFB; CBL; CBX6; CCM2; CCNA2; CCNB1; CCNB2; CCNC; CCND1; CCND2; CCNE2; CCNG1; CCNG2; CCNH; CCNI; CCNT2; CDC25C; CDC6; CDK2AP1; CDK7; CDKN1A; CDYL; CEBPG; CENPA; CENPE; CENPF; CENTA2; CENTD1; CENTD2; CFL2; CHD1; CHD6; CHEK1; CITED2; CLK1; CNOT2; CNOT7; CNOT8; COPS4; CPSF2; CPSF3; CRAMP1L; CREB3; CREM; CRK; CRNKL1; CRYAB; CSNK2A1; CSRP1; CSRP2; CSTF2; CSTF3; CTBP2; CTCF; CTNNBIP1; CTNNBL1; CUL1; CUL3; CUL4A; CUL4B; DAPK3; DCK; DDB2; DDEF1; DDX6; DEK; DFFA; DFFB; DMTF1; DNAJB9; DNASE1L3; DNMT3A; DR1; DTX2; DUSP11; DUSP16; DUT; DYRK1A; E2F1; EED; EGR1; EGR2; EHD2; ELF1; ELK3; EMD; EPC1; ERBB2IP; ETS2; ETV3; ETV6; EZH2; FBL; FEN1; FKBP1A; FKBP1B; FKBP4; FLI1; FNBP1; FUBP1; FUS; FUSIP1; FXR1; GABPA; GABPB1; GIT2; GLRX2; GPS1; GSPT1; GTF2A1; GTF2B; GTF2E2; GTF2F2; GTF2H1; GTF2H2; GTF2I; GTF3C4; H1F0; H2AFZ; H3F3B; HABP4; HAT1; HCLS1; HDAC11; HDAC2; HDAC5; HELLS; HHEX; HIF1A; HIST1H1C; HIST1H2AB; HIST1H2AC; HIST1H2AD; HIST1H2AE; HIST1H3D; HIST1H4A; HIST2H2AC; HIST3H2A; HIVEP1; HIVEP2; HMGB3; HMGN3; HNRPA3; HNRPAB; HNRPDL; HNRPF; HNRPH2; HNRPK; HRB; HRBL; HSBP1; HSPA1A; HSPA1B; ID2; ID3; IFI35; IKBKG; INCENP; IPO7; IRF3; IRF4; IRF5; IRF6; IRF7; KHDRBS3; KIF23; KIF2C; KLF3; KPNA1; KPNA2; KPNA3; KPNB1; LGALS3; LIG1; LIMD1; LITAF; LMO2; LPIN2; LRRFIP1; LSM3; LYL1; MAD2L1; MAFB; MAPK14; MAPK8; MAPK9; MAPKAPK2; MBD4; MBNL3; MBP; MCM2; MCM3; MCM4; MCM6; MDM2; MDM4; MEF2A; MEF2C; MFHAS1; MITF; MKI67; MKI67IP; MKL1; MLF2; MLH3; MNDA; MTAP; MVP; MXI1; MYB; MYCBP; MYCL1; MYNN; NAP1L1; NCBP2; NCOA1; NCOA3; NDRG1; NEDD9; NFAT5; NFATC1; NFIX; NFKB1; NFKB2; NFYA; NFYB; NMNAT1; NOLC1; NOTCH2; NOTCH4; NPEPPS; NR2C2; NR3C1; NUFIP1; NUP153; NUP50; NUP54; NUP62; NUPL1; NUTF2; NVL; OGT; ORC4L; PA2G4; PAPOLG; PCAF; PCNXL3; PDCD7; PDGFA; PES1; PFTK1; PHTF2; PIAS1; PKNOX1; PLAGL2; PLRG1; PML; PNN; POLB; POLD4; POLE4; POLR2B; POLR2F; POLR2H; POLR3K; POU2AF1; PPARG; PPIH; PPIL2; PPP1CC; PPP1R7; PPP2R1B; PPP2R5C; PRC1; PREB; PRPF39; PRPF4B; PRPF8; PRRG2; PSEN1; PSMA4; PSMA6; PSMA7; PSMB3; PSMB4; PSMB5; PSMB7; PSMB8; PSMB9; PSMC1; PSMC2; PSMC6; PSMD10; PSMD14; PSMD2; PSMD4; PSMD8; PSME3; PTP4A1; PTTG1IP; PURA; PXN; RAD17; RAD23A; RAD23B; RAD51; RAD51L1; RAD51L3; RAD54L; RANBP2; RASA1; RB1; RBBP4; RBBP8; RBL1; RBM12; RBM5; RBMS1; RBMX; RECQL; RELB; RERE; REV3L; RFC1; RFC3; RFC4; RFX5; RFXAP; RNF103; RNF12; RNF13; RNF14; RNF6; RNF7; RNMT; ROD1; RPA3; RPS6KA2; RREB1; RRS1; RTCD1; RTN4; RUNX1; RUVBL1; RXRA; SALL2; SAP30; SDCBP; SEC63; SF1; SF3A2; SF3A3; SF3B1; SF3B2; SFPQ; SFRS1; SFRS10; SFRS11; SFRS2; SFRS2IP; SFRS3; SFRS7; SFRS9; SHPRH; SIAH2; SIN3B; SIRT2; SLC9A3R2; SMARCA5; SMARCB1; SMARCC1; SMARCE1; SNAPC3; SNRPA1; SNRPB2; SNRPD1; SON; SP100; SPIB; SPOP; SREBF2; SRF; SRPK2; SRRM1; SSB; SSBP3; SSNA1; STAT1; STAT3; STAT5A; STAT6; STK17B; STK39; STRN3; SUPT4H1; TAF13; TAF1B; TAF7; TAF9; TARDBP; TBPL1; TCEA1; TCEB1; TCEB3; TCERG1; TCF19; TCF4; TCF7; TCF7L2; TDG; TDP1; TEP1; TFDP1; TFPT; TGFBR2; THOC2; TJP2; TLE3; TLK2; TMPO; TOB2; TOP2A; TOP2B; TPR; TREX1; TRIM32; TRIM33; TRIP13; TTC3; TTF1; TULP3; UBE2A; UBE2B; UBE2J1; UBE2V1; UBE2V2; UBE3A; UBP1; UBTF; UCHL5; USP18; USP4; UTX;

				VAV1; WBP4; WDR13; XBP1; XPO1; XPO7; XRN2; YAF2; YY1; ZBTB1; ZBTB2; ZDHHC14; ZDHHC2; ZDHHC3; ZDHHC6; ZDHHC9; ZFP161; ZFP36L1; ZFR; ZFX; ZNRD1; ZWINT
GO Cellular Component	integral to membrane	402	1672	ABCA3; ABCB7; ABCD1; ABHD3; ACP2; ACVR1; ACVRL1; ADAM10; ADAM17; ADAM19; ADAM23; ADAM8; ADAM9; ADCY7; AGPAT3; ALCAM; ALDH3A2; ALOX5AP; AMPD3; ANPEP; APP; ATF6; ATP11A; ATP11B; ATP1B1; ATP2A2; ATP2C1; ATP5A1; ATP5C1; ATP5E; ATP6V0A2; ATP6V0B; ATP6V1A; ATP6V1B2; ATP6V1C1; ATP7A; ATP8A1; AXL; B4GALT4; B4GALT6; BFAR; BNIP3L; BRI3; C6; CACNA1S; CACNB3; CALCRL; CANX; CAST; CCR5; CCR9; CD163; CD36; CD38; CD44; CD48; CD5; CD68; CD74; CD80; CD81; CD83; CD86; CD8A; CD9; CD96; CD97; CD99L2; CHRNB1; CKLF; CLCN3; CLDN1; CLN3; CLN8; CNR2; CPD; CRIM1; CRLF2; CSF1R; CSF2RA; CSF2RB; CXCL16; CXCR3; CYB561; CYC1; CYP8B1; CYSLTR1; DDR1; DEK; DGCR2; DPAGT1; DPP4; DSCR3; EBP; ECE1; EEF1E1; EIF2AK3; EIF2AK4; EMD; EMR1; ENPP4; ENTPD1; EPHX1; ERO1L; ETV6; EVI2A; EVI2B; EXTL2; EXTL3; FADS1; FCGR2B; FCGRT; FLNB; FLT1; FLT3; FMO5; FPR1; FZD7; GABBR1; GALNT1; GALNT3; GHITM; GJA1; GLG1; GPR34; GPR35; GPR65; GPSN2; GYPC; HABP4; HERPUD1; HFE; HMGCR; HRB; HRBL; HRH2; HS2ST1; HS6ST1; ICAM1; ICMT; ICOS; IFITM3; IFNAR1; IFNAR2; IFNGR2; IGF2R; IL10RA; IL13RA1; IL15; IL15RA; IL1RAP; IL2RG; IL6ST; INPP5B; IPO7; IRAK1; ITGA4; ITGA8; ITGA9; ITGAE; ITGAV; ITGAX; ITGB1; ITGB2; ITM2A; ITM2B; ITM2C; ITPR1; ITPR2; JAG2; JTB; KCNJ10; KCNN4; KIT; KLRC1; KMO; KPNA1; KPNA3; KPNB1; KTN1; LAMP2; LANCL2; LAPTM4A; LAPTM4B; LARGE; LEPROTL1; LIFR; LILRB3; LIMD1; LMAN1; LPP; LRMP; LST1; LY75; M6PR; MAN1A2; MAN2A1; MCL1; MERTK; METAP1; MGAT2; MRC1; MS4A1; NAALAD2; NDFIP1; NDFIP2; NDST1; NDST2; NNT; NOTCH1; NOTCH2; NOTCH4; NRP1; NUMB; NUP153; NUP50; NUP54; NUP62; NUTF2; ORMDL2; P2RX4; P2RY6; PCNX; PCNXL3; PEPD; PEX13; PEX3; PIGC; PIGF; PIGM; PIGN; PIGQ; PIGS; PITPNM1; PLA2G4A; PLP2; PLSCR1; PLSCR3; PLXNC1; PPAP2A; PPAP2B; PREB; PRKRIR; PROCR; PRRG2; PSAP; PSEN1; PSME4; PTDSS1; PTGER1; PTGER2; PTGER4; PTGIS; PTGS1; PTPN9; PTPRE; PTPRJ; PTPRS; PTTG1IP; PVR; RAB6IP1; RAMP1; RANBP2; RDH11; RECQL; RNF121; RNF44; RPN1; RRBP1; RTN1; RTN3; RTN4; RYR1; SACM1L; SC4MOL; SCAMP1; SCAMP2; SCARB1; SCARB2; SDC3; SDCBP; SDHC; SEC63; SEMA4D; SEMA4F; SFXN2; SGCB; SGPL1; SGPP1; SLC11A1; SLC12A2; SLC13A3; SLC14A1; SLC15A2; SLC1A5; SLC22A5; SLC25A11; SLC25A13; SLC25A14; SLC25A20; SLC25A5; SLC2A9; SLC30A4; SLC30A5; SLC31A1; SLC31A2; SLC33A1; SLC35A1; SLC35A5; SLC35B1; SLC4A1; SLC4A7; SLC6A6; SLC7A6; SLC7A7; SLC8A1; SLMAP; SOAT1; SPINT2; SPTLC1; SPTLC2; SQLE; SREBF2; SSR2; SSR3; SSR4; STARD3; STARD3NL; STOM; STX17; STX18; STX5A; STX6; STX7; STX8; SURF4; SYNGR2; SYNJ2BP; SYPL; SYT11; TACSTD1; TAP1; TAP2; TAPBP; TBXAS1; TCIRG1; TGFBR1; TGFBR2; TGOLN2; TIMM17B; TIMM22; TJP2; TLR1; TLR2; TLR3; TLR4; TM6SF1; TM9SF2; TMEFF1; TMEM1; TMEM8; TMPO; TNFAIP1; TNFRSF1A; TNFRSF21; TNFRSF9; TOMM70A; TPR; TPST1; TRAM1; TRIM37; TRIP6; TRPM7; TRPV2; TYROBP; UBE3A; UCP2; UGT1A1; UGT1A10; UGT1A5; UGT1A9; UNC93B1; UPF2; UQCRFS1; VAMP3; VAMP4; VAPB; VCAM1; VDAC1; VDAC3; VPS41; VRK2; WASF2; XCR1; XPO1; XPO7; ZDHHC14; ZDHHC2; ZDHHC3; ZDHHC6; ZDHHC9; ZYX
GO Cellular Compo	plasma membrane	261	1672	ACVR1; ACVRL1; ADAM10; ADAM17; ADAM23; ADAM8; ADAM9; ADCY7; ALCAM; ANPEP; AP1G1; AP1S2; APP; ARF1; ARRB1; ATP1B1; ATP2A2; ATP6V1A; ATP6V1C1; ATP7A; AXL; BAIAP2; BASP1; BFAR; BST1; CABP4; CACNA1S; CACNB3; CALCRL; CALM1; CALM2; CANX; CASK; CCR5; CCR9; CD14; CD163; CD36; CD38; CD44; CD48; CD5; CD80; CD81; CD83; CD86; CD8A; CD9; CD96; CD97; CDC42; CDCA7; CHRNB1; CLDN1; CLTA; CLTB; CLTC; CNR2; CSF1R; CSF2RA; CSF2RB; CSNK2A1; CTNNA1; CXCR3; CYB561; CYSLTR1; DDR1;

nent				DLG1; DLG3; EBI3; EBP; EMR1; ENTPD1; ERBB2IP; ETV6; EVI2B; EVL; EZH2; FCGR2B; FLNB; FLT1; FLT3; FPR1; FTH1; FZD7; GABARAPL1; GABBR1; GCA; GIT2; GJA1; GNA13; GNAI3; GNB2; GNB4; GNG10; GNG12; GNG2; GPR34; GYPC; HFE; HRH2; HS6ST1; ICAM1; IFNAR1; IFNAR2; IFNGR2; IGF2R; IL10RA; IL13RA1; IL15; IL15RA; IL2RG; IL6ST; ILK; IRAK1; ITGA4; ITGA8; ITGA9; ITGAE; ITGAV; ITGAX; ITGB1; ITGB2; ITM2B; ITPR2; JAG2; JTB; KATNA1; KCNJ10; KCNN4; KLRC1; LAMP2; LANCL2; LGALS3; LIFR; LIMD1; LIMS1; LIN7C; LPP; LRMP; LRRC1; LST1; LY75; LY86; LY96; M6PR; MADD; MARCKS; MERTK; METAP1; MRAS; MRC1; MS4A1; NOTCH1; NOTCH2; NOTCH4; NUCB2; NUMB; P2RX4; P2RY6; PAK1; PAK2; PCNXL3; PDPK1; PEX3; PIP5K1C; PLCE1; PLEC1; PLSCR1; PLSCR3; PLXNC1; PNN; PPAP2A; PRKCB1; PRKCI; PRNP; PROCR; PRRG2; PSCD2; PSEN1; PTGER1; PTGER2; PTPN9; PTPRE; PTPRJ; PTPRS; RAC1; RALA; RALB; RAMP1; RASGRP4; RDX; RECQL; RGS19; RNF44; RRAS2; RYR1; SC4MOL; SCARB2; SDCBP; SEMA4F; SGCB; SLC11A1; SLC12A2; SLC14A1; SLC15A2; SLC1A5; SLC22A5; SLC25A11; SLC25A13; SLC25A14; SLC25A5; SLC30A5; SLC31A1; SLC31A2; SLC33A1; SLC35A1; SLC4A1; SLC6A6; SLC7A6; SLC7A7; SLC8A1; SLC9A3R2; SLMAP; SNAP23; SSFA2; STOM; STX6; STX7; STX8; SYNGR2; SYPL; SYT11; TACSTD1; TAP1; TAP2; TCIRG1; TGFBR1; TJP2; TLE3; TLR3; TLR4; TM9SF2; TMEM8; TNFAIP1; TNFRSF1A; TNFRSF9; TRIM37; TRIO; TRIP6; TRPV2; TULP3; TYROBP; UBE3A; UPF2; VAPB; VCAM1; VCL; VDAC3; XCR1; ZYX
GO Cellular Component	integral to plasma membrane	171	1672	ACVR1; ACVRL1; ADAM10; ADAM17; ADAM23; ADAM8; ADAM9; ADCY7; ALCAM; ANPEP; APP; ATP1B1; ATP2A2; ATP6V1A; ATP7A; AXL; BFAR; CACNA1S; CACNB3; CALCRL; CANX; CCR5; CCR9; CD163; CD36; CD44; CD48; CD5; CD81; CD83; CD8A; CD9; CD96; CD97; CHRNB1; CLDN1; CNR2; CSF1R; CSF2RA; CSF2RB; CXCR3; CYB561; CYSLTR1; DDR1; EBP; EMR1; ENTPD1; ETV6; EVI2B; FLNB; FLT1; FLT3; GABBR1; GJA1; GPR34; GYPC; HFE; HRH2; HS6ST1; ICAM1; IFNAR1; IFNAR2; IFNGR2; IGF2R; IL13RA1; IL15; IL15RA; IL2RG; IL6ST; IRAK1; ITGA4; ITGA8; ITGA9; ITGAE; ITGAV; ITGAX; ITGB1; ITGB2; ITM2B; JAG2; JTB; KCNJ10; KCNN4; KLRC1; LAMP2; LANCL2; LIFR; LIMD1; LPP; LRMP; LST1; LY75; M6PR; MERTK; METAP1; MRC1; MS4A1; NOTCH1; NOTCH2; NOTCH4; NUMB; P2RX4; P2RY6; PCNXL3; PEX3; PROCR; PRRG2; PSEN1; PTGER1; PTGER2; PTPN9; PTPRE; PTPRJ; PTPRS; RAMP1; RECQL; RNF44; RYR1; SCARB2; SDCBP; SEMA4F; SGCB; SLC11A1; SLC12A2; SLC14A1; SLC15A2; SLC1A5; SLC25A11; SLC25A13; SLC25A14; SLC25A5; SLC30A5; SLC31A1; SLC31A2; SLC33A1; SLC35A1; SLC4A1; SLC6A6; SLC7A6; SLC7A7; SLC8A1; SLMAP; STOM; STX6; STX7; STX8; SYNGR2; SYPL; SYT11; TAP1; TAP2; TCIRG1; TGFBR1; TJP2; TLR3; TLR4; TM9SF2; TMEM8; TNFAIP1; TNFRSF1A; TNFRSF9; TRIM37; TRIP6; TRPV2; TYROBP; UBE3A; UPF2; VAPB; VDAC3; XCR1; ZYX
GO Cellular Component	nucleoplasm	108	1672	AHR; ASF1B; ATF1; ATF2; ATF3; ATF6; BACH1; BCL3; BCL6; CBFB; CCM2; CCNH; CDK7; CPSF2; CPSF3; CSTF2; CSTF3; CTCF; DDB2; DR1; E2F1; EGR1; EGR2; FBL; FUS; FUSIP1; GTF2A1; GTF2B; GTF2E2; GTF2F2; GTF2H1; GTF2H2; GTF3C4; HCLS1; HDAC11; HDAC2; HDAC5; HELLS; HHEX; HIF1A; HIVEP1; HIVEP2; HNRPA3; HNRPK; ID2; ID3; KLF3; KPNA2; LMO2; LYL1; MCM4; MCM6; MEF2A; MEF2C; MITF; MKI67IP; MXI1; MYNN; NAP1L1; NFKB2; NFYA; NFYB; NUP54; PHTF2; PKNOX1; PLAGL2; POLD4; POLR2B; POLR2F; POLR2H; POLR3K; POU2AF1; PPP1CC; RAD54L; RASA1; RBBP4; RELB; REV3L; RNF103; RNF12; RNF6; ROD1; RREB1; RTCD1; RXRA; SAP30; SFPQ; SFRS2IP; SIRT2; SMARCA5; SMARCB1; SMARCC1; SNAPC3; SPIB; TAF13; TAF7; TAF9; TBPL1; TCF4; TDG; TFDP1; TTC3; UBP1; UBTF; XPO1; YAF2; YY1; ZFX
GO Cellular	cytosol	108	1672	ALDH1A2; ALDH9A1; ALS2; APAF1; ARFGAP3; ARHGEF7; BAG5; BID; BZW1; BZW2; CBR3; CCNA2; CCNB1; CCNB2; CCND1; CCND2; CCT3; DFFA; DFFB; DNAJB9; EGLN1; EIF4B; ENO2; FRAP1; GATM; GBP1; GBP2; GBP3; GOT1; GSN; GSPT1; IDH1; LCMT1; LCP1;

Component				MAP3K8; MDH1; MTAP; MTHFS; NCF1; NPEPPS; NT5C2; NUCB2; NUTF2; OGT; PDCL; PFDN2; PFKFB3; PFKL; PFKP; PIK3C2A; PIK3CD; PLA2G4A; PLCE1; PLCG2; PLEKHA1; PLEKHA2; PPP2R1B; PSMA4; PSMA6; PSMA7; PSMB3; PSMB4; PSMB5; PSMB7; PSMB8; PSMB9; PSMC1; PSMC2; PSMC6; PSMD10; PSMD13; PSMD14; PSMD2; PSMD4; PSMD8; PSME3; RGS2; RGS3; RPL11; RPL13; RPL14; RPL30; RPL31; RPL5; RPS10; RPS13; RPS24; RPS6; RPS9; SEC23A; SERPINB9; SH3GLB1; SHMT1; SQSTM1; STMN1; STRN3; SYK; TAP2; TBCD; TPI1; TRIP12; TSG101; UCHL5; ULK1; UNC119; UXT; VPS35; ZAP70
GO Cellular Component	**extracellular**	97	1672	ADAM17; ADFP; AFP; AGL; APOE; APP; BRE; BTG2; C1QA; C1QB; C6; CASP8AP2; CCL22; CD163; CD5L; CNOT7; CNOT8; COL14A1; COL9A3; CRIM1; CRTAP; CST3; CXCL10; CXCL16; CXCL9; **DKK3**; DNASE1L1; DNASE1L3; EBI3; ERBB2IP; FGL2; FLT1; GLIPR1; GRN; GSN; HSBP1; IBSP; IFI30; IFNAR2; IGF1; IK; IL15; IL16; IL18; INSL3; ITGA4; ITGA8; ITGA9; ITGAE; ITGAV; ITGAX; ITGB1; ITGB2; KLK1; LGALS3; LGALS3BP; LPL; LTBP2; LYPLA3; MAP2K1; MAP2K4; MAP2K5; MAP2K6; MAP2K7; MAP3K7IP2; MAPKAP1; MATN2; MFAP3; MGEA5; MST1; NAB2; NUCB2; PDGFA; PDGFC; PLA2G7; PRDX4; PRRG2; PSAP; PTPLA; PVR; QPCT; RTN3; SERPINE2; SGCB; SLPI; SPINT1; SPINT2; SYT11; TGFB3; TGFBI; TGM2; TIMP2; TNFAIP2; TNFRSF1A; TOB2; VAMP3; VWF
GO Cellular Component	membrane fraction	91	1672	ABCA3; ALCAM; ALDH3A2; ALDH3B1; ALOX5AP; ALS2; ARFRP1; ATP2A2; ATP5A1; ATP5C1; BCL2L11; BFAR; BID; CACNA1S; CACNB3; CD36; CD38; CD68; CERK; CHPT1; CLCN3; CPD; CRIM1; CYP8B1; CYSLTR1; ECE1; EPHX1; FMO5; GALNT3; GOLGA4; GP2; HIP1; HMGCR; HMOX1; HSD17B12; ICMT; IL15; ITM2B; JTB; KCNN4; LYPLA1; MAN1A2; MAN2A1; MGAT2; MGST1; NDUFAB1; NDUFB4; NDUFB7; NDUFC2; NDUFS4; NDUFS5; NDUFV1; NRP1; PEX13; PITPNM1; PLCE1; PLP2; PPAP2A; PPIF; PSCD2; PSEN1; RASGRP4; RGS19; SCAMP1; SCAMP2; SCARB2; SEC63; SEMA4F; SLC11A1; SLC12A2; SLC1A5; SLC30A5; SLC33A1; SLC35B1; SNAP23; SPINT1; SQLE; SSR3; STRN3; TAP1; TAP2; TAPBP; TGM1; TPST1; UCP2; UGT1A1; UGT1A10; UGT1A5; UGT1A9; VAMP3; VAMP8
GO Cellular Component	transcription factor complex	61	1672	AHR; ATF1; ATF2; ATF3; BACH1; BCL3; CBFB; CCM2; CCNH; CDK7; CTCF; E2F1; EGR1; EGR2; FUS; GTF2A1; GTF2B; GTF2E2; GTF2F2; GTF2H1; GTF2H2; GTF3C4; HDAC11; HDAC2; HDAC5; HHEX; HIF1A; HIVEP1; HIVEP2; ID2; ID3; KLF3; LMO2; LYL1; MITF; MXI1; MYNN; NFKB2; NFYA; NFYB; PHTF2; PKNOX1; PLAGL2; POLD4; POU2AF1; RELB; RXRA; SAP30; SFPQ; SNAPC3; SPIB; TAF13; TAF7; TAF9; TBPL1; TCF4; TFDP1; UBP1; UBTF; YY1; ZFX
GO Cellular Component	soluble fraction	36	1672	ACP1; ANXA1; ARRB1; ASNA1; CXCL10; DUSP6; EPRS; GYG; HMGCS1; IARS; IK; INSL3; IPO7; KARS; MATK; MERTK; NARS; NCF1; NSMAF; PAFAH1B2; PAFAH1B3; PDE4B; PPP1R11; PPP2R1B; PPP2R4; PPP4R1; PPP4R1L; PTP4A1; PTPN2; PTPRE; QARS; RASGRP4; SPINT2; STMN3; UGCGL1; UNC119
GO Cellular Component	extrinsic to plasma membrane	11	1672	ALCAM; ARRB1; GNA13; GNB2; GNB4; GNG10; GNG12; GNG2; NUMB; RGS19; TLE3

GO Cellular Component	caspase complex	7	1672	BIRC3; CASP2; CASP3; CASP6; CASP7; CASP9; CFLAR
GO Biological Process	cell growth and/or maintenance	624	1702	ABCA3; ABCB7; ABCD1; ABCF1; ABCF3; ABL1; ACO1; ACP2; ADD1; ADD3; AFP; AHR; AIF1; AKAP9; ALS2; ANAPC11; ANLN; AP1G1; AP1GBP1; AP1S2; AP3B1; AP3D1; AP3M1; AP3S1; AP3S2; APC; APOE; APP; APPBP2; ARF1; ARF3; ARF4; ARFGAP3; ARHGAP12; ARHGAP6; ARHGAP9; ARL3; ARL6; ARPC5; ASF1B; ASNA1; ATM; ATOX1; ATP11A; ATP11B; ATP1B1; ATP2A2; ATP2C1; ATP5A1; ATP5C1; ATP5E; ATP6V0A2; ATP6V0B; ATP6V0D1; ATP6V1A; ATP6V1B2; ATP6V1C1; ATP6V1D; ATP6V1H; ATP7A; ATP8A1; ATRX; AXIN1; AXL; BAZ2A; BCL10; BCL3; BCL6; BCL9; BIRC5; BMI1; BRI3; BTG2; BUB1; BUB3; CACNA1S; CACNB3; CALM2; CAPZA1; CAPZA2; CAPZB; CBFA2T3; CBFB; CBL; CBX6; CCNA2; CCNB1; CCNB2; CCNC; CCND1; CCND2; CCNDBP1; CCNE2; CCNG1; CCNG2; CCNH; CCNI; CCNT2; CCT7; CD14; CD36; CD5; CD68; CD81; CD86; CD99L2; CDC16; CDC20; CDC25A; CDC25C; CDC37; CDC42; CDC6; CDK2AP1; CDK4; CDK5; CDK5RAP1; CDK7; CDK8; CDKN1A; CDYL; CENPA; CENPE; CENPF; CETN2; CHD1; CHD6; CHEK1; CHFR; CHPT1; CHRNB1; CKS1B; CKS2; CLASP1; CLCN3; CLIC4; CLK1; CLTA; CLTB; CLTC; COPG2; COPZ2; CPNE1; CPNE3; CRIM1; CRK; CROT; CRTAP; CSF1R; CSK; CSNK2A2; CSRP1; CSRP2; CTBP2; CTCF; CTNNBIP1; CUL1; CUL3; CUL4A; CUL4B; CXCL10; CXCL16; DBI; DBN1; DDX6; DEK; DLEU2; DLG3; DSCR3; DSTN; DTYMK; DUSP1; DUSP16; DUSP22; DUSP6; DUT; E2F1; ECT2; EHD1; EHD2; EHD4; EHHADH; EIF2AK4; EIF4G2; ELK3; EMD; ENSA; EPS15; EPS8; ERBB2IP; ETS2; ETV6; EVI2A; EVI2B; EVI5; EVL; EXTL2; EXTL3; EZH2; FABP5; FBL; FCGR2B; FEN1; FES; FLI1; FLNB; FLT1; FLT3; FRAP1; FSCN1; FTH1; FUS; FUSIP1; FXC1; FYCO1; GABARAPL1; GABARAPL2; GBA; GDI1; GDI2; GFPT1; GJA1; GLG1; GLRX2; GMNN; GNA13; GNAI3; GOLGA4; GPS1; GRN; GRPEL1; GSN; GSPT1; GTF2H1; H1F0; H2AFZ; H3F3B; HDAC11; HDAC2; HDAC5; HFE; HIST1H1C; HIST1H2AB; HIST1H2AC; HIST1H2AD; HIST1H2AE; HIST1H3D; HIST1H4A; HIST2H2AC; HIST3H2A; HK2; HNRPA3; HRB; HSPA1B; HUS1; ICMT; IFI44; IGF1; IGF2R; IL15; IL15RA; IL18; IL2RG; ILK; INCENP; IPO7; IRF5; ITPR1; ITPR2; ITSN1; ITSN2; JAG2; JAK2; JAK3; KATNA1; KCNJ10; KCNN4; KHDRBS1; KIF11; KIF1B; KIF1C; KIF20A; KIF23; KIF2C; KIF3B; KIF5B; KIT; KLHL2; KLHL5; KPNA1; KPNA2; KPNA3; KPNB1; LAMP3; LAPTM4A; LAPTM4B; LIG1; LIMD1; LIMK1; LMAN1; LMO2; LPL; LRMP; LTBP2; LY75; LY86; LYL1; LYN; LZTFL1; M6PR; MAD2L1; MAP2K6; MAP2K7; MAP3K7IP2; MAP3K8; MAPK1; MAPK13; MAPK6; MAPRE1; MAPRE2; MATK; MCL1; MCM2; MCM3; MCM4; MCM6; MDM2; MDM4; MERTK; MKI67; MKL1; MLH3; MRAS; MRC1; MRPL49; MTM1; MTPN; MTX2; MVP; MXI1; MYB; MYCL1; MYL6; MYO1C; MYO5A; MYO6; NAB2; NAP1L1; NCBP2; NDUFA9; NEDD4L; NEDD9; NEK9; NFIX; NFKB2; NFKBIE; NNT; NOLC1; NOTCH2; NRP1; NSF; NUBP1; NUCB2; NUDT4; NUP153; NUP50; NUP54; NUP62; NUPL1; NUTF2; ORC4L; OSBPL11; OSBPL9; P2RX4; PA2G4; PACSIN1; PCAF; PDAP1; PDGFA; PDGFC; PDPK1; PEX11A; PEX13; PEX3; PEX6; PEX7; PFN2; PITPNM1; PLCE1; PLDN; PLEC1; PLP2; PLSCR1; PLSCR3; PML; POLB; POLD4; POU2AF1; PPAP2A; PPAP2B; PPIH; PPP1CC; PPP2R1B; PPP3CB; PPP6C; PRC1; PRKRA; PRKRIR; PRNP; PSAP; PSCD2; PSEN1; PSMD8; PTEN; PTPN6; PTPN9; PTTG1IP; PURA; RAB10; RAB11A; RAB14; RAB24; RAB2B; RAB30; RAB31; RAB32; RAB33B; RAB5A; RAB6B; RAB6IP1; RAB7; RABIF; RAC1; RAD17; RAD51; RAD51L1; RAD51L3; RAD54L; RAMP1; RANBP2; RANBP9; RAP1A; RAP1B; RASA1; RASGRP4; RB1; RBBP4;

				RBBP6; RBBP8; RBL1; RBM5; RBMS1; RDX; REV3L; RFC1; RFC3; RFC4; RGS19; RGS2; ROCK1; ROCK2; RPA3; RPL13; RPL23; RPL5; RPS6KA2; RPS6KB2; RRAS2; RRBP1; RRM1; RRM2; RRS1; RUNX1; RYR1; SAP30; SCAMP1; SCAMP2; SCP2; SDCBP; SDCCAG3; SEC14L1; SEC23A; SEC24B; SEC24C; SEC24D; SEC63; SERPINF1; SFRS9; SFXN2; SHPRH; SIRT2; SKP2; SLC11A1; SLC12A2; SLC13A3; SLC14A1; SLC15A2; SLC1A5; SLC22A5; SLC25A11; SLC25A13; SLC25A14; SLC25A20; SLC25A5; SLC2A9; SLC30A4; SLC30A5; SLC30A7; SLC31A1; SLC31A2; SLC33A1; SLC35A1; SLC35A5; SLC35B1; SLC35E1; SLC37A3; SLC41A1; SLC4A1; SLC4A7; SLC6A6; SLC7A6; SLC7A7; SLC8A1; SMARCA5; SMARCB1; SMARCC1; SMARCE1; SNAP23; SNX10; SNX2; SNX3; SNX4; SNX5; SNX6; SOCS4; SOCS5; SRF; SRI; SRP14; SSFA2; SSR2; SSR4; STAM2; STARD3; STARD4; STARD5; STAT1; STMN1; STRN3; STX12; STX17; STX18; STX5A; STX6; STX7; STX8; SUPT4H1; SYK; SYNGR2; SYPL; SYT11; TACC3; TAP1; TAP2; TAPBP; TARDBP; TBC1D8; TBCD; TCF19; TCIRG1; TEP1; TFDP1; TGFB3; TGFBI; TGFBR2; THOC2; TIMM17B; TIMM22; TLK2; TM9SF2; TMEM1; TNFAIP1; TNFAIP2; TNFRSF9; TOB2; TOP1; TOP2A; TOP2B; TPR; TRAM1; TREX1; TRNT1; TRPM7; TRPV2; TSG101; TTK; TUBGCP5; TXNDC4; UBE2C; UBE2D1; UBE2D3; UBE2V1; UBE2V2; UCP2; USP4; USP8; VAMP3; VAMP8; VAPB; VAV1; VDAC1; VDAC3; VPS18; VPS35; VPS41; VPS4B; WASF2; WASL; XPO1; XPO7; XRN2; YWHAQ; ZFP36L1; ZFYVE16
GO Biological Process	**cell communication**	447	1702	ABL1; ABR; ACVR1; ACVRL1; ADAM10; ADAM17; ADAM9; ADCY7; AHR; AIM1; AKAP9; ALCAM; ANP32A; ANXA1; AP3S1; APC; APOE; APP; ARF1; ARF3; ARF4; ARFRP1; ARHGAP5; ARHGAP6; ARHGEF7; ARL1; ARL3; ARL6; ARRB1; ASAH2; ASB13; ATF6; ATM; ATP2A2; AXIN1; AXL; BAIAP2; BCL3; BCL9; BIRC3; BRD8; BRE; BTK; C1QA; CABP4; CALCRL; CALM1; CALM2; CAMK1; CARD10; CARHSP1; CASK; CASP8AP2; CBL; CCL22; CCR5; CCR9; CD14; CD2AP; CD36; CD38; CD44; CD5; CD80; CD83; CD86; CD8A; CD9; CD96; CD97; CDC42; CENTD1; CENTD2; CERK; CFL2; CHN2; CHRNB1; CHUK; CLDN1; CNOT7; CNP; CNR2; CORO2A; CREM; CRK; CSF1R; CSF2RB; CSK; CSNK1D; CSNK1G1; CSNK2A1; CSNK2A2; CSNK2B; CTNNA1; CTNNBIP1; CXCL10; CXCL9; CXCR3; CYSLTR1; DAPK1; DAPK3; DAPP1; DBN1; DDR1; DEK; DFFA; DFFB; DGCR2; **DKK3**; DUSP16; DUSP22; DUSP6; DUSP7; ECE1; ECT2; ELK3; EMR1; ENSA; ENTPD1; EPS15; EPS8; ERBB2IP; EVL; FCGR2B; FES; FLNB; FLT1; FLT3; FNBP1; FNTA; FPR1; FXC1; FZD7; GABBR1; GADD45B; GADD45G; GALNT1; GCH1; GDI1; GDI2; GIT2; GJA1; GLRX2; GMFB; GNA13; GNAI3; GNB2; GNB4; GNG10; GNG12; GNG2; GPR124; GPR34; GPR35; GPR65; GPS1; GRN; GTF2I; GTPBP2; HABP4; HCK; HCLS1; HIF1A; HIVEP2; HOMER2; HRH2; IBSP; ICAM1; IFNAR1; IFNAR2; IFNGR2; IGF1; IGF2R; IK; IKBKG; IL10RA; IL13RA1; IL15; IL15RA; IL18; IL2RG; IL6ST; ILK; IMPA1; INPP1; INPP4A; INPP5D; INPPL1; INSL3; IPO7; IQGAP1; IRAK1; IRF7; ITGA4; ITGA8; ITGA9; ITGAE; ITGAV; ITGAX; ITGB1; ITGB2; ITPR1; ITPR2; JAG2; JAK1; JAK2; JAK3; KHDRBS1; KIF1B; KIT; KLRC1; LANCL2; LARGE; LGALS3; LGALS3BP; LIFR; LIMD1; LIMK1; LMAN1; LSP1; LTBP2; LY75; LY86; LY96; LYN; MADD; MAN1A2; MAP2K1; MAP2K4; MAP2K5; MAP2K6; MAP2K7; MAP3K3; MAP3K4; MAP3K7; MAP4K1; MAP4K3; MAP4K4; MAP4K5; MAPK1; MAPK13; MAPK14; MAPK6; MAPK8; MAPK9; MAPKAPK2; MAPRE2; MATK; MBP; MERTK; MFAP3; MFHAS1; MKLN1; MKNK1; MRAS; MRC1; MX1; MYD88; MYO9A; NCF1; NCOA1; NCOA3; NEDD9; NFAT5; NFKB1; NFKB2; NMI; NOTCH1; NOTCH2; NOTCH4; NR3C1; NRP1; NSMAF; NUDT4; OGT; OSTF1; P2RX4; P2RY6; PAK1; PAK2; PDAP1; PDCD6IP; PDCL; PDE1B; PDE4B; PDE8A; PDGFA; PDK1; PDK3; PDPK1; PELI1; PEX11A; PIAS1; PIK3C2A; PIK3CD; PLCE1; PLCG2; PLDN; PLEK; PLXNC1; PNN; PPAP2A; PPARG; PPFIA4; PPP2R1B; PPP2R2A; PPP2R5C; PPP3CB; PPP4R1; PPP4R1L; PRDX4; PRKCB1; PRKCD; PRKCH; PRKCI; PRKRA; PRKRIR; PRNP; PSCD2; PSEN1; PTGER1; PTGER2; PTGER4; PTPLA; PTPN11; PTPN6; PTPRE; PTPRJ; PTPRS; PXN; RAB10; RAB11A; RAB14; RAB24; RAB2B; RAB30; RAB31;

				RAB32; RAB33B; RAB5A; RAB6B; RAB7; RAC1; RALA; RALB; RAMP1; RAP1A; RAP1B; RAP2A; RASA1; RASGRP4; RASSF3; RASSF5; RGS10; RGS18; RGS19; RGS2; RGS3; RNF14; ROCK1; ROCK2; RPS6KA2; RPS6KB1; RPS6KB2; RPS6KC1; RRAS2; RRBP1; RREB1; RTN1; RXRA; SCARB1; SCARB2; SDCBP; SEMA4D; SEMA4F; SHOC2; SIAH2; SLA; SLC9A3R2; SNX10; SNX2; SNX3; SNX4; SNX5; SNX6; SOCS4; SOCS5; SQSTM1; SRF; SRI; STAT1; STAT3; STAT5A; STAT6; STK17B; STK3; STMN1; STMN3; SULT1A1; SYK; SYPL; TANK; TBK1; TCF7; TCF7L2; TEC; TGFB3; TGFBI; TGFBR1; TGFBR2; TGM2; TIAM1; TLE3; TLK2; TLR1; TLR3; TLR4; TMEM8; TNFAIP2; TNFRSF1A; TNFRSF21; TRAF3; TRAF5; TRIM37; TRIO; TULP3; TXK; TXNRD1; TYK2; TYROBP; ULK1; UNC119; VAV1; VAV3; VCAM1; VCL; VWF; WASF2; XCR1; YWHAB; YWHAE; YWHAQ; YWHAZ; ZAP70; ZFYVE16; ZFYVE21; ZYX
GO Biological Process	signal transduction	392	1702	ABL1; ABR; ACVR1; ACVRL1; ADAM9; ADCY7; AHR; AKAP9; ALCAM; ANP32A; ANXA1; AP3S1; APC; APP; ARF1; ARF3; ARF4; ARFRP1; ARHGAP5; ARHGAP6; ARHGEF7; ARL1; ARL3; ARL6; ARRB1; ASAH2; ASB13; ATF6; ATM; AXIN1; AXL; BAIAP2; BCL3; BCL9; BIRC3; BRD8; BRE; BTK; CABP4; CALCRL; CALM1; CALM2; CAMK1; CARD10; CARHSP1; CASP8AP2; CBL; CCL22; CCR5; CCR9; CD14; CD2AP; CD38; CD80; CD83; CD8A; CD97; CDC42; CENTD1; CENTD2; CERK; CFL2; CHN2; CHRNB1; CHUK; CNOT7; CNR2; CORO2A; CREM; CRK; CSF1R; CSF2RB; CSK; CSNK1D; CSNK1G1; CSNK2A1; CSNK2A2; CSNK2B; CTNNBIP1; CXCL10; CXCL9; CXCR3; CYSLTR1; DAPK1; DAPK3; DAPP1; DBN1; DDR1; DEK; DFFA; DFFB; **DKK3**; DUSP16; DUSP22; DUSP6; DUSP7; ECT2; ELK3; EMR1; EPS15; EPS8; ERBB2IP; EVL; FCGR2B; FES; FLNB; FLT1; FLT3; FNBP1; FNTA; FPR1; FZD7; GABBR1; GADD45B; GADD45G; GDI1; GDI2; GIT2; GLRX2; GMFB; GNA13; GNAI3; GNB2; GNB4; GNG10; GNG12; GNG2; GPR124; GPR34; GPR35; GPR65; GPS1; GRN; GTF2I; GTPBP2; HABP4; HCK; HCLS1; HIF1A; HIVEP2; HOMER2; HRH2; IFNAR1; IFNAR2; IFNGR2; IGF1; IGF2R; IKBKG; IL10RA; IL13RA1; IL15; IL15RA; IL2RG; IL6ST; ILK; IMPA1; INPP1; INPP4A; INPP5D; INPPL1; IPO7; IQGAP1; IRAK1; ITGA4; ITGA8; ITGA9; ITGAE; ITGAV; ITGAX; ITGB1; ITGB2; ITPR1; ITPR2; JAG2; JAK1; JAK2; JAK3; KHDRBS1; KIT; KLRC1; LANCL2; LGALS3BP; LIFR; LIMD1; LIMK1; LSP1; LTBP2; LY86; LY96; LYN; MADD; MAN1A2; MAP2K1; MAP2K4; MAP2K5; MAP2K6; MAP2K7; MAP3K3; MAP3K4; MAP3K7; MAP4K1; MAP4K3; MAP4K4; MAP4K5; MAPK1; MAPK13; MAPK14; MAPK6; MAPK8; MAPK9; MAPKAPK2; MAPRE2; MATK; MERTK; MFAP3; MFHAS1; MKLN1; MKNK1; MRAS; MX1; MYD88; MYO9A; NCF1; NCOA1; NCOA3; NEDD9; NFAT5; NFKB1; NFKB2; NMI; NOTCH1; NOTCH2; NOTCH4; NR3C1; NRP1; NSMAF; NUDT4; OGT; OSTF1; P2RX4; P2RY6; PAK1; PAK2; PDAP1; PDCD6IP; PDCL; PDE1B; PDE4B; PDE8A; PDGFA; PDK1; PDK3; PDPK1; PELI1; PEX11A; PIAS1; PIK3C2A; PIK3CD; PLCE1; PLCG2; PLEK; PPAP2A; PPARG; PPP2R1B; PPP2R2A; PPP2R5C; PPP3CB; PPP4R1; PPP4R1L; PRDX4; PRKCB1; PRKCD; PRKCH; PRKCI; PRKRA; PRKRIR; PRNP; PSCD2; PSEN1; PTGER1; PTGER2; PTGER4; PTPLA; PTPN11; PTPN6; PTPRE; PTPRJ; PXN; RAB10; RAB11A; RAB14; RAB24; RAB2B; RAB30; RAB31; RAB32; RAB33B; RAB5A; RAB6B; RAB7; RAC1; RALA; RALB; RAMP1; RAP1A; RAP1B; RAP2A; RASA1; RASGRP4; RASSF3; RASSF5; RGS10; RGS18; RGS19; RGS2; RGS3; RNF14; ROCK1; ROCK2; RPS6KA2; RPS6KB1; RPS6KB2; RPS6KC1; RRAS2; RRBP1; RREB1; RTN1; RXRA; SDCBP; SHOC2; SIAH2; SLA; SLC9A3R2; SNX10; SNX2; SNX3; SNX4; SNX5; SNX6; SOCS4; SOCS5; SQSTM1; SRF; SRI; STAT1; STAT3; STAT5A; STAT6; STK17B; STK3; STMN1; STMN3; SYK; TANK; TBK1; TCF7; TCF7L2; TEC; TGFB3; TGFBR1; TGFBR2; TGM2; TIAM1; TLE3; TLK2; TLR1; TLR3; TLR4; TNFRSF1A; TNFRSF21; TRAF3; TRAF5; TRIM37; TRIO; TULP3; TXK; TXNRD1; TYK2; TYROBP; ULK1; VAV1; VAV3; WASF2; XCR1; YWHAB; YWHAE; YWHAQ; YWHAZ; ZAP70; ZFYVE16; ZFYVE21; ZYX
GO	transcripti	265	1702	ABL1; ADNP; AHR; AP3D1; ARHGAP6; ASF1B; ASXL1; ATF1; ATF2; ATF3; ATF6; ATF7IP; ATRX; BACH1; BAD; BASP1; BAZ1B; BAZ2A;

Biological Process	on			BAZ2B; BBX; BCL11A; BCL11B; BCL3; BCL6; BMI1; BRD8; CARHSP1; CBFA2T3; CBFB; CBX6; CCNC; CCNH; CCNT2; CD80; CD86; CDK7; CDK8; CEBPG; CHD1; CITED2; CNOT2; CNOT7; CNOT8; CRAMP1L; CREB3; CREM; CRK; CTCF; CTDP1; CTNNBIP1; CTNNBL1; DEK; DMTF1; DNMT3A; DR1; DRG1; E2F1; EED; EGR1; EGR2; ELF1; ELK3; EPC1; ETS2; ETV3; ETV6; EZH2; FBXO3; FKBP1A; FKBP1B; FLI1; FNBP1; FUBP1; FUSIP1; FXR1; GABPA; GABPB1; GLRX2; GSPT1; GTF2A1; GTF2B; GTF2E2; GTF2F2; GTF2H1; GTF2H2; GTF2I; GTF3C4; H1F0; HABP4; HCLS1; HDAC11; HDAC2; HDAC5; HHEX; HIF1A; HIST1H1C; HIVEP1; HIVEP2; HMGB3; HMGN3; HSBP1; IKBKG; IRAK1; IRF3; IRF4; IRF5; IRF6; IRF7; KLF3; LIMD1; LITAF; LRRFIP1; LYL1; MAFB; MBP; MCM2; MCM3; MCM4; MCM6; MEF2A; MEF2C; MFHAS1; MITF; MKI67IP; MKL1; MNDA; MRPS25; MXI1; MYB; MYCBP; MYCL1; MYD88; MYNN; NAB2; NAP1L1; NCOA1; NCOA3; NFAT5; NFATC1; NFIX; NFKB1; NFKB2; NFYA; NFYB; NMI; NOTCH1; NOTCH2; NOTCH4; NR2C2; NR3C1; PAPOLG; PCAF; PCNXL3; PDCD7; PDGFA; PHF10; PKNOX1; PLAGL2; PML; POLR2B; POLR2F; POLR2H; POLR3K; POU2AF1; PPARG; PPP2R1B; PPP3CB; PREB; PRKCBP1; PRNP; PRPF4B; PRRG2; PURA; PXN; RAD51L1; RB1; RBBP8; RBL1; RBMX; RELB; RERE; RFC1; RFX5; RFXAP; RNF12; RNF14; RREB1; RRS1; RUNX1; RUVBL1; RXRA; SALL2; SF1; SFRS1; SFRS11; SFRS3; SFRS9; SHPRH; SIN3B; SIRT2; SMARCA5; SMARCB1; SMARCC1; SMARCE1; SNAPC3; SNRPD1; SP100; SPIB; SREBF2; SRF; SRRM1; SSB; SSBP3; SSX2IP; STAT1; STAT3; STAT5A; STAT6; SUPT4H1; TAF13; TAF1B; TAF7; TAF9; TARDBP; TBPL1; TCEA1; TCEB1; TCEB3; TCERG1; TCF19; TCF4; TCF7; TCF7L2; TFDP1; TFPT; TGFBR2; TIAL1; TJP2; TLE3; TOP2B; TRIM33; TRIP13; TTF1; TULP3; UBE2V1; UBP1; UBTF; UBXD2; UGP2; UHRF1; VPS4B; XBP1; YAF2; YME1L1; YY1; ZBTB1; ZBTB2; ZDHHC14; ZDHHC2; ZDHHC3; ZDHHC6; ZDHHC9; ZFP161; ZFX; ZNRD1
GO Biological Process	regulation of transcription	241	1702	ABL1; ADNP; AHR; AP3D1; ARHGAP6; ASF1B; ASXL1; ATF1; ATF2; ATF3; ATF6; ATF7IP; ATRX; BACH1; BAD; BASP1; BAZ1B; BAZ2A; BAZ2B; BBX; BCL11A; BCL11B; BCL3; BCL6; BMI1; BRD8; CARHSP1; CBFA2T3; CBX6; CCNC; CCNH; CCNT2; CD80; CD86; CDK7; CDK8; CEBPG; CHD1; CITED2; CNOT2; CNOT7; CNOT8; CRAMP1L; CREB3; CREM; CRK; CTCF; CTNNBIP1; CTNNBL1; DEK; DMTF1; DNMT3A; DR1; E2F1; EED; EGR1; EGR2; ELF1; ELK3; ETS2; ETV3; ETV6; EZH2; FKBP1A; FKBP1B; FLI1; FNBP1; FUBP1; FUSIP1; FXR1; GABPA; GABPB1; GLRX2; GSPT1; GTF2A1; GTF2B; GTF2E2; GTF2F2; GTF2H1; GTF2H2; GTF2I; H1F0; HABP4; HCLS1; HDAC11; HDAC2; HDAC5; HHEX; HIF1A; HIST1H1C; HIVEP1; HIVEP2; HMGB3; HSBP1; IKBKG; IRAK1; IRF3; IRF4; IRF5; IRF6; IRF7; KLF3; LIMD1; LITAF; LRRFIP1; LYL1; MAFB; MBP; MCM2; MCM3; MCM4; MCM6; MEF2A; MEF2C; MFHAS1; MITF; MKL1; MNDA; MRPS25; MXI1; MYB; MYCBP; MYCL1; MYD88; NAB2; NCOA3; NFAT5; NFATC1; NFIX; NFKB1; NFKB2; NFYA; NFYB; NOTCH1; NOTCH2; NOTCH4; NR2C2; NR3C1; PCAF; PCNXL3; PDCD7; PDGFA; PHF10; PKNOX1; PLAGL2; PML; POLR3K; POU2AF1; PPARG; PPP2R1B; PREB; PRKCBP1; PRNP; PRPF4B; PRRG2; PURA; PXN; RB1; RBBP8; RBL1; RBMX; RELB; RERE; RFC1; RFX5; RNF12; RNF14; RREB1; RRS1; RUNX1; RUVBL1; RXRA; SALL2; SF1; SFRS1; SFRS11; SFRS3; SFRS9; SHPRH; SIN3B; SIRT2; SMARCA5; SMARCB1; SMARCC1; SMARCE1; SNAPC3; SNRPD1; SP100; SPIB; SREBF2; SRF; SRRM1; SSBP3; SSX2IP; STAT1; STAT3; STAT5A; STAT6; SUPT4H1; TAF13; TAF7; TAF9; TARDBP; TBPL1; TCEA1; TCEB1; TCEB3; TCF19; TCF4; TCF7; TCF7L2; TFDP1; TFPT; TGFBR2; TIAL1; TJP2; TLE3; TOP2B; TRIM33; TULP3; UBE2V1; UBP1; UBTF; UBXD2; UGP2; UHRF1; VPS4B; XBP1; YAF2; YME1L1; YY1; ZBTB1; ZBTB2; ZDHHC14; ZDHHC2; ZDHHC3; ZDHHC6; ZDHHC9; ZFP161; ZFX; ZNRD1
GO Biologi	cell proliferatio	237	1702	ABL1; ACP2; AHR; AIF1; ANAPC11; ANLN; APC; ATM; AXIN1; AXL; BCL10; BCL3; BCL6; BIRC5; BTG2; BUB1; BUB3; CALM2; CBFA2T3; CCNA2; CCNB1; CCNB2; CCNC; CCND1; CCND2; CCNE2; CCNG1; CCNG2; CCNH; CCNI; CCNT2; CCT7; CD5; CD68; CD81; CD86;

cal Process	n			CD99L2; CDC16; CDC20; CDC25A; CDC25C; CDC37; CDC6; CDK2AP1; CDK4; CDK5; CDK5RAP1; CDK7; CDK8; CDKN1A; CENPE; CENPF; CETN2; CHEK1; CHFR; CKS1B; CKS2; CLK1; CRK; CRTAP; CSF1R; CSK; CSNK2A2; CSRP2; CTBP2; CTCF; CTNNBIP1; CUL1; CUL3; CUL4A; CUL4B; CXCL10; DLEU2; DLG3; DTYMK; DUSP1; DUSP22; DUSP6; DUT; E2F1; EIF2AK4; EIF4G2; ELK3; EPS15; EPS8; ERBB2IP; ETS2; EVI2A; EVI5; FEN1; FES; FLT1; FLT3; FRAP1; FSCN1; FTH1; GMNN; GPS1; GRN; GSPT1; GTF2H1; HDAC5; HK2; HSPA1B; HUS1; IGF1; IL15; IL15RA; IL18; IL2RG; ILK; INCENP; JAG2; JAK2; KATNA1; KHDRBS1; KIF11; KIF23; KIF2C; KPNA2; LAMP3; LIG1; LTBP2; LY86; LYN; MAD2L1; MAP2K6; MAP2K7; MAP3K8; MAPK1; MAPK13; MAPK6; MAPRE1; MAPRE2; MATK; MCM2; MCM3; MCM4; MCM6; MDM2; MDM4; MKI67; MLH3; MVP; MXI1; MYB; NAB2; NAP1L1; NEDD9; NEK9; NFIX; NOLC1; NOTCH2; NRP1; NUBP1; ORC4L; PA2G4; PCAF; PDAP1; PDGFA; PLCE1; POLB; POLD4; PPAP2A; PPP1CC; PPP2R1B; PPP3CB; PPP6C; PRC1; PRKRA; PRKRIR; PSEN1; PSMD8; PTEN; PTPN6; PURA; RAB6IP1; RAC1; RAD17; RAD51; RAD51L1; RAD51L3; RAD54L; RAP1A; RAP1B; RASGRP4; RB1; RBBP4; RBBP6; RBBP8; RBL1; RBM5; RBMS1; REV3L; RFC1; RFC3; RFC4; RGS2; ROCK2; RPA3; RPS6KB2; RRM1; RRM2; SAP30; SERPINF1; SIRT2; SKP2; SMARCB1; STAT1; STRN3; SYK; TARDBP; TBC1D8; TCF19; TCIRG1; TEP1; TFDP1; TGFB3; TGFBI; TGFBR2; TLK2; TNFRSF9; TOB2; TOP1; TOP2A; TOP2B; TREX1; TTK; UBE2C; UBE2D1; UBE2D3; UBE2V1; UBE2V2; USP8; VAV1; YWHAQ; ZFP36L1
GO Biological Process	regulation of transcription\, DNA-dependent	234	1702	ABL1; ADNP; AHR; AP3D1; ARHGAP6; ASF1B; ASXL1; ATF1; ATF2; ATF3; ATF6; ATF7IP; ATRX; BACH1; BAD; BASP1; BAZ1B; BAZ2A; BAZ2B; BBX; BCL11A; BCL11B; BCL3; BCL6; BMI1; BRD8; CARHSP1; CBFA2T3; CBX6; CCNC; CCNH; CCNT2; CDK7; CDK8; CEBPG; CHD1; CITED2; CNOT2; CNOT7; CNOT8; CRAMP1L; CREB3; CREM; CRK; CTCF; CTNNBIP1; CTNNBL1; DEK; DMTF1; DNMT3A; DR1; E2F1; EGR1; EGR2; ELF1; ELK3; ETS2; ETV3; ETV6; EZH2; FKBP1A; FKBP1B; FLI1; FNBP1; FUBP1; FXR1; GABPA; GABPB1; GSPT1; GTF2A1; GTF2B; GTF2E2; GTF2F2; GTF2H1; GTF2H2; GTF2I; H1F0; HABP4; HCLS1; HDAC11; HDAC2; HDAC5; HHEX; HIF1A; HIST1H1C; HIVEP1; HIVEP2; HMGB3; HSBP1; IKBKG; IRF3; IRF4; IRF5; IRF6; IRF7; KLF3; LIMD1; LITAF; LRRFIP1; LYL1; MAFB; MBP; MCM2; MCM3; MCM4; MCM6; MEF2A; MEF2C; MFHAS1; MITF; MKL1; MNDA; MRPS25; MXI1; MYB; MYCBP; MYCL1; MYD88; NAB2; NCOA3; NFAT5; NFATC1; NFIX; NFKB1; NFKB2; NFYA; NFYB; NOTCH1; NOTCH2; NOTCH4; NR2C2; NR3C1; PCAF; PCNXL3; PDCD7; PDGFA; PHF10; PKNOX1; PLAGL2; PML; POLR3K; POU2AF1; PPARG; PREB; PRKCBP1; PRNP; PRPF4B; PRRG2; PURA; PXN; RB1; RBBP8; RBL1; RBMX; RELB; RERE; RFC1; RFX5; RNF12; RNF14; RREB1; RRS1; RUNX1; RUVBL1; RXRA; SALL2; SF1; SFRS1; SFRS11; SFRS3; SFRS9; SHPRH; SIN3B; SIRT2; SMARCA5; SMARCB1; SMARCC1; SMARCE1; SNAPC3; SNRPD1; SP100; SPIB; SREBF2; SRF; SRRM1; SSBP3; SSX2IP; STAT1; STAT3; STAT5A; STAT6; SUPT4H1; TAF13; TAF7; TAF9; TARDBP; TBPL1; TCEA1; TCEB1; TCEB3; TCF19; TCF4; TCF7; TCF7L2; TFDP1; TFPT; TGFBR2; TIAL1; TJP2; TLE3; TOP2B; TRIM33; TULP3; UBE2V1; UBP1; UBTF; UBXD2; UGP2; UHRF1; VPS4B; XBP1; YAF2; YME1L1; YY1; ZBTB1; ZBTB2; ZDHHC14; ZDHHC2; ZDHHC3; ZDHHC6; ZDHHC9; ZFP161; ZFX; ZNRD1
GO Biological Process	development	200	1702	ADAM23; ALAD; ALDH3A2; ANPEP; AP3D1; APAF1; APOE; ARIH2; ASF1B; ATF7IP; ATP2A2; ATP2C1; ATRX; AXIN1; BAIAP2; BMI1; BST1; BTK; CCNI; CD80; CD86; CDK5; CDK5RAP1; CDYL; CHEK1; CHUK; CLN8; CRAMP1L; CRIM1; CRLF3; CRYAB; CSF1R; CSF2RA; CSNK2A2; CSRP2; CTNNBIP1; CUGBP2; CXCL10; DBN1; DFFA; DFFB; DGCR2; DICER1; **DKK3**; DNMT3A; DRG1; DUSP22; DYRK1A; EBP; EGR2; ELAVL1; EMD; ETS2; EVI5; EVL; FABP5; FECH; FES; FLI1; FLII; FLNB; FLT1; FZD7; GADD45B; GADD45G; GJA1; GLRX2; GMFB; GNA13; GNPAT; GPX4; GYPC; HCCS; HCK; HDAC5; HELLS; HHEX; HMBS; HMGB3; HMGCR; HMOX1; IBSP; ID2; ID3; IGF1; IL18; INSL3;

s				IRF4; ITGAX; ITGB1; ITGB2; ITM2B; JAG2; JAK2; JAK3; KHDRBS3; KIF1B; KIF3B; KLF3; KRT17; LARGE; LIG1; LIMD1; LIMK1; LIMS1; LMO2; LRMP; LRRC1; MAFB; MAP4K1; MAPK14; MATK; MBNL3; MBP; MCL1; MEF2A; MEF2C; MITF; MRAS; MTM1; MTPN; MYD88; MYL6; MYOM1; NAB2; NAGLU; NDRG1; NDUFB7; NOTCH1; NOTCH2; NOTCH4; NR2C2; NRP1; NUMB; OLFM1; OSTF1; PAFAH1B3; PAPSS1; PCNXL3; PDGFC; PES1; PHYH; PITPNM1; PLCE1; PLXNB2; PLXNC1; PPAP2A; PPAP2B; PPAP2C; PPP2R1B; PPT1; PTEN; PTPLA; PTTG1IP; RAC1; RASGRP4; RNF103; ROD1; RREB1; RTN1; RTN3; RTN4; RUNX1; RUVBL1; SACM1L; SCMH1; SEMA4D; SEMA4F; SERPINF1; SGCB; SIAH2; SIRT2; SNCA; SOCS5; SRI; STAT3; STMN3; STRBP; SYK; TCF4; TGFB3; TLE3; TLR3; TLR4; TNFAIP2; TNNI2; TOB2; TOP2B; TPD52; TPM1; TPM2; TPM3; TPM4; TRIM3; UBE2V1; UBE3A; UFD1L; USP9X; XRN2; YAF2
GO Biological Process	intracellular signaling cascade	180	1702	ABL1; ABR; ADAM9; ADCY7; ANP32A; ARF1; ARF3; ARF4; ARFRP1; ARHGAP5; ARHGAP6; ARL1; ARL3; ARL6; ASB13; BCL3; BTK; CALCRL; CALM2; CARD10; CARHSP1; CD80; CDC42; CFL2; CHN2; CHUK; CNR2; CORO2A; CRK; CSK; DAPK1; DAPK3; DAPP1; DBN1; DFFA; DFFB; DUSP16; DUSP22; DUSP6; DUSP7; ECT2; FES; FPR1; GABBR1; GADD45B; GADD45G; GDI2; GNA13; GNAI3; GPS1; GTPBP2; HCK; HCLS1; HRH2; IFNAR1; IFNAR2; IGF1; IKBKG; INPP5D; INPPL1; IQGAP1; IRAK1; JAK1; JAK2; JAK3; KHDRBS1; LIMK1; LYN; MAP2K4; MAP3K3; MAP3K4; MAP4K1; MAP4K3; MAP4K4; MAP4K5; MAPK13; MAPK14; MAPK8; MAPK9; MAPKAPK2; MATK; MFHAS1; MKNK1; MRAS; MYO9A; NCF1; NMI; NOTCH2; NUDT4; PAK1; PDK1; PIAS1; PIK3C2A; PLCE1; PLCG2; PLEK; PPAP2A; PPP2R1B; PRDX4; PRKCB1; PRKCD; PRKCH; PRKCI; PSEN1; PTGER4; PTPN11; PTPN6; RAB10; RAB11A; RAB14; RAB24; RAB2B; RAB30; RAB31; RAB32; RAB33B; RAB5A; RAB6B; RAB7; RAC1; RALA; RALB; RAP1A; RAP1B; RAP2A; RASA1; RASGRP4; RASSF5; RGS19; RGS3; RNF14; ROCK1; ROCK2; RPS6KA2; RPS6KC1; RRAS2; RREB1; SDCBP; SHOC2; SIAH2; SLA; SLC9A3R2; SNX10; SNX2; SNX3; SNX4; SNX5; SNX6; SOCS4; SOCS5; SRI; STAT1; STAT3; STAT5A; STAT6; STK17B; STMN1; STMN3; SYK; TBK1; TEC; TGM2; TIAM1; TLK2; TLR1; TLR3; TLR4; TXK; TYK2; TYROBP; VAV1; VAV3; WASF2; XCR1; YWHAB; YWHAE; YWHAQ; YWHAZ; ZAP70; ZFYVE21
GO Biological Process	cell cycle	179	1702	ABL1; ACP2; AHR; AIF1; ANAPC11; ANLN; APC; ATM; AXIN1; AXL; BCL10; BCL3; BIRC5; BUB1; BUB3; CALM2; CCNA2; CCNB1; CCNB2; CCNC; CCND1; CCND2; CCNE2; CCNG1; CCNG2; CCNH; CCNI; CCNT2; CCT7; CD99L2; CDC16; CDC20; CDC25A; CDC25C; CDC37; CDC6; CDK2AP1; CDK4; CDK5; CDK5RAP1; CDK7; CDK8; CDKN1A; CENPE; CENPF; CETN2; CHEK1; CHFR; CKS1B; CKS2; CLK1; CRK; CRTAP; CSK; CSNK2A2; CTCF; CUL1; CUL3; CUL4A; CUL4B; DLEU2; DTYMK; DUSP1; DUSP6; DUT; E2F1; EIF2AK4; EIF4G2; ELK3; ERBB2IP; ETS2; FEN1; FRAP1; GMNN; GPS1; GSPT1; GTF2H1; HDAC5; HK2; HUS1; IGF1; INCENP; JAG2; JAK2; KATNA1; KHDRBS1; KIF11; KIF23; KIF2C; KPNA2; LIG1; LTBP2; LYN; MAD2L1; MAP2K6; MAP2K7; MAP3K8; MAPK1; MAPK13; MAPK6; MAPRE1; MATK; MCM2; MCM3; MCM4; MCM6; MKI67; MLH3; MVP; MYB; NAP1L1; NEDD9; NEK9; NFIX; NOLC1; NOTCH2; ORC4L; PA2G4; PCAF; PDGFA; POLB; POLD4; PPP2R1B; PPP3CB; PPP6C; PRC1; PSEN1; PSMD8; PTEN; PURA; RAB6IP1; RAD17; RAD51; RAD51L1; RAD51L3; RAD54L; RAP1A; RAP1B; RB1; RBBP4; RBBP6; RBBP8; RBL1; RBM5; RBMS1; REV3L; RFC1; RFC3; RFC4; RGS2; RPA3; RPS6KB2; RRM1; RRM2; SAP30; SIRT2; SKP2; SMARCB1; STAT1; STRN3; TARDBP; TCF19; TEP1; TFDP1; TGFB3; TLK2; TOB2; TOP1; TOP2A; TOP2B; TREX1; TTK; UBE2C; UBE2D1; UBE2D3; UBE2V1; UBE2V2; VAV1; YWHAQ
GO Biologi	defense response	134	1702	ABCF1; ADA; ADAR; AFP; AIF1; ALCAM; ALOX5AP; ANXA1; APAF1; APOE; ATP6V0A2; BCL6; BECN1; BMI1; BST1; C1QA; C1QB; C6; CCL22; CCR5; CCR9; CD14; CD48; CD5L; CD74; CD80; CD81; CD83; CD86; CD8A; CD96; CD97; CHUK; CNR2; CSF1R; CSF2RB; CTSC; CTSS; CXCL10; CXCL16; CXCL9; CXCR3; CYSLTR1; DPP4; DPP8; EBI3; ENTPD1; FCGR2B; FCGRT; FPR1; FTH1; GBP1; GBP2; GBP3;

cal Process				GZMA; HDAC5; HFE; HHEX; HRH2; HSPA1B; ICOS; IFI30; IFI35; IFIT1; IFIT2; IFITM3; IK; IKBKG; IL15; IL16; IL18; IL2RG; IL6ST; IRAK1; IRF4; IRF7; ITGB1; ITGB2; JAG2; KCNN4; KLRC1; LGALS3; LGALS3BP; LILRB3; LSP1; LST1; LY75; LY86; LY96; MAPK13; MAPK14; MAPRE2; MBP; MGLL; MNDA; MS4A1; MX1; MYD88; NCF1; NFKB1; NMI; NOTCH1; NR3C1; PLA2G7; POU2AF1; PRKRA; PROCR; PSMB8; PSMB9; PTGER4; RAC1; SAMHD1; SEMA4D; SOCS4; SOCS5; STAT3; STAT5A; TACSTD1; TAP1; TAP2; TAPBP; TCF7; TCIRG1; TLR1; TLR2; TLR3; TLR4; TNFRSF9; TPST1; TYROBP; XBP1; XCR1; YY1; ZAP70
GO Biological Process	**cell surface receptor linked signal transduction**	131	1702	ACVR1; ACVRL1; ANXA1; AP3S1; APC; ARL3; AXIN1; BAIAP2; BCL9; BIRC3; BRD8; CALCRL; CALM1; CALM2; CBL; CCR5; CCR9; CD14; CD8A; CD97; CENTD1; CENTD2; CERK; CNR2; CSF1R; CSNK1D; CSNK1G1; CSNK2A1; CSNK2A2; CTNNBIP1; CXCL10; CXCL9; CXCR3; CYSLTR1; DDR1; **DKK3**; EMR1; EPS15; EPS8; ERBB2IP; EVL; FLT1; FLT3; FNTA; FPR1; FZD7; GABBR1; GIT2; GNA13; GNAI3; GNB2; GNB4; GNG10; GNG12; GNG2; GPR124; GPR34; GPR35; GPR65; HOMER2; HRH2; IFNAR1; IFNAR2; IFNGR2; IL10RA; IL13RA1; IL6ST; ILK; IRAK1; ITGA4; ITGA8; ITGA9; ITGAE; ITGAV; ITGAX; ITGB1; ITGB2; JAG2; KIT; KLRC1; LANCL2; LIFR; LTBP2; LY96; MADD; MAP3K7; MAPK14; MERTK; MYD88; MYO9A; NEDD9; NOTCH2; NOTCH4; P2RY6; PDGFA; PDPK1; PLCE1; PLCG2; PPAP2A; PPP2R1B; PTGER1; PTGER2; PTGER4; PTPN6; PTPRE; PTPRJ; PXN; RAMP1; RASGRP4; RASSF3; RASSF5; RGS19; RGS2; RGS3; SHOC2; SNX6; SOCS5; SQSTM1; SYK; TCF7; TCF7L2; TGFBR1; TGFBR2; TGM2; TLE3; TRIM37; TRIO; TULP3; WASF2; XCR1; ZFYVE16
GO Biological Process	immune response	126	1702	ABCF1; ADA; ADAR; AFP; AIF1; ALCAM; ALOX5AP; ANXA1; APOE; ATP6V0A2; BCL6; BECN1; BMI1; BST1; C1QA; C1QB; C6; CCL22; CCR5; CCR9; CD14; CD5L; CD74; CD80; CD83; CD86; CD8A; CD96; CD97; CHUK; CNR2; CSF1R; CSF2RB; CTSC; CTSS; CXCL10; CXCL16; CXCL9; CXCR3; DPP4; DPP8; EBI3; ENTPD1; FCGR2B; FCGRT; FPR1; FTH1; GBP1; GBP2; GBP3; GZMA; HDAC5; HFE; HHEX; HRH2; HSPA1B; ICOS; IFI30; IFI35; IFIT1; IFIT2; IFITM3; IK; IKBKG; IL15; IL16; IL18; IL2RG; IL6ST; IRF4; IRF7; ITGB1; ITGB2; JAG2; KLRC1; LGALS3; LGALS3BP; LILRB3; LSP1; LST1; LY75; LY86; LY96; MAPK13; MAPK14; MAPRE2; MBP; MGLL; MNDA; MS4A1; MX1; MYD88; NCF1; NFKB1; NMI; NOTCH1; NR3C1; PLA2G7; POU2AF1; PRKRA; PROCR; PSMB8; PSMB9; PTGER4; RAC1; SAMHD1; SEMA4D; SOCS5; STAT3; STAT5A; TAP1; TAP2; TAPBP; TCF7; TCIRG1; TLR1; TLR2; TLR3; TLR4; TNFRSF9; TPST1; TYROBP; XBP1; XCR1; YY1; ZAP70
GO Biological Process	phosphorylation	123	1702	ABL1; ACVR1; ACVRL1; AXL; BTK; BUB1; CAMK1; CASK; CD80; CDK2AP1; CDK4; CDK5; CDK7; CDK8; CHEK1; CHUK; CLK1; CSF1R; CSK; CSNK1D; CSNK1G1; CSNK2A1; CSNK2A2; DAPK1; DAPK3; DDR1; DYRK1A; EIF2AK3; EIF2AK4; FES; FLT1; FLT3; GMFB; HCK; ILK; IRAK1; IRAK4; JAK1; JAK2; JAK3; KIT; LATS2; LIMK1; LYN; MAP2K1; MAP2K4; MAP2K5; MAP2K6; MAP2K7; MAP3K3; MAP3K4; MAP3K7; MAP3K8; MAP4K1; MAP4K3; MAP4K4; MAP4K5; MAPK1; MAPK13; MAPK14; MAPK6; MAPK8; MAPK9; MAPKAPK2; MATK; MELK; MERTK; MKNK1; NDUFB4; NDUFS4; NDUFS5; NDUFV1; NEK6; NEK7; NEK9; PAK1; PAK2; PDPK1; PFTK1; PIK3CD; PIM2; PIP5K1C; PKIB; PKIG; PLCE1; PMVK; PPP2R1B; PRDX4; PRKCB1; PRKCD; PRKCH; PRKCI; PRKRA; PRKX; PRPF4B; ROCK1; ROCK2; RPS6KA2; RPS6KB1; RPS6KB2; RPS6KC1; SAP30; SRPK2; STAT1; STK17B; STK3; STK39; SYK; TBK1; TEC; TGFBR1; TGFBR2; TLK2; TRIO; TRPM7; TTK; TXK; TYK2; UGP2; ULK1; UQCRB; VRK2; ZAP70
GO Biologi	morphogenesis	122	1702	ADAM23; ALDH3A2; ANPEP; APAF1; APOE; ATP2A2; ATP2C1; BAIAP2; BMI1; BTK; CD80; CD86; CDK5; CDK5RAP1; CHUK; CLN8; CRIM1; CRYAB; CSRP2; CUGBP2; CXCL10; DBN1; DGCR2; **DKK3**; DYRK1A; EBP; EGR2; EMD; ETS2; EVL; FABP5; FLI1; FLNB; FLT1; GJA1;

cal Process				GMFB; GNA13; GNPAT; GYPC; HCCS; HCK; HDAC5; HELLS; HHEX; HMGCR; IBSP; ID2; IGF1; IL18; IRF4; ITGAX; ITM2B; JAG2; JAK2; JAK3; KRT17; LARGE; LIG1; LIMK1; LRMP; LRRC1; MAFB; MAP4K1; MAPK14; MATK; MBP; MEF2A; MEF2C; MRAS; MTM1; MTPN; MYL6; MYOM1; NAB2; NAGLU; NOTCH1; NOTCH2; NOTCH4; NR2C2; NRP1; NUMB; OLFM1; OSTF1; PAFAH1B3; PAPSS1; PCNXL3; PDGFC; PES1; PHYH; PITPNM1; PLCE1; PPT1; RAC1; RASGRP4; RNF103; ROD1; RTN3; RTN4; SCMH1; SEMA4D; SEMA4F; SERPINF1; SGCB; SNCA; SOCS5; SRI; STAT3; STMN3; SYK; TGFB3; TLE3; TNFAIP2; TNNI2; TOP2B; TPD52; TPM1; TPM2; TPM3; TPM4; TRIM3; UBE3A; UFD1L
GO Biological Process	regulation of cell cycle	107	1702	ABL1; ACP2; AIF1; ANAPC11; ANLN; APC; ATM; AXIN1; AXL; BCL10; BCL3; BUB1; BUB3; CCNA2; CCNB1; CCNB2; CCNC; CCND1; CCND2; CCNE2; CCNG1; CCNG2; CCNH; CCNI; CCNT2; CCT7; CDC16; CDC20; CDC25A; CDC25C; CDC37; CDC6; CDK2AP1; CDK4; CDK5RAP1; CDK7; CDK8; CDKN1A; CENPF; CHEK1; CHFR; CKS1B; CKS2; CLK1; CRK; CSK; CSNK2A2; CTCF; CUL1; CUL3; CUL4A; DLEU2; DUSP6; E2F1; EIF4G2; ELK3; ETS2; FRAP1; GMNN; GSPT1; GTF2H1; HDAC5; HK2; HUS1; JAK2; KHDRBS1; LTBP2; LYN; MAD2L1; MAP2K6; MAP2K7; MAP3K8; MAPRE1; MATK; MKI67; MYB; NEDD9; NOTCH2; PA2G4; PCAF; PDGFA; PPP2R1B; PPP3CB; PSMD8; PTEN; RAD17; RAP1A; RAP1B; RB1; RBBP6; RBBP8; RBL1; RBM5; RPS6KB2; SKP2; SMARCB1; STAT1; TCF19; TFDP1; TGFB3; TOB2; TTK; UBE2C; UBE2V1; UBE2V2; VAV1; YWHAQ
GO Biological Process	intracellular protein transport	101	1702	AP1G1; AP1GBP1; AP1S2; AP3B1; AP3D1; AP3M1; AP3S1; AP3S2; APPBP2; ARF1; ARF3; ARF4; ARFGAP3; BCL3; CDC37; CLTA; CLTB; CLTC; COPZ2; CROT; DEK; DSCR3; DUSP16; FXC1; GABARAPL2; GRPEL1; ICMT; IPO7; KIF20A; KLHL2; KPNA1; KPNA2; KPNA3; KPNB1; LPL; LTBP2; M6PR; MTX2; MXI1; NFKBIE; NSF; NUP50; NUTF2; PEX13; PEX6; PEX7; PPIH; PRNP; PTTG1IP; RAB10; RAB11A; RAB14; RAB24; RAB2B; RAB30; RAB33B; RAB5A; RAB6B; RAB7; RABIF; RANBP2; RPL23; RRBP1; SCAMP1; SCAMP2; SDCBP; SEC23A; SEC24B; SEC24C; SEC24D; SEC63; SNAP23; SNX10; SNX2; SNX3; SNX4; SNX5; SNX6; SRP14; SSR2; SSR4; STAM2; STX12; STX17; STX18; STX5A; STX6; STX7; STX8; TAP2; TIMM17B; TIMM22; TPR; TRAM1; TRNT1; TSG101; VPS18; VPS35; XPO1; XPO7; ZFYVE16
GO Biological Process	mitotic cell cycle	96	1702	ABL1; ANAPC11; ANLN; BIRC5; BUB1; BUB3; CCNA2; CCNB1; CCNB2; CCND1; CCNE2; CCNG1; CCNG2; CCNH; CCNT2; CD99L2; CDC16; CDC20; CDC25A; CDC25C; CDC37; CDC6; CDK2AP1; CDK4; CDK5RAP1; CDK7; CDKN1A; CENPE; CENPF; CETN2; CHEK1; CHFR; CKS1B; CKS2; CUL1; CUL3; CUL4A; DUT; E2F1; EIF2AK4; FEN1; GMNN; GSPT1; GTF2H1; IGF1; INCENP; KATNA1; KHDRBS1; KIF11; KIF23; KIF2C; KPNA2; LIG1; MAD2L1; MCM2; MCM3; MCM4; MCM6; MLH3; MVP; NAP1L1; NEDD9; NEK9; NFIX; NOLC1; ORC4L; POLB; POLD4; PPP2R1B; PPP6C; PRC1; PTEN; PURA; RAB6IP1; RAD17; RBBP4; RBMS1; REV3L; RFC1; RFC3; RFC4; RPA3; RRM1; RRM2; SAP30; SIRT2; SKP2; TARDBP; TOP1; TOP2A; TOP2B; TREX1; TTK; UBE2C; UBE2D1; UBE2D3
GO Biological Process	cell death	95	1702	ABL1; AHR; APAF1; API5; APOE; APP; AXIN1; BAD; BAG5; BCL10; BCL2L11; BECN1; BFAR; BID; BIRC3; BIRC5; BIRC6; BNIP2; BNIP3L; BTK; C6; CARD10; CASP2; CASP3; CASP6; CASP7; CASP8AP2; CASP9; CD14; CD38; CD5L; CDKN1A; CFLAR; CUL1; CUL3; CUL4A; CYCS; DAPK1; DAPK3; DFFA; DFFB; DNASE1L3; DUSP22; DUSP6; E2F1; EIF4G2; FAIM; FEM1B; FGL2; FXR1; GADD45B; GADD45G; GLRX2; GPR65; GZMA; GZMB; IKBKG; IL18; LIMS1; LY86; MAPK1; MCL1; MOAP1; MX1; NFKB1; NOTCH2; PAK1; PDCD6IP; PDCD7; PDE1B; PMAIP1; PPP2R1B; PRDX2; PSEN1; PTPN6; RNF7; RTN4; SEMA4D; SGPL1; SH3GLB1; SNCA; SON; STAT1; STK17B; STK3; TAX1BP1; TGM2; TIA1; TIAL1; TNFRSF1A; TNFRSF21; TNFRSF9; TRAF3; TRAF5; VDAC1

GO Biological Process	lipid metabolism	95	1702	ACAA2; ACADL; ACADVL; ACAT1; ACOX1; AGPAT3; ALDH3A2; ALDH3B1; ALOX5AP; ANXA1; APOE; ASAH1; ASAH2; B4GALT4; B4GALT6; CD36; CERK; CHPT1; CPNE1; CPNE3; CROT; CRYL1; DDHD1; DPAGT1; EBP; EHHADH; FABP5; FADS1; GALC; GBA; GM2A; GNPAT; GPD1; GPD2; GPX4; GRN; HADHB; HEXA; HEXB; HMGCR; HMGCS1; HPGD; HSD17B4; HSD3B7; IDI1; IMPA1; LARGE; LIPA; LPL; LYPLA3; MGLL; MGST1; NDUFAB1; NSMAF; OSBPL11; OSBPL9; PAFAH1B2; PAFAH1B3; PCCA; PHYH; PIGC; PIGF; PIGH; PIK3C2A; PITPNM1; PLA2G4A; PLA2G7; PLCE1; PLCG2; PMVK; PPAP2A; PPAP2B; PPARG; PPP2R1B; PRKAG2; PSAP; PTDSS1; PTGIS; PTGS1; SC4MOL; SCP2; SGPL1; SOAT1; SPTLC1; SQLE; SREBF2; STARD3; STARD4; STARD5; SULT1A1; TBXAS1; TMPO; TPI1; UGCGL1; UGT1A1
GO Biological Process	death	95	1702	ABL1; AHR; APAF1; API5; APOE; APP; AXIN1; BAD; BAG5; BCL10; BCL2L11; BECN1; BFAR; BID; BIRC3; BIRC5; BIRC6; BNIP2; BNIP3L; BTK; C6; CARD10; CASP2; CASP3; CASP6; CASP7; CASP8AP2; CASP9; CD14; CD38; CD5L; CDKN1A; CFLAR; CUL1; CUL3; CUL4A; CYCS; DAPK1; DAPK3; DFFA; DFFB; DNASE1L3; DUSP22; DUSP6; E2F1; EIF4G2; FAIM; FEM1B; FGL2; FXR1; GADD45B; GADD45G; GLRX2; GPR65; GZMA; GZMB; IKBKG; IL18; LIMS1; LY86; MAPK1; MCL1; MOAP1; MX1; NFKB1; NOTCH2; PAK1; PDCD6IP; PDCD7; PDE1B; PMAIP1; PPP2R1B; PRDX2; PSEN1; PTPN6; RNF7; RTN4; SEMA4D; SGPL1; SH3GLB1; SNCA; SON; STAT1; STK17B; STK3; TAX1BP1; TGM2; TIA1; TIAL1; TNFRSF1A; TNFRSF21; TNFRSF9; TRAF3; TRAF5; VDAC1
GO Biological Process	apoptosis	91	1702	ABL1; AHR; APAF1; API5; APOE; APP; AXIN1; BAD; BAG5; BCL10; BCL2L11; BECN1; BFAR; BID; BIRC3; BIRC5; BIRC6; BNIP2; BNIP3L; BTK; CARD10; CASP2; CASP3; CASP6; CASP7; CASP8AP2; CASP9; CD14; CD38; CD5L; CDKN1A; CFLAR; CUL1; CUL3; CUL4A; CYCS; DAPK1; DAPK3; DFFA; DFFB; DNASE1L3; DUSP22; DUSP6; E2F1; FAIM; FEM1B; FXR1; GADD45B; GADD45G; GLRX2; GPR65; GZMA; GZMB; IKBKG; IL18; LY86; MAPK1; MCL1; MOAP1; MX1; NFKB1; NOTCH2; PAK1; PDCD6IP; PDCD7; PDE1B; PMAIP1; PPP2R1B; PRDX2; PSEN1; PTPN6; RNF7; RTN4; SEMA4D; SGPL1; SH3GLB1; SNCA; SON; STAT1; STK17B; STK3; TAX1BP1; TGM2; TIA1; TIAL1; TNFRSF1A; TNFRSF21; TNFRSF9; TRAF3; TRAF5; VDAC1
GO Biological Process	programmed cell death	91	1702	ABL1; AHR; APAF1; API5; APOE; APP; AXIN1; BAD; BAG5; BCL10; BCL2L11; BECN1; BFAR; BID; BIRC3; BIRC5; BIRC6; BNIP2; BNIP3L; BTK; CARD10; CASP2; CASP3; CASP6; CASP7; CASP8AP2; CASP9; CD14; CD38; CD5L; CDKN1A; CFLAR; CUL1; CUL3; CUL4A; CYCS; DAPK1; DAPK3; DFFA; DFFB; DNASE1L3; DUSP22; DUSP6; E2F1; FAIM; FEM1B; FXR1; GADD45B; GADD45G; GLRX2; GPR65; GZMA; GZMB; IKBKG; IL18; LY86; MAPK1; MCL1; MOAP1; MX1; NFKB1; NOTCH2; PAK1; PDCD6IP; PDCD7; PDE1B; PMAIP1; PPP2R1B; PRDX2; PSEN1; PTPN6; RNF7; RTN4; SEMA4D; SGPL1; SH3GLB1; SNCA; SON; STAT1; STK17B; STK3; TAX1BP1; TGM2; TIA1; TIAL1; TNFRSF1A; TNFRSF21; TNFRSF9; TRAF3; TRAF5; VDAC1
GO Biological Process	response to pest/pathogen/parasite	81	1702	ABCF1; ADA; ADAR; AIF1; ALCAM; ALOX5AP; ANXA1; BCL6; BECN1; BMI1; BST1; C1QA; C1QB; C6; CCL22; CCR5; CCR9; CD14; CD5L; CD80; CD83; CD86; CD8A; CD97; CSF1R; CSF2RB; CXCL10; CXCL9; CXCR3; EBI3; ENTPD1; FPR1; HDAC5; HHEX; HSPA1B; IFI44; IFNAR1; IFNAR2; IFNGR2; IL18; IRF4; IRF7; ITGB1; ITGB2; KLRC1; LGALS3; LGALS3BP; LSP1; LST1; LY75; LY86; LY96; MAPK13; MAPK14; MAPRE2; MGLL; MNDA; MYD88; NCF1; NFKB1; NMI; NR3C1; PLA2G7; POU2AF1; PROCR; RAC1; SAMHD1; SLC11A1; STAT1; STAT3; TAP1; TAP2; TCIRG1; TLR1; TLR2; TLR3; TLR4; TPST1; TYROBP; XCR1; YY1

GO Biological Process	cell motility	69	1702	AAMP; ACTB; ANXA1; APOE; ARPC4; ARPC5; ATP2A2; CABP4; CACNA1S; CAPZA1; CAPZA2; CD2AP; CD97; CHRNB1; CKB; CNN3; CRK; CRYAB; CXCL10; CXCR3; EMD; EVL; FKBP1B; FLII; FPR1; GJA1; GNA13; HMGCR; HMMR; IGF1; JAG2; JAK2; LIMK1; LSP1; MAP2K1; MAPK14; MAPK8; MARCKS; MKLN1; MYO6; MYOM1; NRP1; PAFAH1B2; PLCE1; PPAP2A; PPAP2B; PPAP2C; PXN; RAC1; RNF121; ROCK2; RTN3; RTN4; RYR1; SDCBP; SEMA4F; SERPINE2; SLC8A1; SLMAP; SPINT2; SRI; STAT3; STRBP; TNNI2; TPM1; TPM2; TPM3; VASP; WASL
GO Biological Process	ion transport	60	1702	ASNA1; ATOX1; ATP11A; ATP11B; ATP1B1; ATP2A2; ATP2C1; ATP5A1; ATP5C1; ATP5E; ATP6V0A2; ATP6V0B; ATP6V0D1; ATP6V1A; ATP6V1B2; ATP6V1C1; ATP6V1D; ATP6V1H; ATP7A; ATP8A1; CACNA1S; CACNB3; CHRNB1; CLCN3; CLIC4; FTH1; HFE; ITPR1; ITPR2; KCNJ10; KCNN4; NDUFA9; NEDD4L; NNT; P2RX4; PLP2; RYR1; SFXN2; SLC11A1; SLC12A2; SLC13A3; SLC1A5; SLC22A5; SLC30A4; SLC30A5; SLC30A7; SLC31A1; SLC31A2; SLC41A1; SLC4A1; SLC4A7; SLC8A1; TCIRG1; TMEM1; TNFAIP1; TRPM7; TRPV2; UCP2; VDAC1; VDAC3
GO Biological Process	cell adhesion	58	1702	AIM1; ALCAM; APC; APP; ARHGAP5; ATP2A2; CASK; CD36; CD44; CD5; CD9; CD96; CD97; CLDN1; CTNNA1; CXCR3; DDR1; DGCR2; EMR1; ENTPD1; ERBB2IP; FXC1; GALNT1; IBSP; ICAM1; IL18; ILK; ITGA4; ITGA8; ITGA9; ITGAE; ITGAV; ITGAX; ITGB1; ITGB2; KLRC1; LGALS3; LMAN1; LY75; MKLN1; MRC1; NEDD9; NRP1; PLXNC1; PNN; PPP2R1B; PTPRS; PXN; RAC1; SCARB1; SCARB2; SEMA4D; TGFBI; TMEM8; VCAM1; VCL; VWF; ZYX
GO Biological Process	protein kinase cascade	54	1702	ADAM9; BCL3; CARD10; CHUK; DAPK1; DAPK3; DBN1; DUSP16; DUSP22; DUSP6; DUSP7; FPR1; GADD45B; GADD45G; GNA13; GPS1; IFNAR1; IFNAR2; IKBKG; IRAK1; JAK2; MAP2K4; MAP3K3; MAP3K4; MAP4K1; MAP4K3; MAP4K4; MAP4K5; MAPK13; MAPK14; MAPK8; MAPK9; MAPKAPK2; MKNK1; NMI; PAK1; PIAS1; PLCE1; PPP2R1B; PRDX4; RGS3; RPS6KA2; SOCS4; SOCS5; STAT1; STAT3; STAT5A; STK17B; TBK1; TEC; TLR1; TLR3; TLR4; ZAP70
GO Biological Process	small GTPase mediated signal transduction	54	1702	ABR; ARF1; ARF3; ARF4; ARFRP1; ARHGAP5; ARHGAP6; ARL1; ARL3; ARL6; CDC42; CFL2; GDI2; GNA13; GNAI3; GTPBP2; IGF1; IQGAP1; KHDRBS1; LIMK1; MFHAS1; MRAS; NOTCH2; PDK1; PLCE1; RAB10; RAB11A; RAB14; RAB24; RAB2B; RAB30; RAB31; RAB32; RAB33B; RAB5A; RAB6B; RAB7; RAC1; RALA; RALB; RAP1A; RAP1B; RAP2A; RASGRP4; RGS19; ROCK1; RRAS2; RREB1; SHOC2; SIAH2; VAV3; YWHAB; YWHAQ; YWHAZ

GO Biological Process	G-protein coupled receptor protein signaling pathway	53	1702	ARL3; CALCRL; CALM1; CALM2; CCR5; CCR9; CD97; CENTD1; CENTD2; CERK; CNR2; CXCL9; CXCR3; CYSLTR1; EMR1; FPR1; FZD7; GABBR1; GIT2; GNA13; GNAI3; GNB2; GNB4; GNG10; GNG12; GNG2; GPR124; GPR34; GPR35; GPR65; HOMER2; HRH2; LANCL2; MYO9A; P2RY6; PLCE1; PPAP2A; PTGER1; PTGER2; PTGER4; PTPN6; RAMP1; RASGRP4; RASSF3; RASSF5; RGS19; RGS2; RGS3; SYK; TGM2; TULP3; WASF2; XCR1
GO Biological Process	regulation of biological process	52	1702	AIF1; BCL6; BTG2; CD86; CDC6; CDKN1A; CHEK1; CHPT1; CRIM1; CTBP2; CUL1; CUL3; CUL4A; CXCL10; DLG3; FLT1; FLT3; FTH1; GLRX2; GRN; IGF1; IL15; IL18; JAG2; MATK; MDM2; MDM4; MXI1; NAP1L1; NEDD9; NOTCH2; NRP1; PCAF; PLCE1; PPAP2A; PPP2R1B; PRKRA; PRKRIR; PTPN6; RBBP4; SOCS4; SOCS5; TBC1D8; TCIRG1; TGFBR2; TNFRSF9; TNIP2; TOB2; TSG101; TTK; TXNDC4; UBE2C
GO Biological Process	regulation of apoptosis	52	1702	ABL1; API5; APOE; BAD; BCL10; BCL2L11; BECN1; BFAR; BID; BIRC3; BIRC5; BIRC6; BNIP2; BNIP3L; BTK; CASP2; CASP3; CASP6; CASP8AP2; CD38; CDKN1A; CFLAR; CUL1; CUL3; CUL4A; CYCS; DAPK1; DAPK3; FEM1B; IKBKG; IL18; MAPK1; MCL1; MX1; NFKB1; NOTCH2; PMAIP1; PPP2R1B; PRDX2; PSEN1; RNF7; RTN4; SEMA4D; SNCA; SON; STK17B; TAX1BP1; TGM2; TIA1; TIAL1; TNFRSF9; TRAF3
GO Biological Process	response to wounding	52	1702	ABCF1; AIF1; ALOX5AP; ANXA1; BCL6; BECN1; CCL22; CCR5; CCR9; CD14; CD5L; CD80; CD86; CD8A; CD97; CXCL10; CXCL9; EBI3; FPR1; HDAC5; IL18; IRF4; IRF7; ITGB1; LGALS3; LGALS3BP; LSP1; LST1; LY75; LY86; LY96; MAPRE2; MGLL; MNDA; MYD88; NCF1; NFKB1; NMI; NR3C1; PLA2G7; PROCR; RAC1; TAP1; TAP2; TCIRG1; TLR1; TLR2; TLR3; TLR4; TPST1; TYROBP; XCR1
GO Biological Process	response to endogenous stimulus	47	1702	ABL1; ATM; ATRX; BTG2; CCNH; CDK7; CHEK1; CSNK1D; DCLRE1A; DDB2; FEN1; FRAP1; GADD45G; GTF2H1; GTF2H2; HUS1; IRF7; LIG1; MAP2K6; MBD4; MLH3; NUDT1; POLB; POLK; RAD17; RAD23A; RAD23B; RAD51; RAD51L1; RAD51L3; RAD54L; RBBP4; RBBP8; RECQL; REV3L; RFC1; RPA3; TDG; TDP1; TLK2; TREX1; UBE2A; UBE2B; UBE2C; UBE2V1; UBE2V2; XRN2

GO Biological Process	protein amino acid dephosphorylation	36	1702	ACP1; CDC25A; CDC25C; CTDP1; DUSP1; DUSP11; DUSP16; DUSP19; DUSP22; DUSP6; DUSP7; ILKAP; KIT; MTM1; MTMR1; MTMR4; MTMR6; PPEF2; PPM1A; PPM1B; PPP2R1B; PPP2R2A; PPP2R4; PPP3CA; PPP3CB; PPP6C; PTEN; PTP4A1; PTPLA; PTPN11; PTPN2; PTPN6; PTPN9; PTPRE; PTPRJ; PTPRS
GO Biological Process	positive regulation of programmed cell death	35	1702	ABL1; APOE; BAD; BCL10; BCL2L11; BID; BNIP3L; BTK; CASP2; CASP3; CASP6; CASP8AP2; CD38; CDKN1A; CFLAR; CUL1; CUL3; CUL4A; CYCS; DAPK1; DAPK3; FEM1B; IKBKG; IL18; MAPK1; MX1; NOTCH2; PMAIP1; PPP2R1B; RNF7; STK17B; TIA1; TIAL1; TNFRSF9; TRAF3
GO Biological Process	regulation of programmed cell death	35	1702	ABL1; APOE; BAD; BCL10; BCL2L11; BID; BNIP3L; BTK; CASP2; CASP3; CASP6; CASP8AP2; CD38; CDKN1A; CFLAR; CUL1; CUL3; CUL4A; CYCS; DAPK1; DAPK3; FEM1B; IKBKG; IL18; MAPK1; MX1; NOTCH2; PMAIP1; PPP2R1B; RNF7; STK17B; TIA1; TIAL1; TNFRSF9; TRAF3
GO Biological Process	induction of apoptosis	35	1702	ABL1; APOE; BAD; BCL10; BCL2L11; BID; BNIP3L; BTK; CASP2; CASP3; CASP6; CASP8AP2; CD38; CDKN1A; CFLAR; CUL1; CUL3; CUL4A; CYCS; DAPK1; DAPK3; FEM1B; IKBKG; IL18; MAPK1; MX1; NOTCH2; PMAIP1; PPP2R1B; RNF7; STK17B; TIA1; TIAL1; TNFRSF9; TRAF3
GO Biological Process	positive regualtion of apoptosis	35	1702	ABL1; APOE; BAD; BCL10; BCL2L11; BID; BNIP3L; BTK; CASP2; CASP3; CASP6; CASP8AP2; CD38; CDKN1A; CFLAR; CUL1; CUL3; CUL4A; CYCS; DAPK1; DAPK3; FEM1B; IKBKG; IL18; MAPK1; MX1; NOTCH2; PMAIP1; PPP2R1B; RNF7; STK17B; TIA1; TIAL1; TNFRSF9; TRAF3

GO Biological Process	inflammatory response	32	1702	ABCF1; AIF1; ALOX5AP; ANXA1; BCL6; CCL22; CCR5; CD14; CD97; CXCL10; CXCL9; FPR1; HDAC5; IRF7; LGALS3; LY75; LY86; LY96; MGLL; MYD88; NFKB1; NMI; NR3C1; PLA2G7; PROCR; RAC1; TLR1; TLR2; TLR3; TLR4; TPST1; XCR1
GO Biological Process	innate immune response	32	1702	ABCF1; AIF1; ALOX5AP; ANXA1; BCL6; CCL22; CCR5; CD14; CD97; CXCL10; CXCL9; FPR1; HDAC5; IRF7; LGALS3; LY75; LY86; LY96; MGLL; MYD88; NFKB1; NMI; NR3C1; PLA2G7; PROCR; RAC1; TLR1; TLR2; TLR3; TLR4; TPST1; XCR1
GO Biological Process	enzyme linked receptor protein signaling pathway	31	1702	ACVR1; ACVRL1; AP3S1; BAIAP2; CD8A; CSF1R; DDR1; EPS15; EPS8; ERBB2IP; FLT1; FLT3; FNTA; IRAK1; KIT; LTBP2; MAP3K7; PDPK1; PLCE1; PTPRE; PTPRJ; PXN; RASGRP4; SHOC2; SNX6; SQSTM1; SYK; TGFBR1; TGFBR2; TRIO; ZFYVE16
GO Biological Process	humoral immune response	30	1702	ADA; ADAR; ALCAM; BMI1; BST1; C1QA; C1QB; C6; CCL22; CD83; CD86; CSF1R; CSF2RB; CXCR3; EBI3; ENTPD1; HHEX; HSPA1B; IL18; IRF4; ITGB2; KLRC1; LY86; LY96; MAPK13; MAPK14; NFKB1; POU2AF1; XCR1; YY1
GO Biological Process	antimicrobial humoral response	17	1702	ADA; ADAR; ALCAM; CCL22; CSF1R; CSF2RB; CXCR3; ENTPD1; HHEX; ITGB2; KLRC1; LY96; MAPK13; MAPK14; NFKB1; XCR1; YY1

GO Biological Process	chemotaxis	16	1702	CCL22; CCR5; CCR9; CKLF; CXCL10; CXCL16; CXCL9; CXCR3; FPR1; IL16; MAN1A2; MAP2K1; MAPK1; MAPK14; RALA; XCR1
GO Biological Process	second-messenger-mediated signaling	14	1702	CALCRL; CALM2; CNR2; FPR1; GABBR1; GNAI3; HRH2; NUDT4; PLCE1; PPP2R1B; PTGER4; TGM2; WASF2; XCR1
GO Biological Process	Wnt receptor signaling pathway	14	1702	APC; AXIN1; BCL9; CSNK1D; CSNK1G1; CSNK2A1; CSNK2A2; CTNNBIP1; **DKK3**; FZD7; PPP2R1B; TCF7; TCF7L2; TLE3
GO Biological Process	cell-cell adhesion	14	1702	AIM1; CD44; DGCR2; GALNT1; ICAM1; ITGA8; ITGAE; ITGB1; KLRC1; LGALS3; LMAN1; LY75; MRC1; VCAM1
GO Biological Process	embryogenesis and morphogenesis	14	1702	AK2; CAMTA2; CST3; CUL1; **DKK3**; HIST1H2AB; HIST1H2AD; HIST1H2AE; HIST1H3D; HIST3H2A; PSME4; SCMH1; SMARCC1; TPD52

GO Biological Process	cell migration	14	1702	APOE; CD2AP; EVL; HMGCR; JAG2; NRP1; PPAP2A; PPAP2B; PPAP2C; RTN3; RTN4; SDCBP; SEMA4F; SERPINE2
GO Biological Process	negative regulation of cell cycle	14	1702	APC; ATM; AXIN1; BCL10; CDK2AP1; CDK5RAP1; CTCF; DLEU2; PTEN; RAP1A; RB1; RBL1; RBM5; SMARCB1
GO Biological Process	apoptotic program	12	1702	BAD; BID; CASP2; CASP7; CASP9; CYCS; DFFA; DFFB; MCL1; SH3GLB1; STAT1; VDAC1
GO Biological Process	hemopoiesis	11	1702	CD80; CD86; HDAC5; IRF4; JAG2; LRMP; MAP4K1; NOTCH2; NOTCH4; RASGRP4; SOCS5
GO Biological Process	immune cell activation	11	1702	CD80; CD86; CD8A; HDAC5; IL18; IRF4; JAG2; MS4A1; SOCS5; TLR1; TLR4

GO Biological Process	lymphocyte activation	9	1702	CD80; CD86; CD8A; HDAC5; IL18; IRF4; JAG2; MS4A1; SOCS5
GO Biological Process	pathogenesis	8	1702	CCR5; GLIPR1; IFI44; MX1; SNCA; TTC3; UBE2D1; UBE2D3
GO Biological Process	secretion	7	1702	ARFGAP3; CANX; LTBP2; PLDN; RAB14; TNFAIP2; UNC93B1
GO Biological Process	induction of apoptosis by extracellular signals	7	1702	BID; BTK; CASP8AP2; CD38; CFLAR; DAPK1; IL18
GO Biological Process	inactivation of MAPK	7	1702	DUSP16; DUSP22; DUSP6; DUSP7; GPS1; PPP2R1B; RGS3

GO Biological Process	T-cell activation	7	1702	CD80; CD86; CD8A; IL18; IRF4; JAG2; SOCS5
GO Biological Process	cytokine biosynthesis	7	1702	CD80; CD86; IL18; IRF4; TLR1; TLR3; TLR4
GO Biological Process	cytokine metabolism	7	1702	CD80; CD86; IL18; IRF4; TLR1; TLR3; TLR4
GO Biological Process	TGFbeta receptor signaling pathway	7	1702	ACVRL1; FNTA; LTBP2; MAP3K7; TGFBR1; TGFBR2; ZFYVE16
GO Biological Process	induction of apoptosis by intracellular signals	6	1702	ABL1; CDKN1A; CUL1; CUL3; CUL4A; RNF7

GO Biological Process	cAMP-mediated signaling	6	1702	FPR1; GABBR1; GNAI3; PTGER4; TGM2; WASF2
GO Biological Process	lymphocyte differentiation	6	1702	CD80; CD86; HDAC5; IRF4; JAG2; SOCS5
GO Biological Process	regulation of cytokine biosynthesis	6	1702	CD80; CD86; IRF4; TLR1; TLR3; TLR4
GO Biological Process	protein ubiquitination	6	1702	FBXO4; NEDD4L; TGM2; TRIP12; UBE2V1; UBE2V2
GO Biological Process	embryonic development	5	1702	BMI1; JAG2; KIF1B; LRRC1; NOTCH4

GO Biological Process	T-cell differentiation	5	1702	CD80; CD86; IRF4; JAG2; SOCS5
GO Biological Process	frizzled signaling pathway	3	1702	AXIN1; FZD7; TLE3
GO Molecular Function	**signal transducer activity**	274	1716	ACVR1; ACVRL1; ADAM23; ADAM9; ADFP; AHR; AKAP9; ALCAM; ANPEP; ANXA1; APOE; ARF1; ARHGAP6; ARL3; AXIN1; AXL; BAIAP2; BID; BRD8; CALCRL; CARD10; CARHSP1; CBL; CCL22; CCR5; CCR9; CD14; CD163; CD36; CD44; CD5; CD5L; CD74; CD80; CD86; CD8A; CD97; CDK2AP1; CHD6; CHN2; CHRNB1; CHUK; CKLF; CNOT7; CNR2; CRIM1; CRK; CRLF2; CRLF3; CRTAP; CSF1R; CSF2RA; CSF2RB; CXCL10; CXCL16; CXCL9; CXCR3; CYSLTR1; DBI; DDR1; DGCR2; **DKK3**; DUSP1; EBI3; EBP; EEF1E1; EMR1; ENSA; EPS8; ERBB2IP; EVI2A; EXTL3; FCGR2B; FCGRT; FEM1B; FGL2; FKBP1A; FLT1; FLT3; FPR1; FZD7; GABARAPL1; GABBR1; GLG1; GMFB; GNA13; GNAI3; GNB2; GNB4; GNG10; GNG12; GNG2; GPR124; GPR34; GPR35; GPR65; GPRC5B; GRINL1A; GRN; HABP4; HAVCR2; HFE; HIF1A; HMGN3; HOMER2; HRH2; ICAM1; IFITM3; IFNAR1; IFNAR2; IFNGR2; IGF1; IGF2R; IK; IKBKG; IL10RA; IL13RA1; IL15; IL15RA; IL16; IL18; IL1RAP; IL2RG; IL6ST; INSL3; IRAK1; IRAK4; ITGA4; ITGA8; ITGA9; ITGAE; ITGAV; ITGAX; ITGB1; ITGB2; ITPR1; ITPR2; ITSN2; JAG2; JAK1; JAK2; JAK3; KIT; KLRC1; LANCL2; LASP1; LGALS3BP; LIFR; LILRB3; LSP1; LY75; LY86; LY96; LYN; M6PR; MADD; MAN1A2; MAP2K7; MAP3K3; MAP3K4; MAP3K7; MAPK1; MAPK13; MAPK14; MAPK6; MAPK8; MAPK9; MAPKAPK2; MERTK; MRC1; MS4A1; MYD88; NCOA1; NCOA3; NEDD9; NOTCH1; NOTCH2; NOTCH4; NR2C2; NR3C1; NRP1; NSMAF; OLFM1; P2RX4; P2RY6; PDCL; PDE8A; PDGFA; PDGFC; PEX11A; PEX7; PLCE1; PLCG2; PLRG1; PLXNB2; PLXNC1; PPARG; PPFIA4; PRKCB1; PRKCD; PRKCH; PRKCI; PRKRA; PROCR; PTGER1; PTGER2; PTGER4; PTPN6; PTPN9; PTPRE; PTPRJ; PTPRS; PTTG1IP; PVR; RAMP1; RGS10; RGS18; RGS19; RGS2; RGS3; RNF121; RRBP1; RTN1; RXRA; RYR1; SCARB1; SCARB2; SDCBP; SEMA4D; SEMA4F; SH3BGRL; SLA; SLC1A5; SRI; SSR4; STAM2; STAT1; STAT3; STAT5A; STAT6; STK39; STMN1; SYK; TACSTD1; TAP2; TAPBP; TGFB3; TGFBI; TGFBR1; TGFBR2; TIAM1; TLR1; TLR2; TLR3; TLR4; TNFRSF1A; TNFRSF21; TNFRSF9; TOB2; TOMM70A; TRAF3; TRAM1; TRIP12; TRIP13; TRIP6; TRPV2; TYK2; TYROBP; VAV3; WASF2; WBP1; XCR1; XPO7; ZYX
GO Molecul	transcription	174	1716	ADNP; AHR; ATF1; ATF2; ATF3; ATF6; ATF7IP; ATRX; BACH1; BAZ1B; BAZ2A; BCL11A; BCL3; BCL6; BRD8; BTG2; CAMTA2; CBFA2T3; CBFB; CBL; CD80; CD86; CEBPG; CITED2; CNOT2; CNOT7; CNOT8; CREB3; CREM; CTCF; DEK; DMTF1; DR1; E2F1; EED; EGR1; ELF1; ELK3; EPC1; ETS2; ETV3; ETV6; FLI1; FUS; GABPA; GABPB1; GTF2A1; GTF2B; GTF2E2; GTF2F2; GTF2H1; GTF2I; GTF3C4; HCLS1;

ar Function	regulator activity			HDAC2; HDAC5; HHEX; HIF1A; HMGN3; HSBP1; ID3; IER5; IRAK1; IRF3; IRF4; IRF5; IRF6; IRF7; KLF3; LITAF; LMO2; LRRFIP1; MEF2A; MEF2C; MITF; MRPS25; MXI1; MYB; MYCBP; MYCL1; MYNN; NAB2; NCOA1; NCOA3; NFAT5; NFATC1; NFIX; NFKB1; NFKB2; NFYA; NFYB; NMI; NOTCH2; NR2C2; NR3C1; PCAF; PIAS1; PKNOX1; PLAGL2; PLRG1; PML; POLR3K; POU2AF1; PPARG; PURA; RB1; RELB; RERE; RFX5; RFXAP; RNF12; RNF14; RREB1; RUNX1; RXRA; SALL2; SAP30; SCMH1; SF1; SIAH2; SIN3B; SMARCA5; SMARCB1; SMARCC1; SMARCE1; SOLH; SPIB; SQSTM1; SREBF2; SRF; SSBP3; STAT1; STAT3; STAT5A; STAT6; SUPT4H1; TAF13; TAF1B; TAF7; TAF9; TARDBP; TBPL1; TCEA1; TCEB1; TCEB3; TCERG1; TCF19; TCF4; TCF7; TFDP1; TIAL1; TRIM32; TRIM33; TRIP13; TSG101; TTF1; UBE2V1; UBP1; UBTF; UBXD2; UGP2; UTX; VAV1; XBP1; YAF2; YY1; ZDHHC14; ZDHHC2; ZDHHC3; ZDHHC6; ZDHHC9; ZFP36L1; ZFX; ZNRD1
GO Molecular Function	kinase activity	169	1716	ABL1; ACVR1; ACVRL1; ADK; AK2; AK3; ATM; AXL; BAIAP2; BTK; BUB1; CALM2; CAMK1; CASK; CDK4; CDK5; CDK7; CDK8; CDKN1A; CERK; CHEK1; CHUK; CKB; CKS1B; CKS2; CLK1; CPNE3; CRIM1; CSF1R; CSK; CSNK1D; CSNK1G1; CSNK2A1; CSNK2A2; CSNK2B; DAPK1; DAPK3; DCK; DDR1; DGUOK; DLG1; DLG3; DTYMK; DUSP1; DUSP22; DYRK1A; EIF2AK3; EIF2AK4; FES; FLT1; FLT3; FRAP1; GTF2H1; HCK; HK2; IGF2R; ILK; ILKAP; IRAK1; IRAK4; JAK1; JAK2; JAK3; KHK; KIT; LATS2; LIMK1; LIN7C; LRMP; LYN; MADD; MAP2K1; MAP2K4; MAP2K5; MAP2K6; MAP2K7; MAP3K3; MAP3K4; MAP3K7; MAP3K7IP2; MAP3K8; MAP4K1; MAP4K3; MAP4K4; MAP4K5; MAPK1; MAPK13; MAPK14; MAPK6; MAPK8; MAPK9; MAPKAPK2; MATK; MELK; MERTK; MKNK1; NAGK; NEK6; NEK7; NEK9; NRP1; NSF; PACSIN1; PAK1; PAK2; PANK1; PANK3; PAPSS1; PCM1; PDK1; PDK3; PDPK1; PDXK; PFKFB3; PFKL; PFKP; PFTK1; PHKA1; PHKB; PIK3C2A; PIK3CD; PIM2; PIP5K1C; PKIG; PMVK; PRKAG2; PRKCB1; PRKCD; PRKCH; PRKCI; PRKRA; PRKX; PRPF4B; PRPSAP2; PSMB7; ROCK1; ROCK2; RPS6KA2; RPS6KB1; RPS6KB2; RPS6KC1; SAP30; SLC9A3R2; SRPK2; STK17B; STK3; STK39; SYK; TBK1; TEC; TGFBR1; TGFBR2; TJP2; TK1; TLE3; TLK2; TPD52; TPK1; TPR; TRIO; TRPM7; TTK; TXK; TYK2; TYROBP; UGP2; ULK1; VRK2; ZAP70
GO Molecular Function	receptor activity	160	1716	ACVR1; ACVRL1; ADFP; AHR; ANPEP; AXL; BAIAP2; BRD8; CALCRL; CCR5; CCR9; CD14; CD163; CD36; CD44; CD5; CD5L; CD74; CD80; CD86; CD8A; CD97; CHD6; CHRNB1; CNR2; CRIM1; CRLF2; CRLF3; CRTAP; CSF1R; CSF2RA; CSF2RB; CXCL16; CXCR3; CYSLTR1; DDR1; DGCR2; DUSP1; EBI3; EBP; EEF1E1; EMR1; EVI2A; EXTL3; FCGR2B; FCGRT; FEM1B; FKBP1A; FLT1; FLT3; FPR1; FZD7; GABARAPL1; GABBR1; GPR124; GPR34; GPR35; GPR65; GPRC5B; GRINL1A; HABP4; HAVCR2; HFE; HRH2; ICAM1; IFNAR1; IFNAR2; IFNGR2; IGF2R; IL10RA; IL13RA1; IL15RA; IL1RAP; IL2RG; IL6ST; IRAK1; IRAK4; ITGA4; ITGA8; ITGA9; ITGAE; ITGAV; ITGAX; ITGB1; ITGB2; ITPR1; ITPR2; KIT; KLRC1; LANCL2; LGALS3BP; LIFR; LILRB3; LY75; LY96; M6PR; MERTK; MRC1; MYD88; NCOA1; NOTCH1; NOTCH2; NOTCH4; NR2C2; NR3C1; NRP1; OLFM1; P2RX4; P2RY6; PEX11A; PEX7; PLXNB2; PLXNC1; PPARG; PRKCB1; PRKCD; PRKCH; PRKCI; PROCR; PTGER1; PTGER2; PTGER4; PTPN6; PTPN9; PTPRE; PTPRJ; PTPRS; PTTG1IP; PVR; RAMP1; RNF121; RRBP1; RXRA; RYR1; SCARB1; SCARB2; SEMA4D; SEMA4F; SLC1A5; SSR4; SYK; TACSTD1; TGFBR1; TGFBR2; TLR1; TLR2; TLR3; TLR4; TNFRSF1A; TNFRSF21; TNFRSF9; TOMM70A; TRAM1; TRIP13; TRPV2; TYROBP; WASF2; XCR1; XPO7; ZYX
GO Molecul	protein kinase	124	1716	ABL1; ACVR1; ACVRL1; ATM; AXL; BTK; BUB1; CAMK1; CASK; CDK4; CDK5; CDK7; CDK8; CDKN1A; CERK; CHEK1; CHUK; CKS1B; CKS2; CLK1; CPNE3; CRIM1; CSF1R; CSK; CSNK1D; CSNK1G1; CSNK2A1; CSNK2A2; CSNK2B; DAPK1; DAPK3; DDR1; DYRK1A; EIF2AK3; EIF2AK4; FES; FLT1; FLT3; GTF2H1; HCK; IGF2R; ILK; IRAK1; IRAK4; JAK1; JAK2; JAK3; KIT; LATS2; LIMK1; LYN; MAP2K1;

ar Function	activity			MAP2K4; MAP2K5; MAP2K6; MAP2K7; MAP3K3; MAP3K4; MAP3K7; MAP3K8; MAP4K1; MAP4K3; MAP4K4; MAP4K5; MAPK1; MAPK13; MAPK14; MAPK6; MAPK8; MAPK9; MAPKAPK2; MATK; MELK; MERTK; MKNK1; NEK6; NEK7; NEK9; NRP1; PACSIN1; PAK1; PAK2; PCM1; PDK1; PDK3; PDPK1; PFTK1; PHKA1; PHKB; PIM2; PRKAG2; PRKCB1; PRKCD; PRKCH; PRKCI; PRKX; PRPF4B; ROCK1; ROCK2; RPS6KA2; RPS6KB1; RPS6KB2; RPS6KC1; SAP30; SRPK2; STK17B; STK3; STK39; SYK; TBK1; TEC; TGFBR1; TGFBR2; TLE3; TLK2; TPR; TRIO; TRPM7; TTK; TXK; TYK2; ULK1; VRK2; ZAP70
GO Molecular Function	transcription factor activity	101	1716	ADNP; AHR; ATF1; ATF3; ATF6; ATRX; BACH1; BAZ1B; BCL6; BTG2; CAMTA2; CBFA2T3; CBFB; CBL; CEBPG; CITED2; CNOT7; CNOT8; CREB3; CREM; CTCF; DMTF1; E2F1; EGR1; ELF1; ELK3; ETS2; ETV3; ETV6; FLI1; GABPA; GABPB1; GTF2I; HCLS1; HDAC2; HHEX; HIF1A; IRF3; IRF4; IRF5; IRF6; IRF7; KLF3; LMO2; MEF2A; MEF2C; MRPS25; MYCL1; MYNN; NFAT5; NFATC1; NFIX; NFKB1; NFKB2; NFYA; NFYB; NR2C2; NR3C1; PKNOX1; PLAGL2; PML; POLR3K; PPARG; PURA; RB1; RELB; RERE; RFX5; RFXAP; RUNX1; RXRA; SALL2; SCMH1; SIN3B; SOLH; SPIB; SRF; STAT1; STAT3; STAT5A; STAT6; SUPT4H1; TAF13; TAF1B; TARDBP; TCEA1; TCF19; TFDP1; UBP1; UBXD2; UGP2; VAV1; XBP1; YY1; ZDHHC14; ZDHHC2; ZDHHC3; ZDHHC6; ZDHHC9; ZFP36L1; ZNRD1
GO Molecular Function	protein serine/threonine kinase activity	92	1716	ACVR1; ACVRL1; ATM; AXL; BUB1; CAMK1; CASK; CDK4; CDK5; CDK7; CDK8; CERK; CHEK1; CHUK; CKS1B; CKS2; CLK1; CPNE3; CSNK1D; CSNK1G1; CSNK2A1; CSNK2A2; CSNK2B; DAPK1; DAPK3; DYRK1A; EIF2AK3; EIF2AK4; GTF2H1; HCK; ILK; IRAK1; LATS2; LIMK1; MAP2K1; MAP2K4; MAP2K5; MAP2K6; MAP2K7; MAP3K3; MAP3K4; MAP3K7; MAP3K8; MAP4K1; MAP4K3; MAP4K4; MAP4K5; MAPK1; MAPK13; MAPK14; MAPK6; MAPK8; MAPK9; MAPKAPK2; MELK; MKNK1; NEK6; NEK7; NEK9; PAK1; PAK2; PDPK1; PFTK1; PHKA1; PHKB; PIM2; PRKAG2; PRKCB1; PRKCD; PRKCH; PRKCI; PRKX; PRPF4B; ROCK1; ROCK2; RPS6KA2; RPS6KB1; RPS6KB2; SAP30; SRPK2; STK17B; STK3; STK39; TBK1; TGFBR1; TGFBR2; TLK2; TRIO; TRPM7; TTK; ULK1; VRK2
GO Molecular Function	transmembrane receptor activity	92	1716	ACVR1; ACVRL1; AXL; CALCRL; CCR5; CCR9; CD14; CD163; CD44; CD5; CD5L; CD74; CD97; CHRNB1; CNR2; CRIM1; CRLF2; CRTAP; CSF1R; CSF2RA; CSF2RB; CXCL16; CXCR3; CYSLTR1; DDR1; EBI3; EBP; EEF1E1; EMR1; EVI2A; FLT1; FLT3; FPR1; FZD7; GABBR1; GPR124; GPR34; GPR35; GPR65; GPRC5B; HABP4; HFE; HRH2; ICAM1; IFNAR1; IFNAR2; IFNGR2; IGF2R; IL10RA; IL13RA1; IL15RA; IL1RAP; IL2RG; IL6ST; ITGA4; ITGA8; ITGA9; ITGAE; ITGAV; ITGAX; ITGB1; ITGB2; KIT; KLRC1; LANCL2; LGALS3BP; LIFR; M6PR; MERTK; MYD88; NOTCH1; NRP1; OLFM1; P2RY6; PEX7; PTGER1; PTGER2; PTGER4; PTPRE; PTPRJ; PTPRS; RRBP1; TGFBR1; TGFBR2; TLR1; TLR2; TLR3; TLR4; TNFRSF1A; WASF2; XCR1; XPO7
GO Molecular Function	structural molecule activity	76	1716	ACTB; ACTR10; ACTR8; ADD1; ADD3; ARPC4; ARPC5; BFAR; CD2AP; CLDN1; CLTC; COL14A1; COL9A3; CRELD1; CRYAB; CTNNA1; ERBB2IP; GADD45B; GADD45G; HIP1; KRT17; LACTB; MBP; MFAP3; MRPL1; MRPL11; MRPL15; MRPL16; MRPL17; MRPL22; MRPL27; MRPL3; MRPL46; MRPL48; MRPL49; MRPL50; MRPS14; MRPS15; MRPS2; MRPS21; MRPS25; MRPS28; MRPS9; MYL6; MYO6; MYOM1; NOLA2; OLFM1; PLEC1; PNN; RDX; ROCK2; RPL11; RPL13; RPL14; RPL15; RPL23; RPL30; RPL31; RPL5; RPS10; RPS13; RPS24; RPS6; RPS6KA2; RPS9; SDCCAG8; SGCB; TNNI2; TPM1; TPM2; TPM3; TPM4; VAPB; VCL; WASF2
GO	calcium	67	1716	AIF1; ANXA1; ANXA4; ANXA5; ANXA6; ANXA7; AP1GBP1; ATP2A2; CABP4; CACNA1S; CALM1; CALM2; CALM3; CANX; CBL; CD97; CETN2; CLTA; CLTB; CRELD1; DNASE1L3; EHD1; EHD2; EHD4; EMR1; EPS15; ERO1L; FKBP9; GCA; GPD2; GRN; GSN; ITSN1; ITSN2;

Molecular Function	ion binding			JAG2; LCP1; LRP4; LTBP2; MAN1A2; MATN2; MRC1; MST1; MYL6; NOTCH1; NOTCH2; NOTCH4; NUCB2; PLCG2; PLEK; PLS3; PLSCR1; PLSCR3; PML; PPEF2; PPP3CA; PPP3CB; PRKCB1; PRNP; PRRG2; RCN2; RYR1; SLC25A13; SRI; SSR4; TGM1; TGM2; TKTL1
GO Molecular Function	transcription factor binding	66	1716	ATF2; ATF3; ATF6; ATF7IP; BCL11A; BCL3; BRD8; CBFB; CREB3; CTCF; DR1; DRG1; E2F1; ELK3; FUS; GABPA; GTF2A1; HDAC11; HDAC2; HDAC5; HMGN3; HSBP1; ID3; IER5; IRF3; IRF4; MEF2A; MEF2C; MXI1; MYCBP; NAB2; NCOA1; NCOA3; NFKB2; NMI; NR2C2; PCAF; PIAS1; PLRG1; PML; POU2AF1; RELB; RFX5; RFXAP; RNF12; RNF14; RXRA; SAP30; SF1; SIAH2; SMARCC1; SMARCE1; SQSTM1; TAF7; TAF9; TBPL1; TCERG1; TFDP1; TRIM32; TRIM33; TRIP13; TSG101; UBP1; YAF2; YY1; ZFX
GO Molecular Function	protein-tyrosine kinase activity	63	1716	ABL1; AXL; BTK; CASK; CDK5; CHEK1; CHUK; CLK1; CRIM1; CSF1R; CSK; CSNK1D; DDR1; DYRK1A; FES; FLT1; FLT3; HCK; IGF2R; ILK; IRAK4; JAK1; JAK2; JAK3; KIT; LIMK1; LYN; MAP2K1; MAP2K4; MAP2K5; MAP2K6; MAP2K7; MAP3K7; MAPK1; MAPK13; MAPK14; MAPK9; MATK; MERTK; NEK6; NEK7; NRP1; PAK2; PDPK1; PRKCD; PRKCH; PRKX; PRPF4B; ROCK2; RPS6KA2; SRPK2; STK3; STK39; SYK; TBK1; TEC; TGFBR1; TLK2; TPR; TTK; TXK; TYK2; ZAP70
GO Molecular Function	transcription cofactor activity	62	1716	ATF2; ATF3; ATF6; ATF7IP; BCL11A; BCL3; BRD8; CBFB; CREB3; CTCF; DR1; E2F1; ELK3; FUS; GABPA; GTF2A1; HDAC5; HMGN3; HSBP1; ID3; IER5; IRF3; MEF2A; MEF2C; MXI1; MYCBP; NAB2; NCOA1; NCOA3; NFKB2; NMI; NR2C2; PCAF; PIAS1; PLRG1; PML; POU2AF1; RELB; RFX5; RFXAP; RNF12; RNF14; RXRA; SAP30; SF1; SIAH2; SMARCC1; SMARCE1; SQSTM1; TAF7; TAF9; TBPL1; TCERG1; TFDP1; TRIM32; TRIM33; TRIP13; TSG101; UBP1; YAF2; YY1; ZFX
GO Molecular Function	molecular_function unknown	59	1716	ABHD3; ABL1; AIF1; AIM1; APOA1BP; ATP6V0D1; CBFB; CD44; CDK5RAP1; CENTA2; CLTA; CLTB; COPZ2; CSRP2; CUL4B; DSCR3; EHD1; ETV3; FUS; HERPUD1; HRASLS3; IFIT1; IFIT2; ITSN1; LPP; LRBA; MATN2; MKRN1; MLH3; MRPL49; MRPS28; MST1; NUBP1; PCCA; PIGF; PPFIA4; PPIL2; PRKAG2; PTPN6; PTTG1IP; RNF6; RTN1; RTN3; RTN4; SEC24C; SEC24D; SHOC2; SPIB; STRN3; SURF4; TGM2; TM6SF1; TMEM8; TNFAIP1; TPM1; TPM3; TRIM17; UBE2V1; UXT
GO	cytoskelet	58	1716	ADD1; ANLN; BAIAP2; CAPZA1; CAPZA2; CAPZB; CFL2; CLASP1; CNN3; CORO1B; CORO2A; DBN1; DLG1; DSTN; EVL; FLII; FLNB; FSCN1; GABARAPL1; GABARAPL2; GMFB; GSN; HIP1; HOMER2; KIF1B; KLHL2; KLHL5; LCP1; LSP1; MAPRE1; MAPRE2; MARCKS;

Molecular Function	al protein binding			MYO1C; MYO5A; MYO6; NEDD9; PDLIM2; PFN2; PLEC1; PLS3; RDX; SDC3; SDCBP; SEC24C; STMN3; TARDBP; TMOD3; TNNI2; TPM1; TPM2; TPM3; TPM4; TUBGCP5; VASP; VCL; WASF2; WASL; WDR1
GO Molecular Function	phosphoric ester hydrolase activity	56	1716	ACP1; ACP2; CCR5; CDC25A; CDC25C; CNP; CTDP1; DUSP1; DUSP11; DUSP16; DUSP19; DUSP22; DUSP6; DUSP7; ILKAP; IMPA1; INPP1; INPP4A; INPP5B; INPP5D; INPPL1; MTM1; MTMR1; MTMR4; MTMR6; NT5C2; PDE1B; PDE4B; PDE8A; PFKFB3; PLCE1; PLCG2; PPAP2A; PPAP2B; PPAP2C; PPEF2; PPM1A; PPM1B; PPP1CC; PPP2R1B; PPP2R2A; PPP3CA; PPP3CB; PPP6C; PTEN; PTP4A1; PTPLA; PTPN11; PTPN2; PTPN6; PTPN9; PTPRE; PTPRJ; PTPRS; SACM1L; UNC119
GO Molecular Function	ligase activity	56	1716	ARIH1; BIRC6; CBL; CD48; CD68; CDCA7; CORO2A; CTPS; CUL1; CUL3; CUL4A; CUL4B; EPRS; FBXO11; FBXO25; FBXO3; FBXO4; FBXO6; HARS; HLCS; IARS; KARS; LAMP2; LAMP3; LIG1; LYPLA1; MDM2; MTHFS; NARS; NEDD4; NEDD4L; PAICS; PCCA; PJA1; QARS; QRSL1; RNF12; RNF14; RTCD1; SUCLG1; TRIP12; UBE2A; UBE2B; UBE2C; UBE2D1; UBE2D3; UBE2E1; UBE2E3; UBE2G1; UBE2J1; UBE2L3; UBE2L6; UBE2M; UBE2V1; UBE2V2; UBE3A
GO Molecular Function	ion transporter activity	55	1716	ASNA1; ATOX1; ATP11A; ATP11B; ATP1B1; ATP2A2; ATP2C1; ATP5A1; ATP5C1; ATP5E; ATP6V0A2; ATP6V0B; ATP6V0D1; ATP6V1A; ATP6V1B2; ATP6V1C1; ATP6V1D; ATP6V1H; ATP7A; ATP8A1; COX15; COX5B; COX7C; GJA1; ITPR2; NDUFA5; NDUFA9; NDUFAB1; NDUFB4; NDUFB7; NDUFC2; NDUFS4; NDUFS5; NDUFV1; NNT; PLP2; SFXN2; SLC1A5; SLC22A5; SLC25A11; SLC30A4; SLC30A5; SLC30A7; SLC31A1; SLC31A2; SLC41A1; SLC4A1; SLC4A7; SLC6A6; SLC8A1; TCIRG1; TMEM1; TRPV2; UQCRB; UQCRFS1
GO Molecular Function	GTPase regulator activity	52	1716	ABL1; ABR; ALCAM; ALS2; ARFGAP3; ARHGAP12; ARHGAP5; ARHGAP6; ARHGAP8; ARHGAP9; ARHGEF10; ARHGEF7; BNIP2; CENTA2; CENTD2; CHN2; CYFIP1; CYFIP2; DDEF1; ECT2; EIF2B2; FGD2; GDI1; GDI2; GIT2; GNG12; GPS1; IPO7; IQGAP1; ITSN1; MAP4K1; MAP4K3; MAP4K4; MAP4K5; MAPKAP1; PLCE1; PSCD2; RABIF; RAP1GDS1; RASA1; RASGRP4; RGS19; RGS2; RGS3; SHOC2; STARD8; TBC1D8; TIAM1; TRIO; VAV1; VAV3; WASL
GO	receptor	48	1716	ADAM23; ADAM9; AKAP9; ALCAM; ANXA1; APOE; BID; CCL22; CD80; CD8A; CKLF; CXCL10; CXCL16; CXCL9; DBI; **DKK3**; ENSA; ERBB2IP; FEM1B; FGL2; GLG1; GMFB; GPRC5B; GRN; HMGN3; IGF1; IK; IL15; IL16; IL18; INSL3; JAG2; MADD; MAP2K7; MYD88; NCOA3;

Molecular Function	binding			PDGFA; PDGFC; PLXNC1; SDCBP; SRI; TAP2; TAPBP; TGFB3; TGFBI; TRIP12; TRIP6; WBP1
GO Molecular Function	GTPase activity	48	1716	ARF1; ARF3; ARF4; ARFRP1; ARHGAP5; ARL1; ARL3; ARL6; CDC42; GBP1; GBP2; GBP3; GNA13; GNAI3; GNB2; GNB4; GNG10; GNG12; GNG2; GSPT1; GTPBP2; MFHAS1; MRAS; MX1; NCF1; NUDT1; RAB10; RAB11A; RAB14; RAB24; RAB2B; RAB30; RAB31; RAB32; RAB33B; RAB5A; RAB6B; RAB7; RAC1; RALA; RALB; RAP1A; RAP1B; RAP2A; RRAS2; SAMHD1; TGM2; TUFM
GO Molecular Function	guanyl nucleotide binding	47	1716	AK3; ARF1; ARF3; ARF4; ARFRP1; ARL1; ARL3; ARL6; CDC42; DEK; DRG1; EIF2B2; EIF2B4; GBP1; GBP2; GBP3; GNA13; GNAI3; GSPT1; GTPBP2; MFHAS1; MRAS; MX1; NCF1; NOLC1; RAB10; RAB11A; RAB14; RAB24; RAB2B; RAB30; RAB31; RAB32; RAB33B; RAB5A; RAB6B; RAB7; RAC1; RALA; RALB; RAP1A; RAP1B; RAP2A; RRAS2; SUCLG1; TGM2; TUFM
GO Molecular Function	GTP binding	47	1716	AK3; ARF1; ARF3; ARF4; ARFRP1; ARL1; ARL3; ARL6; CDC42; DEK; DRG1; EIF2B2; EIF2B4; GBP1; GBP2; GBP3; GNA13; GNAI3; GSPT1; GTPBP2; MFHAS1; MRAS; MX1; NCF1; NOLC1; RAB10; RAB11A; RAB14; RAB24; RAB2B; RAB30; RAB31; RAB32; RAB33B; RAB5A; RAB6B; RAB7; RAC1; RALA; RALB; RAP1A; RAP1B; RAP2A; RRAS2; SUCLG1; TGM2; TUFM
GO Molecular Function	cation transporter activity	47	1716	ATOX1; ATP11A; ATP11B; ATP1B1; ATP2A2; ATP2C1; ATP5A1; ATP5C1; ATP5E; ATP6V0A2; ATP6V0B; ATP6V0D1; ATP6V1A; ATP6V1B2; ATP6V1C1; ATP6V1D; ATP6V1H; ATP7A; ATP8A1; COX15; COX5B; COX7C; ITPR2; NDUFA5; NDUFA9; NDUFAB1; NDUFB4; NDUFB7; NDUFC2; NDUFS4; NDUFS5; NDUFV1; NNT; SFXN2; SLC1A5; SLC25A11; SLC30A4; SLC30A5; SLC30A7; SLC31A1; SLC31A2; SLC41A1; SLC8A1; TCIRG1; TMEM1; UQCRB; UQCRFS1
GO	actin	46	1716	ADD1; ANLN; CAPZA1; CAPZA2; CAPZB; CFL2; CNN3; CORO1B; CORO2A; DBN1; DSTN; EVL; FLII; FLNB; FSCN1; GABARAPL2; GMFB; GSN; HIP1; HOMER2; KLHL2; KLHL5; LCP1; LSP1; MARCKS; MYO1C; MYO5A; MYO6; NEDD9; PFN2; PLEC1; PLS3; RDX; SDCBP;

Molecular Function	binding			SEC24C; TMOD3; TNNI2; TPM1; TPM2; TPM3; TPM4; VASP; VCL; WASF2; WASL; WDR1
GO Molecular Function	receptor signaling protein activity	46	1716	ACVR1; ACVRL1; ARF1; ARHGAP6; CARD10; CHN2; CHUK; CRK; EPS8; GNA13; HOMER2; IFITM3; IRAK1; ITSN2; JAK1; JAK2; JAK3; KIT; LASP1; LYN; MAP3K3; MAP3K4; MAP3K7; MAPK1; MAPK13; MAPK14; MAPK6; MAPK8; MAPK9; MS4A1; NSMAF; PDCL; PLCE1; SH3BGRL; SLA; STAM2; STAT1; STAT3; STK39; TGFBR1; TGFBR2; TIAM1; TOB2; TYK2; TYROBP; VAV3
GO Molecular Function	small GTPase regulatory/ interacting protein activity	38	1716	ABL1; ABR; ALCAM; ALS2; ARFGAP3; ARHGAP12; ARHGAP5; ARHGAP6; ARHGAP9; ARHGEF10; ARHGEF7; CYFIP1; CYFIP2; ECT2; EIF2B2; FGD2; GDI1; GDI2; GNG12; IPO7; IQGAP1; ITSN1; MAP4K1; MAP4K3; MAP4K4; MAP4K5; MAPKAP1; PLCE1; PSCD2; RABIF; RASA1; RASGRP4; SHOC2; TIAM1; TRIO; VAV1; VAV3; WASL
GO Molecular Function	chaperone activity	36	1716	ATOX1; BAG5; CANX; CCT3; CCT7; CD74; CDC37; CLN3; CRYAB; DNAJA1; DNAJB11; DNAJB4; DNAJB6; DNAJB9; DNAJC5; FKBP4; FUSIP1; GRPEL1; HSPA1A; HSPA1B; HSPA4; HSPA5; HSPA8; HSPH1; LMAN1; PFDN2; PPIH; PTPLA; RBBP4; SEC63; SSFA2; TAPBP; TBCD; TXNDC4; UXT; YWHAQ
GO Molecular Function	apoptosis regulator activity	31	1716	APAF1; API5; BAD; BAG5; BCL10; BCL2L11; BFAR; BID; BIRC3; BIRC5; BIRC6; BNIP2; BNIP3L; CARD10; CASP2; CASP9; CFLAR; DAPK1; DAPK3; DFFA; DFFB; FAIM; IL18; MCL1; PRDX2; RNF7; RTN4; SH3GLB1; SON; STK17B; TAX1BP1

GO Molecular Function	small monomeric GTPase activity	29	1716	ARF1; ARF3; ARF4; ARFRP1; ARL1; ARL3; ARL6; CDC42; MFHAS1; MRAS; RAB10; RAB11A; RAB14; RAB24; RAB2B; RAB30; RAB31; RAB32; RAB33B; RAB5A; RAB6B; RAB7; RAC1; RALA; RALB; RAP1A; RAP1B; RAP2A; RRAS2
GO Molecular Function	defense/immunity protein activity	29	1716	APAF1; C1QA; C1QB; C6; CCL22; CD14; CD96; FTH1; HSPA1B; ICOS; IFI35; IFI44; IFNAR2; IFNGR2; LST1; LY75; MLF2; MST1; MX1; NOTCH1; PPP2R1B; PRKRA; SAMHD1; TAP2; TAPBP; TIAL1; TLR1; TLR3; TLR4
GO Molecular Function	receptor signaling protein serine/threonine kinase activity	16	1716	ACVR1; ACVRL1; CHUK; IRAK1; MAP3K3; MAP3K4; MAP3K7; MAPK1; MAPK13; MAPK14; MAPK6; MAPK8; MAPK9; STK39; TGFBR1; TGFBR2
GO Molecular Function	hematopoietin/interferon-class (D200-domain) cytokine receptor activity	14	1716	CRLF2; CSF2RA; CSF2RB; EBI3; IFNAR1; IFNAR2; IFNGR2; IL10RA; IL13RA1; IL15RA; IL1RAP; IL2RG; IL6ST; LIFR
GO	cytokine	14	1716	CCL22; CKLF; CXCL10; CXCL16; CXCL9; ERBB2IP; GRN; IK; IL15; IL16; IL18; PDGFA; SDCBP; TGFB3

Molecular Function	activity			
GO Molecular Function	kinase regulator activity	14	1716	CCNDBP1; CDKN1A; CSNK2B; CXCL10; GMFB; HMOX1; MADD; PHKA1; PHKB; PKIB; PKIG; PTGIS; SOCS5; YWHAQ
GO Molecular Function	apoptosis inhibitor activity	14	1716	API5; BFAR; BIRC3; BIRC5; BIRC6; BNIP2; BNIP3L; CASP2; CFLAR; FAIM; PRDX2; RNF7; SON; TAX1BP1
GO Molecular Function	transmembrane receptor protein kinase activity	14	1716	ACVR1; ACVRL1; AXL; CRIM1; CSF1R; DDR1; FLT1; FLT3; IGF2R; KIT; MERTK; NRP1; TGFBR1; TGFBR2
GO Molecular Function	growth factor activity	11	1716	**DKK3**; GMFB; GRN; IGF1; IL18; JAG2; MAP2K7; PDGFA; PDGFC; SDCBP; TGFB3

GO Molecular Function	interleukin binding	6	1716	CSF2RB; IL10RA; IL15RA; IL1RAP; IL2RG; IL6ST
GO Molecular Function	interleukin receptor activity	6	1716	CSF2RB; IL10RA; IL15RA; IL1RAP; IL2RG; IL6ST
GO Molecular Function	growth factor binding	6	1716	CRIM1; CSF2RB; IL10RA; IL1RAP; IL2RG; IL6ST
GO Molecular Function	apoptosis activator activity	6	1716	APAF1; DAPK1; DAPK3; IL18; SH3GLB1; STK17B
GO Molecular Function	caspase activity	6	1716	CASP2; CASP3; CASP6; CASP7; CASP9; CFLAR

GO Molecular Function	transforming growth factor-beta receptor activity	4	1716	ACVR1; ACVRL1; TGFBR1; TGFBR2
GO Molecular Function	death receptor binding	4	1716	BID; FEM1B; MADD; MYD88
GO Molecular Function	chemokine receptor activity	4	1716	CCR5; CCR9; CXCR3; XCR1
GO Molecular Function	chemokine receptor binding	4	1716	CCL22; CXCL10; CXCL16; CXCL9
GO Molecular Function	MAP kinase phosphatase activity	4	1716	DUSP1; DUSP16; DUSP6; DUSP7

GO Molecular Function	Ras interactor activity	3	1716	MAPKAP1; PLCE1; SHOC2

The above list was generated by use of the EASE version 2.0 software (Hosack et al. 2003). The "population" of genes is all genes assayed (i.e. all differentially expressed genes) and annotated within a given system of classifying genes (e.g. the 'Molecular Function' branch of the Gene Ontology). Therefore the population can change from one system to the next. "Hits" refers to genes falling within the gene category in question. Therefore "Population hits" for the Biological Process "apoptosis" refers to the number of genes falling within the category "apoptosis" out of all genes in the population annotated with a Biological Process. EASE first maps all gene identifiers in the population to "primary gene identifiers". The default "primary gene identifier" in EASE is the LocusLink number. This step controls for the possibility of multiple identifiers on the list referring to the same gene (typical of Genbank accessions), and that gene therefore receiving multiple spurious "votes" for its categories in the over-representation analysis. The primary gene identifiers are then mapped to gene categories within various categorical systems, the "Population Total" is determined for each system of gene categorization, and the "Population Hits" is determined for every category within those systems.

Definitions of default fields in the results:

System = the system of categorizing genes

Gene Category = the specific category of genes within the System

Population Hits = number of genes in the total group of genes assayed that belong to the specific Gene Category

Population Total = number of genes in the total group of genes assayed that belong to any Gene Category within the System

Genbank accessions = List of identifiers (in this case: Genbank accessions) from the gene list that fall into the Gene Category.

Abarzua, F., M. Sakaguchi, M. Takaishi, Y. Nasu, K. Kurose, S. Ebara, M. Miyazaki, M. Namba, H. Kumon and N. H. Huh (2005). "Adenovirus-mediated overexpression of REIC/Dkk-3 selectively induces apoptosis in human prostate cancer cells through activation of c-Jun-NH2-kinase." Cancer Res **65**(21): 9617-22.

Abarzua, F., M. Sakaguchi, R. Tanimoto, H. Sonegawa, D. W. Li, K. Edamura, T. Kobayashi, M. Watanabe, Y. Kashiwakura, H. Kaku, T. Saika, K. Nakamura, Y. Nasu, H. Kumon and N. H. Huh (2007). "Heat shock proteins play a crucial role in tumor-specific apoptosis by REIC/Dkk-3." Int J Mol Med **20**(1): 37-43.

Abi-Hanna, D., D. Wakefield and S. Watkins (1988). "HLA antigens in ocular tissues. I. In vivo expression in human eyes." Transplantation **45**(3): 610-3.

Aktas, O., T. Prozorovski and F. Zipp (2006). "Death ligands and autoimmune demyelination." Neuroscientist **12**(4): 305-16.

Albert, M. L., B. Sauter and N. Bhardwaj (1998). "Dendritic cells acquire antigen from apoptotic cells and induce class I-restricted CTLs." Nature **392**(6671): 86-9.

Alderson, M. R., T. W. Tough, T. Davis-Smith, S. Braddy, B. Falk, K. A. Schooley, R. G. Goodwin, C. A. Smith, F. Ramsdell and D. H. Lynch (1995). "Fas ligand mediates activation-induced cell death in human T lymphocytes." J Exp Med **181**(1): 71-7.

Alferink, J., B. Schittek, G. Schonrich, G. J. Hammerling and B. Arnold (1995). "Long life span of tolerant T cells and the role of antigen in maintenance of peripheral tolerance." Int Immunol **7**(2): 331-6.

Alferink, J., A. Tafuri, D. Vestweber, R. Hallmann, G. J. Hammerling and B. Arnold (1998). "Control of neonatal tolerance to tissue antigens by peripheral T cell trafficking." Science **282**(5392): 1338-41.

Algood, H. M. and J. L. Flynn (2004). "CCR5-deficient mice control Mycobacterium tuberculosis infection despite increased pulmonary lymphocytic infiltration." J Immunol **173**(5): 3287-96.

Anderson, G., J. J. Owen, N. C. Moore and E. J. Jenkinson (1994). "Thymic epithelial cells provide unique signals for positive selection of CD4+CD8+ thymocytes in vitro." J Exp Med **179**(6): 2027-31.

Andrade, F., L. A. Casciola-Rosen and A. Rosen (2004). "Granzyme B-induced cell death." Acta Haematol **111**(1-2): 28-41.

Apostolou, I., A. Sarukhan, L. Klein and H. von Boehmer (2002). "Origin of regulatory T cells with known specificity for antigen." Nat Immunol **3**(8): 756-63.

Apostolou, I. and H. von Boehmer (2004). "In vivo instruction of suppressor commitment in naive T cells." J Exp Med **199**(10): 1401-8.

Aranami, T. and T. Yamamura (2008). "Th17 Cells and Autoimmune Encephalomyelitis (EAE/MS)." Allergol Int **57**(2): 115-20.

Askenasy, N., E. S. Yolcu, I. Yaniv and H. Shirwan (2005). "Induction of tolerance using Fas ligand: a double-edged immunomodulator." Blood **105**(4): 1396-404.

Azuma, M., M. Cayabyab, D. Buck, J. H. Phillips and L. L. Lanier (1992). "CD28 interaction with B7 costimulates primary allogeneic proliferative responses and cytotoxicity mediated by small, resting T lymphocytes." J Exp Med **175**(2): 353-60.

Banchereau, J. and R. M. Steinman (1998). "Dendritic cells and the control of immunity." Nature **392**(6673): 245-52.

Barrantes Idel, B., A. Montero-Pedrazuela, A. Guadano-Ferraz, M. J. Obregon, R. Martinez de Mena, V. Gailus-Durner, H. Fuchs, T. J. Franz, S. Kalaydjiev, M. Klempt, S. Holter, B. Rathkolb, C. Reinhard, G. Morreale de Escobar, J. Bernal, D. H. Busch, W. Wurst, E. Wolf, H. Schulz, S. Shtrom, E. Greiner, M. Hrabe de Angelis, H. Westphal and C. Niehrs (2006). "Generation and characterization of dickkopf3 mutant mice." Mol Cell Biol **26**(6): 2317-26.

Belkaid, Y., C. A. Piccirillo, S. Mendez, E. M. Shevach and D. L. Sacks (2002). "CD4+CD25+ regulatory T cells control Leishmania major persistence and immunity." Nature **420**(6915): 502-7.

Bennett, C. L., J. Christie, F. Ramsdell, M. E. Brunkow, P. J. Ferguson, L. Whitesell, T. E. Kelly, F. T. Saulsbury, P. F. Chance and H. D. Ochs (2001). "The immune dysregulation, polyendocrinopathy, enteropathy, X-linked syndrome (IPEX) is caused by mutations of FOXP3." Nat Genet **27**(1): 20-1.

Bettelli, E., M. Pagany, H. L. Weiner, C. Linington, R. A. Sobel and V. K. Kuchroo (2003). "Myelin oligodendrocyte glycoprotein-specific T cell receptor transgenic mice develop spontaneous autoimmune optic neuritis." J Exp Med **197**(9): 1073-81.

Bluestone, J. A. and A. K. Abbas (2003). "Natural versus adaptive regulatory T cells." Nat Rev Immunol **3**(3): 253-7.

Bopp, T., C. Becker, M. Klein, S. Klein-Hessling, A. Palmetshofer, E. Serfling, V. Heib, M. Becker, J. Kubach, S. Schmitt, S. Stoll, H. Schild, M. S. Staege, M. Stassen, H. Jonuleit and E. Schmitt (2007). "Cyclic adenosine monophosphate is a key component of regulatory T cell-mediated suppression." J Exp Med **204**(6): 1303-10.

Bouneaud, C., P. Kourilsky and P. Bousso (2000). "Impact of negative selection on the T cell repertoire reactive to a self-peptide: a large fraction of T cell clones escapes clonal deletion." Immunity **13**(6): 829-40.

Brocker, T., M. Riedinger and K. Karjalainen (1997). "Targeted expression of major histocompatibility complex (MHC) class II molecules demonstrates that dendritic cells can induce negative but not positive selection of thymocytes in vivo." J Exp Med **185**(3): 541-50.

Bruder, D., M. Probst-Kepper, A. M. Westendorf, R. Geffers, S. Beissert, K. Loser, H. von Boehmer, J. Buer and W. Hansen (2004). "Neuropilin-1: a surface marker of regulatory T cells." Eur J Immunol **34**(3): 623-30.

Burkly, L. C., S. Degermann, J. Longley, J. Hagman, R. L. Brinster, D. Lo and R. A. Flavell (1993). "Clonal deletion of V beta 5+ T cells by transgenic I-E restricted to thymic medullary epithelium." J Immunol **151**(8): 3954-60.

Cadigan, K. M. and Y. I. Liu (2006). "Wnt signaling: complexity at the surface." J Cell Sci **119**(Pt 3): 395-402.

Calne, R. Y., H. J. White, R. M. Binns, B. M. Herbertson, P. R. Millard, J. Pena, J. R. Salaman, J. R. Samuel and D. R. Davis (1969). "Immunosuppressive effects of the orthotopically transplanted porcine liver." Transplant Proc **1**(1): 321-4.

Cantrell, D. (1996). "T cell antigen receptor signal transduction pathways." Annu Rev Immunol **14**: 259-74.

Cao, X., S. F. Cai, T. A. Fehniger, J. Song, L. I. Collins, D. R. Piwnica-Worms and T. J. Ley (2007). "Granzyme B and perforin are important for regulatory T cell-mediated suppression of tumor clearance." Immunity **27**(4): 635-46.

Cardell, S., B. Sander and G. Moller (1992). "Primary stimulation of CD4+ cells in the presence of IL-4 or IFN-gamma alters the frequencies of cytokine-producing cells at restimulation." Scand J Immunol **36**(6): 769-77.

Chatila, T. A., F. Blaeser, N. Ho, H. M. Lederman, C. Voulgaropoulos, C. Helms and A. M. Bowcock (2000). "JM2, encoding a fork head-related protein, is mutated in X-linked autoimmunity-allergic disregulation syndrome." J Clin Invest **106**(12): R75-81.

Chen, W., M. S. Ford, K. J. Young and L. Zhang (2004). "The role and mechanisms of double negative regulatory T cells in the suppression of immune responses." Cell Mol Immunol **1**(5): 328-35.

Chen, W., W. Jin, N. Hardegen, K. J. Lei, L. Li, N. Marinos, G. McGrady and S. M. Wahl (2003). "Conversion of peripheral CD4+CD25- naive T cells to CD4+CD25+ regulatory T cells by TGF-beta induction of transcription factor Foxp3." J Exp Med **198**(12): 1875-86.

Chen, Y., V. K. Kuchroo, J. Inobe, D. A. Hafler and H. L. Weiner (1994). "Regulatory T cell clones induced by oral tolerance: suppression of autoimmune encephalomyelitis." Science **265**(5176): 1237-40.

Collison, L. W., C. J. Workman, T. T. Kuo, K. Boyd, Y. Wang, K. M. Vignali, R. Cross, D. Sehy, R. S. Blumberg and D. A. Vignali (2007). "The inhibitory cytokine IL-35 contributes to regulatory T-cell function." Nature **450**(7169): 566-9.

Crabtree, G. R. (1989). "Contingent genetic regulatory events in T lymphocyte activation." Science **243**(4889): 355-61.

Crispe, I. N., M. Giannandrea, I. Klein, B. John, B. Sampson and S. Wuensch (2006). "Cellular and molecular mechanisms of liver tolerance." Immunol Rev **213**: 101-18.

Deaglio, S., K. M. Dwyer, W. Gao, D. Friedman, A. Usheva, A. Erat, J. F. Chen, K. Enjyoji, J. Linden, M. Oukka, V. K. Kuchroo, T. B. Strom and S. C. Robson (2007). "Adenosine generation catalyzed by CD39 and CD73 expressed on regulatory T cells mediates immune suppression." J Exp Med **204**(6): 1257-65.

Derbinski, J., A. Schulte, B. Kyewski and L. Klein (2001). "Promiscuous gene expression in medullary thymic epithelial cells mirrors the peripheral self." Nat Immunol **2**(11): 1032-9.

Derynck, R. and Y. E. Zhang (2003). "Smad-dependent and Smad-independent pathways in TGF-beta family signalling." Nature **425**(6958): 577-84.

Devergne, O., M. Birkenbach and E. Kieff (1997). "Epstein-Barr virus-induced gene 3 and the p35 subunit of interleukin 12 form a novel heterodimeric hematopoietin." Proc Natl Acad Sci U S A **94**(22): 12041-6.

Dorr, J., I. Bechmann, S. Waiczies, O. Aktas, H. Walczak, P. H. Krammer, R. Nitsch and F. Zipp (2002). "Lack of tumor necrosis factor-related apoptosis-inducing ligand but presence of its receptors in the human brain." J Neurosci **22**(4): RC209.

Dubois, P. M., M. Pihlgren, M. Tomkowiak, M. Van Mechelen and J. Marvel (1998). "Tolerant CD8 T cells induced by multiple injections of peptide antigen show impaired TCR signaling and altered proliferative responses in vitro and in vivo." J Immunol **161**(10): 5260-7.

Edamura, K., Y. Nasu, M. Takaishi, T. Kobayashi, F. Abarzua, M. Sakaguchi, Y. Kashiwakura, S. Ebara, T. Saika, M. Watanabe, N. H. Huh and H. Kumon (2007). "Adenovirus-mediated REIC/Dkk-3 gene transfer inhibits tumor growth and metastasis in an orthotopic prostate cancer model." Cancer Gene Ther **14**(9): 765-72.

Endharti, A. T., I. M. s. Rifa, Z. Shi, Y. Fukuoka, Y. Nakahara, Y. Kawamoto, K. Takeda, K. Isobe and H. Suzuki (2005). "Cutting edge: CD8+CD122+ regulatory T cells produce IL-10 to suppress IFN-gamma production and proliferation of CD8+ T cells." J Immunol **175**(11): 7093-7.

Etheridge, S. L., G. J. Spencer, D. J. Heath and P. G. Genever (2004). "Expression profiling and functional analysis of wnt signaling mechanisms in mesenchymal stem cells." Stem Cells **22**(5): 849-60.

Fathman, C. G. and N. B. Lineberry (2007). "Molecular mechanisms of CD4+ T-cell anergy." Nat Rev Immunol **7**(8): 599-609.

Fedders, H., R. Augustin and T. C. Bosch (2004). "A Dickkopf- 3-related gene is expressed in differentiating nematocytes in the basal metazoan Hydra." Dev Genes Evol **214**(2): 72-80.

Ferber, I., G. Schonrich, J. Schenkel, A. L. Mellor, G. J. Hammerling and B. Arnold (1994). "Levels of peripheral T cell tolerance induced by different doses of tolerogen." Science **263**(5147): 674-6.

Fields, P. E., T. F. Gajewski and F. W. Fitch (1996). "Blocked Ras activation in anergic CD4+ T cells." Science **271**(5253): 1276-8.

Filaci, G., M. Fravega, D. Fenoglio, M. Rizzi, S. Negrini, R. Viggiani and F. Indiveri (2004). "Non-antigen specific CD8+ T suppressor lymphocytes." Clin Exp Med **4**(2): 86-92.

Floess, S., J. Freyer, C. Siewert, U. Baron, S. Olek, J. Polansky, K. Schlawe, H. D. Chang, T. Bopp, E. Schmitt, S. Klein-Hessling, E. Serfling, A. Hamann and J. Huehn (2007). "Epigenetic control of the foxp3 locus in regulatory T cells." PLoS Biol **5**(2): e38.

Fontenot, J. D., M. A. Gavin and A. Y. Rudensky (2003). "Foxp3 programs the development and function of CD4+CD25+ regulatory T cells." Nat Immunol **4**(4): 330-6.

Friese, M. A. and L. Fugger (2005). "Autoreactive CD8+ T cells in multiple sclerosis: a new target for therapy?" Brain **128**(Pt 8): 1747-63.

Gallegos, A. M. and M. J. Bevan (2004). "Central tolerance to tissue-specific antigens mediated by direct and indirect antigen presentation." J Exp Med **200**(8): 1039-49.

Glass, W. G., M. T. Liu, W. A. Kuziel and T. E. Lane (2001). "Reduced macrophage infiltration and demyelination in mice lacking the chemokine receptor CCR5 following infection with a neurotropic coronavirus." Virology **288**(1): 8-17.

Glinka, A., W. Wu, H. Delius, A. P. Monaghan, C. Blumenstock and C. Niehrs (1998). "Dickkopf-1 is a member of a new family of secreted proteins and functions in head induction." Nature **391**(6665): 357-62.

Glinka, Y. and G. J. Prud'homme (2008). "Neuropilin-1 is a receptor for transforming growth factor beta-1, activates its latent form, and promotes regulatory T cell activity." J Leukoc Biol **84**(1): 302-10.

Gondek, D. C., L. F. Lu, S. A. Quezada, S. Sakaguchi and R. J. Noelle (2005). "Cutting edge: contact-mediated suppression by CD4+CD25+ regulatory cells involves a granzyme B-dependent, perforin-independent mechanism." J Immunol **174**(4): 1783-6.

Gordon, L. B., P. M. Knopf and H. F. Cserr (1992). "Ovalbumin is more immunogenic when introduced into brain or cerebrospinal fluid than into extracerebral sites." J Neuroimmunol **40**(1): 81-7.

Greenwald, R. J., G. J. Freeman and A. H. Sharpe (2005). "The B7 family revisited." Annu Rev Immunol **23**: 515-48.

Griffiths, G. M. (1995). "The cell biology of CTL killing." Curr Opin Immunol **7**(3): 343-8.

Grossman, W. J., J. W. Verbsky, W. Barchet, M. Colonna, J. P. Atkinson and T. J. Ley (2004). "Human T regulatory cells can use the perforin pathway to cause autologous target cell death." Immunity **21**(4): 589-601.

Groux, H. (2001). "An overview of regulatory T cells." Microbes Infect **3**(11): 883-9.

Groux, H., A. O'Garra, M. Bigler, M. Rouleau, S. Antonenko, J. E. de Vries and M. G. Roncarolo (1997). "A CD4+ T-cell subset inhibits antigen-specific T-cell responses and prevents colitis." Nature **389**(6652): 737-42.

Guder, C., S. Pinho, T. G. Nacak, H. A. Schmidt, B. Hobmayer, C. Niehrs and T. W. Holstein (2006). "An ancient Wnt-Dickkopf antagonism in Hydra." Development **133**(5): 901-11.

Harling-Berg, C., P. M. Knopf, J. Merriam and H. F. Cserr (1989). "Role of cervical lymph nodes in the systemic humoral immune response to human serum albumin microinfused into rat cerebrospinal fluid." J Neuroimmunol **25**(2-3): 185-93.

Harling-Berg, C. J., P. M. Knopf and H. F. Cserr (1991). "Myelin basic protein infused into cerebrospinal fluid suppresses experimental autoimmune encephalomyelitis." J Neuroimmunol **35**(1-3): 45-51.

Harrington, L. E., P. R. Mangan and C. T. Weaver (2006). "Expanding the effector CD4 T-cell repertoire: the Th17 lineage." Curr Opin Immunol **18**(3): 349-56.

Harris, J. E., K. D. Bishop, N. E. Phillips, J. P. Mordes, D. L. Greiner, A. A. Rossini and M. P. Czech (2004). "Early growth response gene-2, a zinc-finger transcription factor, is required for full induction of clonal anergy in CD4+ T cells." J Immunol **173**(12): 7331-8.

Hayday, A. and R. Tigelaar (2003). "Immunoregulation in the tissues by gammadelta T cells." Nat Rev Immunol **3**(3): 233-42.

Heath, W. R., C. Kurts, J. F. Miller and F. R. Carbone (1998). "Cross-tolerance: a pathway for inducing tolerance to peripheral tissue antigens." J Exp Med **187**(10): 1549-53.

Heissmeyer, V. and A. Rao (2004). "E3 ligases in T cell anergy--turning immune responses into tolerance." Sci STKE **2004**(241): pe29.

Hermann, M., D. Pirkebner, A. Draxl, P. Berger, G. Untergasser, R. Margreiter and P. Hengster (2007). "Dickkopf-3 is expressed in a subset of adult human pancreatic beta cells." Histochem Cell Biol **127**(5): 513-21.

Holscher, C. (2004). "The power of combinatorial immunology: IL-12 and IL-12-related dimeric cytokines in infectious diseases." Med Microbiol Immunol **193**(1): 1-17.

Hori, S., T. Nomura and S. Sakaguchi (2003). "Control of regulatory T cell development by the transcription factor Foxp3." Science **299**(5609): 1057-61.

Horwitz, D. A., S. G. Zheng and J. D. Gray (2003). "The role of the combination of IL-2 and TGF-beta or IL-10 in the generation and function of CD4+ CD25+ and CD8+ regulatory T cell subsets." J Leukoc Biol **74**(4): 471-8.

Hosack, D. A., G. Dennis, Jr., B. T. Sherman, H. C. Lane and R. A. Lempicki (2003). "Identifying biological themes within lists of genes with EASE." Genome Biol **4**(10): R70.

Hsieh, C. S., Y. Zheng, Y. Liang, J. D. Fontenot and A. Y. Rudensky (2006). "An intersection between the self-reactive regulatory and nonregulatory T cell receptor repertoires." Nat Immunol **7**(4): 401-10.

Hsieh, S. Y., P. S. Hsieh, C. T. Chiu and W. Y. Chen (2004). "Dickkopf-3/REIC functions as a suppressor gene of tumor growth." Oncogene **23**(57): 9183-9.

Hu, D., K. Ikizawa, L. Lu, M. E. Sanchirico, M. L. Shinohara and H. Cantor (2004). "Analysis of regulatory CD8 T cells in Qa-1-deficient mice." Nat Immunol **5**(5): 516-23.

Hua, C., C. Boyer, M. Buferne and A. M. Schmitt-Verhulst (1986). "Monoclonal antibodies against an H-2Kb-specific cytotoxic T cell clone detect several clone-specific molecules." J Immunol **136**(6): 1937-44.

Huesmann, M., B. Scott, P. Kisielow and H. von Boehmer (1991). "Kinetics and efficacy of positive selection in the thymus of normal and T cell receptor transgenic mice." Cell **66**(3): 533-40.

Huffnagle, G. B., L. K. McNeil, R. A. McDonald, J. W. Murphy, G. B. Toews, N. Maeda and W. A. Kuziel (1999). "Cutting edge: Role of C-C chemokine receptor 5 in organ-specific and innate immunity to Cryptococcus neoformans." J Immunol **163**(9): 4642-6.

Huseby, E. S., D. Liggitt, T. Brabb, B. Schnabel, C. Ohlen and J. Goverman (2001). "A pathogenic role for myelin-specific CD8(+) T cells in a model for multiple sclerosis." J Exp Med **194**(5): 669-76.

Huseby, E. S., C. Ohlen and J. Goverman (1999). "Cutting edge: myelin basic protein-specific cytotoxic T cell tolerance is maintained in vivo by a single dominant epitope in H-2k mice." J Immunol **163**(3): 1115-8.

Itoh, M., T. Takahashi, N. Sakaguchi, Y. Kuniyasu, J. Shimizu, F. Otsuka and S. Sakaguchi (1999). "Thymus and autoimmunity: production of CD25+CD4+ naturally anergic and suppressive T cells as a key function of the thymus in maintaining immunologic self-tolerance." J Immunol **162**(9): 5317-26.

Jenkins, M. K., D. M. Pardoll, J. Mizuguchi, H. Quill and R. H. Schwartz (1987). "T-cell unresponsiveness in vivo and in vitro: fine specificity of induction and molecular characterization of the unresponsive state." Immunol Rev **95**: 113-35.

Jeremias, I., I. Herr, T. Boehler and K. M. Debatin (1998). "TRAIL/Apo-2-ligand-induced apoptosis in human T cells." Eur J Immunol **28**(1): 143-52.

Ji, Q. and J. Goverman (2007). "Experimental autoimmune encephalomyelitis mediated by CD8+ T cells." Ann N Y Acad Sci **1103**: 157-66.

Jiang, H., S. Curran, E. Ruiz-Vazquez, B. Liang, R. Winchester and L. Chess (2003). "Regulatory CD8+ T cells fine-tune the myelin basic protein-reactive T cell receptor V beta repertoire during experimental autoimmune encephalomyelitis." Proc Natl Acad Sci U S A **100**(14): 8378-83.

Jiang, L., P. Yang, H. He, B. Li, X. Lin, S. Hou, H. Zhou, X. Huang and K. Aize (2007). "Increased expression of Foxp3 in splenic CD8+ T cells from mice with anterior chamber-associated immune deviation." Mol Vis **13**: 968-74.

Jordan, M. S., A. Boesteanu, A. J. Reed, A. L. Petrone, A. E. Holenbeck, M. A. Lerman, A. Naji and A. J. Caton (2001). "Thymic selection of CD4+CD25+ regulatory T cells induced by an agonist self-peptide." Nat Immunol **2**(4): 301-6.

Jorgensen, S. H., P. E. Jensen, H. Laursen and P. S. Sorensen (2005). "Intravenous immunoglobulin ameliorates experimental autoimmune encephalomyelitis and reduces neuropathological abnormalities when administered prophylactically." Neurol Res **27**(6): 591-7.

Jorgensen, S. H., N. Storm, P. E. Jensen, H. Laursen and P. S. Sorensen (2007). "IVIG enters the central nervous system during treatment of experimental autoimmune encephalomyelitis and is localised to inflammatory lesions." Exp Brain Res **178**(4): 462-9.

June, C. H., J. A. Bluestone, L. M. Nadler and C. B. Thompson (1994). "The B7 and CD28 receptor families." Immunol Today **15**(7): 321-31.

Kaech, S. M., S. Hemby, E. Kersh and R. Ahmed (2002). "Molecular and functional profiling of memory CD8 T cell differentiation." Cell **111**(6): 837-51.

Kang, S. M., B. Beverly, A. C. Tran, K. Brorson, R. H. Schwartz and M. J. Lenardo (1992). "Transactivation by AP-1 is a molecular target of T cell clonal anergy." Science **257**(5073): 1134-8.

Kaplan, H. J. and J. W. Streilein (1977). "Immune response to immunization via the anterior chamber of the eye. I. F. lymphocyte-induced immune deviation." J Immunol **118**(3): 809-14.

Kapp, J. A., K. Honjo, L. M. Kapp, X. Xu, A. Cozier and R. P. Bucy (2006). "TCR transgenic CD8+ T cells activated in the presence of TGFbeta express FoxP3 and mediate linked suppression of primary immune responses and cardiac allograft rejection." Int Immunol **18**(11): 1549-62.

Kappler, J. W., N. Roehm and P. Marrack (1987). "T cell tolerance by clonal elimination in the thymus." Cell **49**(2): 273-80.

Kawabe, Y. and A. Ochi (1990). "Selective anergy of V beta 8+,CD4+ T cells in Staphylococcus enterotoxin B-primed mice." J Exp Med **172**(4): 1065-70.

Kawahata, K., Y. Misaki, M. Yamauchi, S. Tsunekawa, K. Setoguchi, J. Miyazaki and K. Yamamoto (2002). "Generation of CD4(+)CD25(+) regulatory T cells from autoreactive T cells simultaneously with their negative selection in the thymus and from nonautoreactive T cells by endogenous TCR expression." J Immunol **168**(9): 4399-405.

Kawano, Y., M. Kitaoka, Y. Hamada, M. M. Walker, J. Waxman and R. M. Kypta (2006). "Regulation of prostate cell growth and morphogenesis by Dickkopf-3." Oncogene **25**(49): 6528-37.

Kawano, Y. and R. Kypta (2003). "Secreted antagonists of the Wnt signalling pathway." J Cell Sci **116**(Pt 13): 2627-34.

Kearney, E. R., K. A. Pape, D. Y. Loh and M. K. Jenkins (1994). "Visualization of peptide-specific T cell immunity and peripheral tolerance induction in vivo." Immunity **1**(4): 327-39.

Kim, J. M., J. P. Rasmussen and A. Y. Rudensky (2007). "Regulatory T cells prevent catastrophic autoimmunity throughout the lifespan of mice." Nat Immunol **8**(2): 191-7.

Kimpton, W. G., E. A. Washington and R. N. Cahill (1995). "Virgin alpha beta and gamma delta T cells recirculate extensively through peripheral tissues and skin during normal development of the fetal immune system." Int Immunol **7**(10): 1567-77.

Kingsley, C. I., M. Karim, A. R. Bushell and K. J. Wood (2002). "CD25+CD4+ regulatory T cells prevent graft rejection: CTLA-4- and IL-10-dependent immunoregulation of alloresponses." J Immunol **168**(3): 1080-6.

Kisielow, P. (1988). "The true function of the thymus." Immunol Today **9**(12): 367.

Knolle, P. A., E. Schmitt, S. Jin, T. Germann, R. Duchmann, S. Hegenbarth, G. Gerken and A. W. Lohse (1999). "Induction of cytokine production in naive CD4(+) T cells by antigen-presenting murine liver sinusoidal endothelial cells but failure to induce differentiation toward Th1 cells." Gastroenterology **116**(6): 1428-40.

Kobayashi, K., M. Ouchida, T. Tsuji, H. Hanafusa, M. Miyazaki, M. Namba, N. Shimizu and K. Shimizu (2002). "Reduced expression of the REIC/Dkk-3 gene by promoter-hypermethylation in human tumor cells." Gene **282**(1-2): 151-8.

Kohn, A. D. and R. T. Moon (2005). "Wnt and calcium signaling: beta-catenin-independent pathways." Cell Calcium **38**(3-4): 439-46.

Korn, T., M. Oukka, V. Kuchroo and E. Bettelli (2007). "Th17 cells: effector T cells with inflammatory properties." Semin Immunol **19**(6): 362-71.

Krakowski, M. and T. Owens (1996). "Interferon-gamma confers resistance to experimental allergic encephalomyelitis." Eur J Immunol **26**(7): 1641-6.

Kretschmer, K., I. Apostolou, D. Hawiger, K. Khazaie, M. C. Nussenzweig and H. von Boehmer (2005). "Inducing and expanding regulatory T cell populations by foreign antigen." Nat Immunol **6**(12): 1219-27.

Krupnik, V. E., J. D. Sharp, C. Jiang, K. Robison, T. W. Chickering, L. Amaravadi, D. E. Brown, D. Guyot, G. Mays, K. Leiby, B. Chang, T. Duong, A. D. Goodearl, D. P. Gearing, S. Y. Sokol and S. A. McCarthy (1999). "Functional and structural diversity of the human Dickkopf gene family." Gene **238**(2): 301-13.

Kumar, V. (2004). "Homeostatic control of immunity by TCR peptide-specific Tregs." J Clin Invest **114**(9): 1222-6.

Kuphal, S., S. Lodermeyer, F. Bataille, M. Schuierer, B. H. Hoang and A. K. Bosserhoff (2006). "Expression of Dickkopf genes is strongly reduced in malignant melanoma." Oncogene **25**(36): 5027-36.

Kurts, C., W. R. Heath, H. Kosaka, J. F. Miller and F. R. Carbone (1998). "The peripheral deletion of autoreactive CD8+ T cells induced by cross-presentation of self-antigens involves signaling through CD95 (Fas, Apo-1)." J Exp Med **188**(2): 415-20.

Kwidzinski, E. and I. Bechmann (2007). "IDO expression in the brain: a double-edged sword." J Mol Med **85**(12): 1351-9.

Lampson, L. A. and C. A. Fisher (1984). "Weak HLA and beta 2-microglobulin expression of neuronal cell lines can be modulated by interferon." Proc Natl Acad Sci U S A **81**(20): 6476-80.

Langrish, C. L., Y. Chen, W. M. Blumenschein, J. Mattson, B. Basham, J. D. Sedgwick, T. McClanahan, R. A. Kastelein and D. J. Cua (2005). "IL-23 drives a pathogenic T cell population that induces autoimmune inflammation." J Exp Med **201**(2): 233-40.

Leifeld, L., C. Trautwein, F. L. Dumoulin, M. P. Manns, T. Sauerbruch and U. Spengler (1999). "Enhanced expression of CD80 (B7-1), CD86 (B7-2), and CD40 and their ligands CD28 and CD154 in fulminant hepatic failure." Am J Pathol **154**(6): 1711-20.

Lenardo, M., K. M. Chan, F. Hornung, H. McFarland, R. Siegel, J. Wang and L. Zheng (1999). "Mature T lymphocyte apoptosis--immune regulation in a dynamic and unpredictable antigenic environment." Annu Rev Immunol **17**: 221-53.

Li, M. O., Y. Y. Wan and R. A. Flavell (2007). "T cell-produced transforming growth factor-beta1 controls T cell tolerance and regulates Th1- and Th17-cell differentiation." Immunity **26**(5): 579-91.

Li, W., C. D. Whaley, A. Mondino and D. L. Mueller (1996). "Blocked signal transduction to the ERK and JNK protein kinases in anergic CD4+ T cells." Science **271**(5253): 1272-6.

Limmer, A., J. Ohl, C. Kurts, H. G. Ljunggren, Y. Reiss, M. Groettrup, F. Momburg, B. Arnold and P. A. Knolle (2000). "Efficient presentation of exogenous antigen by liver endothelial cells to CD8+ T cells results in antigen-specific T-cell tolerance." Nat Med **6**(12): 1348-54.

Liu, Y. J., V. Soumelis, N. Watanabe, T. Ito, Y. H. Wang, W. Malefyt Rde, M. Omori, B. Zhou and S. F. Ziegler (2007). "TSLP: an epithelial cell cytokine that regulates T cell differentiation by conditioning dendritic cell maturation." Annu Rev Immunol **25**: 193-219.

Lodygin, D., A. Epanchintsev, A. Menssen, J. Diebold and H. Hermeking (2005). "Functional epigenomics identifies genes frequently silenced in prostate cancer." Cancer Res **65**(10): 4218-27.

Loeser, S. and J. M. Penninger (2007). "Regulation of peripheral T cell tolerance by the E3 ubiquitin ligase Cbl-b." Semin Immunol **19**(3): 206-14.

Lohse, A. W., P. A. Knolle, K. Bilo, A. Uhrig, C. Waldmann, M. Ibe, E. Schmitt, G. Gerken and K. H. Meyer Zum Buschenfelde (1996). "Antigen-presenting function and B7 expression of murine sinusoidal endothelial cells and Kupffer cells." Gastroenterology **110**(4): 1175-81.

Lord, S. J., R. V. Rajotte, G. S. Korbutt and R. C. Bleackley (2003). "Granzyme B: a natural born killer." Immunol Rev **193**: 31-8.

Lutz, M. B. and G. Schuler (2002). "Immature, semi-mature and fully mature dendritic cells: which signals induce tolerance or immunity?" Trends Immunol **23**(9): 445-9.

Lyakh, L., P. Ghosh and N. R. Rice (1997). "Expression of NFAT-family proteins in normal human T cells." Mol Cell Biol **17**(5): 2475-84.

Macian, F., F. Garcia-Cozar, S. H. Im, H. F. Horton, M. C. Byrne and A. Rao (2002). "Transcriptional mechanisms underlying lymphocyte tolerance." Cell **109**(6): 719-31.

Madakamutil, L. T., I. Maricic, E. Sercarz and V. Kumar (2003). "Regulatory T cells control autoimmunity in vivo by inducing apoptotic depletion of activated pathogenic lymphocytes." J Immunol **170**(6): 2985-92.

Mahic, M., K. Henjum, S. Yaqub, B. A. Bjornbeth, K. M. Torgersen, K. Tasken and E. M. Aandahl (2008). "Generation of highly suppressive adaptive CD8(+)CD25(+)FOXP3(+) regulatory T cells by continuous antigen stimulation." Eur J Immunol **38**(3): 640-6.

Maloy, K. J. and F. Powrie (2001). "Regulatory T cells in the control of immune pathology." Nat Immunol **2**(9): 816-22.

Maloy, K. J., L. Salaun, R. Cahill, G. Dougan, N. J. Saunders and F. Powrie (2003). "CD4+CD25+ T(R) cells suppress innate immune pathology through cytokine-dependent mechanisms." J Exp Med **197**(1): 111-9.

Mao, B., W. Wu, G. Davidson, J. Marhold, M. Li, B. M. Mechler, H. Delius, D. Hoppe, P. Stannek, C. Walter, A. Glinka and C. Niehrs (2002). "Kremen proteins are Dickkopf receptors that regulate Wnt/beta-catenin signalling." Nature **417**(6889): 664-7.

Mao, B., W. Wu, Y. Li, D. Hoppe, P. Stannek, A. Glinka and C. Niehrs (2001). "LDL-receptor-related protein 6 is a receptor for Dickkopf proteins." Nature **411**(6835): 321-5.

Mariani, S. M. and P. H. Krammer (1998). "Surface expression of TRAIL/Apo-2 ligand in activated mouse T and B cells." Eur J Immunol **28**(5): 1492-8.

McLean, J. M. and R. J. Scothorne (1970). "The lymphatics of the endometrium in the rabbit." J Anat **107**(Pt 1): 39-48.

Medawar (1948). "Immunity to homologous skin grafting III. The fate of skin homografts transplanted to the brain and to the anterior chamber of the eye." Br J Exp Path **29**: 58-69.

Micklem, H. S., C. E. Ford, E. P. Evans and J. Gray (1966). "Interrelationships of myeloid and lymphoid cells: studies with chromosome-marked cells transfused into lethally irradiated mice." Proc R Soc Lond B Biol Sci **165**(998): 78-102.

Micsenyi, A., X. Tan, T. Sneddon, J. H. Luo, G. K. Michalopoulos and S. P. Monga (2004). "Beta-catenin is temporally regulated during normal liver development." Gastroenterology **126**(4): 1134-46.

Modigliani, Y., A. Coutinho, P. Pereira, N. Le Douarin, V. Thomas-Vaslin, O. Burlen-Defranoux, J. Salaun and A. Bandeira (1996). "Establishment of tissue-specific tolerance is driven by regulatory T cells selected by thymic epithelium." Eur J Immunol **26**(8): 1807-15.

Mogil, R. J., L. Radvanyi, R. Gonzalez-Quintial, R. Miller, G. Mills, A. N. Theofilopoulos and D. R. Green (1995). "Fas (CD95) participates in peripheral T cell deletion and associated apoptosis in vivo." Int Immunol **7**(9): 1451-8.

Monaghan, A. P., P. Kioschis, W. Wu, A. Zuniga, D. Bock, A. Poustka, H. Delius and C. Niehrs (1999). "Dickkopf genes are co-ordinately expressed in mesodermal lineages." Mech Dev **87**(1-2): 45-56.

Moore, M. A. and J. J. Owen (1965). "Chromosome marker studies on the development of the haemopoietic system in the chick embryo." Nature **208**(5014): 956 passim.

Moore, M. A. and J. J. Owen (1967). "Experimental studies on the development of the thymus." J Exp Med **126**(4): 715-26.

Morelli, A. E. and A. W. Thomson (2003). "Dendritic cells: regulators of alloimmunity and opportunities for tolerance induction." Immunol Rev **196**: 125-46.

Mukhopadhyay, M., S. Shtrom, C. Rodriguez-Esteban, L. Chen, T. Tsukui, L. Gomer, D. W. Dorward, A. Glinka, A. Grinberg, S. P. Huang, C. Niehrs, J. C. Belmonte and H. Westphal (2001). "Dickkopf1 is required for embryonic head induction and limb morphogenesis in the mouse." Dev Cell **1**(3): 423-34.

Murai, M., H. Yoneyama, T. Ezaki, M. Suematsu, Y. Terashima, A. Harada, H. Hamada, H. Asakura, H. Ishikawa and K. Matsushima (2003). "Peyer's patch is the essential site in initiating murine acute and lethal graft-versus-host reaction." Nat Immunol **4**(2): 154-60.

Murphy, P. M., M. Baggiolini, I. F. Charo, C. A. Hebert, R. Horuk, K. Matsushima, L. H. Miller, J. J. Oppenheim and C. A. Power (2000). "International union of pharmacology. XXII. Nomenclature for chemokine receptors." Pharmacol Rev **52**(1): 145-76.

Nagata, S. (1997). "Apoptosis by death factor." Cell **88**(3): 355-65.

Najafian, N., T. Chitnis, A. D. Salama, B. Zhu, C. Benou, X. Yuan, M. R. Clarkson, M. H. Sayegh and S. J. Khoury (2003). "Regulatory functions of CD8+CD28- T cells in an autoimmune disease model." J Clin Invest **112**(7): 1037-48.

Nakao, A., T. Imamura, S. Souchelnytskyi, M. Kawabata, A. Ishisaki, E. Oeda, K. Tamaki, J. Hanai, C. H. Heldin, K. Miyazono and P. ten Dijke (1997). "TGF-beta receptor-mediated signalling through Smad2, Smad3 and Smad4." Embo J **16**(17): 5353-62.

Nelson, W. J. and R. Nusse (2004). "Convergence of Wnt, beta-catenin, and cadherin pathways." Science **303**(5663): 1483-7.

Neumann, H., I. M. Medana, J. Bauer and H. Lassmann (2002). "Cytotoxic T lymphocytes in autoimmune and degenerative CNS diseases." Trends Neurosci **25**(6): 313-9.

Ng-Cashin, J., J. J. Kuhns, S. E. Burkett, J. D. Powderly, R. R. Craven, H. W. van Deventer, S. L. Kirby and J. S. Serody (2003). "Host absence of CCR5 potentiates dendritic cell vaccination." J Immunol **170**(8): 4201-8.

Niederkorn, J. Y. (2006). "See no evil, hear no evil, do no evil: the lessons of immune privilege." Nat Immunol **7**(4): 354-9.

Niehrs, C. (2006). "Function and biological roles of the Dickkopf family of Wnt modulators." Oncogene **25**(57): 7469-81.

Nikcevich, K. M., K. B. Gordon, L. Tan, S. D. Hurst, J. F. Kroepfl, M. Gardinier, T. A. Barrett and S. D. Miller (1997). "IFN-gamma-activated primary murine astrocytes express B7 costimulatory molecules and prime naive antigen-specific T cells." J Immunol **158**(2): 614-21.

Noh, D. Y., S. H. Shin and S. G. Rhee (1995). "Phosphoinositide-specific phospholipase C and mitogenic signaling." Biochim Biophys Acta **1242**(2): 99-113.

Ono, M., H. Yaguchi, N. Ohkura, I. Kitabayashi, Y. Nagamura, T. Nomura, Y. Miyachi, T. Tsukada and S. Sakaguchi (2007). "Foxp3 controls regulatory T-cell function by interacting with AML1/Runx1." Nature **446**(7136): 685-9.

Oshima, T., F. S. Laroux, L. L. Coe, Z. Morise, S. Kawachi, P. Bauer, M. B. Grisham, R. D. Specian, P. Carter, S. Jennings, D. N. Granger, T. Joh and J. S. Alexander (2001). "Interferon-gamma and interleukin-10 reciprocally regulate endothelial junction integrity and barrier function." Microvasc Res **61**(1): 130-43.

Ouyang, W., J. K. Kolls and Y. Zheng (2008). "The biological functions of T helper 17 cell effector cytokines in inflammation." Immunity **28**(4): 454-67.

Pacholczyk, R., J. Kern, N. Singh, M. Iwashima, P. Kraj and L. Ignatowicz (2007). "Nonself-antigens are the cognate specificities of Foxp3+ regulatory T cells." Immunity **27**(3): 493-504.

Pandiyan, P., L. Zheng, S. Ishihara, J. Reed and M. J. Lenardo (2007). "CD4+CD25+Foxp3+ regulatory T cells induce cytokine deprivation-mediated apoptosis of effector CD4+ T cells." Nat Immunol **8**(12): 1353-62.

Phillips, T. A., J. Ni, G. Pan, S. M. Ruben, Y. F. Wei, J. L. Pace and J. S. Hunt (1999). "TRAIL (Apo-2L) and TRAIL receptors in human placentas: implications for immune privilege." J Immunol **162**(10): 6053-9.

Pickart, C. M. and D. Fushman (2004). "Polyubiquitin chains: polymeric protein signals." Curr Opin Chem Biol **8**(6): 610-6.

Pinho, S. and C. Niehrs (2007). "Dkk3 is required for TGF-beta signaling during Xenopus mesoderm induction." Differentiation **75**(10): 957-67.

Pitkanen, J. and P. Peterson (2003). "Autoimmune regulator: from loss of function to autoimmunity." Genes Immun **4**(1): 12-21.

Pollard, S. L. and P. W. Holland (2000). "Evidence for 14 homeobox gene clusters in human genome ancestry." Curr Biol **10**(17): 1059-62.

Popko, B. and K. D. Baerwald (1999). "Oligodendroglial response to the immune cytokine interferon gamma." Neurochem Res **24**(2): 331-8.

Praseedom, R. K., K. D. McNeil, C. J. Watson, G. J. Alexander, R. Y. Calne, J. Wallwork and P. J. Friend (2001). "Combined transplantation of the heart, lung, and liver." Lancet **358**(9284): 812-3.

Puccetti, P. and U. Grohmann (2007). "IDO and regulatory T cells: a role for reverse signalling and non-canonical NF-kappaB activation." Nat Rev Immunol **7**(10): 817-23.

Qin, H. Y., R. Mukherjee, E. Lee-Chan, C. Ewen, R. C. Bleackley and B. Singh (2006). "A novel mechanism of regulatory T cell-mediated down-regulation of autoimmunity." Int Immunol **18**(7): 1001-15.

Quill, H. and R. H. Schwartz (1987). "Stimulation of normal inducer T cell clones with antigen presented by purified Ia molecules in planar lipid membranes: specific induction of a long-lived state of proliferative nonresponsiveness." J Immunol **138**(11): 3704-12.

Read, S., R. Greenwald, A. Izcue, N. Robinson, D. Mandelbrot, L. Francisco, A. H. Sharpe and F. Powrie (2006). "Blockade of CTLA-4 on CD4+CD25+ regulatory T cells abrogates their function in vivo." J Immunol **177**(7): 4376-83.

Refaeli, Y., L. Van Parijs, C. A. London, J. Tschopp and A. K. Abbas (1998). "Biochemical mechanisms of IL-2-regulated Fas-mediated T cell apoptosis." Immunity **8**(5): 615-23.

Reibke, R., N. Garbi, R. Ganss, G. J. Hammerling, B. Arnold and T. Oelert (2006). "CD8+ regulatory T cells generated by neonatal recognition of peripheral self-antigen." Proc Natl Acad Sci U S A **103**(41): 15142-7.

Reinke, E. and Z. Fabry (2006). "Breaking or making immunological privilege in the central nervous system: the regulation of immunity by neuropeptides." Immunol Lett **104**(1-2): 102-9.

Roman-Gomez, J., A. Jimenez-Velasco, X. Agirre, J. A. Castillejo, G. Navarro, M. Barrios, E. J. Andreu, F. Prosper, A. Heiniger and A. Torres (2004). "Transcriptional silencing of the Dickkopfs-3 (Dkk-3) gene by CpG hypermethylation in acute lymphoblastic leukaemia." Br J Cancer **91**(4): 707-13.

Romeo, P. H., V. Lemarchandel and R. Tordjman (2002). "Neuropilin-1 in the immune system." Adv Exp Med Biol **515**: 49-54.

Safford, M., S. Collins, M. A. Lutz, A. Allen, C. T. Huang, J. Kowalski, A. Blackford, M. R. Horton, C. Drake, R. H. Schwartz and J. D. Powell (2005). "Egr-2 and Egr-3 are negative regulators of T cell activation." Nat Immunol **6**(5): 472-80.

Saha, D., P. K. Datta and R. D. Beauchamp (2001). "Oncogenic ras represses transforming growth factor-beta /Smad signaling by degrading tumor suppressor Smad4." J Biol Chem **276**(31): 29531-7.

Sakaguchi, S., T. Yamaguchi, T. Nomura and M. Ono (2008). "Regulatory T cells and immune tolerance." Cell **133**(5): 775-87.

Sarris, M., K. G. Andersen, F. Randow, L. Mayr and A. G. Betz (2008). "Neuropilin-1 expression on regulatory T cells enhances their interactions with dendritic cells during antigen recognition." Immunity **28**(3): 402-13.

Sato, N., W. A. Kuziel, P. C. Melby, R. L. Reddick, V. Kostecki, W. Zhao, N. Maeda, S. K. Ahuja and S. S. Ahuja (1999). "Defects in the generation of IFN-gamma are overcome to control infection with Leishmania donovani in CC chemokine receptor (CCR) 5-, macrophage inflammatory protein-1 alpha-, or CCR2-deficient mice." J Immunol **163**(10): 5519-25.

Schartner, J. M., C. G. Fathman and C. M. Seroogy (2007). "Preservation of self: an overview of E3 ubiquitin ligases and T cell tolerance." Semin Immunol **19**(3): 188-96.

Schmitt, E., P. Hoehn, C. Huels, S. Goedert, N. Palm, E. Rude and T. Germann (1994). "T helper type 1 development of naive CD4+ T cells requires the coordinate action of interleukin-12 and interferon-gamma and is inhibited by transforming growth factor-beta." Eur J Immunol **24**(4): 793-8.

Schroeder, A., O. Mueller, S. Stocker, R. Salowsky, M. Leiber, M. Gassmann, S. Lightfoot, W. Menzel, M. Granzow and T. Ragg (2006). "The RIN: an RNA integrity number for assigning integrity values to RNA measurements." BMC Mol Biol **7**: 3.

Schwartz, R. H. (2003). "T cell anergy." Annu Rev Immunol **21**: 305-34.

Seddon, B. and D. Mason (2000). "The third function of the thymus." Immunol Today **21**(2): 95-9.

Sharabi, A. and E. Mozes (2008). "The suppression of murine lupus by a tolerogenic peptide involves foxp3-expressing CD8 cells that are required for the optimal induction and function of foxp3-expressing CD4 cells." J Immunol **181**(5): 3243-51.

Shevach, E. M., R. S. McHugh, C. A. Piccirillo and A. M. Thornton (2001). "Control of T-cell activation by CD4+ CD25+ suppressor T cells." Immunol Rev **182**: 58-67.

Sloan-Lancaster, J., B. D. Evavold and P. M. Allen (1993). "Induction of T-cell anergy by altered T-cell-receptor ligand on live antigen-presenting cells." Nature **363**(6425): 156-9.

Sonobe, Y., S. Jin, J. Wang, J. Kawanokuchi, H. Takeuchi, T. Mizuno and A. Suzumura (2007). "Chronological changes of CD4(+) and CD8(+) T cell subsets in the experimental autoimmune encephalomyelitis, a mouse model of multiple sclerosis." Tohoku J Exp Med **213**(4): 329-39.

Steinman, L. (2001). "Myelin-specific CD8 T cells in the pathogenesis of experimental allergic encephalitis and multiple sclerosis." J Exp Med **194**(5): F27-30.
Steinman, R. M., D. Hawiger and M. C. Nussenzweig (2003). "Tolerogenic dendritic cells." Annu Rev Immunol **21**: 685-711.
Steinman, R. M. and M. C. Nussenzweig (2002). "Avoiding horror autotoxicus: the importance of dendritic cells in peripheral T cell tolerance." Proc Natl Acad Sci U S A **99**(1): 351-8.
Steinman, R. M. and M. D. Witmer (1978). "Lymphoid dendritic cells are potent stimulators of the primary mixed leukocyte reaction in mice." Proc Natl Acad Sci U S A **75**(10): 5132-6.
Stephens, G. L. and E. M. Shevach (2007). "Foxp3+ regulatory T cells: selfishness under scrutiny." Immunity **27**(3): 417-9.
Stockinger, B. and M. Veldhoen (2007). "Differentiation and function of Th17 T cells." Curr Opin Immunol **19**(3): 281-6.
Stone, J. C. (2006). "Regulation of Ras in lymphocytes: get a GRP." Biochem Soc Trans **34**(Pt 5): 858-61.
Street, N. E. and T. R. Mosmann (1991). "Functional diversity of T lymphocytes due to secretion of different cytokine patterns." Faseb J **5**(2): 171-7.
Streilein, J. W. (2003). "Ocular immune privilege: therapeutic opportunities from an experiment of nature." Nat Rev Immunol **3**(11): 879-89.
Sun, C. M., J. A. Hall, R. B. Blank, N. Bouladoux, M. Oukka, J. R. Mora and Y. Belkaid (2007). "Small intestine lamina propria dendritic cells promote de novo generation of Foxp3 T reg cells via retinoic acid." J Exp Med **204**(8): 1775-85.
Sun, D., J. N. Whitaker, Z. Huang, D. Liu, C. Coleclough, H. Wekerle and C. S. Raine (2001). "Myelin antigen-specific CD8+ T cells are encephalitogenic and produce severe disease in C57BL/6 mice." J Immunol **166**(12): 7579-87.
Suwa, T., M. Chen, C. L. Hawks and P. J. Hornsby (2003). "Zonal expression of dickkopf-3 and components of the Wnt signalling pathways in the human adrenal cortex." J Endocrinol **178**(1): 149-58.
Takeuchi, H., J. Wang, J. Kawanokuchi, N. Mitsuma, T. Mizuno and A. Suzumura (2006). "Interferon-gamma induces microglial-activation-induced cell death: a hypothetical mechanism of relapse and remission in multiple sclerosis." Neurobiol Dis **22**(1): 33-9.
Tang, Q. and J. A. Bluestone (2008). "The Foxp3+ regulatory T cell: a jack of all trades, master of regulation." Nat Immunol **9**(3): 239-44.
Thakker, P., M. W. Leach, W. Kuang, S. E. Benoit, J. P. Leonard and S. Marusic (2007). "IL-23 is critical in the induction but not in the effector phase of experimental autoimmune encephalomyelitis." J Immunol **178**(4): 2589-98.
van Leeuwen, J. E. and L. E. Samelson (1999). "T cell antigen-receptor signal transduction." Curr Opin Immunol **11**(3): 242-8.
van Meerwijk, J. P., S. Marguerat, R. K. Lees, R. N. Germain, B. J. Fowlkes and H. R. MacDonald (1997). "Quantitative impact of thymic clonal deletion on the T cell repertoire." J Exp Med **185**(3): 377-83.
Volkmann, A., T. Zal and B. Stockinger (1997). "Antigen-presenting cells in the thymus that can negatively select MHC class II-restricted T cells recognizing a circulating self antigen." J Immunol **158**(2): 693-706.
Wagner, D. H., Jr. (2007). "Re-shaping the T cell repertoire: TCR editing and TCR revision for good and for bad." Clin Immunol **123**(1): 1-6.
Wan, Y. Y. and R. A. Flavell (2007). "Regulatory T cells, transforming growth factor-beta, and immune suppression." Proc Am Thorac Soc **4**(3): 271-6.

Wang, S., Z. F. Boonman, H. C. Li, Y. He, M. J. Jager, R. E. Toes and J. Y. Niederkorn (2003). "Role of TRAIL and IFN-gamma in CD4+ T cell-dependent tumor rejection in the anterior chamber of the eye." J Immunol **171**(6): 2789-96.

Wenkel, H., J. W. Streilein and M. J. Young (2000). "Systemic immune deviation in the brain that does not depend on the integrity of the blood-brain barrier." J Immunol **164**(10): 5125-31.

Willenborg, D. O., S. Fordham, C. C. Bernard, W. B. Cowden and I. A. Ramshaw (1996). "IFN-gamma plays a critical down-regulatory role in the induction and effector phase of myelin oligodendrocyte glycoprotein-induced autoimmune encephalomyelitis." J Immunol **157**(8): 3223-7.

Wu, Y., M. Borde, V. Heissmeyer, M. Feuerer, A. D. Lapan, J. C. Stroud, D. L. Bates, L. Guo, A. Han, S. F. Ziegler, D. Mathis, C. Benoist, L. Chen and A. Rao (2006). "FOXP3 controls regulatory T cell function through cooperation with NFAT." Cell **126**(2): 375-87.

Wysocki, C. A., Q. Jiang, A. Panoskaltsis-Mortari, P. A. Taylor, K. P. McKinnon, L. Su, B. R. Blazar and J. S. Serody (2005). "Critical role for CCR5 in the function of donor CD4+CD25+ regulatory T cells during acute graft-versus-host disease." Blood **106**(9): 3300-7.

Yue, W., Q. Sun, S. Dacic, R. J. Landreneau, J. M. Siegfried, J. Yu and L. Zhang (2008). "Downregulation of Dkk3 activates beta-catenin/TCF-4 signaling in lung cancer." Carcinogenesis **29**(1): 84-92.

Yurchenko, E., M. Tritt, V. Hay, E. M. Shevach, Y. Belkaid and C. A. Piccirillo (2006). "CCR5-dependent homing of naturally occurring CD4+ regulatory T cells to sites of Leishmania major infection favors pathogen persistence." J Exp Med **203**(11): 2451-60.

Zehntner, S. P., L. Bourbonniere, M. Hassan-Zahraee, E. Tran and T. Owens (2004). "Bone marrow-derived versus parenchymal sources of inducible nitric oxide synthase in experimental autoimmune encephalomyelitis." J Neuroimmunol **150**(1-2): 70-9.

Zinkernagel, R. M., M. F. Bachmann, T. M. Kundig, S. Oehen, H. Pirchet and H. Hengartner (1996). "On immunological memory." Annu Rev Immunol **14**: 333-67.

Zinkernagel, R. M. and P. C. Doherty (1974). "Restriction of in vitro T cell-mediated cytotoxicity in lymphocytic choriomeningitis within a syngeneic or semiallogeneic system." Nature **248**(450): 701-2.

Zinkernagel, R. M. and P. C. Doherty (1979). "MHC-restricted cytotoxic T cells: studies on the biological role of polymorphic major transplantation antigens determining T-cell restriction-specificity, function, and responsiveness." Adv Immunol **27**: 51-177.